



POLYMER ELECTROLYTE MEMBRANE (PEM) FUEL CELL SEALS DURABILITY

By Sebnem Pehlivan-Davis

A Doctoral Thesis

Submitted in partial fulfilment of the requirements for the award of
Degree of Doctor of Philosophy of Loughborough University

October 2015

Supervisor: Dr Jane Clarke

© by Sebnem Pehlivan- Davis

“Anybody who has been seriously engaged in scientific work of any kind realizes that over the entrance to the gates of the temple of science are written the words: '*Ye must have faith.*' It is a quality which the scientist cannot dispense with.”

- Max Planck (1932)

Abstract

Polymer electrolyte membrane fuel cell (PEMFC) stacks require sealing around the perimeter of the cells to prevent the gases inside the cell from leaking. Elastomeric materials are commonly used for this purpose. The overall performance and durability of the fuel cell is heavily dependent on the long-term stability of the gasket. In this study, the degradation of three elastomeric gasket materials (silicone rubber, commercial EPDM and a developed EPDM 2 compound) in an accelerated ageing environment was investigated.

The change in properties and structure of a silicone rubber gasket caused by use in a real fuel cell was studied and compared to the changes in the same silicone rubber gasket material brought about by accelerated aging. The accelerated aging conditions were chosen to relate to the PEM fuel cell environment, but with more extreme conditions of elevated temperature (140°C) and greater acidity. Three accelerated ageing media were used. The first one was dilute sulphuric acid solution with the pH values of 1, 2 and 4. Secondly, Nafion® membrane suspended in water was used for accelerated ageing at a pH 3 to 4. Finally, diluted trifluoroacetic acid (TFA) solution of pH 3.3 was chosen. Weight change and the tensile properties of the aged gasket samples were measured. In addition, compression set behaviour of the elastomeric seal materials was investigated in order to evaluate their potential sealing performance in PEM fuel cells.

The results showed that acid hydrolysis was the most likely mechanism of silicone rubber degradation and that similar degradation occurred under both real fuel cell and accelerated aging conditions. The effect of TFA solution on silicone rubber was more aggressive than sulphuric acid and Nafion® solutions with the same acidity (pH value) suggesting that TFA accelerated the acid hydrolysis of silicone rubber. In addition, acid ageing in all three acidic solutions caused visible surface damage and a significant decrease in tensile strength of the silicone rubber material, but did not significantly affect the EPDM materials. EPDM 2 compound had a desirable (low) compression set value which was similar to silicone rubber and much better than the commercial EPDM. It also showed a very good performance in the fuel cell test rig conforming that it a potential replacement for silicone rubber in PEMFCs.

Acknowledgement

I wish to express my sincere appreciation to my supervisor, Dr. Jane Clarke for her consistent guidance, patience, and tremendous support throughout my research period and during the preparation of this thesis.

I would like to also thank my project sponsors, Technology Strategy Board (TSB) and Intelligent Energy, giving me this opportunity to participate in the project (BH064B).

Additionally, I am grateful to all the staff at the Department of Materials for their help and support.

I especially would like to thank to my husband Jason, for his understanding, patience, encouragement and unconditional love, without which I would not have succeeded this far. Finally, I want to thank to my sister Sinem and my lovely son Ethan-Sarp for their love, inspiration and support over the years.

Table of Contents

Abstract	i
Acknowledgement	ii
Table of Contents	iii
List of Figures	x
List of Tables	xv
1. CHAPTER 1: Introduction	1
1.1. Background	1
1.2. Reasons for the Study	2
1.3. Objectives of the Study	3
1.4. Outline of the Thesis	4
1.5. REFERENCES	6
2. CHAPTER 2: Background to Fuel Cells	7
2.1. What is a Fuel Cell	7
2.2. Types of Fuel Cell	9
2.2.1. Direct Methanol Fuel Cell (DMFC)	11
2.2.2. Polymer Electrolyte Membrane Fuel Cell (PEMFC)	11
2.2.3. Alkaline Fuel Cell (AFC)	11
2.2.4. Phosphoric Acid Fuel Cell (PAFC)	12
2.2.5. Molten Carbonate Fuel Cell (MCFC)	12
2.2.6. Solid Oxide Fuel Cell (SOFC)	13
2.3. Advantages and Applications of Fuel Cells	14
2.4. The PEM Fuel Cell	16
2.4.1. Electrolyte Membrane	19

2.4.2. The Electrode/Catalyst Layer.....	21
2.4.3. The Membrane Electrode Assembly.....	23
2.4.4. The Gas Diffusion Layer.....	24
2.4.5. The Bipolar Plate.....	25
2.4.6. Sealing.....	26
2.5. Characteristics and Applications of PEM Fuel Cells.....	26
2.6. Limitations of PEM Fuel Cell Technology.....	29
2.7. REFERENCES.....	33
3. CHAPTER 3: Sealing Gasket.....	37
3.1. Introduction.....	37
3.2. Function of the Sealing Gasket.....	38
3.3. Environment of the Sealing Gasket.....	39
3.4. Requirements of the Sealing Gasket.....	40
3.5. Design and Fabrication Methods.....	43
3.6. Seal Materials.....	49
3.6.1. Background.....	49
3.6.2. Elastomers for Seal/ Gasket Applications.....	54
3.6.3. Current PEM Fuel Cell Gasket Materials.....	55
Silicone Rubber (Q).....	55
Ethylene-Propylene -Diene Monomer (EPDM).....	60
Fluoroelastomers (FKM).....	63
Fluorosilicone Rubber (FMQ , FVMQ).....	67
3.7. Summary.....	68
3.8. REFERENCES.....	70
4. CHAPTER 4: Seal / Gasket Degradation.....	74

4.1. Introduction	74
4.2. Chemical Degradation of Sealing Material	74
4.2.1. Degradation of Seals in Various Environments.....	75
4.2.2. Degradation in Accelerated and Simulated PEM Fuel Cell Environments....	81
Weight Change:.....	82
Surface Change-Optical Microscopy:	87
ATR-FTIR (Fourier Transform Infrared).....	90
X-ray Photoelectron Spectroscopy (XPS).....	94
Atomic Adsorption Spectrometry	96
The Effect of Hardness (Shore A) of the Sealing Materials on Degradation..	96
Change in Physical and Mechanical Properties with Chemical Degradation.	97
Microindentation Test:	98
4.2.3. Degradation of Silicone Rubber Seals during PEM Fuel Cell Operation.....	102
Proposed Degradation Mechanism of Silicone Rubber Gasket Material in PEMFC	
.....	104
4.3. Stress Relaxation in Sealing Materials.....	107
4.3.1. Modelling of Stress Relaxation Behaviour and Lifetime Predictions of Seals	
.....	108
4.3.2. Stress Relaxation Studies for PEMFC Seals	112
4.4. Compression Set	117
4.5. REFERENCES	120
5. CHAPTER 5: Experimental.....	125
5.1. Materials	125
5.2. Mixing.....	131
5.3. Curing Properties & Conditions.....	132
5.4. Characterization Methods	133

5.4.1. Scanning Electron Microscopy (SEM)	133
5.4.2. Atomic Force Microscopy (AFM).....	133
5.4.3. X-Ray Photoelectron Spectroscopy (XPS)	133
5.4.4. Attenuated Total Reflection Fourier Transform Infrared Spectroscopy (ATR-FTIR)	134
5.4.5. Solvent Swelling Method	134
5.5. Accelerated Acid Ageing Method	135
5.5.1. Accelerated Ageing Solutions	136
5.5.2. Weight Change	137
5.6. Tensile Testing.....	137
5.7. Compression Set	138
5.8. Hardness.....	139
5.9. REFERENCES	140
6. CHAPTER 6: Degradation of Silicone Rubber Gasket Material	141
6.1. Aging of Silicone Rubber Gasket in an actual PEM Fuel cell Environment	141
6.1.1. Observed Surface Degradation of the Silicone Rubber Gasket	142
6.1.2. Scanning Electron Microscopy (SEM) – Change in the Thickness of the Gasket	143
6.1.3. Atomic Force Microscopy (AFM) – Change in the Stiffness of the Gasket .	145
6.1.4. X-Ray Photoelectron Spectroscopy (XPS) – Change in Surface Atomic Composition.....	148
6.1.5. Attenuated Total Reflection Fourier Transform Infrared Spectroscopy (ATR-FTIR) – Change in Surface Chemistry with Degradation	151
6.1.6. Solvent Swelling Method – Change in the Cross-link Density	154
6.2. Aging of Silicone Rubber Gasket Material in an Accelerated Aging Environment	155

6.2.1 In Acidic H ₂ SO ₄ Solutions of pH 1, 2 and 4.....	155
Effect of Aging on the Mechanical Properties	155
Effect of Aging on the Surface Appearance	158
6.2.2. Aging of Silicone Rubber Gasket Material in Nafion® Solution with pH 3 to 4	160
Acidity (pH) of Nafion® Solution	160
Comparison of Degradation in Nafion® (pH 3–4) and H ₂ SO ₄ (pH 2 & pH 4) Solutions.....	161
6.2.3. Aging of Silicone Rubber in Trifluoroacetic acid (TFA) (pH 3.3), Nafion® (pH ~ 3.2) and H ₂ SO ₄ (pH ~ 3) Solutions	163
Acidity (pH) Change of the Aging Solutions.....	164
Weight Change.....	165
Effect of Aging on the Mechanical Properties	166
Effect of Aging on the Surface Appearance.....	167
6.3. Summary.....	168
6.4. REFERENCES	170
7. CHAPTER 7: Material Development for Improved PEM Fuel Cell Seal	171
7.1. Commercial EPDM.....	171
7.1.1. Accelerated Aging of Commercial EPDM Compound and Silicone Rubber (in pH 2 sulfuric acid solution).....	171
7.1.2. Compression Set	173
7.2. The Requirements For an Ideal EPDM Fuel Cell Seal Compound	173
7.3. EPDM Compound Optimisation	174
7.3.1. Initial Compounding.....	174
Tensile Properties of the initial EPDM Compounds	175
Compression Set of the initial EPDM Compounds.....	177

7.3.2. Final Compounding.....	179
Tensile Properties of the final EPDM Compounds.....	179
Hardness of the final EPDM Compounds	182
Compression Set of the final EPDM Compounds	183
7.4. Comparison of Accelerated Aging Behaviour of EPDM 2 with Silicone Rubber	189
7.4.1. Weight Change	189
7.4.2. Effect of Aging on the Mechanical Properties	190
7.4.3. Compression Set	193
7.5. Accelerated Aging of Moulded Gaskets in Single Fuel Cells (in stack test)	194
7.5.1. Daily Cross- over Test (Failure Test) of the Gaskets	195
7.5.2. Thickness Loss in Gasket Samples	196
7.6. Summary.....	198
7.7. REFERENCES	199
8. CHAPTER 8: Conclusions and Recommendations	200
8.1. Conclusions.....	200
8.1.1. Effect of Aging on the properties of silicone rubber gasket in a real PEM fuel cell environment.....	200
8.1.2. Effect of Aging on the Properties of Silicone Rubber Gasket Material in an Accelerated Aging Environment	201
8.1.3. Effect of chemical Aging on the properties of commercial EPDM gasket material with comparison to silicone rubber	203
8.1.4. EPDM Compound development	203
8.1.5. Effect of chemical Aging on the properties of EPDM 2 gasket material with comparison to silicone rubber	204
8.1.6. Compression set behaviour of silicone rubber, commercial EPDM and EPDM 2 compound	205

8.1.7. Stability of silicone rubber and EPDM 2 gasket materials in the fuel cell accelerated aging test rig.....	205
8.2. Recommendations for Future Work	205
APPENDIX	207
Publications from this Thesis.....	207

List of Figures

<u>FIGURE 2.1.</u> Basic working principle of a fuel cell	7
<u>FIGURE 2.2.</u> Schematic of a fuel cell ⁴	8
<u>FIGURE 2.3.</u> PEM Fuel Cell Stack ²⁰	19
<u>FIGURE 2.4.</u> Chemical Formula of Nafion® ²¹	20
<u>FIGURE 2.5.</u> Structure of Nafion® ²²	20
<u>FIGURE 2.6.</u> The structure of Carbon supported Catalyst ²⁴	22
<u>FIGURE 2.7.</u> Simplified structure of a PEM fuel cell electrode ²⁴	22
<u>FIGURE 2.8.</u> A diagram of membrane electrode assembly (MEA) ²⁵	24
<u>FIGURE 3.1.</u> Illustration of a single PEM fuel cell ⁶	38
<u>FIGURE 3.2.</u> Loose style profile gaskets ²⁵	47
<u>FIGURE 3.3.</u> Methods for seal integration to bipolar plate (BPP) ²⁵	48
<u>FIGURE 3.4.</u> Cross-linked network of an elastomer ³⁷	51
<u>FIGURE 3.5.</u> The ring opening reaction of elemental sulfur at 150°C	51
<u>FIGURE 3.6.</u> Peroxide reactions ³⁶	53
<u>FIGURE 3.7.</u> Polydimethylsiloxane (PDMS) ⁴⁰	56
<u>FIGURE 3.8.</u> A structural formula of ENB-containing EPDM ⁵⁰	61
<u>FIGURE 3.9.</u> Most common monomers used for the preparation of FKM ⁴³	64
<u>FIGURE 3.10.</u> The chemical structure of Fluorosilicone rubber ⁵⁵	67
<u>FIGURE 4.1.</u> The hydrothermal degradation mechanism for LSR in Deionised (DI) water ⁹	78
<u>FIGURE 4.2.</u> Weight loss of silicone rubber with exposure time in the aging solution (12 ppm H ₂ SO ₄ , 1.8 ppm HF) and at 60°C & 80°C ²¹	83
<u>FIGURE 4.3.</u> Weight loss of silicone rubber with exposure time at 70°C ²⁴	84
<u>FIGURE 4.4.</u> Weight change with exposure time for samples having 120° bend angle in ADT solution at 60°C and 80°C ²⁶	85
<u>FIGURE 4.5.</u> The weight change of five gasket materials over time in Regular (pH 3.35) and ADT (pH < 1) solutions at 80°C ²¹	86

FIGURE 4.6. Optical micrographs of silicone rubber samples before and after exposure to ADT solution at 80 and 60°C. (a) Before exposure, (b) 1-week exposure at 80°C, (c) 3-week exposure at 80°C, (d) 5-week exposure at 80°C, (e) 17-week exposure at 80°C, (f) 5-week exposure at 60°C, (g) 17-week exposure at 60°C, (h) 45-week exposure at 60°C ²²	88
FIGURE 4.7. Optical micrographs of EPDM samples before and after exposure to the solution at 80 and 60°C. (a) Before exposure, (b) 10-week exposure at 80°C, (c) 17-week exposure at 80°C, (d) 24-week exposure at 80°C, (e) 35-week exposure at 80°C, (f) 35-week exposure at 60°C ²⁸	89
FIGURE 4.8. ATR-FTIR results for silicone rubber material exposed to aging solution at 80°C and subjected to compressive load : a-without exposure and after b-3 week, c-5 week, d-7 week, e-10 week and f- 12 week exposure. ATR-FTIR spectra from (A) 800 – 1450cm ⁻¹ and (B) 2500 – 3500 cm ⁻¹ ²⁸	91
FIGURE 4.9. ATR-FTIR results for EPDM material in the aging solution at 80°C : a-without exposure and after b-5 week, c-24 week, d-28 week and e-35 week exposure ²⁸	93
FIGURE 4.10. XPS spectra for silicone rubber sample (a) before and (b) after 4 week exposure to ADT solution at 80°C ²³	95
FIGURE 4.11. Weight loss of silicone rubbers with different hardness after exposure to simulated solution (a) and of silicone rubber with hardness of 40 exposure to different aqueous solutions (b) ³⁰	97
FIGURE 4.12. Load-indentation depth curves of the silicone samples before exposure (a) and after 35 week exposure to the aging solution (pH ~ 3.35) at 60°C (b) and 80°C (c) at a peak indentation depth of 0.20mm ²¹	99
FIGURE 4.13. Bar charts of indentation load for silicone (SS) samples before exposure (a) and after 35 week exposure to the aging solution (pH ~ 3.35) at 60°C (b) and 80°C (c) ²¹	99
FIGURE 4.14. Load-indentation depth curves of the EPDM samples before exposure (a) and after 35 week exposure to the solution (pH ~ 3.35) at 60°C (b) and 80°C (c) at a peak indentation depth of 0.20mm ²⁸	100

<u>FIGURE 4.15.</u> Bar charts of indentation load for the EPDM samples before exposure (A) and after 35 week exposure to the aging solution (pH ~ 3.35) at 60°C (B) and 80°C (C) at a peak indentation depth of 0.020 mm ²⁸	101
<u>FIGURE 4.16.</u> Silicone gasket of cell # 2 and cathode GDL attached to the bipolar plate ³³	103
<u>FIGURE 4.17.</u> The degradation mechanisms of silicone rubber at cross-linked sites of the rubber and combination reaction (in the ageing solution pH < 1) ²⁴	106
<u>FIGURE 4.18.</u> Time – temperature superposition ³⁸	110
<u>FIGURE 4.19.</u> Stress relaxation curves of LSR – comparison of test data with the estimation from the Prony series ³⁹	112
<u>FIGURE 4.20.</u> Stress relaxation data of LSR in DI water at three temperatures in logarithmic scale ³⁹	113
<u>FIGURE 4.21.</u> Master curve of stress relaxation of LSR at a reference temperature of 70°C ³⁹	114
<u>FIGURE 4.22.</u> Arrhenius plot for stress relaxation tests of LSR in air and DI water ³⁷	116
<u>FIGURE 5.1.</u> The order for compound mixing.....	132
<u>FIGURE 5.2.</u> The parts of a pressure cooker.....	135
<u>FIGURE 5.3.</u> (a) Accelerated aging test pressure cooker and (b) arrangement of the samples in the cooker	136
<u>FIGURE 5.4.</u> (a) Dimensions of a tensile test piece and (b) tensile grip with specimen clamped on.....	138
<u>FIGURE 6.1.</u> Cross section of a PEM fuel cell showing gasket	142
<u>FIGURE 6.2.</u> Sections of silicone rubber gasket (a) unused (b) after 8000 h use in fuel cell.....	143
<u>FIGURE 6.3.</u> SEM images of silicone rubber gasket (a) unused (b) used for 5000 h (c) used for 8000 h	144
<u>FIGURE 6.4.</u> Average thicknesses of silicone rubber gaskets measured from SEM images.....	145
<u>FIGURE 6.5.</u> Topographic images of used silicone rubber gasket: Location 4. The points (1, 2, 3, and 4) on right bottom image indicate the points at which AFM modulus was calculated for each location	146

<u>FIGURE 6.6.</u> Force/distance curves of the used silicone rubber gasket – location 4 (In and out represents the force measurement of the AFM probe with the amount of indentation on the surface).....	147
<u>FIGURE 6.7.</u> AFM Modulus of unused and used (5000 h in the fuel cell) silicone rubber gaskets (from less degraded area, Location 1, to highly degraded area, Location 5, and at each location four different points were measured).....	148
<u>FIGURE 6.8.</u> Stained and degraded areas of used silicone rubber gasket.....	149
<u>FIGURE 6.24.</u> (a) Unexposed silicone rubber and after 4 days exposure to pH 3 solutions (b) sulfuric acid, (c) Nafion® and (d) TFA at 140°C.....	168
<u>FIGURE 7.1.</u> Tensile strength of commercial EPDM and silicone rubber compounds in pH 2 sulfuric acid (H ₂ SO ₄) solution at 140°C.....	172
<u>FIGURE 7.2.</u> Tensile strength of commercial EPDM and silicone rubber compounds in pH 3 – 4 Nafion® solution at 140°C.....	172
<u>FIGURE 7.3.</u> Compression set of commercial EPDM and silicone rubber at 140°C and 25% compression for 72 hrs.....	173
<u>FIGURE 7.4.</u> Tensile strength of EPDM compounds (A to F).....	175
<u>FIGURE 7.5.</u> Elongation at break of EPDM compounds (A to F).....	176
<u>FIGURE 7.6.</u> 50 % Modulus of EPDM compounds (A to F).....	176
<u>FIGURE 7.7.</u> Compression set of EPDM compounds (A to F).....	178
<u>FIGURE 7.8.</u> Tensile Strength of new EPDM compounds and compound F.....	180
<u>FIGURE 7.9.</u> Elongation at break of new EPDM compounds and compound F.....	181
<u>FIGURE 7.10.</u> 100 % Modulus of new EPDM compounds and compound F.....	182
<u>FIGURE 7.11.</u> Hardness of EPDM new compounds and compound F.....	183
<u>FIGURE 7.12.</u> Compression set of EPDM new compounds and compound F at 140°C and 25% compression for 72 hrs.....	184
<u>FIGURE 7.13.</u> Effect of lithene and silica concentrations on the tensile strength of EPDM compounds.....	185
<u>FIGURE 7.14.</u> Effect of lithene and silica concentrations on the elongation at break of EPDM compounds.....	185
<u>FIGURE 7.15.</u> Effect of lithene and silica concentrations on the 50 % modulus of EPDM compounds.....	186

<u>FIGURE 7.16.</u> Effect of lithene and silica concentrations on the hardness of EPDM compounds.....	187
<u>FIGURE 7.17.</u> Effect of lithene and silica concentrations on the compression set of EPDM compounds.....	188
<u>FIGURE 7.18.</u> Weight change of silicone rubber (SR) and EMPD 2 aged in Nafion® (pH 3-4) solution @ 140°C.....	190
<u>FIGURE 7.19.</u> Tensile strength of silicone rubber (SR) and EPDM 2 aged in Nafion® (pH 3-4) solution at 140°C.....	191
<u>FIGURE 7.20.</u> Elongation at break of silicone rubber (SR) and EPDM 2 aged in Nafion® (pH 3-4) solution at 140°C.....	192
<u>FIGURE 7.21.</u> 100 % Modulus of silicone rubber (SR) and EPDM 2 aged in Nafion® (pH 3– 4) solution at 140°C.....	193
<u>FIGURE 7.22.</u> Compression set of EPDM 2 and silicone rubber at 140°C and 25% compression for 72 hrs.....	194
<u>FIGURE 7.23.</u> Intelligent Energy’s accelerated aging test rig	195
<u>FIGURE 7.24.</u> Cross over leak rate (flow rate) of hydrogen through the membrane for EPDM 2 and silicone rubber 001,002 and 003 gaskets.....	196
<u>FIGURE 7.25.</u> Eight points for gasket thickness measurements.....	197
<u>FIGURE 7.26.</u> Average thickness loss of silicone rubber, EPDM 2 and commercial EPDM gaskets after 121 - 158 hrs exposure to accelerated aging in the fuel cell test rig	197

List of Tables

Table 2.1.Characteristics of Fuel Cells	10
Table 2.2 Application areas of PEM fuel cells with a various power level	27
Table 3.1 Classification of different sealing designs	46
Table 4.1. Surface atomic concentration of each element and ratios of atomic concentrations of O and C to Si	95
Table 5.1. The rubber compounds used in the project	125
Table 5.2. Properties of the Silicone Rubber compound	126
Table 5.3. Formulation of initial EPDM compounds (A–F)	127
Table 5.4. Functions of the ingredients in EPDM compounds	127
Table 5.5 Formulation of final EPDM compounds	128
Table 5.6. Recipe for the EPDM Compound F	129
Table 5.7. Recipe for the EPDM 2 Compound	129
Table 5.8. Cure Properties of Gasket Materials	132
Table 6.1. Atomic Composition of Silicone Rubber Gasket from XPS Measurements	149
Table 7.1. EPDM Compounds with different combinations	174
Table 7.2. Hardness of EPDM compound F and silicone rubber	179

1. CHAPTER 1: Introduction

1.1. Background

Fossil fuels, which meet 80 % of the world energy demand today, are limited and sooner or later will be depleted. Because of the fact that, the rate of fossil fuel consumption is higher than the rate of the fossil production by the nature. They are also causing serious environmental problems, such as global warming, climate changes, melting of ice caps, rising sea levels, acid rains, pollution, ozone layer depletion, oil spills¹.

Fuel cells (FC) appear to be a solution to these problems and are promising candidates as alternative energy sources to the fossil fuels. Specifically, Polymer Electrolyte Membrane also known as Proton Exchange Membrane (PEM) Fuel Cells are considered a potential power source for automotive and stationary applications due to their high efficiency, low temperature of operation and environmentally friendly properties. Although significant progress has been made recently in the field of Polymer Electrolyte Membrane Fuel Cell (PEMFC) technology, there are still a number of problems need to be solved before their successful commercialisation. Such problems arise from their performance, durability and cost effectiveness as well as the distribution and storage difficulties related to the use of pure hydrogen as the most desirable fuel for PEM fuel cells^{1,2}.

Durability is described as the ability of a PEMFC or stack to resist permanent change in performance over time. There are many internal and external factors affect the performance of a PEMFC or stack, such as fuel cell design and assembly, materials degradation, operational conditions, and impurities or contaminants. Especially, automotive applications require PEM fuel cells to operate under a wide range of conditions which may have a negative effect on the long-time durability².

Seals / gaskets are one of the fuel cell components and are used to prevent the leaking of reactant gases and coolants.

The gaskets are usually made of elastomeric materials. The degradation of the gasket can impact on the performance of the cell. For this reason, the long term chemical and mechanical stability of the seals need to be examined.

1.2. Reasons for the Study

Although there is a large amount of published research on durability of PEM fuel cell components, relatively little work on gaskets have been reported in the literature. Therefore, there is a need to carry out more systematic studies of degradation of the elastomeric sealing materials in order to determine the best materials for durable fuel cell seals. Just in recent years, the studies related to the stability of the gasket materials have started to increase. However, they have mainly focused on the silicone rubber as the sealing material. Due to the fact that silicone rubber is still the most commonly used gasket material in PEM fuel cells; the issue of chemical degradation of silicone rubber in the PEM fuel cell environment remains as a problem. There are just a few published works which report the durability of commercially available EPDM and the other elastomeric gasket materials for PEM fuel cell stack sealing. Hence, the purpose of this thesis is to draw attention to EPDM as an alternative gasket material to silicone rubber.

Furthermore, much work carried out on the ageing of gasket materials at low temperatures and similar accelerated ageing conditions by trying to simulate the real fuel cell environments. In this study, elevated temperatures and different accelerated aging agents have been used to create more extreme and realistic conditions.

In the literature, mechanical properties of the elastomeric gasket materials before and after being exposed to accelerated ageing conditions have been assessed by using indentation test and dynamic mechanical analysis (DMA), however, there is very little published work where the tensile and compression set tests have been utilised as standard mechanical tests.

It is quite important to model the compression set behaviour of the gasket material in order to predict the suitability of the material for the sealing applications. Thus, in this project, the compression set test and tensile test have been applied on to the materials both to compare mechanical properties and also to evaluate the changes in the properties with ageing.

1.3. Objectives of the Study

The aim of the current research is to improve the durability of seals by obtaining a better understanding of the degradation phenomena of the seals in the fuel cells thus increase the functional life of cells. It is hoped that if the long term stability of the seal material can be achieved then this will lead to the elimination of one of the factors that hinder fuel cell technology from being fully commercialised.

Specific objectives of the project are listed below:

1. To investigate the effect of the fuel cell conditions on the properties of silicone rubber, as the existing gasket material, after operation in the fuel cell,
2. To determine the mechanisms by which silicone rubber degrades in the fuel cell environment and to quantify the key controlling factors affecting the extent of degradation,
3. To develop an accelerated ageing test in order to assess acid, time and temperature resistance of sealing material which can be exposed to similar conditions in the real fuel cell environment,
4. To carry out experiments to quantify the effects of temperature and acidity (pH) on degradation behaviour, using tensile strength as a measure of degradation,
5. To assess the suitability of new elastomeric materials, particularly commercial EPDM rubber, in comparison to silicone rubber,

6. To develop new EPDM compounds as an alternative sealing material to silicone rubber so as to determine the best material for durable fuel cells,
7. To investigate and compare the degradation behaviour of silicone rubber and selected (i.e., optimum) EPDM compound under accelerated aging conditions,
8. To carry out tensile and compression set tests on the silicone rubber, EPDM compound and commercial EPDM in order to study the effect of aging on the mechanical properties,
9. To supply moulded EPDM gaskets to the sponsor company (Intelligent Energy) for them to undertake accelerated aging tests in the fuel cell.

1.4. Outline of the Thesis

The main body of the thesis is made up of 8 chapters, which are divided as follows;

Chapter 1: Provides a very brief introduction to PEM fuel cells in relation to the current energy systems, durability issues in the PEMFC technologies, and the sealing used in the cell. It describes the significance and the objectives of the current research along with the organisation of the dissertation.

Chapter 2: Gives a general background on the description of a fuel cell as well as its basic operational functions. It then introduces the main types of the fuel cells and their main advantages and applications. Subsequently, it focuses on the PEM fuel cell which is the type under investigation in this research project. First, it describes the working principles of the PEM fuel cells followed by a presentation of the different components that make up a PEMFC. It then discusses the major characteristics and application areas along with the limitations of the PEM fuel cells.

Chapter 3: Provides information about the sealing / gasket of the PEM fuel cells which is the main subject of this study. It explains the functions of the gasket as well as the environment in which they are subjected to in the fuel cells and the main property and design requirements expected to be met from the durable gaskets.

After that, it outlines the elastomeric materials for PEMFC sealing applications with a special emphasis on the silicone rubber and ethylene propylene – diene monomer (EPDM) rubber.

Chapter 4: Summarises the studies, currently present in literature which investigate the chemical degradation of the sealing materials particularly in the simulated fuel cell conditions and the characterisation methods used in these studies in order to determine the effect of degradation on the material properties.

Chapter 5: Describes the experimental techniques and apparatus used as well as the test methods applied in this study especially focuses the accelerated aging test which is developed during the study. It further, gives details about the materials that are both commercially provided and also compounded for the project.

Chapter 6: Presents and discusses the results of the experimental work with regard to the changes in the silicone rubber gasket properties after operating in the actual fuel cell. It then highlights the main degradation modes in the real fuel cell and compares them to those of brought about by accelerated aging test.

Chapter 7: Reviews the development of an optimal EPDM compound to use as a fuel cell gasket by applying tensile test and compression set test. Compares the acid aging resistance of EPDM compound with that of silicone rubber in- situ and ex-situ (i.e., in fuel cell accelerated aging rig) conditions to determine the most suitable gasket material.

Chapter 8: Summarizes the thesis conclusions and provides recommendations for future work.

1.5. REFERENCES

- [1] F. Barbir 1954-, *PEM fuel cells theory and practice*. Amsterdam ; Boston: Elsevier Academic Press, 2005.
- [2] H. H. Wang, H. Li 1964-, and X.-Z. Yuan, *PEM fuel cell diagnostic tools*. Boca Raton, Fla.: CRC, 2012.

2. CHAPTER 2: Background to Fuel Cells

2.1. What is a Fuel Cell

A fuel cell electrochemically combines a fuel and oxidant to produce electricity. It transforms the chemical energy stored in a fuel into electrical energy. Fuel cells and batteries have similarities because both rely on the electrochemical nature of the power generation process except that a fuel cell does not need recharging (like batteries) as the fuel is constantly being supplied. The fuel cell operates quietly and efficiently, and when hydrogen is used as fuel, it produces only power and water. Therefore, a fuel cell has low emissions.

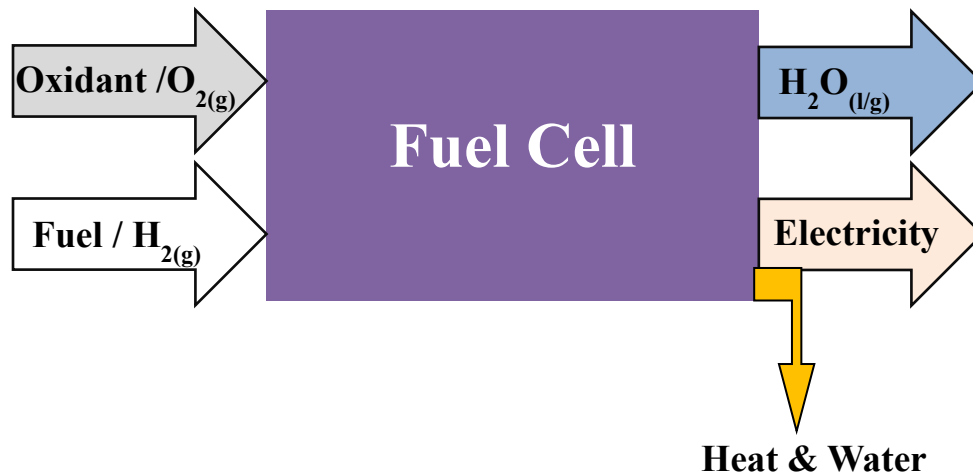


Figure 2.1. Basic working principle of a fuel cell

The first basic fuel cell was invented by Sir William Grove in 1839 and it was called a “gaseous voltaic battery”. In his experiment, Grove used platinum electrodes and sulfuric acid electrolyte, with hydrogen and oxygen as reactants. The basic principle of this first fuel cell was to obtain electricity and water by reversing the electrolysis procedure as shown in Figure 2.1.

Since 1932, when Francis Bacon demonstrated the first fuel cell stack capable of 5 kW power, a substantial amount of research has been done in this area to develop higher performance and more durable fuel cells^{1,2}.

All fuel cells consist of an anode (fuel electrode), a cathode (oxidant electrode) and an electrolyte sandwiched in between. The majority of fuel cell electrolytes are solid however some are liquid. In most fuel cells, there is a layer with catalyst particles between the electrode and electrolyte where the electrochemical reactions occur. At the anode of a hydrogen fuel cell, the fuel (hydrogen) reacts by an oxidizing reaction with the loss of electrons (e.g. $\text{H}_2 \rightarrow 2\text{H}^+ + 2\text{e}^-$). At the cathode, oxygen reacts by a reduction reaction, gaining electrons (e.g. $2\text{H}^+ + \frac{1}{2}\text{O}_2 + 2\text{e}^- \rightarrow \text{H}_2\text{O}$). The electrons released from the reaction drive an external circuit. The basic process is illustrated in Figure 2.2.³

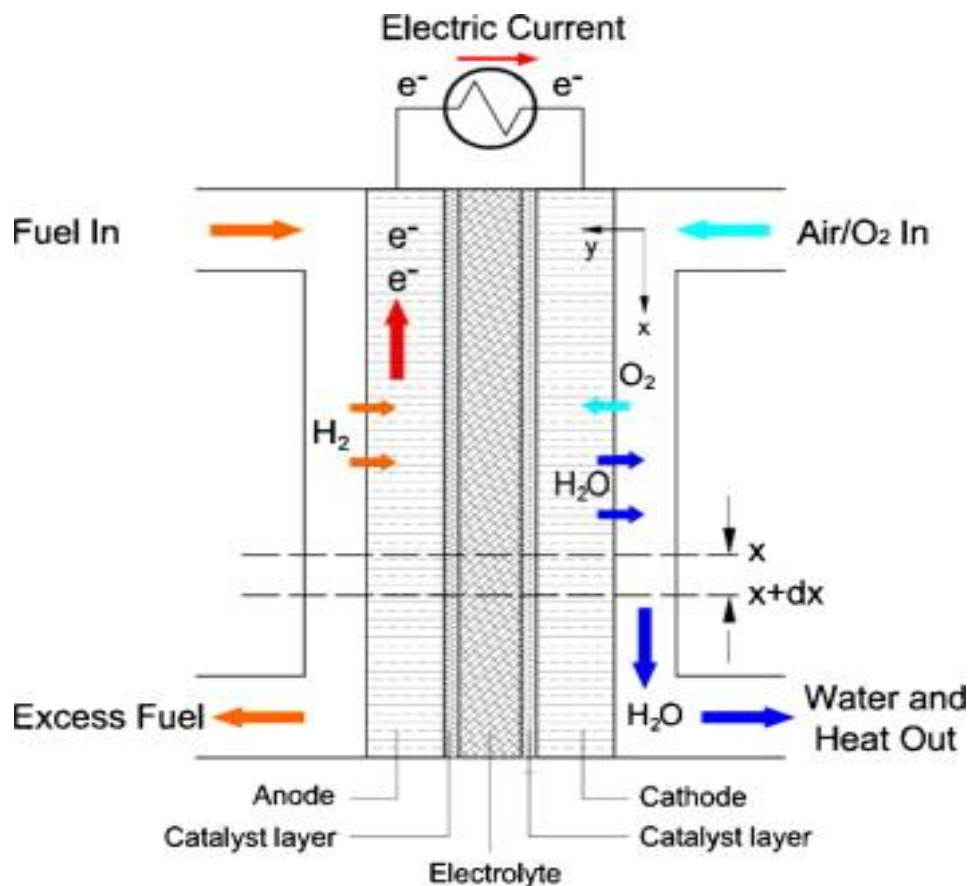


Figure 2.2. Schematic of a fuel cell⁴

2.2. Types of Fuel Cell

Fuel cells can be classified on the basis of various parameters which are related to the fuel cell operation or construction. These parameters include the type of electrolyte used, the type of ion transferred through the electrolyte, the type of reactants (e.g. primary fuel and oxidants), operating temperature and pressure, direct or indirect use of the primary fuels, and primary or regenerative systems. The choice of the electrolyte defines the main features of a fuel cell, including operation temperature, power-up time, type of fuel, migration ions, and shock resistance as well as the materials which can be used for the cell and stack components. Thus, fuel cells are primarily named by the nature of their electrolyte used. This classification leads to:

1. Direct Methanol Fuel Cells (DMFC),
2. Polymer Electrolyte (Proton Exchange) Membrane Fuel Cells (PEMFC)
3. Alkaline Fuel Cells (AFC)
4. Phosphoric Acid Fuel Cells (PAFC)
5. Molten Carbonate Fuel Cells (MCFC)
6. Solid Oxide Fuel Cells (SOFC)

Table 2.1 provides a summary of the operational characteristics of the six major types of fuel cell. Fuel cells can be classified into low temperature fuel cells such as direct methanol, polymer electrolyte membrane and alkaline fuel cells; medium temperature fuel cells such as the phosphoric acid fuel cell and high temperature fuel cells such as the molten carbonate and solid oxide fuel cells^{3,5,6}.

Table 2.1.Characteristics of Fuel Cells

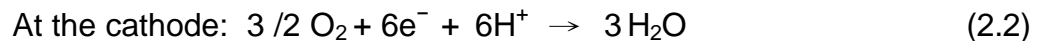
Fuel Cell	Mobile Ion	Operating Temp.	Electrolyte Material	Overall Reaction Process	Electric Efficiency (System)	Power Level (kW)
DMFC	H ⁺	50- 90°C	Sulphonated PTFE	$\text{CH}_3\text{OH} + 3/2\text{O}_2 \rightarrow 2\text{H}_2\text{O} + \text{CO}_2$	40 %	0.001-100
PEMFC	H ⁺	80 °C	Sulphonated PTFE	$\text{H}_2 + 1/2\text{O}_2 \rightarrow \text{H}_2\text{O}$	40– 50%	0.01-1000
AFC	OH ⁻	60-220°C	Potassium Hydroxide	$\text{H}_2 + 1/2\text{O}_2 \rightarrow \text{H}_2\text{O}$	50%	10-100
PAFC	H ⁺	200 °C	Concentrated Phosphoric Acid	$\text{H}_2 + 1/2 \text{O}_2 \rightarrow \text{H}_2\text{O}$	40%	100-5000
MCFC	CO ₃ ⁻²	650 °C	Molten Carbonate	$\text{H}_2 + 1/2 \text{O}_2 + \text{CO}_2 \rightarrow \text{H}_2\text{O} + \text{CO}_2$	45-55%	1000-100,000
SOFC	O ⁻	600-100°C	Yttrium-stabilised Zirkondioxide	$\text{H}_2 + 1/2 \text{O}_2 \rightarrow \text{H}_2\text{O}$	50-60%	100-100,000

2.2.1. Direct Methanol Fuel Cell (DMFC)

The direct methanol fuel cell operates on a liquid fuel, methanol, and it requires water as an additional reactant at the anode at which methanol reacts with to produce carbon dioxide (CO₂) as a waste product and hydrogen ions (H⁺).



The hydrogen ions (H⁺) pass through a polymer membrane to combine with oxygen at the cathode to produce water.



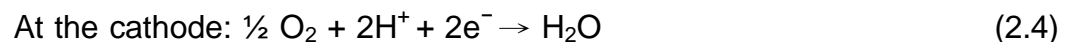
Both electrodes include platinum (Pt) catalysts. In DMFC, methanol (as fuel) can be supplied to a fuel cell for direct electro-oxidation of methanol. Alternatively, methanol can initially be reformed to give hydrogen in a high temperature step^{3,6,7}.

2.2.2. Polymer Electrolyte Membrane Fuel Cell (PEMFC)

Polymer electrolyte membrane fuel cells (PEMFCs) are also known as proton exchange membrane fuel cells. They utilise hydrogen gas at the anode where the electro-oxidation of hydrogen occurs with the production of protons and electrons.



At the cathode hydrogen ions (H⁺) combine with the oxygen to form water.



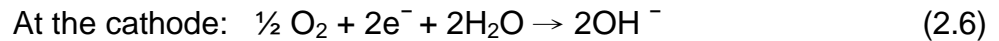
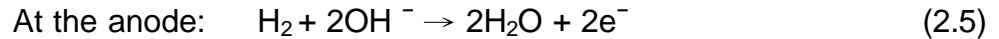
They use a proton conducting polymer membrane as an electrolyte and carbon electrodes with platinum (Pt) catalyst. The only liquid in this fuel cell is water; therefore, corrosion problems are minimal. The operating temperature is low, typically around 60 to 80°C compared to other types of fuel cell^{8,9,10}.

2.2.3. Alkaline Fuel Cell (AFC)

The alkaline fuel cell uses a liquid potassium hydroxide (KOH) electrolyte. Unlike acidic fuel cells where H⁺ is transferred from the anode to the cathode, in an alkaline fuel cell OH⁻ is conducted from the cathode to the anode. Therefore, hydrogen oxidation occurs at the anode where hydrogen gas and hydroxyl ions (OH⁻) from the potassium hydroxide electrolyte combine to produce water and electrons.

Electrons travel through the external circuit, generating useful electric energy output while a part of water generated is transferred to the cathode where molecular oxygen is reduced to form hydroxyl ions (OH^-).

The anode and cathode reactions are:



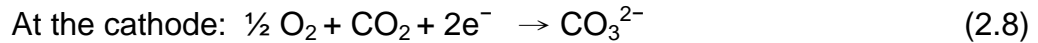
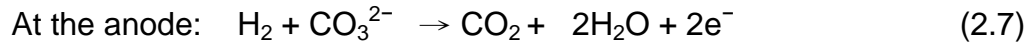
Thus, water is consumed at the cathode of an alkaline fuel cell whereas it is produced (twice as fast) at the anode. The AFC can operate at temperatures between 60 and 250°C dependent on the KOH concentration in the electrolyte^{3,9}.

2.2.4. Phosphoric Acid Fuel Cell (PAFC)

Phosphoric acid fuel cells employ liquid phosphoric acid (H_3PO_4) as an electrolyte (either pure or highly concentrated) to facilitate the passage of hydrogen ions toward the cathode. The hydrogen ions are produced from hydrogen gas at the anode in the same way as DMFCs and PEMFCs. Phosphoric acid (electrolyte) is retained in a thin silicon carbide (SiC) matrix between two porous graphite electrodes coated with platinum (Pt) catalyst. The PAFC typically operates at 150 to 220°C. The use of concentrated acid (100 percent) minimises the water vapour pressure so water management in the cell is not difficult^{5,7,9}.

2.2.5. Molten Carbonate Fuel Cell (MCFC)

The molten carbonate fuel cell (MCFC) operates at high temperature (around 600 °C ~ 700°C). The electrolyte in the molten carbonate fuel cell is a molten mixture of alkali metal carbonates, lithium carbonate (Li_2CO_3) and potassium carbonate (K_2CO_3) restrained in a porous ceramic matrix of LiAlO_2 . At the high operating temperatures, the alkali carbonates form a highly conductive molten salt, with carbonate CO_3^{2-} ions providing ionic conduction. Carbonate ions (CO_3^{2-}) in the electrolyte react with hydrogen gas at the anode to produce water and carbon dioxide and release electrons to the external circuit. At the cathode, oxygen is reduced to carbonate ions by combining with carbon dioxide and electrons from the external circuit. The anode and cathode reactions are therefore:



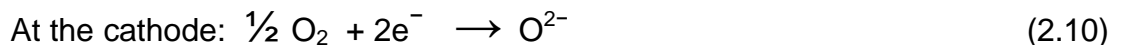
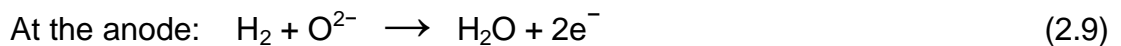
Thanks to their high operating temperatures (i.e. 600°C and above) MCFCs can be equipped with facilities for internal reforming process which converts hydrocarbon fuels into hydrogen directly within the fuel cell. Therefore they are not limited to use pure hydrogen as fuel but can use gaseous hydrocarbons such as methane, methanol and petroleum or gasified coal.

The electrodes in a MCFC are nickel based; the anode consists of a nickel/chromium alloy whereas the cathode comprises of a lithiated nickel oxide powder which is prepared by oxidation of a porous Ni plate in the cathode environment. The nickel provides catalytic activity and conductivity. The main disadvantage of MCFC arises from using a very corrosive and molten (mobile) electrolyte^{5,7,9}.

2.2.6. Solid Oxide Fuel Cell (SOFC)

The solid oxide fuel cell (SOFC) has the highest operating temperature (about 1000°C) between all the important fuel cells under development. They use a solid ceramic electrolyte, Yttria- stabilized zirconia (YSZ) which is an oxygen ion conductor.

At the anode, hydrogen gas reacts with oxide ions (O^{2-}) which is the mobile conductor in this case, to form water and release electrons. These electrons travel through the external circuit to reach the cathode and they combine with oxygen gas at the cathode to produce oxide ions (O^{2-}). The anode and cathode reactions are:



The high operating temperature offers some advantages such as fuel flexibility and high efficiency (around 50 – 60 % electric efficiency). But also creates some challenges including stack hardware, sealing and mechanical issues. Like MCFCs, internal reforming can be accomplished due to the high operating temperatures^{3,7}.

2.3. Advantages and Applications of Fuel Cells

There are many advantages of fuel cells depending on the different types. Most importantly, fuel cells are more efficient than combustion engines. They convert fuel into electricity at more than double the efficiency of internal combustion engines. In transportation, hydrogen fuel-cell engines operate at an efficiency of up to 65%, compared to 25% for present - day petrol - driven car engines ¹⁰.

One of the main advantages of fuel cells is to reduce carbon dioxide (CO₂) emission when using renewable hydrogen, e.g. hydrogen produced from the electrolysis of water using energy from renewable sources. CO₂ is the largest source of greenhouse gasses accounting for 77 % of total emissions (from fossil fuels use) and road transport contributes to 10.5 % of global CO₂ emissions ¹¹.

The by-product of the main fuel cell reaction, when hydrogen is used as a fuel, is pure water. This contrasts with the generation of electricity from high temperature combustion of fossil fuels which produce harmful chemical pollutants such as nitride oxides (NO_x), sulphide oxides (SO_x) and carbon monoxide (CO).

However, even if fuel cells use hydrocarbon fuels, they still can contribute to a substantial reduction in both greenhouse gases and local pollution thanks to their clean and quiet energy conversion ^{3,5,12}.

Another important characteristic of fuel cells is their fuel flexibility. Fuel cell systems mainly use hydrogen gas as fuel, which can be produced from renewable sources (i.e. sunlight, wind, and biomass) or conventional fossil fuel fuels. Additionally, they operate on methanol or natural gas directly or indirectly, which can also be derived from renewable sources. This diverse variety of fuel options makes fuel cells suitable candidates for sustainable energy systems in the future ³.

Fuel cells operate quietly with minimal vibration or noise, unlike traditional combustion engines such as diesel generators, because a fuel cell stack has no mechanical moving parts. This simplicity in the essentials of the fuel cells makes them reliable and long lasting systems as well as reducing the maintenance cost^{3,5}.

Other advantages of fuel cells include the modular design and fabrication process which allows a wide variation in the power plant size. This is because many cells are connected together to form a stack and one or a number of stacks to form a fuel cell system. The fuel cells can be monitored remotely, reducing maintenance time and cost, especially in isolated installations such as telecommunications backup-power sites^{3,7,10}.

The main disadvantage of fuel cells today is the same for all types: The cost. Fuel availability and storage are considered the next most important problems. Hydrogen is the best fuel for fuel cells however it is not commonly available, has a low volumetric energy density and is difficult to store. In addition, alternative fuels (e.g. methane, methanol, formic acid) are difficult to use directly and so usually require reforming. The other limitations of fuel cells include susceptibility to environmental poisons especially low temperature fuel cells (i.e. PEMFC & DMFC) are quite sensitive to reactant contaminations including CO, sulfur species, and ammonia.

Low temperature operation requires a noble-metal catalyst (typically platinum) to be used to separate the hydrogen's electrons and protons. However, the platinum catalyst is extremely sensitive to CO poisoning. This makes it necessary to use an additional reactor to reduce CO in the fuel gas if the hydrogen is obtained from an alcohol or hydrocarbon fuel. This also adds cost.

Durability under start-stop cycling and reliable operating conditions such as in the ambient temperatures of 40°C to +40°C and very high or low relative humidity are also some of the limiting factors of fuel cells^{13,14}.

Fuel cells can be used in a variety of potential applications from residential (SOFCs, PAFCs and MCFCs), terrestrial and marine vehicles (PEMFCs) to space applications¹⁵.

They can provide power for diverse applications, such as: consumer electronics (up to 100 W), homes (1–5 kW), backup power generators (1–5 kW), forklifts (5–20 kW), vehicles such as cars, buses and minivans (50–125 kW), and centralized power generation (1–200 MW or more)¹².

Fuel cells can produce combined heat and power in an efficient way. Combined heat and power (CHP) means the simultaneous generation of electricity and heat from the same energy source. A CHP power plant produces both electric power and heat. This heat can be recovered for a useful purpose such as warming a building space or water or for a useful industrial process. Many stationary CHP fuel cell systems are designed to convert the chemical energy of the fuel into both electrical power and useful heat in one system^{2,5,16}.

Eventually it is expected that fuel cells will be used extensively in three main applications: transportation, stationary power generation and portable applications.

PEM fuel cells have the highest power densities of all the fuel cell types (300-1000 mW/cm²). Power density states how much power a fuel cell can produce per unit volume or per unit mass. They operate at relatively low temperatures, which bring the further benefit that a PEMFC can start quickly⁷.

This makes them particularly suitable for use in automotive applications and is the type of fuel cell in which is the subject of this thesis.

2.4. The PEM Fuel Cell

The proton exchange membrane fuel cell (PEMFC) was the first type of fuel cell developed as the power source for NASA's Gemini space flights in the 1960s. In these flights, 1 kW PEMFCs supplied additional power requirements in the space vehicles and drinking water for the astronauts. However, PEMFC technology was abandoned in the 1970s due to high cost and poor durability issues. From the 1980s, a return in the research and development of PEMFCs happened in industry and especially portable and transport applications initiated by the Canadian company Ballard Power Systems.

Since then more and more universities and institutes all over the world are becoming involved in PEM fuel cells^{5,6,17}.

PEM fuel cells use a solid proton conductive membrane as electrolyte. A schematic diagram of a PEM fuel cell is shown in Figure 2.3.

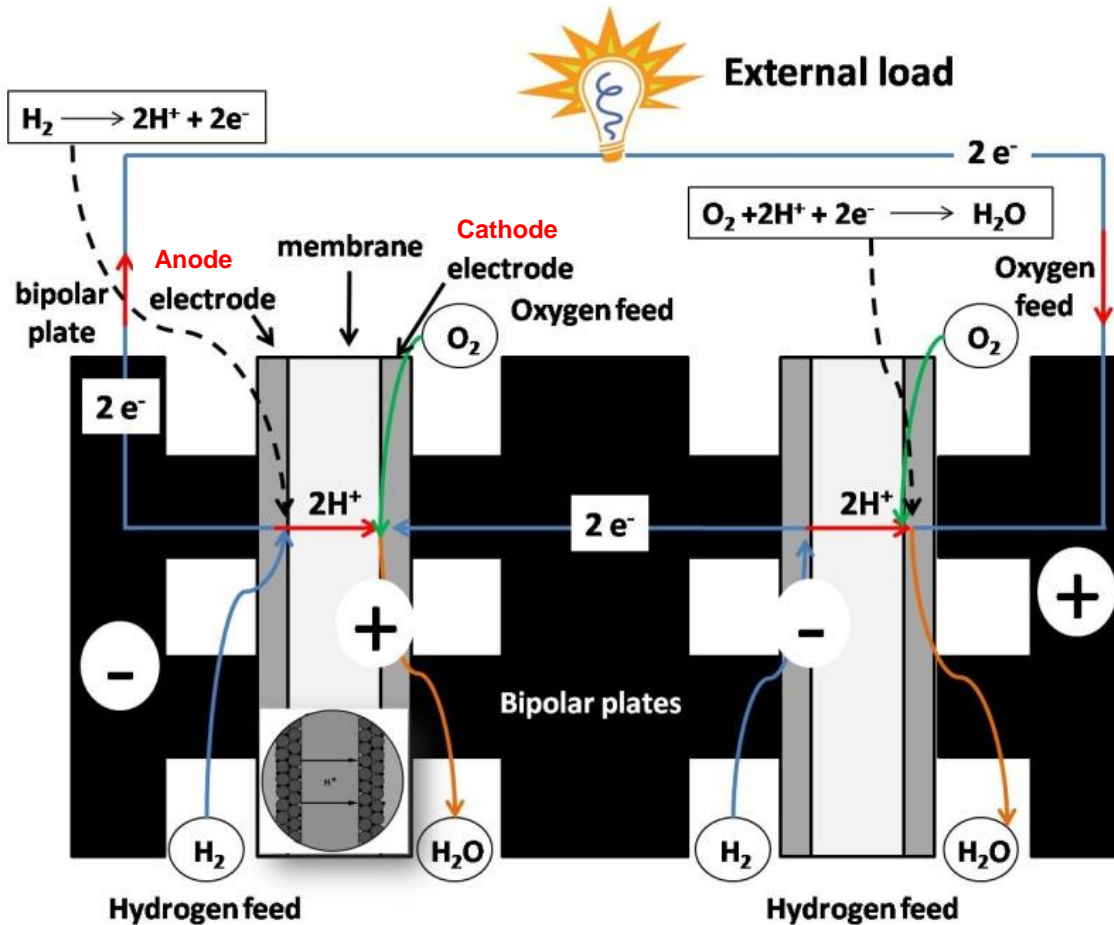
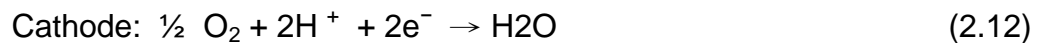


Figure 2.3 Schematic diagram of a PEM fuel cell¹⁸

The electrolyte (polymer membrane) is placed between two porous, electrically conductive electrodes (anode and cathode). The membrane is impermeable to reactant gases but it conducts protons. At the interface between the electrode and the membrane there is a catalyst layer¹⁴. Electrochemical reactions happen at the surface of the catalyst on both sides of the membrane, the anode and the cathode. Hydrogen gas enters the anode, the negative side of the fuel cell, where the atoms react with the platinum catalyst and they split into individual protons and electrons. The protons travel across the membrane to the cathode, the positive side of the fuel cell whereas electrons travel through electrically conductive electrodes, through the external circuit where they produce the electricity and come back to the other side of the membrane (cathode side).

At the catalyst sites between the membrane and the cathode, the electrons combine with the protons that went through the membrane and oxygen which is fed on the cathode side. Consequently, the products of PEMFC reactions are water, electricity and heat^{17,19}.

Below are the reactions at each electrode.



A single PEM fuel cell includes only one anode and one cathode and it can generate approximately 0.6-0.7 V. In order to produce useful voltages many cells are connected together in series to form a “stack”. A typical PEM fuel cell stack is shown in Figure 2.4. Each cell in the stack is formed of a solid polymer electrolyte and porous electrodes. Individual cells are electrically connected (the anode of one cell to the cathode of the next) with bipolar plates. Bipolar plates deliver reactant gases, remove exhaust gases and liquid water and carry a cooling fluid if required. The individual cells can be around only 2 mm thick with a complicated symmetrical form^{17,19}. PEM fuel cell components and their properties are explained below.

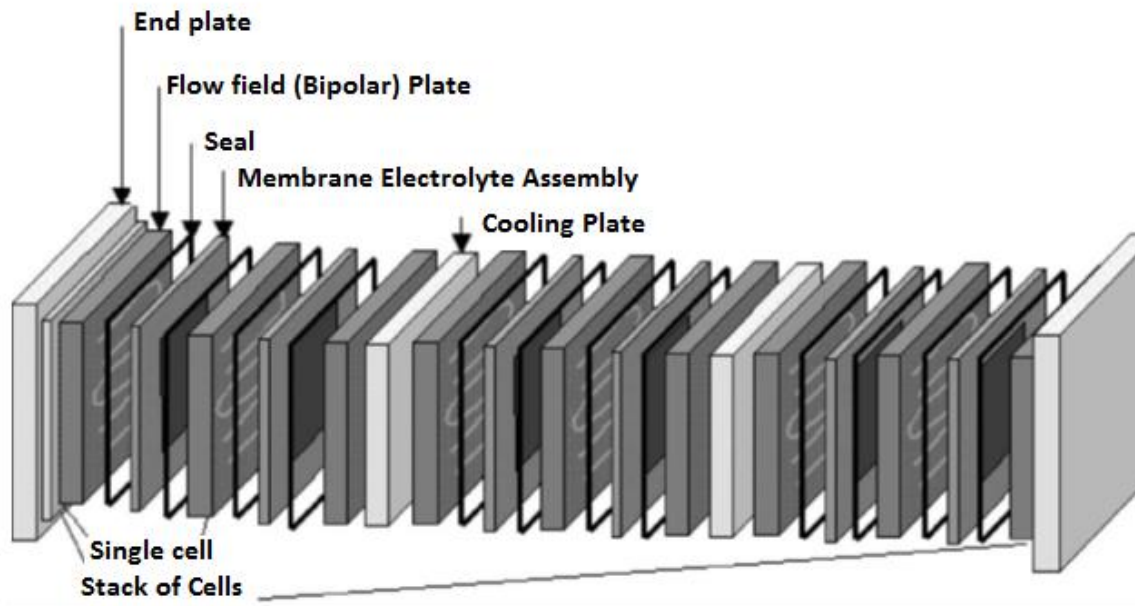


Figure 2.3. PEM Fuel Cell Stack²⁰

2.4.1. Electrolyte Membrane

The main function of electrolyte is to transfer protons from the anode to the cathode. Nafion® (Dupont) is the most widely used electrolyte which is a polymer based on sulfonated polytetrafluoroethylene (PTFE). It has a backbone structure similar to polytetrafluoroethylene (Teflon). But, unlike Teflon, Nafion® contains sulphonic acid ($\text{SO}_3^- \text{H}^+$) functional groups which are shown in Figure 2.5. The Teflon backbone provides mechanical strength whereas the sulphonic acid ($\text{SO}_3^- \text{H}^+$) groups provide charge sites for proton transport. Because Nafion® is based on Teflon like polymer; it is very stable and durable. It is also called a perfluorinated ionomer because the SO_3H group is ionically bonded; therefore the end of the chain is actually an SO_3^- ion with H^+ ion. For this reason the resulting structure is called an "ionomer". Due to their ionic nature, the ends of the side chains tend to cluster within the overall structure of the membrane. Nafion® membranes are extruded in different sizes and thicknesses. They are marked with a letter N followed by a 3 or 4 digit number.

The first two digits represent equivalent weight divided by 100, and the last digit or two is the membrane thickness in mills (1 mill = 1/1000 inch = 0.0254 mm).

Nafion® is available in several thicknesses, namely 2, 3.5, 5, 7, and 10 mills (50, 89, 127, 178, 254 μm respectively). For instance, Nafion® N117 has equivalent weight of 1100 and it is 7 mills (0.178 mm) thick^{5,7,17,19}.

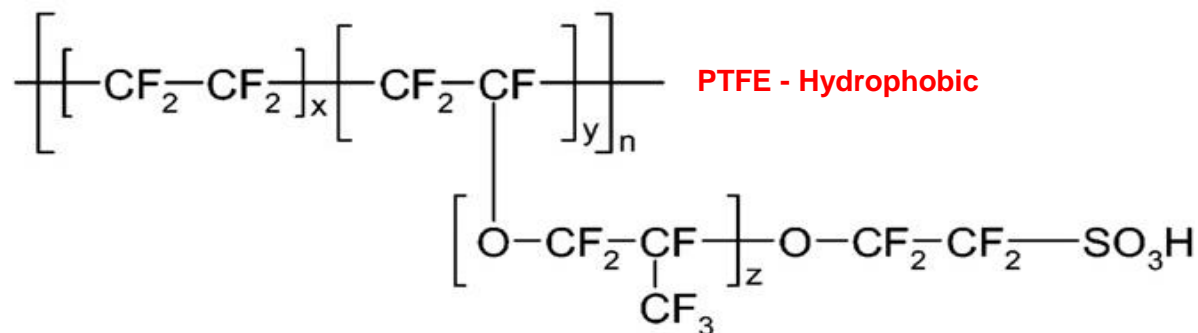


Figure 2.4. Chemical Formula of Nafion®²¹

The main property of Nafion® is its proton conductivity. PTFE is hydrophobic (it repels water) but ionically bonded SO_3^- ions formed at the end of the side chains are hydrophilic (attracts water) and tend to cluster together. This means that in Nafion®, the hydrophilic regions are created within a hydrophobic matrix as shown in Figure 2.6^{1,5,17}.

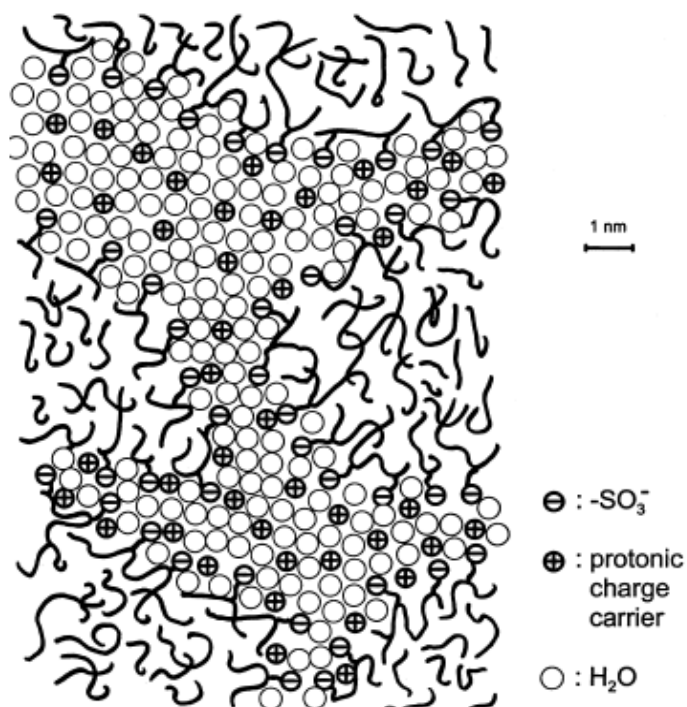


Figure 2.5. Structure of Nafion®²²

Water collects around the clusters of ionised sulfonate (SO_3^-) groups. When the membrane is well hydrated, H^+ ions, which are weakly attracted to SO_3^- groups can move freely between the hydrophilic clusters. Therefore, they are good proton conductors. Usually, the higher the water content, the higher the proton conductivity because the hydrophilic domains become larger and the connections between these domains get better. For this reason, the proton conductivity of the electrolyte is highly dependent on the water content. Normally, in a sufficiently hydrated electrolyte (i.e., boiled in water to equilibrium) there will be around 22 water molecules for each sulfonate (SO_3^-) group^{1,5,19}.

The preparation of pre-treated membrane is described in many papers. For example Yang et al. first immersed Nafion® 115 (Dupont) membrane in 3% hydrogen peroxide (H_2O_2) in water for 1 hour to get rid of any organic impurities and then rinsed it in boiling water. Secondly it was boiled in 1 M H_2SO_4 for 1 h to remove any metallic impurities from the membrane and then it was rinsed in boiling water again. Finally, the membrane was dried at 80°C for 1 h²³.

2.4.2. The Electrode/Catalyst Layer

Fuel cell electrodes must efficiently deliver and collect electrons from the fuel cell and also deliver and collect reactant and product materials from the fuel cell. Therefore, they are required to have high electrical conductivity and high porosity as well as high catalytic activity in the area of the electrode/electrolyte interface⁷.

The electrode is a thin catalyst layer pressed between the electrolyte (ionomer membrane) and a porous, electrically conductive substrate. The electrochemical reactions take place on this layer (catalyst surface). The most common catalyst in PEM fuel cells for hydrogen oxidation reaction at the anode and oxygen reduction reaction at the cathode is platinum (Pt). Usually, small platinum particles are deposited very finely onto larger particles of powdered carbon (Carbon supported catalyst), as shown in Figure. 2.7.

Catalyst Particles

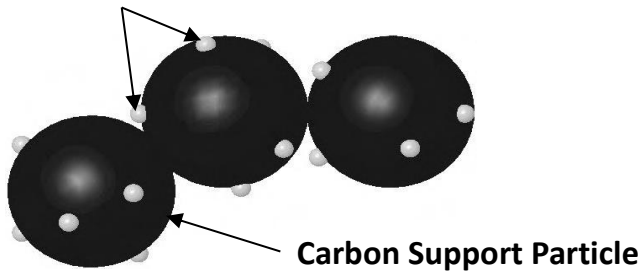


Figure 2.6. The structure of Carbon supported Catalyst²⁴

This way, there will be a maximal surface area of Pt in contact with the reactant. The carbon supported catalyst is then fixed to a porous and conductive material such as carbon cloth or paper.

The purpose of the carbon cloth or paper is to provide the mechanical strength for the electrode as well as to allow diffusion of the gas onto the catalyst. For this reason it is called the “gas diffusion layer”. The electrode is then attached to each side of polymer electrolyte membrane ^{1,17,19}. Figure 2.8 shows the resulting structure of an electrode.

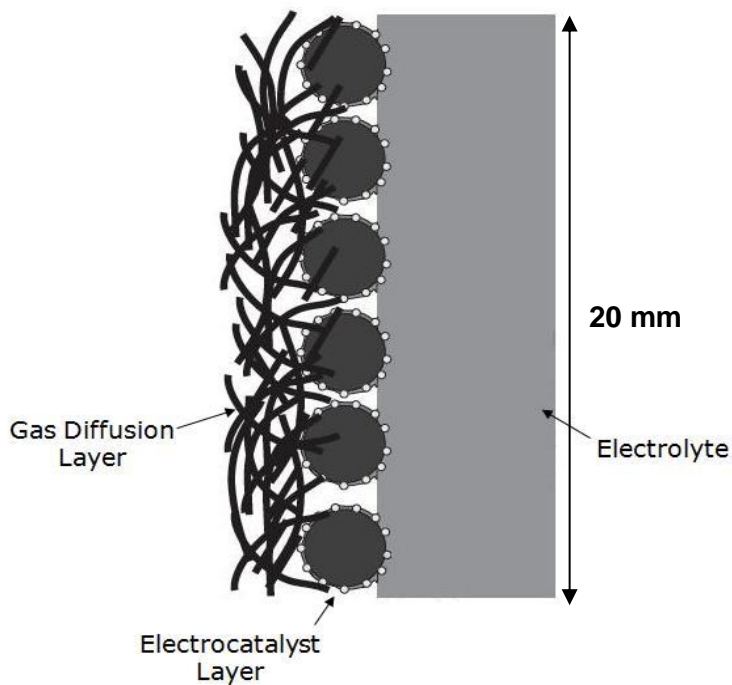


Figure 2.7. Simplified structure of a PEM fuel cell electrode²⁴

2.4.3. The Membrane Electrode Assembly

The electrochemical reactions in the PEM fuel cell can only take place where the electrolyte, electrode and gas phases are all in contact. This reaction zone can be described as a “triple-phase zone” which indicates the regions or points where the gas pores; electrode and electrolyte phases all come together. One of the ways to enlarge these three-phase zones is to attach the catalyst to the ionomer membrane. This combination of membrane and catalyst layers is called the membrane electrolyte assembly or MEA^{7,19}.

There are two methods to fabricate the MEA. The first method is to add a catalyst layer on the porous and conductive substrate (carbon cloth/ paper), so called “gas diffusion layer” (GDL). Then the catalyst-surfaced GDL (electrode) is hot pressed to the pre-treated membrane which has catalyst on each side¹⁷. The whole MEA assembly is completed by putting the electrodes on to the membrane and hot pressing at 140°C and at high pressure (70-90 atm) for three minutes^{5,17}.

The second method of fabricating MEA is to build the electrode directly onto the membrane. In this method, the catalyst which is mixed with hydrophobic PTFE, is fixed directly to the membrane (electrolyte). These forms a 3 layer MEA or catalysed MEA. The GDL is then added later once the catalyst is fixed to the membrane⁵. The MEAs assembled by both of above methods will have similar structure as shown in Figure 2.9.

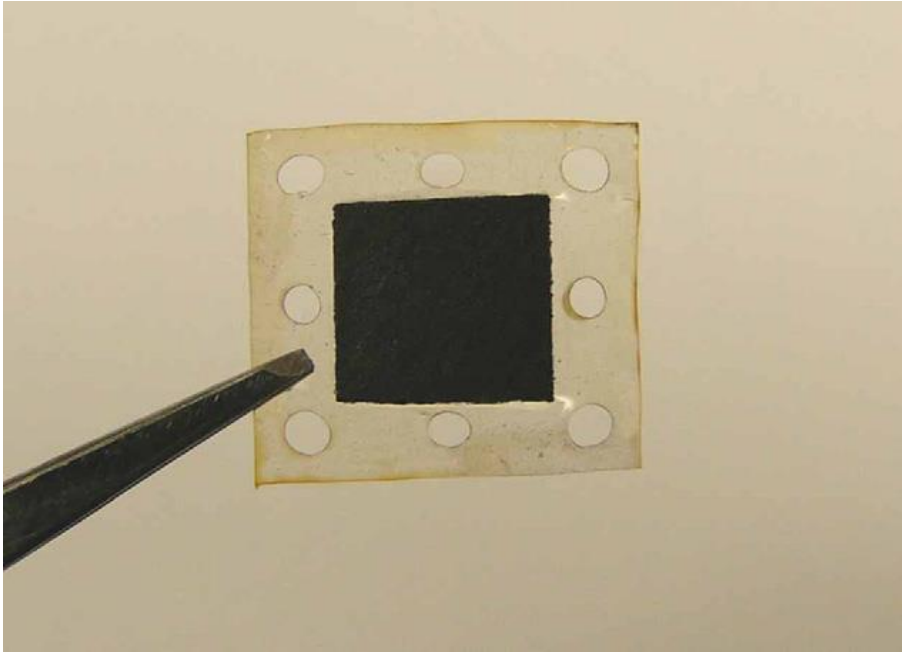


Figure 2.8. A diagram of membrane electrode assembly (MEA)²⁵

The thickness of an MEA relies on the thickness of membrane, catalysts, and GDL. The membrane is usually 0.05 to 0.1 mm thick, the electrodes are about 0.03 mm thick, and GDL is between 0.2 and 0.5 mm thick⁵.

2.4.4. The Gas Diffusion Layer

The key function of the GDL is to allow diffusion of each reactant gas to the catalyst on the MEA through its porous structure. The GDL also enables electrical connection between the carbon-supported catalyst and the bipolar plate or other current collectors. It also carries the product water away from the electrolyte surface.

The most common GDL materials are carbon fibre cloths and carbon fibre papers with a thickness of around 0.2 to 0.5 mm. Carbon fibre materials are selected due to their good electrical conductivity and high porosity as well as their excellent stability and corrosion resistance. In addition, they have a good mechanical strength in order to support the MEA. A hydrophobic material such as PTFE is combined into the carbon fibres to avoid flooding with water which could reduce gas flow to the catalyst sites^{7,17,19}.

2.4.5. The Bipolar Plate

The bipolar plate is also called the flow-field plate since it contains a gas flow field on one side and is flat on the other side. (See Figure 2.4) The main function of the bipolar plate is to distribute the fuel gas over the surface of the anode, and the oxygen/air over the surface of the cathode. They also collect and conduct the current (generated electrochemical reactions) from the anode side of one cell to the cathode of the next. In addition, they connect cells electrically in series so they must be electrically conductive.

The other functions of the bipolar plates are: to separate the gases (H_2 and O_2) in adjacent cells, to remove the product water from cathode and the heat from active cells. Therefore, the plates must have a good thermal conductivity.

Furthermore, the bipolar plates hold the fuel cell stack together thus they must be sufficiently strong. Transport applications in particular require bipolar plates to have low weight and low volume. As bipolar plates are exposed to a very corrosive environment in a fuel cell (pH 2-3 and temperature 60-80 C°), they must have high chemical stability and corrosion resistance. Since the bipolar plate is considered the most costly component of the fuel cell stack, the potential bipolar plate material must be inexpensive and easily manufactured for mass production^{5,17,19}.

The most common materials used for bipolar plates are graphite and metals. Graphite has good electronic conductivity and low density. Above all, it has an excellent corrosion resistance compared to metals. However, graphite is quite brittle which makes it difficult to handle and assemble. Metals have higher mechanical strength and thermal conductivity, but their corrosion resistance is very limited when compared to graphite. The metal bipolar plates can dissolve in the acidic environment of the PEM fuel cell. The leached metal ions can then poison the catalyst, leading to a decrease in the power density of each cell.

Now more alternative materials are being developed for bipolar plates such as graphite polymer composites and metallic materials with coatings^{3,17}.

2.4.6. Sealing

Sealing gaskets in PEM fuel cells are placed between bipolar plates and the MEA (See Figure 2. 4).The main function of gaskets is to prevent the leaking of reactant gases and coolants inside the cell. In addition, they also work as electrical insulators between the parts they separate and provide stack height control. Gaskets are generally made of polymeric materials. A single PEM fuel cell stack may contain 100 or more individual cells in series and elastomeric gaskets are required to keep the reactant gases within their respective regions ^{26,27} .

In the succeeding chapters, the functions, requirements, material selection and degradation mechanisms of seals will be extensively discussed as the durability of seals is the main focus of the Thesis.

2.5. Characteristics and Applications of PEM Fuel Cells

PEMFCs have many beneficial characteristics such as utilising hydrogen as the fuel, low operating temperature (vital for a rapid start up time), low or zero carbon emissions, high operation efficiency and high power density. These advantages make them the most promising technology for the automotive market through the development of environmentally- friendly vehicles^{1,6,17} .

One of the unique features of the PEMFCs, compared with other types of fuel cells (except for the solid oxide fuel cell) is to have a solid proton-conducting electrolyte (membrane). It enables less complex sealing and assembly. The absence of a corrosive liquid electrolyte in the cell also allows minimal corrosion of cell components and thus longer cell life time. PEMFCs have quick start-up due to a low operating temperature (under 90°C). They also operate silently therefore they reduce noise pollution as well as air pollution^{3,6,7} .

PEM fuel cells can generate power from a few Watts to hundreds of kilowatts so they can be used in almost every application where local electricity generation is required. The applications areas of PEMFCs with various power levels are shown in Table 2.2.

Table 2.2 Application areas of PEM fuel cells with a various power level¹⁷

Level of power	Applications
> 1 MV	Local distributed power station
100 kW – 1 MW	Large transportation vehicles, such as naval ships, submarines, and buses; small portable power station; small stationary power station
10 kW – 100 kW	Transportation vehicles such as cars and mid- size buses; back-up power for mid-size communication station; small power station
1 kW – 10 kW	Transportation vehicles such as motorcycles, utility vehicles, cars, yachts; residential power system, various power devices used for field working
100 W –1 kW	Simple riding devices such as bicycles, scooters and wheelchairs; UPS for small services, terminals and computers, backpack power
10 W – 100 W	Portable power such as for emergency working power supply and military equipment; batter replacements; lighting; signal light power
< 10 W	Small portable power device; cell phone

The main application fields for PEMFCs can be categorized into three groups: transportation, stationary power and portable power applications.

Transport applications include, automobiles, buses, utility vehicles, scooters and bicycles. Among the many applications of PEMFCs, transportation is the most competitive. The fuel cell engine is considered the best replacement for an IC (Internal Combustion Engine) due to its potential higher efficiency (and thus lower fuel consumption) and being theoretically zero-emission in an automobile. In March 1998, the first passenger bus powered by PEM fuel cell was demonstrated in Chicago, USA.

It was built by a consortium including Ballard- Daimler Benz Groups, Chicago Transit Authority and had 10 fuel cell stacks for an overall power of 200 kW. The fuel was gaseous hydrogen compressed at 300 bar and stored in seven tanks and was sufficient for 400 km range. Ballard has also been developing PEM fuel cells for automotive applications since late 1980s.

The first PEM fuel cell powered electric cars (NECAR series) have already been demonstrated by cooperation between Ballard, Daimler Chrysler and also Ford which has recently become involved in the project. NECAR 4 vehicle was first developed in 1994 by this cooperation. It can carry 5 passengers and consists of two stacks of 160 fuel cells each. It is fuelled with liquid hydrogen (stored in a 100 l tank) which provides a 450 km range. Other car producers in USA, Japan and Europe also joined in the field and have been making substantial investments annually on the development of PEM fuel cell stacks for hybrid and electric cars^{6,17,19}.

Stationary power applications comprise not only large –scale utility plants but also smaller scale systems, such as individual homes, buildings where distribution of electricity and heat generation is provided. The basis for development of the PEM fuel cells in this market are the same as the ones for automobile sector: higher efficiency and lower emissions. Since mid-1980s, there has been a number of PEM fuel cell stationary applications such as the GPU and Ballard 250 kW plant at Crane Naval Air station in India (1991), a 5 kW PEM unit powering a home in USA^{6,17,19}.

PEM fuel cells have a high potential for portable power applications such as cell phones and laptop computers. In the near future, they might be able to replace the batteries which power these portable electronic devices.

The key advantage of fuel cells over batteries is the shorter charging time (a few minutes' vs several hours). Furthermore, fuel cells can achieve higher power and energy capacity than batteries. Normally, battery performance declines when the charge level decreases, where fuel cells operate at a constant level so long as fuel is supplied. The companies of Ballard Power Systems and H-Power have been working on commercialising of PEM fuel cells for portable applications with the expected power levels of 35 to 250 W where the fuel is hydrogen.

The applications can include video cameras, electric wheelchairs, portable power briefcases, laptop computers, intelligent transportation systems (i.e., road signs and traffic lights) and military communications^{6,17,19}.

2.6. Limitations of PEM Fuel Cell Technology

There are several challenges to be overcome in PEM fuel cells before their extensive commercial use. The main disadvantages of PEM fuel cells are their high cost and the high cost of hydrogen production plus the difficulties related to hydrogen storage. For the full commercialisation of PEMFC system, hydrogen must be easily available and the problems of the lack of hydrogen fuel infrastructure and safety concerns about the hydrogen storage need to be resolved. A stable supply of high-purity hydrogen is also essential. Traditionally, hydrogen is produced by steam reforming of hydrocarbons such as natural gas or by coal gasification. Nevertheless, both methods produce CO₂ as a by-product, which can result in greenhouse effect. Moreover CO formation can lead to poisoning of the anode electrocatalysts in PEMFC. Hydrogen can also be produced by the electrolysis of water, which uses electricity to split hydrogen and oxygen elements. However, this method is more expensive than by reforming natural gas^{19,28,29}.

For large scale storage, hydrogen can be stored underground in caverns, ex-mines or aquifers and it can be transported through pipelines or via gas tankers. It is then used in transportation, industrial, residential and commercial sectors as a fuel¹⁹. Yet, hydrogen delivery and storage is still one of the obstructions to the mass production of the PEM fuel cells for transport applications. The possible infrastructure options and technologies relating to this issue have recently been investigated intensely by researchers. For transport applications, hydrogen can be stored directly as hydrogen or can be produced on board the vehicle by reforming hydrocarbon fuel or methanol.

There are several possibilities to store hydrogen on-board the vehicle such as compressed gas, liquefied hydrogen (in a cryogenic storage vessel), and storage in a metal hydride (hydrogen bound in metals) or in a chemical hydride^{29,30}.

The compressed gaseous hydrogen is bulky even if hydrogen is compressed to 450 bar. Therefore, to be able to store 1 kg hydrogen, it requires about 40- 50 litres of space. In addition, hydrogen liquefaction is an energy-intensive process and use of hydrogen is practical only for large scale applications due to the high costs of liquid hydrogen storage tanks and difficulties to small scale sizes.

However, thanks to the recent developments of ultralight cylinders, compressed gas storage seems to have potential for on board vehicle storage. Moreover, storage of hydrogen in metal hydride is still a development stage. Although, the production of hydrogen by hydrocarbon reformation has been receiving a significant interest, it requires additional equipment thus an additional cost. All these issues related to the hydrogen infrastructure and storage needs to be solved or the safer and more efficient storage systems need to be developed before considering the mass scale applications of PEM fuel cells^{6,19,29}.

The relatively high cost of PEM fuel cell, which is partly due to the high prices of materials including the platinum catalyst, polymer electrolyte membrane and bipolar plate are further barriers to their commercialisation. The total cost of a fuel cell vehicle which is made of using a PEMFC system is 10 times that of a traditional car with an internal combustion engine (ICE). So to reduce the cost, it is essential that there be a more efficient and cost-effective development of each component in a PEMFC. The recent advances in PEM fuel cell technology do indicate that the cost of fuel cells and hydrogen will eventually decline^{14,28}.

Furthermore, durability is one of the main factors that affect the commercialisation potential of PEM fuel cells. The 2015 US Department of Energy (DOE) lifetime requirements are 5000 h for cars and 20000h for buses and 40000h for stationary fuel cell power systems. Currently, the lifetimes of PEM fuel cell vehicles and stationary power systems are about 1700 h and 10000h respectively.

On the other hand, it is very promising that Ballard has already established a durability of more than 2200 h in simulated testing^{14,28}.

Besides the cost of PEMFC and hydrogen supplies mentioned above there are also some other technological challenges in a PEMFC system. They include water and heat management, CO poisoning of the platinum anode electrocatalysts, system size, fuel processing, flow fields and MEA structure.

However, considering the progress that has been made in the fuel cells technologies so far all these problems are expected be solved in the near future^{30,31}.

Another issue of PEM fuel cell systems is their performance degradation with time. PEM fuel cells comprise different components such as membranes, catalysts, catalysts supports, GDLs, bipolar plates and sealing. Each of these components can degrade or fail to function, hence resulting in the fuel cell system degrade or fail.

The durability of each component can be affected by internal and external factors, including the material properties, fuel cell operating conditions, (i.e. humidity, temperature, cell voltage) impurities or contaminants in the reactants, environmental conditions, (such as subfreezing or cold start), operation modes (e.g., start-up, shut-down, potential cycling, etc.), and the design of components and the stack. Besides, the degradation route of different components are often are interconnected in a fuel cell system. So, the long-term durability tests need to be carried out in order to assess the degradation mechanism of these components. However, it is costly and not viable to operate a fuel cell under its normal conditions for several thousand hours for those tests. Thus, accelerated test methods are required to obtain quick information about the main durability concerns^{14,32}.

The durability of sealing material has a great importance on the long-term fuel cell performance. Therefore, material choice, structure and profile design, and processing method are very crucial for preventing seal degradation. The degradation phenomena of seals can have many effects on the fuel cell durability over long-term operation as included below:

- poisoning of Pt catalysts by the products of degradation or leaching out ;
- the leakage of sealing components can diffuse into membrane phase, leading to a decrease in membrane conductivity and a reduction in the mechanical strength of the membrane;
- causing an increased compression force on the GDL, resulting in reduced porosity and increased reactant transport resistance of GDL;

- detrimental effects on the hydrophilic / hydrophobic feature of the GDL, which may affect the water management inside the fuel cell ^{14,33}.

The seals/ gaskets are crucial components in a PEMFC stack. Recently, the importance of durable seals is increasing as a result of the continuous improvement of the fuel cell manufactures about reliable and durable sealing systems. At the same time, sealing technologies are being progressed from the R&D stage to real applications.

2.7. REFERENCES

- [1] A. Varga, "Introduction to Fuel cell Technology," in *Fuel Cell Electronics Packaging*, K. Kuang and K. Easler, Eds. New York ; London: Springer, 2007, pp. 1–32.
- [2] E. Chen, "History," in *Fuel Cell Technology Handbook*, G. Hoogers, Ed. Boca Raton, Fla. ; London: CRC Press, 2003, pp. 2–35.
- [3] X. Li 1962-, *Principles of fuel cells*. New York: Taylor & Francis, 2005.
- [4] V. Meidanshahi and G. Karimi, "Dynamic modeling, optimization and control of power density in a PEM fuel cell," *Appl. Energy*, vol. 93, pp. 98–105, 2012.
- [5] J. Larminie and A. Dicks, *Fuel Cell Systems Explained*, vol. 93. Chichester: John Wiley & Sons Ltd, 2001.
- [6] B. Viswanathan, *Fuel cells : Principles and applications*. Hyderabad: Universities Press India, 2007.
- [7] R. P. O'Hayre, S.-W. Cha, W. G. Colella, and F. B. Prinz, *Fuel cell fundamentals*, 2nd ed.. Hoboken, N.J.: John Wiley & Sons, 2009.
- [8] G. Hoogers, "Fuel Cell Components and Their Impact on Performance," in *Fuel Cell Technology Handbook*, G. Hoogers, Ed. Boca Raton, Fla. ; London: CRC Press, 2003, pp. 4–1, 4–27.
- [9] S. Edition and W. Virginia, "Fuel Cell Handbook. US Department of Energy, 7th Edition.Springfield:US Department of Commence," no. November, 2004.
- [10] P. P. Edwards, V. L. Kuznetsov, W. I. F. David, and N. P. Brandon, "Hydrogen and fuel cells: Towards a sustainable energy future," *Energy Policy*, vol. 36. pp. 4356–4362, 2008.
- [11] T. Herzog, "World Greenhouse Gas Emissions in 2005," *World Resour. Inst.*, pp. 2005–2009, 2009.

- [12] T. Program, E. Efficiency, and R. Energy, "The Department of Energy Hydrogen and Fuel Cells Program Plan," *Fuel*, pp. 1–105, 2011.
- [13] T. Plan and F. Cells, "Technical Plan — Fuel Cells," no. June 2011, pp. 1–49, 2012.
- [14] H. H. Wang, H. Li, and X.-Z. Yuan, "Introduction," in *PEM Fuel Cell Failure Mode*, Wang Haijiang Henry; Li Hui; Yuan Xiao-Zi, Ed. Boca Raton, Fla.: CRC, 2012, pp. 1–2.
- [15] J. H. Hirschenhoffer, *Fuel cells : a handbook*, vol. Rev. 3.. Orinda, Calif.: Business Technology Books, 1996.
- [16] Management Summary, "European Virtual Fuel Cell Power Plant," 2000.
- [17] X.-Z. Yuan and H. Wang, "PEM Fuel cell Fundamentals," in *PEM Fuel Cell Electrocatalysts and Catalyst Layers*, J. Zhang, Ed. London: Springer, 2008, pp. 1–79.
- [18] R. Yeetsorn, M. W. Fowler, and C. Tzoganakis, "A Review of Thermoplastic Composites for Bipolar Plate Materials in PEM Fuel Cells," in *Nanocomposites with Unique Properties and Applications in Medicine and Industry*, .
- [19] F. Barbir 1954-, *PEM fuel cells theory and practice*. Amsterdam ; Boston: Elsevier Academic Press, 2005.
- [20] V. Mehta and J. S. Cooper, "Review and analysis of PEM fuel cell design and manufacturing," *Journal of Power Sources*, vol. 114. pp. 32–53, 2003.
- [21] T. H. Yu, W.-G. Liu, Y. Sha, B. V. Merinov, P. Shirvanian, and W. A. Goddard, "The effect of different environments on Nafion degradation: Quantum mechanics study," *J. Memb. Sci.*, vol. 437, pp. 276–285, 2013.
- [22] K. D. Kreuer, "On the development of proton conducting polymer membranes for hydrogen and methanol fuel cells," *Journal of Membrane Science*, vol. 185. pp. 29–39, 2001.

- [23] C. Yang, P. Costamagna, S. Srinivasan, J. Benziger, and A. B. Bocarsly, "Approaches and technical challenges to high temperature operation of proton exchange membrane fuel cells," *J. Power Sources*, vol. 103, pp. 1–9, 2001.
- [24] J. Larminie, A. Dicks, and M. S. McDonald, *Fuel cell systems explained*, vol. 2. Chichester: John Wiley & Sons Ltd, 2003.
- [25] P.-C. Lin, B. Y. Park, and M. J. Madou, "Development and characterization of a miniature PEM fuel cell stack with carbon bipolar plates," *Journal of Power Sources*, vol. 176. pp. 207–214, 2008.
- [26] L. Frisch, "PEM fuel cell stack sealing using silicone elastomers," *Sealing Technology*, vol. 2001. pp. 7–9, 2001.
- [27] C.-H. Chien, C.-W. Lin, Y.-J. Chao, C. Tong, J. Van Zee, and T.-H. Su, "Variation of Compression of Seals in PEM Fuel Cells," in *Experimental and Applied Mechanics, Volume 6 SE - 40*, 2011, pp. 319–327.
- [28] J. Wee, "Applications of proton exchange membrane fuel cell systems," *Renew. Sustain. Energy Rev.*, vol. 11, pp. 1720–1738, 2007.
- [29] G. Hoogers, "The Fuelling Problem: Fuel Cell Systems," in *Fuel Cell Technology Handbook*, G. Hoogers, Ed. Boca Raton, Fla. ; London: CRC Press, 2003, pp. 5–1,5–23.
- [30] S. Hajj, K. A. Malinger, S. L. Suib, and E. C, "Fuels and Fuel Processing," in *Fuel Cell Technology*, N. M. Sammes, Ed. Berlin ; London: Springer, 2005, pp. 165–211.
- [31] D. Feroldi and M. Basualdo, "Description of PEM fuel Cell System," in *PEM Fuel Cells with Bio-Ethanol Processor Systems*, M. S. Basualdo, D. Feroldi, and R. Outbib, Eds. London: Springer London, 2012.
- [32] Dhathathreyan K.S; Rajalakshmi N., "Polymer Electrolyte Membrane Fuel Cell," in *Title: Recent Trends Fuel Cell Science and Technology*, S. Basu, Ed. Springer and Anayama, 2007, pp 40-115.

- [33] J. Wu, X. Z. Yuan, J. J. Martin, H. Wang, J. Zhang, J. Shen, S. Wu, and W. Merida, "A review of PEM fuel cell durability: Degradation mechanisms and mitigation strategies," *Journal of Power Sources*, vol. 184. pp. 104–119, 2008.

3. CHAPTER 3: Sealing Gasket

3.1. Introduction

The sealing component has a significant impact on safety, durability, reliability, functional performance and cost of a PEM fuel cell stack. Utilising hydrogen gas as a fuel can cause two different types of safety concerns in PEMFCs: escaping of hydrogen from the fuel cell due to inadequate sealing and mixing of hydrogen with oxygen (air) inside the cell due to a defect (rupture) in the membrane. Besides, a successful commercialisation of PEM fuel cells is heavily depend on the production of cost-effective systems which can be achieved by durable seals as well as the other cell components¹⁻³. Every single component in the cell can degrade or fail to operate affecting the durability of the whole fuel cell system. If a gasket degrades or fails during the fuel cell operation, the reactant gases can mix with each other directly causing an impact on the performance and operation of the fuel cell. Apart from degradation of materials, there are also the other factors such as fuel cell design and assembly, operational conditions, and impurities which determine the performance of a PEM fuel cell. Among all the other fuel cell stack components, the function and the degradation problems of the seals have been neglected. Nevertheless, the long term chemical and mechanical stability of the gaskets are crucial for both sealing and the electrochemical performance of the fuel cells^{4, 5}.

A single PEM fuel cell consists of a membrane electrode assembly (MEA), a gasket on the perimeter of the MEA with a gas diffusion layer, and catalyst in the centre on the anode and cathode side of the membrane, bipolar (flow field) plates, current collectors and end plates as shown in Figure 3.1. Two sealing gaskets are required for one MEA unit, placed between each side of the MEA and the bipolar (flow field) plates^{1,3}.

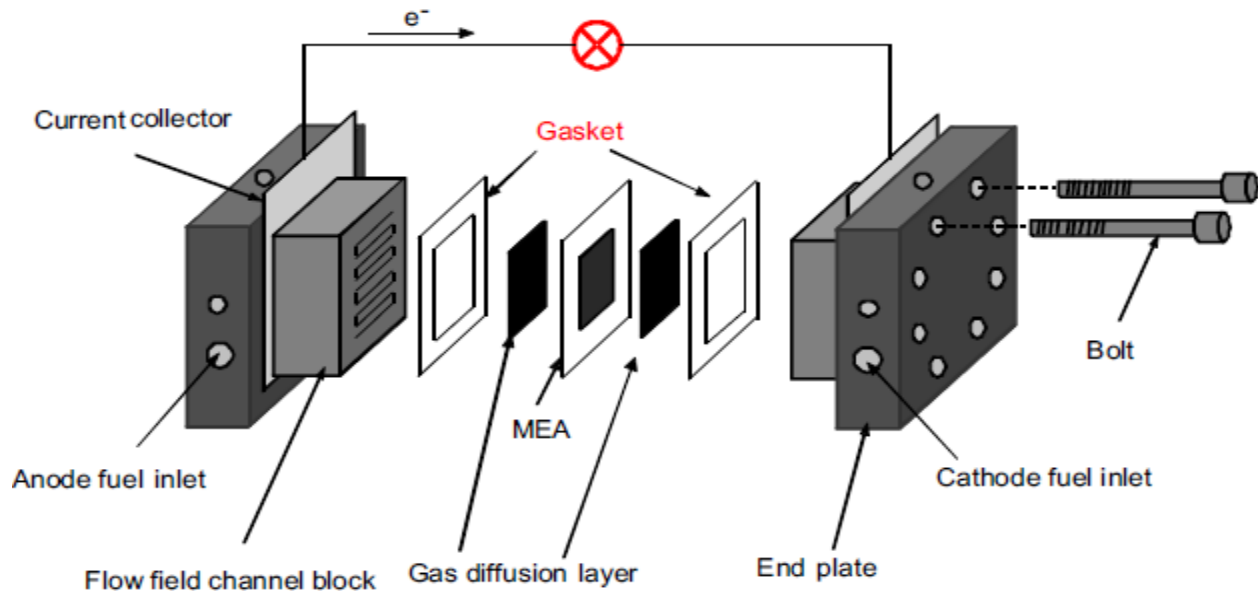


Figure 3.1 Illustration of a single PEM fuel cell⁶

3.2. Function of the Sealing Gasket

The main functions of the gaskets are:

1. To prevent the reactant gases and coolants inside the cell from leaking
2. To avoid the mixing of the reactant gases near the catalyst areas
3. To provide electrical insulation in order to prevent the fuel cell from short circuit (shorting)

During the fuel cell operation there are reactant gases and liquids inside the cell. Any gas or fluid leakage between the components due to sealing failure can reduce fuel cell performance, damage the fuel cell stack and cause safety problems^{1,3,7}.

Generally, the gas leaks in a fuel cell are expressed as *Cross over leaks* and *Overboard leaks*. *Cross over leaks* occur when the reactant gas from either the cathode or the anode side escapes to the environment. *Overboard leaks* happen when the gas from one side of the membrane crosses over to the other side of the membrane. Gaskets must prevent both cross over and overboard leaks⁵.

They also prevent the electrical contact between the bipolar plates in the fuel cell stack which can result in the short circuit.

The electrical short circuit causes non-reversible degradation e.g. melting of the electrodes, therefore leading to the failure of the PEM fuel cell stack⁸.

Additionally, the gaskets in the fuel cell provide stack height and variability control, and compression control as well as mechanical sealing between bipolar plates and gas diffusion layers^{1,3,7}.

3.3. Environment of the Sealing Gasket

The sealing material in the fuel cell is exposed to acidic liquid solution, hydrogen, humid air, coolant, temperature cycles, electrochemical environment as well as mechanical stress^{9,10}.

Mechanical stress: Seals or gaskets used in PEM fuel cells (or stacks) are under compressive stress so as to prevent any leakage of the liquid and gas inside the cells. The components in the fuel cells are assembled together by bolts or a combination of bolts and springs. This applies a clamping pressure to fuel cell stack therefore a compressive stress on the seal^{11,12}.

Humidity: The polymer membrane can only function when it is fully hydrated in other words; it becomes ion conductive only after it absorbs water. For this reason, it is necessary to humidify reactant gases (up to 100 % relative humidity- RH) before entering the fuel cell stack in order to maintain membrane's proton conductivity. Hence the gasket is exposed to 100 % RH in the cell¹³.

Temperature: PEMFC units are required to function at ambient temperatures around the world^{1,10}. Hence, the PEM fuel cells typically operate at a temperature range between – 40 and 100°C.

Chemical environment: There is a strong acidic environment inside the fuel cell which comes from the chemical structure of the polymer electrolyte membrane (the side chain sulfonic acid radicals). Since the sealing gasket is in direct contact with the membrane, it will be affected by this corrosive condition¹⁰.

The sealing gasket will also be exposed to reactant gases (hydrogen and oxygen), coolants, water (pH 4-9), steam and reaction by-products (carbon monoxide and carbon dioxide) as well as traces of hydrogen fluoride (HF). The typical coolants used in PEM fuel cells include synthetic hydrocarbons, perfluorocarbons, fluorosilicone fluids, deionized water and water-glycol mixtures^{1, 14}.

3.4. Requirements of the Sealing Gasket

For durable fuel cells, it is necessary that the seals should meet the following properties:

Excellent mechanical stability and suitable compressibility: As it is mentioned before in the section 3.1.2, the components of a fuel cell should be clamped together with a sufficient assembly force to prevent overboard leakage of the reactants. In other words, the adequate compression has to be applied to seals. Consequently, the internal pressure inside the cell can be quite high and the gasket must withstand this pressure during extended operation. Compression set is the most important property for the mechanical stability. Gasket material should possess a required set value which will prevent over-compression of stacks components. Because over-compression can cause a change in the gas permeability of the GDL which will affect the fuel cell performance^{10,15}. Moreover, soft or resilient sealing materials are preferable in order to allow compression of the stack to help intimate contact of all components. Most designs for PEM fuel cell seals require the hardness of 20 to 60 Shore A durometer¹.

Thermal, chemical and electrochemical stability: Sealing materials should stand the conditions and internal environment of a PEM fuel cell stack for instance, high humidity, temperature changes (– 40 to 100°C), reactive chemicals, strong redox environment, certain trace hydrocarbons and inorganic species as previously explained in section 3.1.2¹⁰. For transport applications, PEM fuel cells must operate at the temperature range from – 40 to 80°C for at least 5000 hours (approximately 7 months) according to the U.S. Department of Energy's (DOE) PEM fuel cell technical targets for the year 2012. Automotive fuel cell power systems should survive at and start-up from freezing temperatures (– 40°C)¹⁶.

Therefore, the seals must be durable enough in order to endure the load under the normal operating temperature after exposed to above temperature changes¹⁷. It also has to be considered that quick temperature cycles to which a sealing material can be subjected to are normally more challenging than a maximum long term service temperature¹⁰. One of the other requirements is that the sealing material should not interfere with the electrochemistry in the fuel cell¹⁴.

Compatible with membrane and all other materials (used in the fuel cell): Suitable sealing materials must be resistant to the proton-exchange membrane and the other materials such as bipolar plates. The chemical nature of the membrane and very chemically active operating environment in a PEM fuel cell stack as well as the presence of catalyst, protons and localized current flow will all have an impact on the durability of seal^{1,14}.

In the case of direct contact with the catalyst layer of the MEA, the sealing material should not contain any substance which in the presence of the catalyst will initiate unwanted side reactions. Additionally, the sealing material should not include any components which can perform as catalyst poisons that can contaminate the electrocatalyst resulting in reduced cell efficiency¹⁴.

Furthermore, the sealing materials should be free of any components such as bivalent cations which might restrict the function of the membrane that can cause an irreversible complication the ionic sites leading to reduced membrane conductivity¹⁴.

Low ion elution and low leachability: Appropriate sealing materials are required to have least possible ion elution. This is because if the small ions leach out of the sealing material, they can attack above-mentioned membrane's sulfonic acid (ionic) groups adversely affecting its proton conductivity. Moreover, the eluted ions can migrate to the surface of the catalyst and influence its catalytic activity^{15,18}.

In addition, the other components such as plasticisers, oligomers, internal and external process aids used during production should not elute from the sealing materials.

Since, they may diffuse through the cell and block the pores in the gas diffusion layer or accumulate on the other areas of the cell. This will cause cell contamination and an increase in contact resistance eventually bringing about increased Ohmic losses¹⁴.

Good electrical insulation: Sealing gasket should be electrically insulating in order to prevent:

- Drain of the direct current obtained from each cell.
- Short-circuit between the cells^{14,19}.

Moisture resistance: The seal material is exposed to water vapour inside the cell. This is because water vapour is one of the by-products of PEM fuel cell reactions. Plus high relative humidity (RH) is required inside the cell so as to sustain the function (proton conductivity) of polymer membrane. Therefore the gasket material should be hydrophobic which will not absorb the water unlike the hydrophilic ones that can absorb the humidity even in the air flow. Undesirable level of moisture can degrade the gasket material and damage fuel cell performance^{13,20}.

Coolant resistance: Depending on the design, the sealing can encounter with substances used for cooling of the cell. Such materials are water-glycol mixtures, deionized water and hydrocarbon based coolants. The sealing material should be resistant against these cooling media^{1,14}. The main factors which determine the seal resistance to coolant fluids includes swelling in the fluids, leaching of additives from the seal material into the coolant and resistance to degradation caused by the coolant.

The materials used for seals in PEMFCs must not swell in the coolants more than around 5 % because the swelling above this percentage can damage the bipolar plates, cause misalignment of the fuel cell components and be more susceptible to leaks. Seal materials must not contain any components (i.e. plasticisers) which can be easily leached out on exposure to cooling fluids. Because any leachate can contaminate the coolant resulting in coolant failure or blocking the coolant channels¹.

Resistance to the reactant gases (hydrogen & oxygen) and **reaction by – products** (CO & CO₂).

Low gas permeability: Permeation of gases especially the hydrogen gas promotes the safety concerns in the PEM fuel cells. For this reason, low permeation rates of gases through the sealing material are desirable¹.

Efficient seal integration: A PEM fuel cell stack may have hundreds of fuel cells stacked on top of each other to attain a desired current and voltage output. Hence a great number of gaskets are needed to prevent the leakage of hydrogen and air. For the cost effective mass production, the sealing can be integrated with the MEA or bipolar plate into one component. This not only allows high capacity manufacture also reduces the chance of defects¹⁰.

Low cost and easy fabrication: The cost of sealing together with an easy and fast assembly process will be essential when PEMFC manufactures reach the high capacity of production of PEM fuel cells (i.e. millions of cell units) in the near future¹

3.5. Design and Fabrication Methods

As mentioned in section 2.4, a single cell generates relatively low voltages (~ 0.7 V). In order to provide useful amounts of power at usable voltages, fuel cells are usually formed into stacks which can have 60 to 100 in some applications and even as many as 200 fuel cells in a single stack.

The design of a single stack can be very complicated and can involve various elements, all of which must be carefully assembled. A precise technique needs to be applied to achieve the proper alignment of these cell components¹.

As was previously described, a single cell is constructed by virtually stacking the cathode bipolar plate, cathode gasket, MEA, the anode gasket, and the anode bipolar plate in sequence on an end plate (fitted with the necessary bolts) and finally completing the assembly with the other end plate (See Figure 3.1).

A fuel cell stack consists of many those single cells connected in series. The integration of the gasket on the bipolar plates and GDL are required a number of steps with the consideration of several important parameters. These parameters include gasket thickness, the assembly and the alignment of the gasket to the bipolar plate (BPP) and GDL^{3,21,22}.

In recent years, several sealing designs have been developed in parallel with MEA development and flow field designs. The choice of the appropriate gasket design as well as a suitable gasket material is essential in terms of avoiding a mechanical overload on the seal^{3,14}.

Correct sealing decreases the internal electric resistance of the stack by allowing compression of the stack so as to ensure intimate contact of all conductive components.

As part of the mechanical requirements, the seals also have to compensate for all the tolerances associated with the different fuel cell components within the stack. The different components especially bipolar plates, gas diffusion layers and the seal itself exhibit dimensional tolerances due to their particular production processes. Additionally, single components can show a different permanent set under the applied compacting forces leading to bending of the assembled stack.

Furthermore, all components expand or contract when subjected to temperature changes. All these factors need to be considered in the choice of suitable gasket design and material¹⁴.

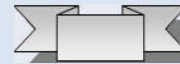
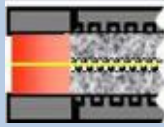
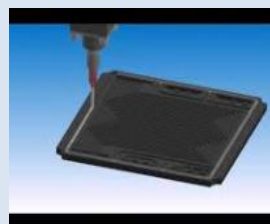
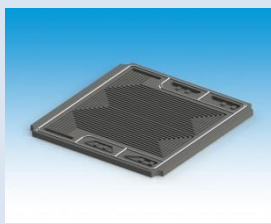
Typically there are two methods used to fabricate elastomeric PEM fuel cell seals: Die cutting and screen printing³. Also the seals can be formed to different designs including the following:

Flat gasket design: Flat gaskets are cut from a suitable solid elastomeric sheet material of suitable thickness using a die-cutter. This is a cheap and simple technique but has the disadvantage of producing gaskets with only a constant thickness. A further disadvantage is that there is significant amount of material wasted^{1, 23}.

Profiled gasket design: Seals are formed by moulding (i.e. injection, transfer or compression moulding) of various profiles which can be fabricated on flat plate surfaces or assembled into channels or grooves in the flow field plates. In this technique the gasket is moulded separately from individual components of the fuel cell and then attached to the bipolar plate or MEA. Profile seal design is more advantageous than the flat design because the assembly forces are lower and thus the other fuel cell components will be secured from the damage which can be caused by excessive assembly forces^{23,24}.

Formed in place gasket (FIPG): In FIPG technology, a liquid elastomer composition is applied by a robot applicator to the joining surfaces (flanges) of connecting components in the fuel cell stack, such as bipolar plate, MEA or GDL. After application to the liquid elastomers cure with time and temperature [i.e. also called cure in place gasket (CIPG)] and become bonded and integrated with these components. The FIP gaskets have been developed to improve the pressure resistance of the joint surface and to reduce the processing time by excluding the step in which the fixed- shape gasket is attached^{10,23,24}. The comparison of different gasket designs and suitability for use in PEMFCs is shown in Table 3.1.

Table 3.1. Classification of different sealing designs – Adapted from ^{14,25-27}

	Rigid	Elastic	Suitability for use
Flat	Softmetal (elastomer layer appr.50 μm) 	Elastomer 	poor tolerance adjustment
Profiled		Elastomer  Metal 	suitable for all conditions high forces & contact pressure
Adhesion	Adhesive  Duromer Adhesive	Adhesive  Elastomer Adhesive	limited usage
	Liquid Elastomer (Elastic)	Cured in place & bonded to bipolar plate	Suitability for use
FIP			superior adhesion increased production speed

Generally, loose gaskets are suitable for the assembly of single cells or prototype stacks where a simple gasket design preferred. So that the shape can be altered quickly according to the sealing conditions or optimising the geometry. For cost-effective mass production, however, the gasket has to be attached on other fuel cell components (i.e., bipolar plates or GDL).

Figures 3.2 & 3.3 demonstrate the loose profile gasket and the methods of the integration of sealing function onto various other components of PEM fuel cell respectively^{14, 25}.

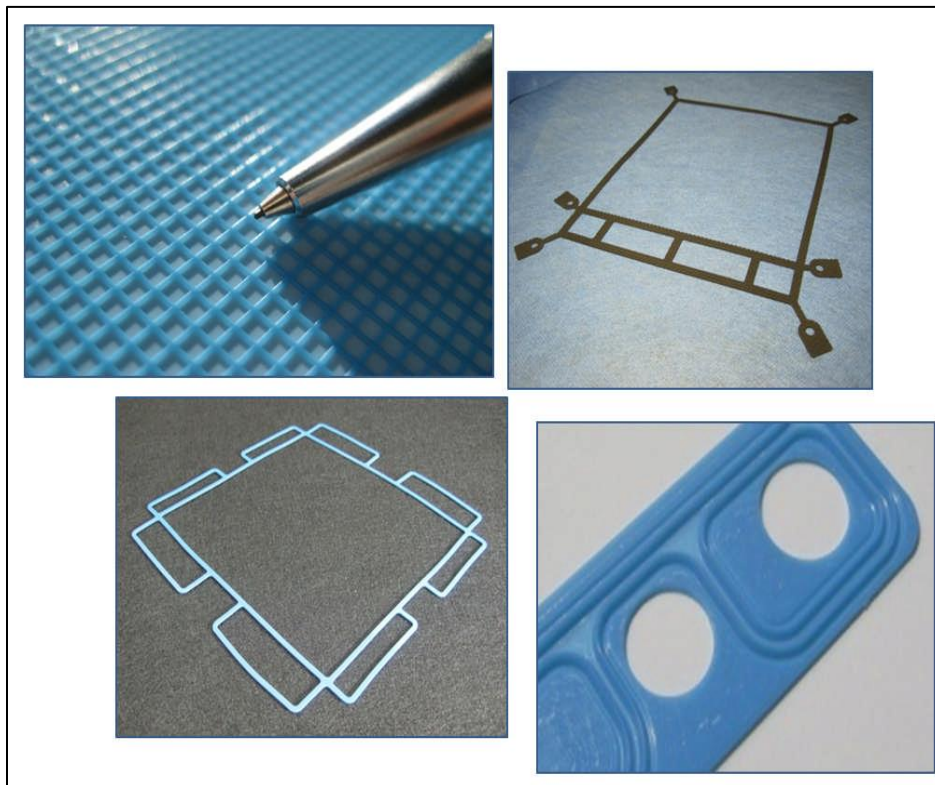


Figure 3.2. Loose style profile gaskets²⁵

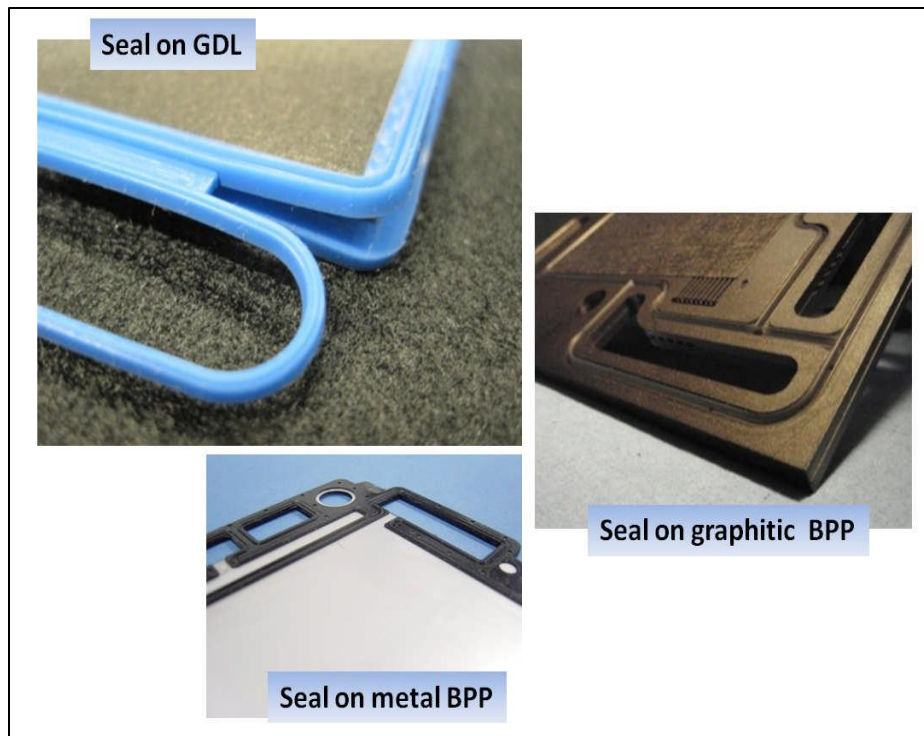


Figure 3.3 Methods for seal integration to bipolar plate (BPP) ²⁵

Suitable material solutions for seals:

Flexible elastomeric sealing systems are generally preferred over the more rigid solutions which include duromeric glues or soft metal which consists of a thin metal layer partially or fully coated with an elastomeric layer usually less than 50 μ m thick, as shown in Figure 3¹⁴. Gasket stress is a general term is used to describe the unit load on its surface. It directly affects the ability of gasket to seal. Different gasket materials may respond differently to a specified stress range. For instance, soft gasket manufactured from flexible elastomers can seal at a relatively low gasket stress whereas, a hard gasket fabricated from rigid systems (i.e. soft metal with the very thin elastomeric layer). In the case of PEM fuel cells, soft (i.e., resilience) sealing materials are favoured to allocate low compression force for the interaction of the stack components²⁷.

The conventional methods for gasket manufacture, of die-cutting or injection moulding, require expensive punch and mould tools which increase the cost of the final product²⁸. One of the new manufacturing methods is liquid elastomer moulding (LEM) which has developed by the US-based Federal- Mogul Corporation. The LEM sealing technology aims to overcome the challenges of mass production such as size, cost and packaging. The principle of a LEM design is that small amounts of elastomeric droplets are moulded under pressure and heat. The total thickness of the gasket is in the range of just 0.3 – 0.5 mm which is half the thickness of the conventional moulded gaskets²⁹. The LEM process also enables manufacturing of seals with very flat surfaces. Furthermore, the gaskets can be integrated directly in to the bipolar plate. All these features of the gaskets fabricated by the LEM method make both assembly and operation much easier³⁰.

3.6. Seal Materials

3.6.1. Background

The seals in PEM fuel cells are typically made of elastomers. Cured elastomers are one of the most applicable classes of polymer materials with distinctive advantages in sealing applications compared to other polymer classes such as thermoplastics, duromers and thermoplastic elastomers. Especially, the excellent stress relaxation behaviour, good flexibility, high chemical resistance and better processability alongside the availability of low-hardness types makes elastomers the most attractive material class for PEM fuel cell sealing¹⁴.

An elastomer is a polymer which is viscoelastic and able to return its original shape and size after large deformation (i.e. being stretched, compressed, twisted or bent). Elastic deformation remains only as long as a deforming force (stress) is applied to the material and disappears when the stress is released.

Elastomers are normally amorphous polymers which comprise of carbon, oxygen and or / silicon and whose glass transition temperatures (T_g) are well below the operating temperature. They can have outstanding properties including large strain, transparency, permeability and insulation³¹.

The chemical and molecular structure of elastomers is closely connected to their elastomeric mechanical response. The ability to experience high strains without breaking needs, a polymer with high molecular weight.

High strain is achieved by the uncoiling of random molecular chains to a less random conformation. This reduces the entropy meaning that molecules are less disordered. As a result, the immediate response to stress and reversibility of deformation of an elastomer can be achieved with macromolecules which have long flexible chains with weak intermolecular forces. When molecules are in fully extended conformation, the elastic response is almost wholly by this entropic mechanism, with little distortion of their covalent bonds or change in their internal energy.³²

In practice, elastomers are not generally used on their own but as compounds, comprising an elastomer and many other components, such a crosslinking system and filler. However, the specific molecular structure of an elastomer is responsible for the compound's basic chemical and physical characteristics, such as its resistance towards heat, cold, oils, solvents or other chemicals^{33,34}. Therefore the choice of base elastomer determines the thermal properties and the media resistance of the elastomer compound¹⁴.

By vulcanisation (curing) elastomeric polymers, useful materials can be formed which possess physical properties such as high tensile strength, low compression set, recoverable elongations, high tear energies and improved dynamic performance. Vulcanisation refers to the crosslinking reaction which occurs under the influence of heat and pressure. During this process, crosslinks are formed between the individual polymer chains to prevent chains from sliding past one another. Figure 3.4 illustrates the cross-links between polymer chains. The connection of adjacent polymer chains allows the rubber part to recover from large deformations quickly and reduces creep^{14,35-36}.

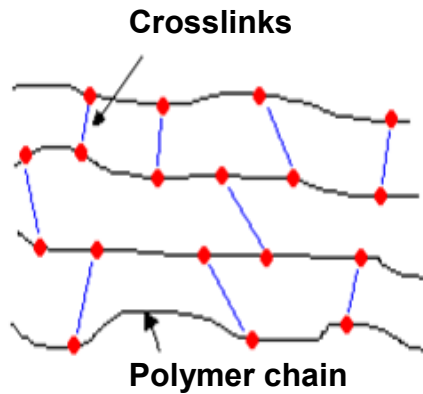


Figure 3.4. Cross-linked network of an elastomer ³⁷

The most commonly used crosslinking processes for elastomers are “sulfur vulcanisation” and “peroxide vulcanisation”.

Sulfur Vulcanisation:

Elemental sulfur was the first material used to cure rubber. It is still today’s most common cure system. For sulfur curing there should be carbon – carbon unsaturation present in the polymer and it results in a three-dimensional rubber network where the polymer chains are connected to each other by sulfur bonds. The sulfur vulcanisation process provides products with good tensile and tear strength, good dynamic properties, but poor high temperature properties such as ageing. One of the downsides of sulfur curing is that it results in rather poor compression set at elevated temperatures and poor high temperature ageing behaviour^{35,36}. When a polymer is cross-linked with elemental sulfur under the effect of heat, free radicals are formed as a result of ring opening of the eight- membered sulfur rings (S₈).

Figure 3.5 shows this ring opening reaction:

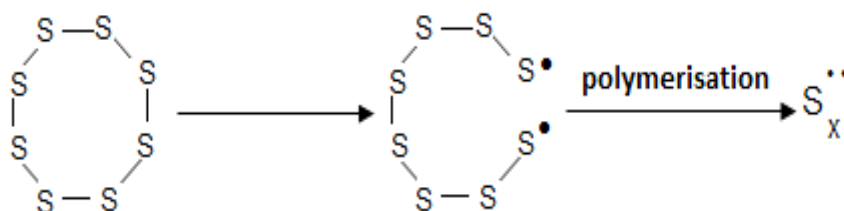


Figure 3.5. The ring opening reaction of elemental sulfur at 150°C



The free radicals then react with the unsaturation (carbon-carbon double bonds) of the polymer in the following way.



Peroxide Vulcanisation:

Peroxide cure has become more popular with the introduction of some fully saturated elastomers, for instance ethylene-propylene rubber (EPM) and fluoroelastomers (FKM), which cannot be cured by sulfur vulcanisation. When polymers are cross-linked with peroxides, the bond formed between individual polymer chains are very stable covalent carbon-carbon (C – C) bonds^{35, 36}. The reaction mechanism for peroxide cure is shown in Figure 3.6. At the first step homolytic cleavage of the oxygen – oxygen (O – O) bond occurs to provide two alkoxy free radicals (R – O[•] and R' – O[•]). Generally alkoxy radicals abstract a hydrogen atom from the polymer to generate a free radical on the polymer chain. In the case of a presence of double bonds in the polymer some alkoxy radicals can add to the polymer chain to obtain slightly different radicals. The final step of peroxide cross - linking involves the joining of two polymer free radicals to form the carbon – carbon (C – C) cross-link. If the polymer contains a high degree of branching or a lot of side groups, (i.e. butyl rubber, propylene) addition of peroxides will result in chain scission and softening instead of cross-linking³⁶.

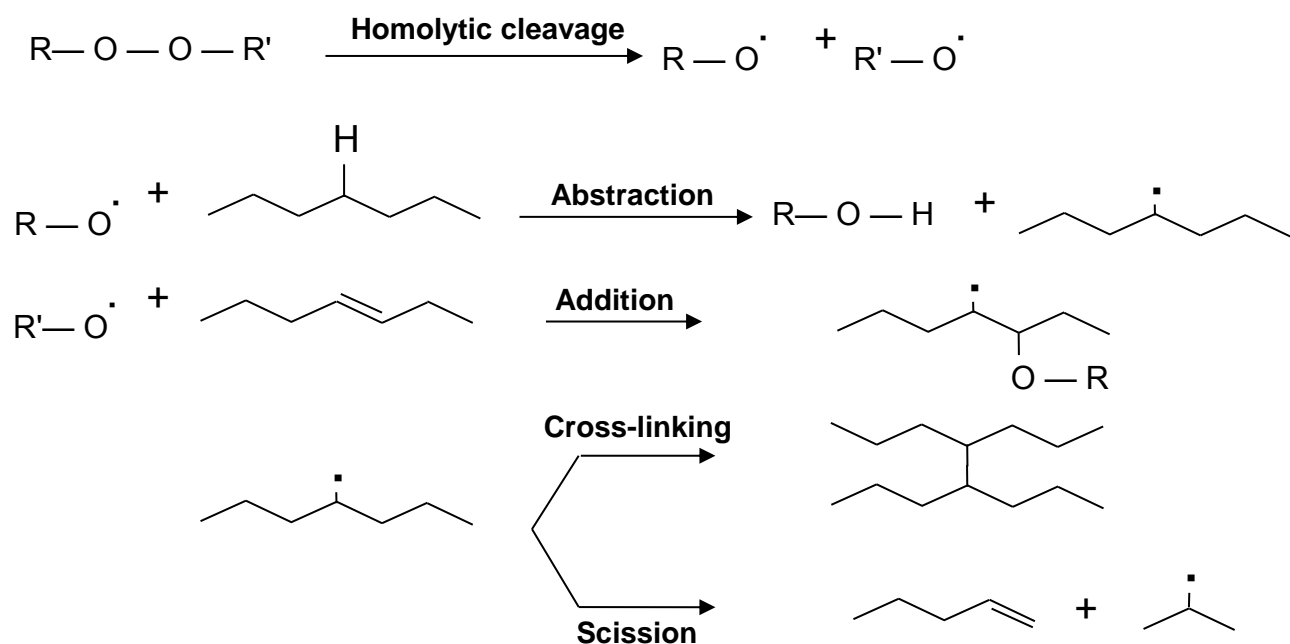


Figure 3.6. Peroxide reactions³⁶

As a result of C – C bonds, peroxide cured articles, have good high temperature properties like heat ageing and compression set, compared to sulfur cured vulcanizates. Moreover, peroxide cure enables vulcanisation of both unsaturated and saturated polymers that is not possible with sulfur vulcanisation. However, some of the mechanical properties of peroxide cured articles are inferior to those accomplished by sulfur vulcanisation, including tensile strength and dynamic properties which limit the use of this vulcanisation method^{35,36}.

Another limitation of peroxide cure is insufficient “scorch time”. Scorch time is defined as the time passed by before vulcanisation starts which is very important in terms of controlling the vulcanisation reaction. It is essential to have a particular scorch time (scorch safety) which is sufficient to provide good processing of the material before it starts vulcanisation.

Apart from sulfur and peroxide cures, the other vulcanisation systems that are initiated using alternative energy initiation mechanisms such as ultraviolet light, electron beam, microwave and resins are gaining more importance^{35,36}.

Other additives such as fillers (carbon black, silica, mineral fillers) are also added to the base rubber of an elastomer in order to attain adequate material strength, whilst plasticisers are added to decrease the compound viscosity and influence low temperature flexibility. Moreover, the ageing resistance can be improved by addition of a range of antidegradants which prevent the part from the effects of heat, UV light and ozone. In addition, processing aids such as lubricants, released agents, silicone modified processing additives are utilized to facilitate easy handling of the compounds plus a consistent and reproducible manufacturing process¹⁴.

Any of the additives included in a rubber compound can have a negative influence on the PEM fuel cell performance if they are chosen wrongly. Thus the formulation of an elastomeric seal is crucial and requires comprehensive rubber knowledge in order to avoid any undesirable side effects which will promote fuel cell degradation. Besides a careful selection of the sealing material's composition, the manufacturing steps need to be considered as well. Such manufacturing steps include mixing of the rubber compound, manufacturing of the gasket, its after- treatment, and packing and assembly¹⁴.

3.6.2. Elastomers for Seal/ Gasket Applications

Most industrial gaskets and seals are manufactured from elastomers such as nitrile rubber (NBR), chloroprene rubber (CR), styrene butadiene rubber (SBR), fluoroelastomers (FKM), and silicone rubber^{29,38}. These elastomeric materials should meet the most important gasket requirements such as a high resistance to stress relaxation, suitable hardness, good mechanical strength and processability, excellent thermal stability and sufficient chemical resistance²⁹.

In the case of PEM fuel cells, the selection of gasket material is determined by the temperature and media requirements which have been explained in section 3.3. The most commonly used elastomers for PEM fuel cells include silicone rubber, EPDM, fluorinated elastomers (fluoroelastomers), polyacrylate, acrylate copolymer, butyl rubber and chloroprene. Silicone rubber is usually employed for low temperature PEM fuel cells while fluorocarbon rubber (FKM) is more suitable for high temperature applications.

EPDM or in general, hydrocarbon-based rubbers with highly saturated backbones can also be chosen due to their excellent chemical and good thermal resistance.

To achieve better fuel, oxygen, water and heat, resistance fluorine-containing elastomers such as fluorosilicone are preferred^{10,14,30}. In addition, other seal materials or material combinations have been subjected to extensive research for PEM fuel cell sealing applications. For example, liquid silicone rubber (LSR) based compounds, glass-fibre reinforced PTFE and an EPDM rubber gasket combined with a PTFE gasket. More details will be given about PEM fuel cell gasket materials and related studies in the subsequent sections.

3.6.3. Current PEM Fuel Cell Gasket Materials

Silicone Rubber (Q)

Silicone rubber's distinctive characteristics arise from its unique molecular structure. The organosiloxane polymers consist of mainly repetitions of the $-R_2SiO-$ unit and hence they possess both organic and inorganic properties. Their backbone contains silicone (Si) and oxygen (O) atoms (Si – O bonds) instead of the carbon (C) backbone structure (C – C bonds) of all other elastomers. Due to this Si – O (siloxane) bond, silicone rubber exhibits the combination of inherent properties which make them the unique choice in a broad range of applications. These properties comprise excellent weather and thermal stability, ozone and oxidation resistance, good electrical properties, extreme low temperature flexibility (due to a very low temperatures of $T_g -120^\circ\text{C}$), high gas permeability, good solvent and oil resistance, good compatibility with body tissue and curability by a variety of methods at both elevated and ambient temperatures. Thanks to these unique features silicone rubber has replaced some hydrocarbon rubbers used in many industries like aerospace, munitions, automobile, construction, electricals, electronics, medical and food processing³⁹⁻⁴¹.

Polydimethylsiloxane (PDMS) silicone rubber is the most common organosilicon polymer having two methyl groups attached to each silicone atom. Figure 3.7 shows the chemical structure of PDMS.

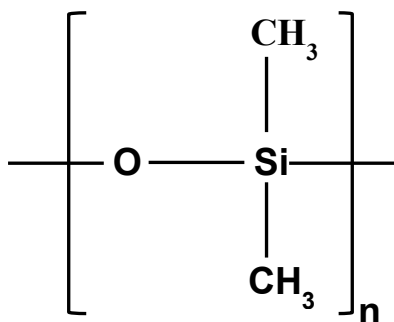


Figure 3.7. Polydimethylsiloxane (PDMS) ⁴⁰

The organic groups on the polysiloxane bond can be methyl (CH₃), vinyl (–CH=CH₂) or phenyl $\left[\begin{array}{c} \text{R} \\ | \\ \text{C}_6\text{H}_5 \end{array} \right]$ groups.

The different silicone polymers are named after these organic side groups connected to silicone atom. Each silicone atom has four chemical bonds; this is why silicone rubber is often abbreviated with a Q for quaternary groups. The structure of the existing polymers available can vary for example, by using different polymer chain lengths, with or without branching or high or low vinyl content. Consequently, this will determine the final properties of the rubber^{42,43}. The most important silicone rubber classes include:

- **MQ** stands for methyl- polysiloxane which contains methyl side groups without double bonds. These are linear polymers with very low viscosities (liquid) and do not react easily with peroxide based cross-linkers^{42,43}.
- **VMQ** is vinyl-methyl-polysiloxane which is similar to MQ but some of the methyl groups have been replaced with vinyl groups. The double bond is a reactive group which is necessary for crosslinking. The presence of vinyl groups improves the peroxide cross-linking efficiency significantly and allows these silicone rubbers to be used in applications requiring enhanced performance and long term-reliability, such as automotive seals^{40,42-43}.
- **PMVQ** represents phenyl-vinyl-methyl-polysiloxane copolymer in which a small number of methyl groups in the VMQ are replaced with phenyl groups.

The large phenyl group means the polymer chains have less tendency to pack closely with adjacent chains at low temperature and hence further improves flexibility at low temperatures^{40,42}.

The unusual combination of properties of silicone rubber are closely related to its chemical structure including strong backbone chain bonds, great backbone chain flexibility, ease of rotation of the organic side chain groups, low intermolecular forces and inorganic-organic character⁴⁰.

The bond energy of the Si – O bond is 452 kJ/mole, greater than that of a C – C bond at 343 kJ/mol hence the polysiloxane chain is thermally, oxidatively and chemically much more stable than organic hydrocarbon chains. The extra energy required to dissociate a siloxane bond is the reason for the excellent heat resistance of silicones, with a maximum service temperature of 316°C^{41,43}.

Silicone rubber also can remain flexible at very low temperatures even below – 50°C which is the result of unique siloxane backbone chain flexibility (freedom of rotation). One of the other consequences of this unique dynamic flexibility is a very low glass transition temperature T_g (–127°C), the lowest amongst all the conventional polymers. Low intermolecular forces between the silicone molecules and relatively unhindered single bonds which connect the alternate silicone and oxygen atoms in the backbone chain contribute to the flexibility of the backbone. These characteristics are also the reasons for high permeability of silicone elastomers to gases^{41, 44}.

The backbone (siloxane) chain flexibility of silicone rubber is the result of free rotation (i.e., low molecular forces) of the methyl (CH₃) groups in PDMS (See Figure 3.6). Besides, the low surface energy of PDMS is due to the non-polar nature of the methyl groups and the fact that they are evenly distributed around the backbone chain. The high degree of hydrophobicity of silicone rubber, which is related to its low surface energy, is exploited in outdoor insulation^{40,44}.

In addition, silicones also are less affected by radiation (UV, alpha, beta and gamma rays) than organic polymers.

This offers the use of silicones in a wide range of fields such as aerospace (low and high temperature performance, electronics (electrical insulation), health care (excellent biocompatibility) or in the building industries (resistance to weathering)³⁹.

Despite the above mentioned useful properties, silicone rubber has a poor resistance towards strong acid and base. This behaviour is caused by the partial ionic / polar character of the Si – O bond (40-50% ionic) due to the difference in the electronegativities of silicone and oxygen. Consequently, this ionic nature of Si – O bond is responsible for the sensitivity of silicone rubber to hydrolysis at extreme pH values. Therefore, it is not desirable to use silicone rubber where it will come in contact with strong acids^{39,44}.

Typically, organic peroxides are used for curing (cross-linking) of silicone rubbers. Unfilled peroxide cured silicone gums are very weak having a tensile strength of only around 0.34 MPa. So it is necessary to compound silicones with reinforcing fillers and additives to obtain improved mechanical and physical properties. For example, tensile strength of the silicone gums can be increased by as much as fifty times (up to 17 MPa) when they are compounded with suitable fillers. Silica fillers such as fumed silica and precipitated silica are particularly preferred for silicone compounds. On the other hand, carbon black is used in only a small number of applications to produce electrically conductive vulcanizates for example from VMQ silicone rubber. A problem with using carbon black is that it has a high content of adsorbed volatiles which can cause the voids in the compound during curing. Additionally, calcium carbonate, graphite (conductive fillers), other silicates and aluminates are also utilised as reinforcing fillers with silicones. Stabilizers, such as inorganic pigments like ferric oxide (Fe_2O_3), are extensively used to improve UV stability. Plasticisers, such as low molecular weight 1.2- polybutadiene, is also mixed to compounds to achieve desired hardness of the material⁴³⁻⁴⁵.

Silicone rubber can be compounded using conventional equipment such as dough mixers, Banburys, and two-roll mills⁴⁵. After compounding, the freshening is the first step in the fabrication procedure. Basically, this is a re-milling process as to reverse the "creep-hardening" or "structuring" which has taken place since the compound was made.

Structuring happens more quickly and proceeds further if the compound has been aged at higher temperatures. It is caused by the formation of hydrogen bonds between the hydroxyl (– OH) groups of the filler and the hydroxyl groups of oxygen atoms of the polymer. The freshening is carried on until the silicone rubber stock reaches the desired consistency⁴⁶. The second step for the fabrication process is moulding. Compression and transfer moulding are the most widely used methods for relatively simple shaped silicone rubber parts in fairly low quantities. However, there is a growing demand for the injection moulding for large volume applications such as are required by the automotive industry^{46,47}.

Alternatively, silicone rubber can be extruded into a variety of shapes and sizes like gaskets, tubing, tape, seals, wires and cables.

Calendering is another technique where the rubber is squeezed between rollers to form sheets of varying thickness^{45,47}. Silicone rubber is often calendered onto fabrics such as glass, nylon, polyester and cotton. Post-curing along with trimming or deflashing (i.e., removing the flash" excess rubber" from moulded parts) is often the final step in the fabrication of silicone rubber parts. Post-curing eliminates volatile species such as low molecular weight silicones and peroxide decomposition products. Removal of low molecular weight silicones result in less shrinkage later and lower extractables. Also, removal of the peroxide decomposition products enhances compression set, electrical properties, chemical resistance and the bond to other substrates⁴⁵.

Silicone rubber has been chosen widely as a sealing material in PEMFCs because of its softness, simple processability and extensive availability rather than its exclusive material properties. Nevertheless, silicone rubber is more expensive than the other commodity rubbers and has poor chemical resistance towards acidic environments which is a key factor for the PEMFC applications where the gaskets are exposed to acidic conditions. For these reasons, silicone rubber seals seem to be more suitable for less demanding, mainly short-term applications rather than long-term applications in PEM fuel cells^{14,29}. During PEM fuel cell operation, it has been found that, silicon containing species accumulate around the membrane edges, mostly around the membrane seal joints.

Calcium (Ca) is thought to come from gasket fillers and silicon (Si) from polymer degradation. In the case of losing Si and Ca will change the sealing property of the gasket, possibly resulting in the leakage of the reactants and coolants from their separate areas. Additionally, these Si and Ca constituents contaminate the membrane and catalyst and therefore reduce their functioning capabilities⁴⁸.

Ethylene-Propylene -Diene Monomer (EPDM)

EPDM continues to be one of the fastest growing and most widely used elastomers among the synthetic rubbers. It has a broad range of applications such as gasket and seals, electrical insulation, tubes, outdoor applications, automotive housing, roof sheeting, wire and cable. EPDM has a useful combination of weather and heat resistance due to its saturated polymer backbone (unlike many other rubbers). Availability of very wide molecular weight range also makes EPDM the polymer of choice in diverse markets⁴⁹.

EPDM rubber is a copolymer of ethylene and propylene with a non-conjugated diene monomer which provides a site of unsaturation (double bonds) for cross-linking as shown in Figure 3.7. The copolymerisation of ethylene and propylene with the Ziegler-Natta catalyst results in an amorphous and rubbery material, so-called EPM rubber (copolymer). EPDMs can only be cross-linked with peroxides as they do not have double bonds (unsaturation). However, during the copolymerization of ethylene and propylene a third monomer (a diene) can be added and the resultant rubber will have unsaturation so that it can be vulcanized with sulfur. These rubbers are called EPDMs (terpolymer)⁴³.

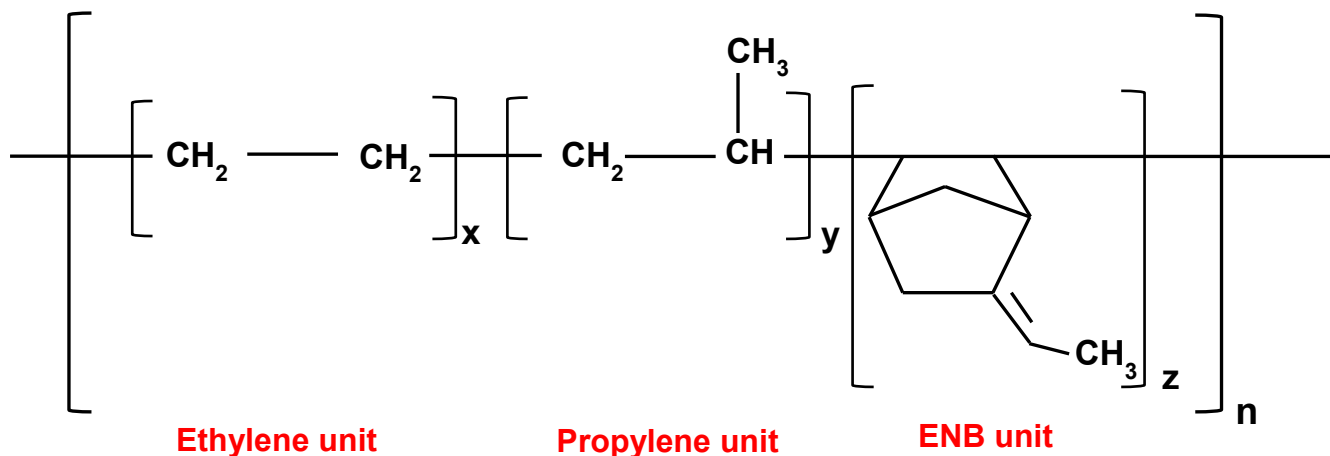


Figure 3.8. A structural formula of ENB-containing EPDM ⁵⁰

The ratio of ethylene to propylene content plays an important role in the main characteristics of EPDM rubber. Ideally this lies between 40 wt % ethylene and 60 wt% propylene. Commercial EPDMs however, comprise between 50 and 80 % ethylene. If the ethylene content is low (i.e. 50-55 wt %), the resulting polymer will be amorphous, soft and flexible and exhibit excellent low temperature flexibility and compression set, but they cannot be loaded with a high quantity of fillers. On the other hand, polymers contain high ethylene content of 68 to 80 %, will have improved modulus and green strength thanks to their crystallinity ⁴⁹.

The choice of diene affects EPDM properties such as compression set, aging and cure rate of the polymer. There are three type of dienes are commonly used in the production of EPDM including: 5-ethylidene- 2- norborne (ENB), dicyclopentadiene (DCPD), and 1,4-hexadiene (HD). ENB and DCDP are cyclic dienes and influence the low-temperature properties of EPDM by increasing the glass transition temperature (T_g) because of their rigid structure but they also reduce crystallinity by breaking up ethylene arrangements. 1,4 HD however is a linear non-conjugated diene therefore, it is less reactive towards the Ziegler Natta catalyst.

Consequently, it is slower curing than both ENB and DCDP due to the absence of cyclic bonds. It also provides a linear polymer structure with narrow molecular weight distribution (MWD) as compared to those of manufactured from ENB and DCDP which are branched with broader MWD. They provide branched EPDM grades with broad molecular weight distribution (MWD).

Between all three, ENB termonomer is used most widely by EPDM producers since it is a fast curing diene with a sulfur cure system because of the six allylic hydrogens on carbon atoms adjacent to the olefinic bond (See Figure 3.8) ⁴⁹.

These aforementioned structural features and compositions all contribute to the main properties of EPDM. For instance, the saturated backbone is responsible for its excellent chemical and weather resistance. Although the double bonds in a polymer are the main areas to attack for oxidants, but in EPDM they are pendant to the backbone and thus, the oxidation of the double bond will not have any significant effect on the physical properties of the rubber ⁴⁹.

EPDM polymers are nonpolar consequently they have very good resistance to water, aqueous solutions and other polar fluids. In addition, being non-polar contributes to the good nonconductive electrical properties as well. EPDM also is inherently resistant to inorganic acids (i.e. sulfuric acid, hydrochloric acid and nitric acid) ⁴⁹.

EPDM can endure a range of temperatures from – 45°C to +120°C. However; it is not very stable at elevated temperatures due to oxidation⁵¹. Because of its good ozone and weather resistance, EPDM rubber is commonly used in outdoor applications. It can also be an excellent choice for automotive brake components, where good ozone and heat resistance, low stress relaxation and resistance to non-mineral oil hydraulic fluids are essential. The other application areas in which EPDM is utilised include, conveyor belting, bridge bearing pads, window gaskets, grommets and seals⁴⁹.

EPDM can be vulcanized in both peroxide and sulfur cured systems due to the presence of double (unsaturated) bonds in the side chains. If peroxide cures and a high level of cross-linking is desired, the rubber must contain at least 50 mole % of ethylene. The termonomer has an effect on the peroxide cure as well. For peroxide cures of EPDM, activators are needed, such as sulfur, sulfur donors, acrylates, maleimides and quinones. With sulfur cures, the type of termonomer in the rubber mainly determines the required amount of sulfur and accelerator ⁴³.

Thanks to its low crystallinity, EPDM needs to be reinforced by fillers to obtain best mechanical properties. Another advantage of EPDM is that it can accept high loading of fillers and plasticisers and still provide good processability and properties in its end products. Carbon black, silica, clay, calcium carbonate with very fine particles and fibre are the most commonly used fillers for EPDM⁴³. If vulcanizates with a good aging resistance are required, the use of a protective agent is necessary, such as aromatic amines and especially p-phenylene diamine, naphthenic oils and paraffinic oils which are the most commonly used softeners for EPDM.

Furthermore, in order to facilitate the mixing of EPDM compounds, and above all to improve the filler dispersion, stearic acid, zinc soaps, calcium soaps of fatty acids are employed as process aids⁴³.

The mixing of EPDM compounds is generally achieved using the internal mixers preferably by the “upside down” technique where the fillers and oils are added to the mixer followed straight after by the polymer. This is unlike the conventional mixing technique where the polymer is added first to the mixer and after a period of mixing, the filler is added followed by any plasticisers or oils⁵².

From a consideration of its properties EPDM rubber would be expected to maintain good durability under the harsh environment of the PEM fuel cell, thanks to its excellent acid ageing resistance²⁹.

Fluoroelastomers (FKM)

Fluoroelastomers are prepared from fluorinated monomers. They have been developed since 1950s in various compositions from copolymers to pentapolymers. The first copolymers were made from vinylidene fluoride (VF2) and chlorotrifluoroethylene (CTFE), and were amorphous polymers with more than 60 % fluorine and with a low T_g . Shortly after, they were replaced by copolymer of VF2 and HFP (hexafluoropropylene), with the trade name of Viton ® from Dupont, in order to meet the demands for high performance sealing material in the aerospace industry.

Subsequently, tetrafluoroethylene (TFE), a third monomer was added to VF2 and HFP so as to increase the fluorine level in the fluoroelastomers and improve its chemical resistance, especially to alcohols. FKM can be prepared through co - or terpolymerisation of the following monomers (See Figure 3.9) ^{43,53} .

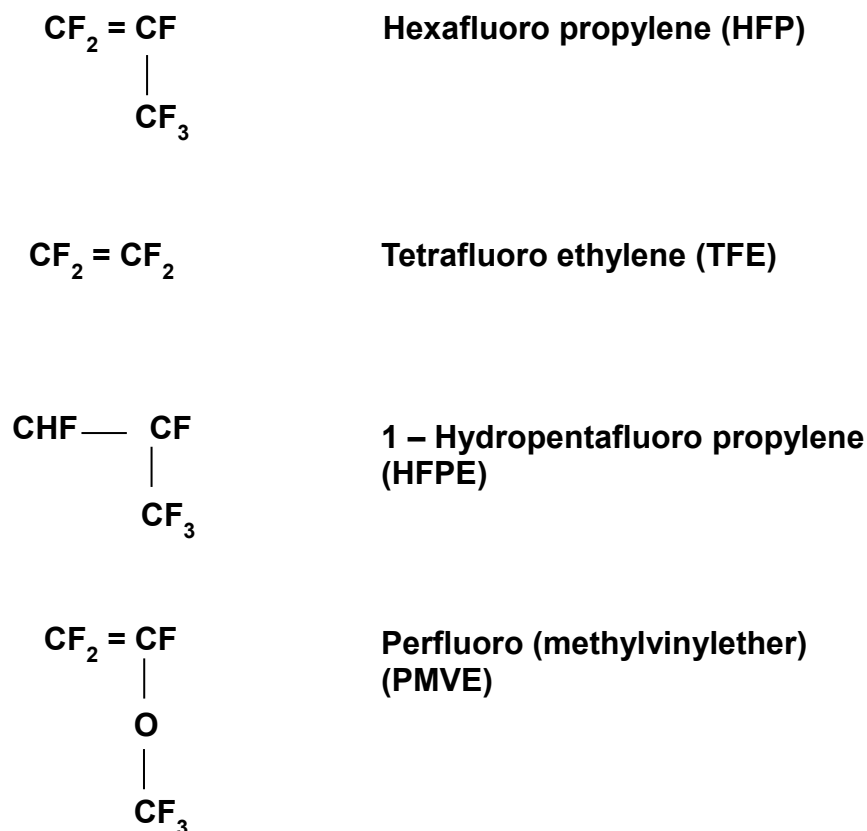


Figure 3.9. Most common monomers used for the preparation of FKM⁴³

The heat and chemical resistance of FKM is superior to that of other elastomers. They withstand most of lubricants, fuels and hydraulic fluids; a wide range of particularly corrosive chemicals and chlorinated solvents⁴¹. Many FKM grades are suitable for long term service interaction with various fluids up to 300°C. Thus, fluoroelastomer seals and other components are extensively used in many areas including automotive, aerospace, oil and chemical industries⁵⁴ .

The bond energy of the carbon-fluorine bond is 442 KJ/mole, considerably higher than that of the carbon-hydrogen bond at 377 KJ/mole.

For this reason, and because of the protecting of the polymer chain by the larger fluorine substituents, as compared with non-substituted chains, FKM shows great resistance towards high heat and chemicals FKM vulcanizates show very good resistance to swelling (with increasing fluorine content) in hot oils and aliphatic compounds as well as in aromatics and chlorinated hydrocarbons, even acids at high concentrations⁴³.

FKM elastomers can exhibit the very good heat resistance with a continuous service temperature of 220°C for 1000 hours.

FKM is fully saturated and it cannot be affected by oxidative processes. So, it is entirely resistant towards oxidation and ozone as well as to motor fuels with hydroperoxides. In addition, FKM has a very low gas permeability⁴³.

Because of its excellent properties, FKM is used in special elastomer products, such as shaft seals and O-rings in automotive industry, components in aircraft and rockets and other moulded parts and extruded shapes (e.g. fuel hose). Fluoroelastomers show much longer operational performance in sealing applications at elevated temperatures compared to other elastomers. Thanks to their low gas permeability and service reliability, fluoroelastomers are increasingly used in the chemical and transportation industries where it is essential to reduce emissions. O-rings and gaskets make up the major product types of fluoroelastomers due to their good compression resistance and fluid resistance at high temperatures for prolonged periods^{43,53-54}.

On the other hand, the glass transition temperature (T_g) of fluoroelastomers range between 0°C to – 30°C which is normally higher than those of hydrocarbon elastomers. They can be used at room temperature and higher (i.e. above their T_g) especially in the sealing applications the desired property is flexibility and elasticity. Because above the T_g the elastomer is in the rubbery state^{43,54}.

In spite of all these exclusive properties, fluoroelastomer compounds are much more costly than most mid-performance elastomers and so only tend to be used when high performance is absolutely essential⁵³.

Initially amine curatives were used for FKM in the late 1950s but they were quickly abandoned because bisphenol cure systems could provide much better scorch safety and better compression set resistance. The most favourable cure systems for FKM are based on bisphenol in combination with magnesium oxide (MgO) and calcium hydroxide [Ca(OH)₂] as acid acceptors. Peroxide curing systems can be utilised with the highly fluorinated FKM grades such as PMVE which contains a cure site monomer which introduces reactive side groups.

The use of coagents (i.e. peroxy-carbamates) as well as acid acceptors such as zinc oxide are required with peroxides^{43,53}.

Generally, FKM has very high viscosity prior to curing and it is difficult to attain low hardness compounds. Therefore non-reinforcing blacks and mineral fillers are employed to achieve the desired hardness, good processability, and good vulcanizate properties and to reduce the compound cost. MT and SRF black fillers are mainly used. MT at low levels can provide good physical properties and processability. Other specialty black fillers such as conductive blacks for electrostatic or conductive properties and Austin black for better compression set can also be considered. Apart from black fillers, barium sulphate (BaSO₄), calcium metasilicate and calcium carbonate are used as white fillers^{43,53}.

FKM is not well-suited for use with traditional plasticisers because they cannot endure the service temperatures and post-cure cycles of fluoroelastomers⁵³.

FKM can be mixed and processed using the conventional methods applied to most of the other elastomers. However, long post curing periods are generally required (i.e. 24 hours at 200 to 260°C) so that the cross-linking reaction can be completed during post cure and also so that high cure states and low compression set values can be achieved⁴³.

Usually, fluoroelastomers (FKM) would be expected to operate well under characteristic PEM fuel cell conditions, with exceptional chemical resistance against acids and water, excellent elasticity, very low compression set and constant hardness.

Nevertheless, they are not the primary choice for the fuel cell manufacturers due to their poor melt processability (i.e., for injection moulding), and relatively poor low – temperature resistance but above all they are much more expensive than the other rubbers²⁹ .

Fluorosilicone Rubber (FMQ , FVMQ)

Fluorosilicone rubber was created by upgrading of dimethyl siloxanes (VMQ) to meet the requirements for increased solvent resistance in harsh environments where VMQ rubbers cannot survive.

One of the methyl (CH₃) groups in VMQ is replaced with — CH₂CH₂CF₃ (trifluoropropyl) group as shown in Figure 3.10. The polymer is known as poly (methyltrifluoropropyl siloxane) or fluorosilicone rubbers (FMQ, FVMQ)^{43,55} .

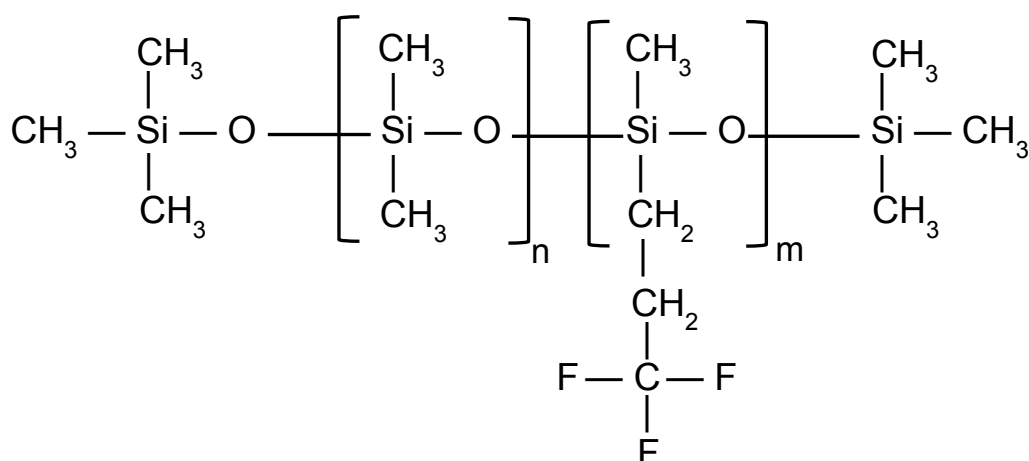


Figure 3.10. The chemical structure of Fluorosilicone rubber ⁵⁵

The addition of fluorine in the side groups increases the polarity of FVMQ significantly over that of VMQ and as a result, FVMQ vulcanizates have a much better resistance to oils and motor fuels. The combination of siloxane backbone and fluorine substitution in the side groups gives FVMQ its exclusive properties.

For example, the lowest known intermolecular forces of fluorocarbon groups between all pendent groups combine with the unique flexibility of the siloxane backbone.

Therefore, fluorosilicone rubber (FSR) is suitable for applications requiring low and high temperature performance under the influence of jet and automotive fuels, many solvents, and engine oils^{43,56-58}.

The solvent resistance and stability of FSR derives from the presence of carbon-fluorine (C – F) bonds in the polymer. Replacement of hydrogen with fluorine reduces solubility and surface energy and increases thermal stability and resistance to chemicals⁵⁷.

The major applications of fluorosilicone rubber include O-ring seals, shaft seals and gaskets, moulded parts, wire and cable insulation⁵⁹.

Fluorosilicones can be cured by using any peroxide classes as they contain typical reactive groups available for typical silicone network chemistry. Additional materials are added for compounding such as reinforcing fillers, extending fillers, pigments, thermal stabilizers, acid acceptors and conductive fillers.

Silicas (silicon dioxide) are usually used as reinforcing fillers due to their thermal stability and their compatibility with the elastomeric silicon-oxygen backbone. Calcium carbonate, iron oxide, titanium oxide and zinc oxide are the other commonly used fillers⁵⁹.

Mixing of the compounds can be carried out with both open-mill and internal mixers. Particularly, Baker-Perkins mixers are used by the industry to prepare original formulations⁶⁰.

3.7. Summary

PEM fuel cell has become a growing research area especially in the attempt of improving its performance and lifetime so that it can compete with the internal combustion engines. The durability and the limited lifetime of the PEMFCs are still main obstacles in their mass production and fully commercialisation. Therefore, most of the research has been focused on the optimization of PEM fuel cell components as well as the cell operating conditions. Seal/gasket is one of the cell components, which has an impact on the stability of PEM fuel cell stack. In this chapter, the different aspects related to the PEM fuel cell seal as well as the potential seal

materials have been discussed. The chemical structures and main properties of silicone rubber, EPDM, FKM and fluorosilicone rubber which, are commonly used elastomers for PEM fuel cell sealing, have been described. Although silicone rubber has been chosen widely as gasket material due to its low cost and easy fabrication, it is unable to endure in the acidic environment of the PEM due to the fact that it is susceptible to the hydrolytic degradation. On the other hand, EPDM seems to have a greater potential as a durable gasket material thanks to its excellent chemical resistance.

FKM is regarded as the other possible gasket material for PEM fuel cell applications because of its superior resistance towards chemicals and water along with the good compression resistance which are the main requirements for a PEM fuel cell gasket material. But FKM is much more expensive than most of the other elastomers and has a high viscosity which can be significant shortcomings for a PEMFC seal material.

Fluorosilicone rubber has already been used as a seal material for the applications required good resistance to automotive fuels, engine oils and various solvents as well as good thermal resistance. Therefore, it is considered as another choice of material for fuel cell gaskets.

In the next chapter the current research about PEMFC sealing and the comparison of the performance of these elastomeric seal materials will be discussed extensively.

3.8. REFERENCES

- [1] L. Frisch, "PEM fuel cell stack sealing using silicone elastomers," *Sealing Technology*, vol. 2001. pp. 7–9, 2001.
- [2] P. C. Ghosh, "Influences of contact pressure on the performances of polymer electrolyte fuel cells," *J. Energy*, vol. 2013, 2013.
- [3] J. Zhang, H. Zhang, J. Wu, and J. Zhang, "Design and Fabrication of PEM Fuel Cell," in *Pem Fuel Cell Testing and Diagnosis*, Elsevier, 2013, pp. 43–80.
- [4] X. Z. Yuan, H. Li, S. Zhang, J. Martin, and H. Wang, "A review of polymer electrolyte membrane fuel cell durability test protocols," *Journal of Power Sources*, vol. 196. pp. 9107–9116, 2011.
- [5] A. Husar, M. Serra, and C. Kunusch, "Description of gasket failure in a 7 cell PEMFC stack," *J. Power Sources*, vol. 169, pp. 85–91, 2007.
- [6] C. W. Lin, C. H. Chien, J. Tan, Y. J. Chao, and J. W. Van Zee, "Dynamic mechanical characteristics of five elastomeric gasket materials aged in a simulated and an accelerated PEM fuel cell environment," *Int. J. Hydrogen Energy*, vol. 36, pp. 6756–6767, 2011.
- [7] C. Kunusch, P. Puleston, and M. Mayosky, "Sliding-Mode Control of PEM Fuel Cells," 2012.
- [8] R. E. Silva, F. Harel, S. Jemeï, R. Gouriveau, D. Hissel, L. Boulon, and K. Agbossou, "Proton Exchange Membrane Fuel Cell Operation and Degradation in Short-Circuit," *Fuel Cells*, vol. 14, no. 6, pp. 894–905, 2014.
- [9] M. Schulze, T. Knöri, A. Schneider, and E. Gülzow, "Degradation of sealings for PEFC test cells during fuel cell operation," in *Journal of Power Sources*, 2004, vol. 127, pp. 222–229.
- [10] B. L. and J. M. Daijun Yang, Junsheng Zheng, "Degradation of Other Components," in *PEM Fuel Cell Failure Mode Analysis*, H. H. Wang, H. Li 1964-, and X.-Z. Yuan, Eds. Boca Raton, Fla.: CRC Press, 2012.
- [11] C.-H. Chien, C.-W. Lin, Y.-J. Chao, C. Tong, J. Van Zee, and T.-H. Su, "Variation of Compression of Seals in PEM Fuel Cells," in *Experimental and Applied Mechanics, Volume 6 SE - 40*, 2011, pp. 319–327.
- [12] J. Z. Tan, Y. J. Chao, W.-K. Lee, and J. W. Van Zee, "Relationship between the applied torque and compression of gasket in a fuel cell assembly," *J. Press. Equip. Syst*, vol. 5, pp. 1–7, 2007.
- [13] F. Barbir and ScienceDirect (Online service), *PEM fuel cells[electronic resource] :] theory and practice*. 2005.

- [14] R. Bieringer, M. Adler, S. Geiss, and M. Viol, "Gaskets: Important Durability Issues," in *Polymer Electrolyte Fuel Cell Durability SE - 13*, F. Büchi, M. Inaba, and T. Schmidt, Eds. Springer New York, 2009, pp. 271–281.
- [15] T. Bond and T. News, "New Series of Fuel Cell Sealing Compounds – ThreeBond 1152/1153." pp. 1–8, 2003.
- [16] A. P. Report, "Annual progress report 2012," 2012.
- [17] T. Cui, Y. Chao, and J. Van Zee, "Understanding the Stress Response of Seals in Fuel Cell Subject to Temperature Cycling," *ECS Trans.*, vol. 41, no. 1, pp. 1927–1934, 2011.
- [18] J. Feng, Q. Zhang, Z. Tu, W. Tu, Z. Wan, M. Pan, and H. Zhang, "Degradation of silicone rubbers with different hardness in various aqueous solutions," *Polym. Degrad. Stab.*, vol. 109, pp. 122–128, Nov. 2014.
- [19] T. Bond and T. News, "New Series of Fuel Cell Sealing Compounds – ThreeBond 1152/1153," *Fuel Cell*, pp. 1–8, 2003.
- [20] D. Authority, C. Energy, and B. Growth, "Advanced Fuel Cell Technology," vol. 15, no. 8, 2011.
- [21] Supramaniam Srinivasan, *Fuel Cells: From Fundamentals to Applications*. Springer, 2006.
- [22] Hartmut Elias, "Integrated seal for a PEM fuel cell," 1999.
- [23] M. T. M. Lawrence Eugene Frisch, Randall Allen Herring, "Seals for fuel cells and fuel cell stacks," US 6761991 B2, 2004.
- [24] David J. Dunn, *Adhesives and Sealants: Technology, Applications and Market*. Shropshire UK: Rapra Technology, 2003.
- [25] M. a Belchuk, "# 293 - Sealing Pem Fuel Cells," *Freudenb. FCCT KG*, pp. 1–8, 2010.
- [26] "Form in Place/ Cure in Place Gaskets." [Online]. Available: <https://www.dymax.com/index.php/en/adhesives/fip-gaskets>. [Accessed: 12-Aug-2015].
- [27] P. M. Page, "Sealing sense," *Pumps*, no. September, pp. 46–47, 2004.
- [28] M. A. K. Mitchell T. Huang, "Photocurable form-in-place gasket for electronic applications," EP 1432936 A1, 2004.
- [29] U. Basuli, J. Jose, R. H. Lee, Y. H. Yoo, K.-U. Jeong, J.-H. Ahn, and C. Nah, "Properties and Degradation of the Gasket Component of a Proton Exchange Membrane Fuel Cell—A Review," *J. Nanosci. Nanotechnol.*, vol. 12, no. 10, pp. 7641–7657, 2012.

- [30] I. Sealing, "LEM Sealing Technology for Fuel Cells," pp. 44–47.
- [31] S. Yang and K. Jiang, "Elastomer Application in Microsystem and Microfluidics," *Adv. Elastomers - Technol. Prop. Appl.*, pp. 203–222, 2012.
- [32] R. Shanks and I. Kong, "Thermoplastic Elastomers," 2012.
- [33] E. Ho, "Elastomeric seals for rapid gas decompression applications in high - pressure services," *Heal. Saf. Exec. BHR Gr. Limited, Res. Rep. No 485*, pp. 1 – 74, 2006.
- [34] Leonard J Martini, *Practical Seal Design*. New York US: Taylor & Francis, 1984.
- [35] E. Manaila, M. D. Stelescu, and G. Craciun, "Aspects Regarding Radiation Crosslinking of Elastomers," pp. 3–34, 2012.
- [36] Robert F. Ohm, "Vulcanisation Agents for Specialty Elastomers," in *Handbook of Specialty Elastomers*, R. C. Klingender, Ed. CRC Press, 2008, pp. 409–427.
- [37] "Peroxide Vulcanisation." [Online]. Available: <https://rubbertech.wordpress.com/2013/07/>. [Accessed: 02-Sep-2015].
- [38] "Fuel Cell and Hydrogen Energy Association, Recommended Standard Test Methods for Fuel Cell Gasket Material," 2011.
- [39] S. C. Shit and P. Shah, "A Review on Silicone Rubber," *Natl. Acad. Sci. Lett.*, vol. 36, no. 4, pp. 355–365, 2013.
- [40] H. S. A.Bhowmick, "Advances in Silicone Rubber Technology Part 1," in *Handbook of elastomers*, 2nd ed.,re., Keith E. Polmantaer, Ed. New York: M.Dekker, 2001.
- [41] C. A. (Charles A. Harper 1926-, *Handbook of plastics, elastomers and composites*, 2nd ed.. London: McGraw-Hill, 1992.
- [42] "Silicone Rubber Technical Information. Mosites Rubber Company." [Online]. Available: <http://www.mositesrubber.com/technical/technical-info/silicone-rubber/>. [Accessed: 10-Sep-2015].
- [43] W. Hofmann 1924-, *Rubber technology handbook*. Munich : New York: Hanser Publishers , 1989.
- [44] J. L. Goudie, M. J. Owen, and D. C. Corporation, "A Review of Possible Degradation Mechanisms of Silicone Elastomers in Voltage Insulation Applications," *Electr. Insul. Dielectr. Phenomena, 1998. Annu. Report. Conf. , vol. 1, no., pp.120,127 vol. 1*, vol. 1, no. 1, pp. 120–127, 1998.
- [45] NPSP Board of Consultant Engineers, *The Complete Book on Rubber Chemicals*. New Delhi: Asia Pasific Business Press.

- [46] NIIR Board of Consultants and Engineers, "Silicone rubber," in *The Complete Book on Rubber Processing and Compounding Technology*, A. K. Gupta, Ed. New Delhi: Asia Pasific Business Press, 2006, pp. 453–489.
- [47] G. Hawley, "Plastics, Filler and Extender Uses," in *Industrial Minerals & Rocks, Commodities, Markets and Uses*, 7 th., Kogel J. E. et al., Ed. SME, 2006, pp. 1321–1364.
- [48] A. B. Choudhury, G. Escobedo, D. E. Curtin, and S. Banerjee, "PEM Hydrogen Fuel Cell Durability : A Perspective Review and Recent Advances Membrane Fuel Cell Components," *Transw. Res. Netw.*, vol. 661, no. 2, pp. 1–25, 2015.
- [49] Anil K..Bhowmick, "EPDM Rubber Technology," in *Handbook of elastomers*, 2nd ed.,re., K. C. B. William H. Klingensmith, Ed. New York: M.Dekker, 2001.
- [50] S. Mitra, A. Ghanbari-Siahkali, P. Kingshott, H. K. Rehmeier, H. Abildgaard, and K. Almdal, "Chemical degradation of crosslinked ethylene-propylene-diene rubber in an acidic environment. Part I. Effect on accelerated sulfur crosslinks," *Polym. Degrad. Stab.*, vol. 91, no. 1, pp. 69–80, 2006.
- [51] A. Fazal and K. S. Fancey, "Performance enhancement of nylon kevlar fiber composites through viscoelastically generated pre-stress," *Polym. Polym. Compos.*, vol. 16, no. 2, pp. 101–113, 2008.
- [52] P.R.Wood, "Rubber Mixing," 1996.
- [53] P. Ferrandez, "Fluoroelastomers, FKM, and FEPM," in *Handbook of Specialty Elastomers*, Robert F. Ohm, Ed. Boca Raton: CRC Press, 2008, pp. 134–152.
- [54] Alber L. Moore, *Fluoroelastomers Handbook:The Definitive User's Guide*. William Andrew Publishing, 2006.
- [55] D. C. Corporation, "FSRs in Extreme Applications."
- [56] H. Zhang and A. Cloud, "Research progress in calenderable fluorosilicone with excellent fuel resistance," *Sampe*, 2007.
- [57] P. Fluorosilicones, "Poly(fluorosilicones) 1.," *Kirk Othmer Encyclopedia Chem. Technol.*, pp. 1–11.
- [58] M.J.Oven, "Surface Properties and Applications," in *Silicon Containing Polymers, The Science and Technology of Their Synthesis and Applications*, J. Richard G.Jones, Wataru Ando, Ed. Kluwer Academic Publishers, 2000, pp. 213–229.
- [59] A. K. Bhowmick and H. L. Stephens, *Handbook of elastomers*, 2nd ed., r. New York: M. Dekker, 2001.

4. CHAPTER 4: Seal / Gasket Degradation

4.1. Introduction

The degradation of sealing materials in PEM fuel cells can be caused by elevated temperature, the chemical environment and mechanical stress and may result in the loss of the sealing force, leading to external leaks of coolant, gas crossover or plate electrical shorting. It will eventually lead to a decrease in the performance of the fuel cell.¹

For instance, the gasket can experience reduced thickness over long term operation which leads to an increased compression force on the gas diffusion layer (GDL) which can change the gas permeability of the GDL. Both the degradation products and leachants from the sealing material can reach the electrodes and change the electrodes' hydrophobic nature negatively and also poison the Pt catalyst. Cross over leakage is one of the consequences of gasket degradation and can cause damage to the membrane. In addition, molecular fragments from the seal material may diffuse into the membrane leading to a reduction in the membrane conductivity. All these outcomes of seal degradation will be detrimental to the fuel cell life time^{1, 2}.

Even though there are a significant number of publications regarding the degradation of elastomeric gasket materials in various environments, only a small number of reports have been published on degradation and its mechanisms, mainly about silicone rubber in the PEMFC environment. Outcomes of this research will be discussed in detail in the following sections.

4.2. Chemical Degradation of Sealing Material

Generally, chemical attack on the elastomeric materials involves specific chemical reactions which lead to degradation. Hydrolysis is one of the causes of polymer degradation, which includes the scission of susceptible molecular groups (i.e., esters, amides, imides, and carbonate groups) by reaction with water, acids and alkalis.

Chain scission occurs if these groups are located in the backbone chain rather than the side chain. Consequently, chain scission causes a reduction in molecular weight which leads to a softening of the polymer.

Upon exposure to elevated temperatures, elastomers can experience oxidative cross-linking reactions which can result in new chemical bonds between different molecules and hardening of the material. Subsequently, chemical degradation of seals will alter the physical and mechanical properties including hardness, modulus, compression set, stress relaxation, and tensile properties.

4.2.1. Degradation of Seals in Various Environments

Silicone Rubber

Besides fuel cells, there are many published reports concerning the degradation of silicone rubber in various environments³⁻⁹. For instance, Gravier et al.³ reported their findings in a review based on other studies about the possible degradation mechanisms of polydimethylsiloxane (PDMS) in an outdoor environment. It was suggested that, upon disposal of the PDMS polymer, most of it enters the soil environment. In soil, PDMS hydrolyses into the low molecular weight dimethylsilandiol (DMSD) which can evaporate to the upper atmosphere, where the Si – C bonds are cleaved by hydroxyl radicals leading to the degradation products of silica, water and carbonyl compounds. The rate of hydrolysis depends on the type of the soil, pH, temperature, organic material, and particularly the moisture content.

In an early study by Thomas⁴, it was reported that network scission in peroxide cured PDMS rubbers at high (i.e., 250°C) temperatures in a closed system was due to hydrolysis reactions, which did not happen in an open system, probably because of evaporation of any water.

Similarly Patel et al.⁵ conducted an experiment for thermal ageing of polysiloxane rubber in the presence of moisture at temperatures of up to 190 °C, in both sealed conditions and open to air. Their results confirmed the findings of Thomas⁴ which was that siloxane rubber aged in a sealed system softened with time, whereas samples aged open to air did not. Patel et al.⁵ also suggested that ageing in the sealed environment led to compression set which was due to hydrolysis of the PDMS.

Chaudhry and Billingham⁶ showed that silica filled PDMS rubber was highly resistant towards oxidative degradation at high temperatures (180 – 200°C) in both air and inert conditions. This proves that silicone rubber vulcanizates are very stable at high temperatures in open systems where the effect of water is minimal. From these studies it became apparent that water is the main trigger for the breakage of siloxane bonds, which leads to network scission in PDMS.

An acidic environment under humid conditions can accelerate the degradation of silicone rubber to a great extent. Umeda et al.⁷ investigated aged silicone rubber housing for a polymer insulator used at a testing station near the sea coast. The FTIR analysis confirmed that the ageing mode was similar to damage caused by nitric acid. A strong acid environment (i.e., pH = 0 – 2.0) was measured on the housing during a fog test, due to corona discharge on the silicone rubber housing under humid conditions. Based on the same approach as Umeda et al., the deterioration mechanism of the silicone rubber housing by corona discharge was examined by Koshino et al.⁸ The polymer insulator samples were exposed to an artificial fog condition in a test chamber and surface changes were observed during the test as a result of the corona discharge. It was suggested that nitric acid generated by corona discharges in humid conditions causes deterioration of the housing rubber surface as discoloration and deposition of a white powdery substance. Consequently, it can be concluded that silicone rubber may not be a good choice of material when a strong acid environment is present.

The change in surface chemistry of liquid silicone rubber (LSR) aged in de-ionized water (at 100°C) for two years was also monitored by Ghanbari-Siahkali et al.⁹ Silicone rubber can be stable at temperatures as high as 300°C in air by replacing of the methyl side groups in the side chain of the rubber backbone (e.g., PDMS) with phenyl groups. Yet, these silicone rubbers have limited hydrothermal stability which constrains their service temperature to a maximum 120°C in the presence of water, steam, acidic and alkaline environments. From their FTIR and XPS results, Ghanbari- Siahkali and his team suggested that the hydrothermal degradation of LSR involves chain scission through hydrolytic attack on Si – O – Si bonds.

The decomposition of methyl groups attached to silicon atoms (in the side chains i.e., $-\text{Si}-\text{CH}_3$) can be replaced with OH (hydroxyl) groups, if acidic or alkaline conditions are present. The authors also assume that the other less likely step in the degradation process could include attack on unreacted vinyl side groups ($-\text{Si}-\text{CH}=\text{CH}_2$), used as cross-link sites, generating OH (hydroxyl) groups. Figure 4.1 shows this possible degradation mechanism of LSR. In all cases, these reactions would result in oxidation and breakdown of the LSR (i.e., hydrolysis). Additionally, they found out that the physical properties of LSR upon the exposure to water for a prolonged time were altered, for instance the surface hardness increased linearly as a function of exposure time due to degradation.

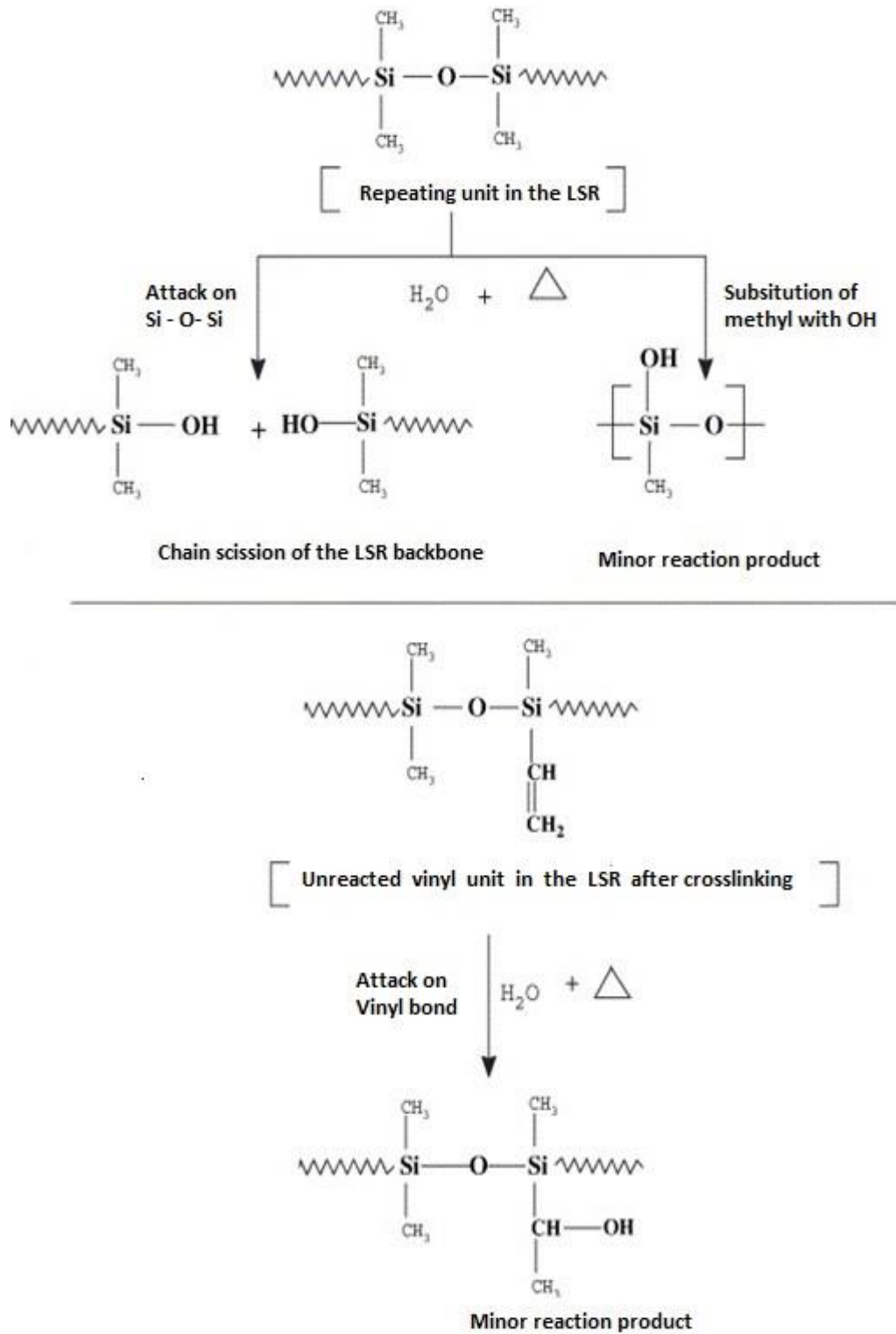


Figure 4.1. The hydrothermal degradation mechanism for LSR in Deionised (DI) water⁹

EPDM Rubber

EPDM rubber is used widely as seals and gaskets in many industrial applications including fuel cells. In published literature, there are just a few reports discussing the chemical degradation of EPDM in specific acidic environments in relation to PEM fuel cells. Mitra et al. conducted a number of studies concerning the chemical degradation of EPDM rubbers in aggressive aqueous chemical environments¹⁰⁻¹³. They investigated the chemical degradation of cross-linked EPDM rubber with both peroxide and sulfur systems in a 20 % Cr/H₂SO₄ (CSA) acidic solution for various periods from 1 to 12 weeks^{10,11}. The XPS and ATR-FTIR results along with crosslink density measurements revealed that the crosslink sites underwent hydrolytic attack. The carbon-carbon double bond (C=C) of ENB present in EPDM as diene was also attacked by aqueous acid solutions. Surface degradation affected the bulk properties, but the EPDM backbone was found to be stable under the examined chemical degradation environment.

In another study by Kole et al.¹⁴ hydrothermal weathering of peroxide cured silicone rubber, EPDM rubber and their 50:50 blends was carried out for various durations at different temperatures. It was found out that silicone rubber was very susceptible to degradation whereas EPDM and its blend (50:50) with silicone rubber showed excellent weathering resistance. The rubber test samples were weathered in water and steam over a range of aging temperatures (170 – 210°C) and aging periods (24 – 384 h) in the pressure vessels. The results indicated that the modulus, tensile strength and elongation at break of silicone rubber decreased linearly with aging period. The elongation at break of the specimens weathered for 72 h at 210°C fell even under 50 %, which means that in practical terms silicone rubber lost its elastomeric property. On the other hand, EPDM and its blend with silicone rubber maintained more than 50 % elongation (its elastomeric nature) over a wide range of aging periods and temperatures (e.g., 96 h at 210°C and 384 h at 170°C). The mode of degradation for silicone rubber was hydrolytic chain scission as confirmed by other researchers⁹. Tensile strength and modulus decreased consistently with degradation. Generally, the reduction in modulus, which is caused by the scission of some of the network chains, gives a qualitative measure for the extent of degradation consequently, the hardness reduced with prolonged aging.

The weight loss of weathered silicone rubber samples was also observed, indicating the leaching of oligomeric species. The weight loss was higher in weathering in water than in condensed steam, suggesting that water is an effective leachant for the oligomeric products. In the case of EPDM, the weathering process was dominated mainly by crosslinking reactions. The modulus remained at the same value as for the un-aged sample. Furthermore, the presence of EPDM in the blend improved the aging behaviour significantly. The authors concluded that the properties of silicone rubber deteriorate in humid environments at high temperatures but this can be improved by blending it with EPDM ¹⁴.

Fluorinated Elastomers

Although fluoroelastomer copolymer (FKM) is an expensive rubber, it is still considered for automotive applications including fuel cells, thanks to its excellent resistance to degradation.

One of the most common application areas of FKM seals is in submerged pumps where they are exposed to a range of aqueous solutions such as strong alkalis. Mitra et al.¹⁵ carried out a study regarding to the chemical degradation mechanism of FKM (Viton ®) under an alkaline (10% NaOH solution) environment at 80°C for various periods of time (1 to 12 weeks). The degradation mechanism was reported as de-crosslinking through hydrolysis of the cross links, followed by chain scission in the backbone via a process of dehydrofluorination. Cracks were observed on the surface after prolonged exposure as an indication of chemical degradation. The extent of this surface degradation also affected bulk mechanical properties.

Sugama. T¹⁶ carried out aging experiments in a hot geothermal brine reservoir at 150°C, in order to determine the changes in the surface chemistry of an FKM bearing material. The main degradation was thermal decomposition due to the high temperature. It was observed that the surface underwent hydrothermal oxidation by the attack of hot brine. This causes the integration of oxygen into the elastomer leading to the scission and breakage of C–F and C–C bonds in the polyfluorocarbon chain.

Kalyafan et al.¹⁷ used a chemical stress –relaxation method to determine the network changes taking place in the thermally aged fluororubber (FKM).

In their work, they carried out stress relaxation measurement at temperatures from 120 to 300°C in various media (including air, nitrogen, and fuel). The results showed that FKM experienced cross-linking as well as chain scission during thermal aging in both air and nitrogen. In addition, the relaxation due to chemical changes is generated more rapidly by atmospheric oxygen than by thermal effects under the experimental test conditions used.

Fluorosilicone rubber (FVMQ) is another material which is considered as a candidate for PEM fuel cell gasket applications. Like FKM, fluorosilicone rubber is deemed as a high-temperature and hydrocarbon fuel resistant rubber. Most of the investigations regarding the chemical degradation of FVMQ in acidic and humid environments have been conducted under PEM fuel cell conditions, which will be discussed in the following section.

In another investigation by Kalfayan et al.¹⁸ accelerated heat ageing (at around 300°C) of FVMQ was carried out by using a chemical stress relation test similar to that used in their degradation study of FKM¹⁷. It was observed that FVMQ underwent a similar degradation mechanism (i.e., chain scission and crosslinking) to FKM during thermal aging¹⁷.

Thomas¹⁹ reported that the chemical degradation of FVMQ at 200°C could lead to hydrolytic scission at siloxane (Si – O – Si) bonds in the main polymer chain and oxidative scission at the hydrocarbon crosslinks, which was the same mechanism suggested for silicone rubber in the literature³⁻⁹.

4.2.2. Degradation in Accelerated and Simulated PEM Fuel Cell Environments **Ex-situ Accelerated Aging Tests:**

It can be very time consuming and costly to operate a fuel cell for thousands of hours to collect durability information about the degradation of elastomeric seals. For this reason, ex-situ accelerated aging test have been developed and are used to gather this information in a shorter time.

This knowledge is utilised to understand the accelerated degradation profile of the seal material and it is incorporated into models to predict the possible lifetime of the seals in the real fuel cells^{5,20}.

In most accelerated aging studies, sealing materials are exposed to a mixture of various acids at temperatures similar to those of real fuel cells. In some cases, compressive load is applied to the materials to simulate the real loading on seals in PEM fuel cells.

Factors such as weight change and the release of the chemicals are used as evidence for the stability of the seals. Samples from the degraded seal material are analysed to reveal changes in the composition of the material. In addition, some mechanical test methods including micro indentation and dynamic mechanical analysis (DMA) are used in the aging studies to assess the effect of chemical degradation on mechanical and physical properties. The used accelerated aging solution can also be analysed to detect any ions which have been leached out from the gasket material as a result of chemical degradation. The conditions of the accelerated aging tests and simulated PEM fuel cell environments as well as descriptions of analysing techniques will be given in detail in the following sub sections.

Accelerated and simulated aging conditions such as the test temperatures and the composition of the accelerated aging solutions are chosen according to the operating temperatures and environment of actual PEM fuel cells. For instance, test temperatures have been selected at 60°C – 80°C which are close to the operating temperature of real PEM fuel cells. An example of a chemical environment used to simulate a real fuel cell is; 12 ppm H₂SO₄, 1.8 ppm HF and a pH value of 3.35²¹. An example of solution used to accelerate the degradation of gasket materials is 1M H₂SO₄, 10 ppm HF with a pH value less than 1²². The strength of the aging solution can be adjusted by changing the concentration of the acid in the solution.

Weight Change:

Tan et al. observed the weight change of gasket materials with degradation in several studies^{21,23 - 25}. All the results agreed that silicone rubber experienced weight loss increasing with exposure time as a result of degradation. For example, Figure 4.2 shows that weight loss of silicone rubber gasket material increases with both time and temperature on exposure to aging solution²¹.

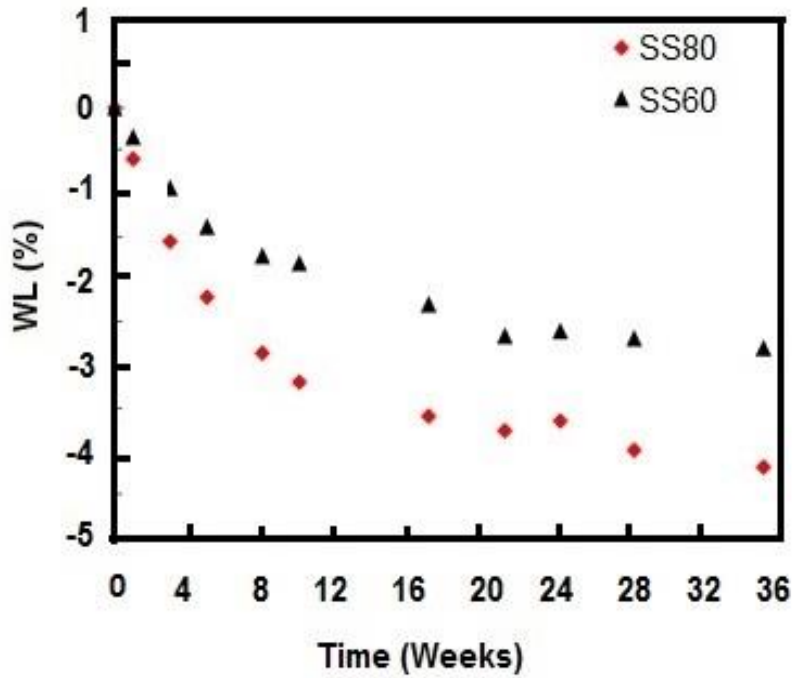


Figure 4.2. Weight loss of silicone rubber with exposure time in the aging solution (12 ppm H₂SO₄, 1.8 ppm HF) and at 60°C & 80°C²¹

Tan et al.²⁴ investigated the effect of concentration of acid on weight loss of silicone rubber seal material on aging. Figure 4.3 demonstrates the weight loss of the silicone rubber samples with exposure time in various test solutions at 70°C. The Regular solution (RS) was similar (pH ~ 3.35) to the real PEM fuel cell environment and the four accelerated durability test (ADT 1, 2, 3, 4) solutions, had higher acid concentrations. The concentration of hydrofluoric acid (HF) increased from ADT1 to ADT4 while the concentration of sulfuric acid (H₂SO₄) remained the same. The data in Figure 4.3 indicates that the higher the concentration of the HF acid in the test solution, the more the weight loss²⁴.

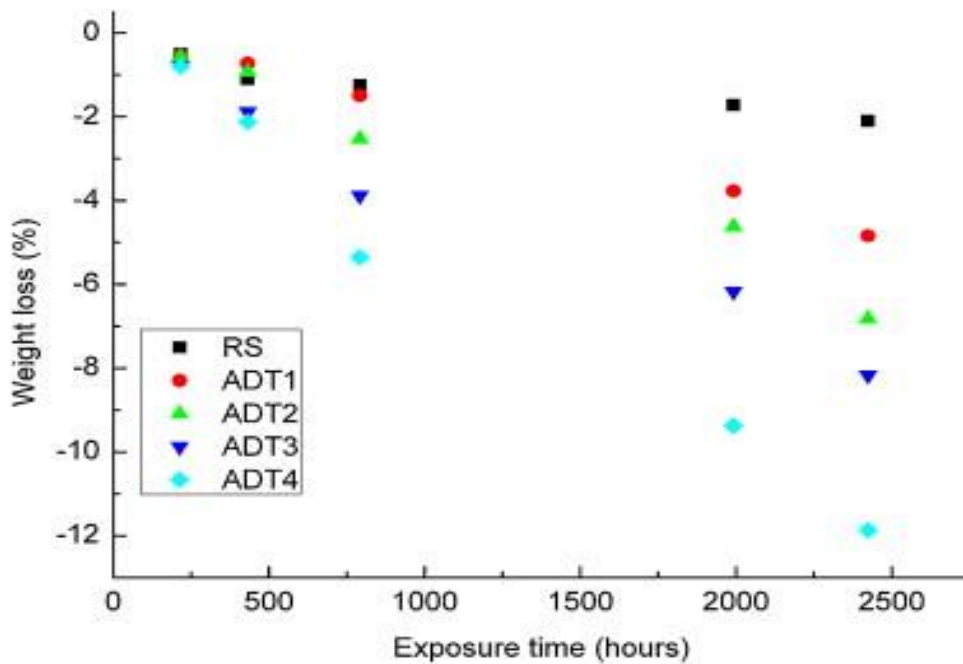


Figure 4.3. Weight loss of silicone rubber with exposure time at 70°C²⁴

In another study by Tan et al.²⁵, the influence of stress on the gasket materials, which is caused by the bending of the sample, in the degradation phenomena was investigated in order to see the effect of the stress in the degradation. Their results showed that the silicone rubber samples which were bent to 120° degraded faster in the aging (ADT) solution at 80°C than the silicone rubber samples with the bend angle of 90° and no bend under the same conditions. Therefore, it was concluded that applied stress in the sample can accelerate the degradation of the materials with time.

The weight change of silicone rubbers S and G grades, EPDM (EP) and fluoroelastomer (FL) sealing materials having 120° bend angle (exposed to ADT solution / short term accelerated aging at 80 and 60°C) was also by measured in the same study by Tan et al.²⁵ and the data is shown in Figure 4.4. It can be seen clearly that both silicone grade materials (SS &SG) degraded as presented by their weight loss. EPDM (EP) and fluoroelastomer (FL) samples showed only a slight increase in weight after 1 week. Afterwards, they maintained a constant weight with time. It was underlined that generally, the higher the temperature, the more material loss. Both EPDM and fluoroelastomer are least affected by degradation compared to silicone rubber²⁶.

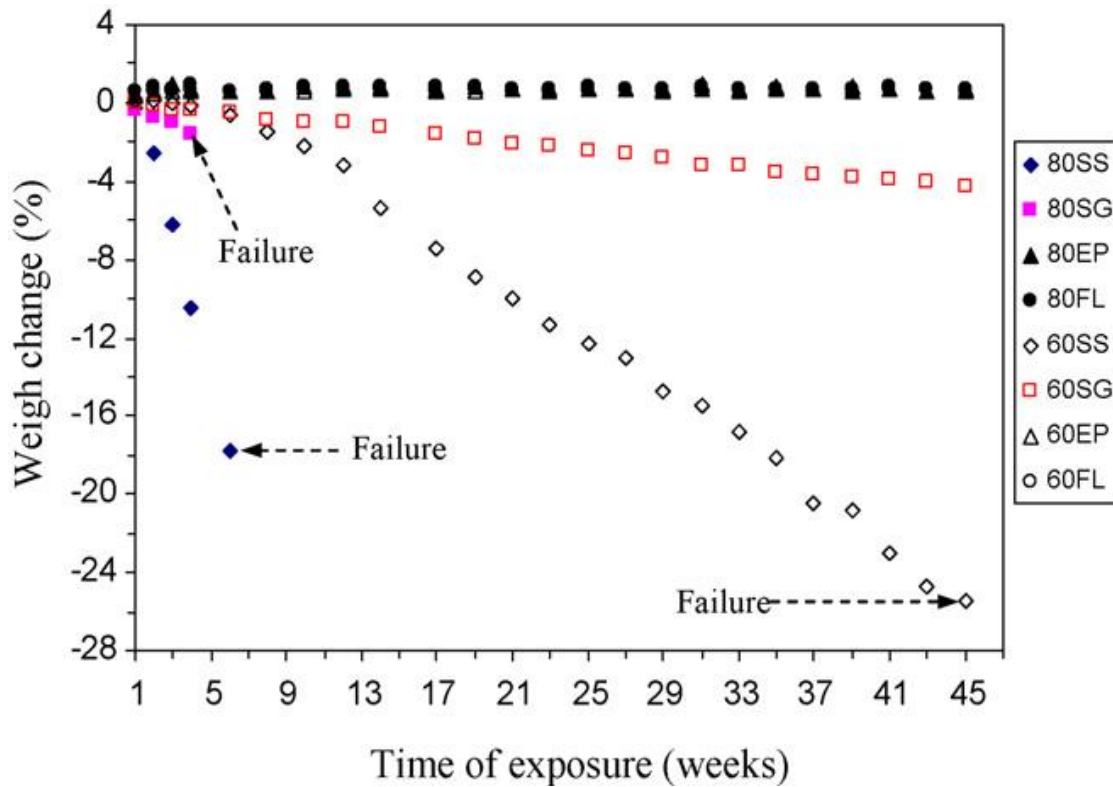


Figure 4.4. Weight change with exposure time for samples having 120° bend angle in ADT solution at 60°C and 80°C²⁶

Lin et al.²¹ inspected the weight change of five gasket materials under similar aging conditions to those discussed in the previous section. In their experiment, they aged EPDM rubber, copolymeric resin (CR – a silicone resin), liquid silicone rubber (LSR), fluorosilicone rubber (FSR) and fluoroelastomer copolymer (FKM) in a regular and an ADT solution at 80°C. Figure 4.5 shows that in the regular solution, both EPDM and FKM gained weight gradually with time. This was explained as being due to the formation of some crystal species on the surface of the EPDM and FKM samples which were observed by optical microscopy. These crystals were expected to be MgSO₄. It could be that MgCO₃ used as filler in the rubber can form MgSO₄ in the sulfuric acid solution and therefore crystals on the surface as hard particles. However, the weights of EPDM and FKM were almost unchanged in the ADT solution even though ADT solution was more acidic than the regular solution signifying their good acid resistance. Copolymer silicone (CR) and liquid silicone rubber (LSR) lost weight progressively in the ADT solution while they remained about the same weight in the regular solution.

It was suggested that higher concentration of the acid in ADT solution corroded more out of CR and LSR materials but not EPDM and FKM.

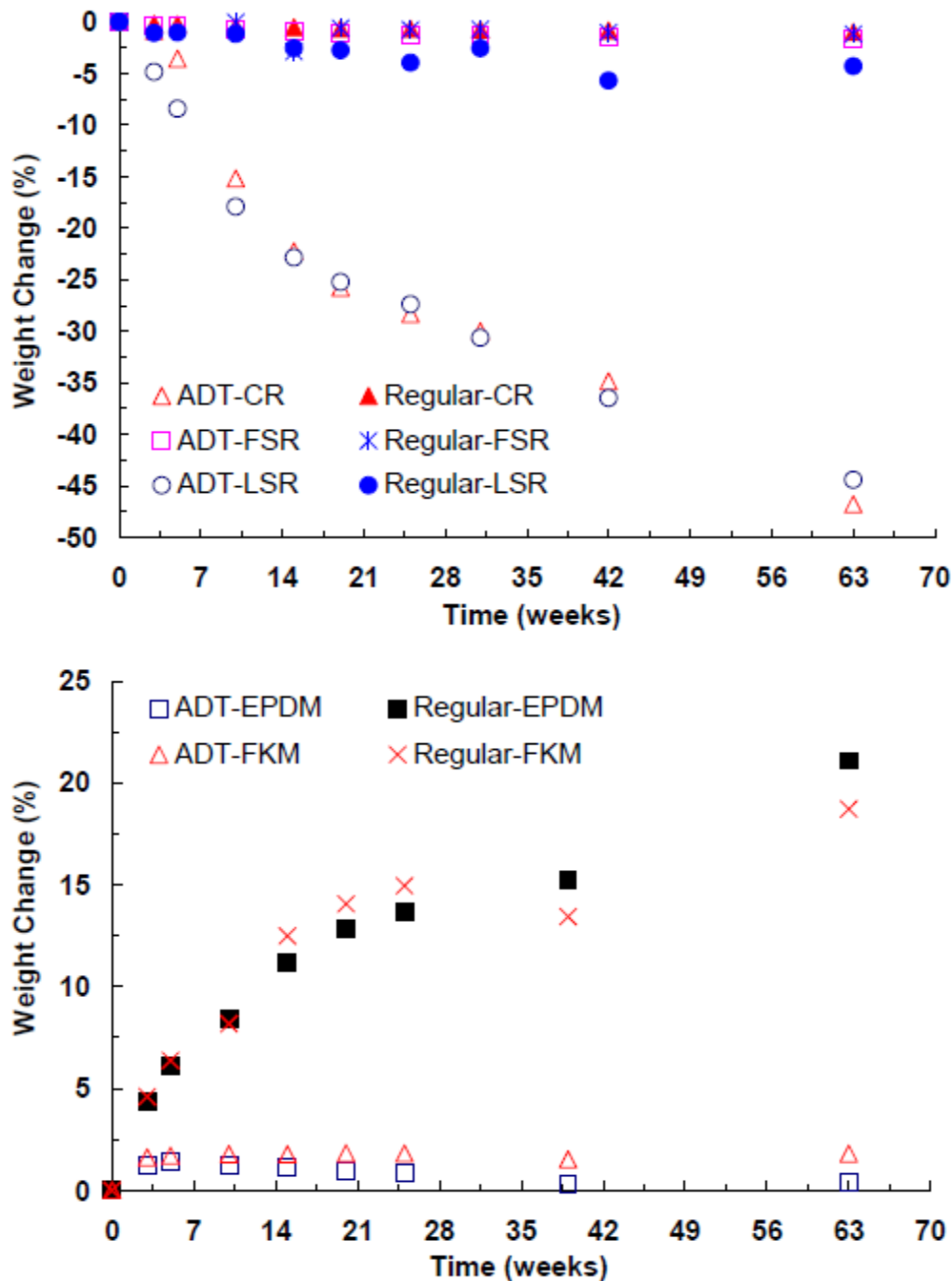


Figure 4.5. The weight change of five gasket materials over time in Regular (pH 3.35) and ADT (pH < 1) solutions at 80°C²¹

Surface Change-Optical Microscopy:

Optical microscopy is employed to observe the topographical changes on the sample surfaces with degradation.

Silicone Rubber

The surfaces of silicone rubber samples which had been subjected to accelerated aging were examined by using optical microscopy by Tan et al.^{22,24-25} and Li et al.^{23,26}. All the results from these studies indicated the same level of surface degradation of silicone rubber over time. It can be clearly seen from Figure 4.6 that the surface of the silicone rubber exposed to ADT solution (pH < 1) changed over time from originally smooth to rough, then to a cracked surface and finally crack propagation was observed. The magnitude of surface damage at 80°C was more severe compared to 60°C under identical acid conditions²².

The surface degradation of the silicone rubber samples, which were bent to different angles, prior to exposure to the same conditions, was also investigated by Tan et al.²⁵ It was proposed that the applied stress (due to the bending) in the samples, contributed to crack propagation.

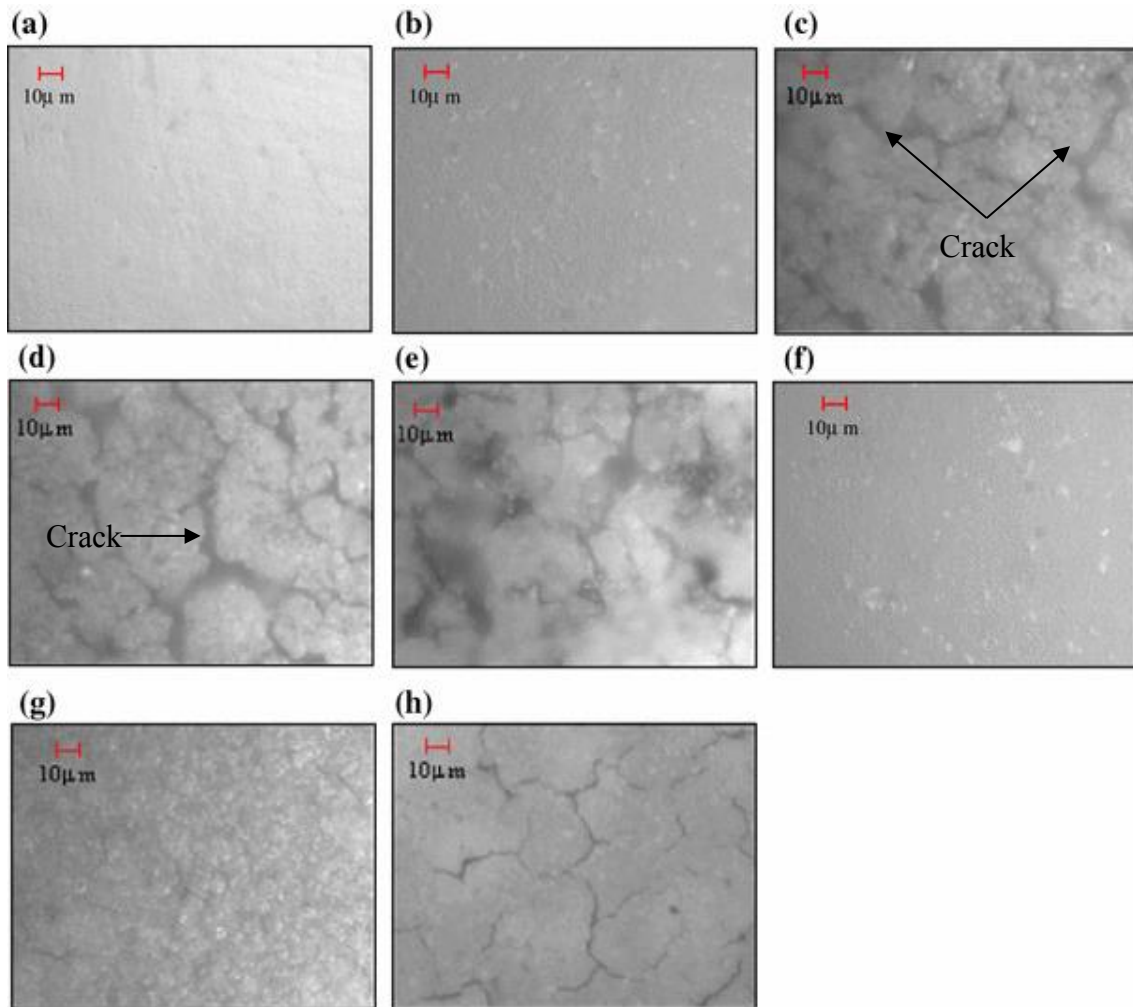


Figure 4.6. Optical micrographs of silicone rubber samples before and after exposure to ADT solution at 80 and 60°C. (a) Before exposure, (b) 1-week exposure at 80°C, (c) 3 -week exposure at 80 C°, (d) 5 -week exposure at 80°C, (e) 17 -week exposure at 80°C, (f) 5- week exposure at 60°C, (g) 17 -week exposure at 60°C, (h) 45 -week exposure at 60°C²²

EPDM

In the case of EPDM,²⁸ the surface condition of the samples did not change with ageing and there were no cracks observed up to 35 week exposure under the same accelerated ageing conditions as those used by Tan et. al^{22, 24-25} for silicone rubber. As demonstrated in Figure 4.7 the optical micrographs for the EPDM did not show a significant change except the slight roughness on the surface appeared after exposure to the solution at 80°C [See Figure 4.7(b), (c), (d) and (e)]. It was reported that unlike silicone rubber, the surface topography of the EPDM material did not present time – dependent chemical degradation under the same test conditions²⁸.

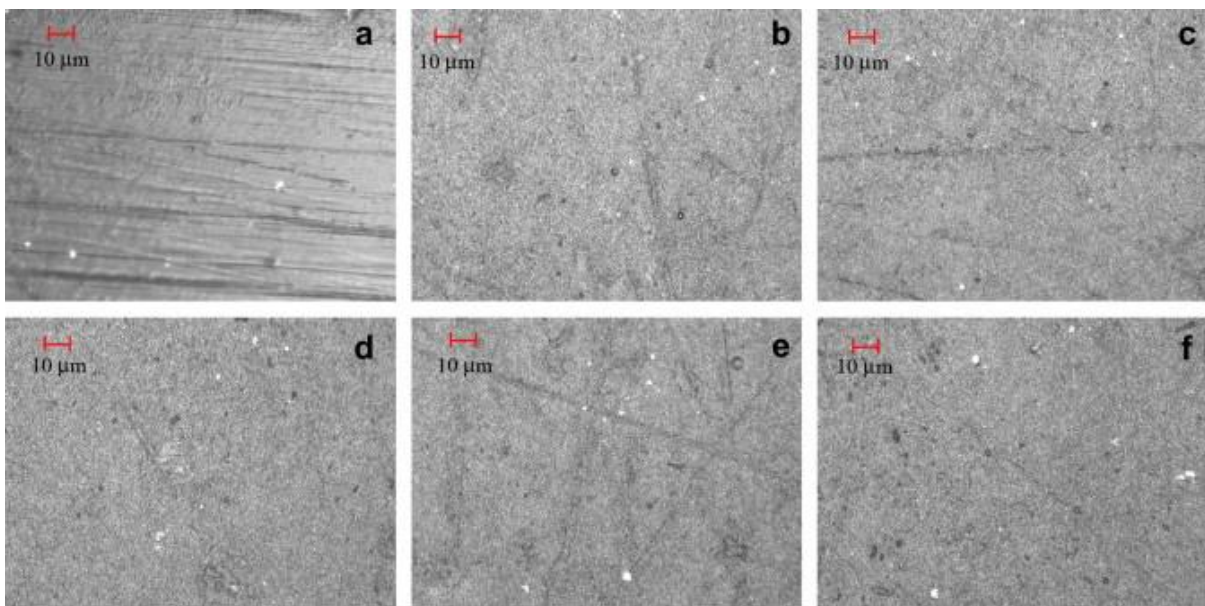


Figure 4.7. Optical micrographs of EPDM samples before and after exposure to the solution at 80 and 60°C. (a) Before exposure, (b) 10 -week exposure at 80°C, (c) 17 –week exposure at 80°C, (d) 24 –week exposure at 80 C°, (e) 35 –week exposure at 80°C, (f) 35 –week exposure at 60°C²⁸

The Other Seal Materials (FKM and FSR)

EPDM and FKM underwent surface degradation to some extent but only the crystals (i.e., MgSO_4) were formed on the surface with time rather than cracks. In addition, they did not face any fading of surface colour either.

The result from optical microscopy also showed that the surface of aged EPDM was smoother than aged FKM material possibly indicating that FKM had more degradation activities than EPDM²⁹. The ageing conditions were the same as some other silicone rubber studies²³⁻²⁶.

ATR-FTIR (Fourier Transform Infrared)

ATR-FTIR analysis was used to determine the change in the surface chemistry of gasket materials with degradation.

Silicone Rubber

A number of other studies including those conducted by Tan et al.^{21,23,25,26} and Li et al.^{24,27} investigated the surface chemical degradation of silicone rubber after exposure to simulated and accelerated PEM fuel cell environments.

Figure 4.8 shows the ATR-FTIR spectra for the silicone rubber samples under a constant compressive load and in the accelerated aging solution ($\text{pH} < 1$) at 80°C up to 12 weeks exposure²⁵. The broadest peaks for the unexposed samples occurred between 1015 and 1080cm^{-1} which was due to the stretching vibrations of Si-O-Si groups in the silicone backbone as seen in Figure 4.8(A). The peaks at 866cm^{-1} and 1260cm^{-1} were from the rocking vibration of Si- CH_3 and the bending vibration of Si- CH_3 . The peak near 1418cm^{-1} was highlighted the rocking vibration of $-\text{CH}_2-$ as a part of the silicone rubber cross-linked region. The peak appeared at 2960cm^{-1} was from the stretching vibration of CH_3 (see Figure 4.8-B). It is clear in Figure 4.8(A) that the intensity of the peaks between 1015cm^{-1} and 1080cm^{-1} decreased sharply after 5 week exposure and almost disappeared after 10 week at 80°C . Similar trends can be observed for the characteristic peaks at 866cm^{-1} , 1260cm^{-1} and 1418cm^{-1} in Figure 4.8 (A). The peak at 2960cm^{-1} also followed a similar trend as shown in Figure 4.8 (B).

Additionally, a group of new peaks emerged at 1040cm^{-1} upon prolonged exposure which could be from the stretching vibration of Si-O as a result of the chemical structure changes²⁵.

All the other papers^{21, 23,24,26,27} obtained similar results from the ATR-FTIR analysis of the aged silicone rubber. In conclusion, all those reports suggested that the silicone rubber backbone and the crosslink sites in the rubber were chemically changed over time as a result of acid hydrolysis.

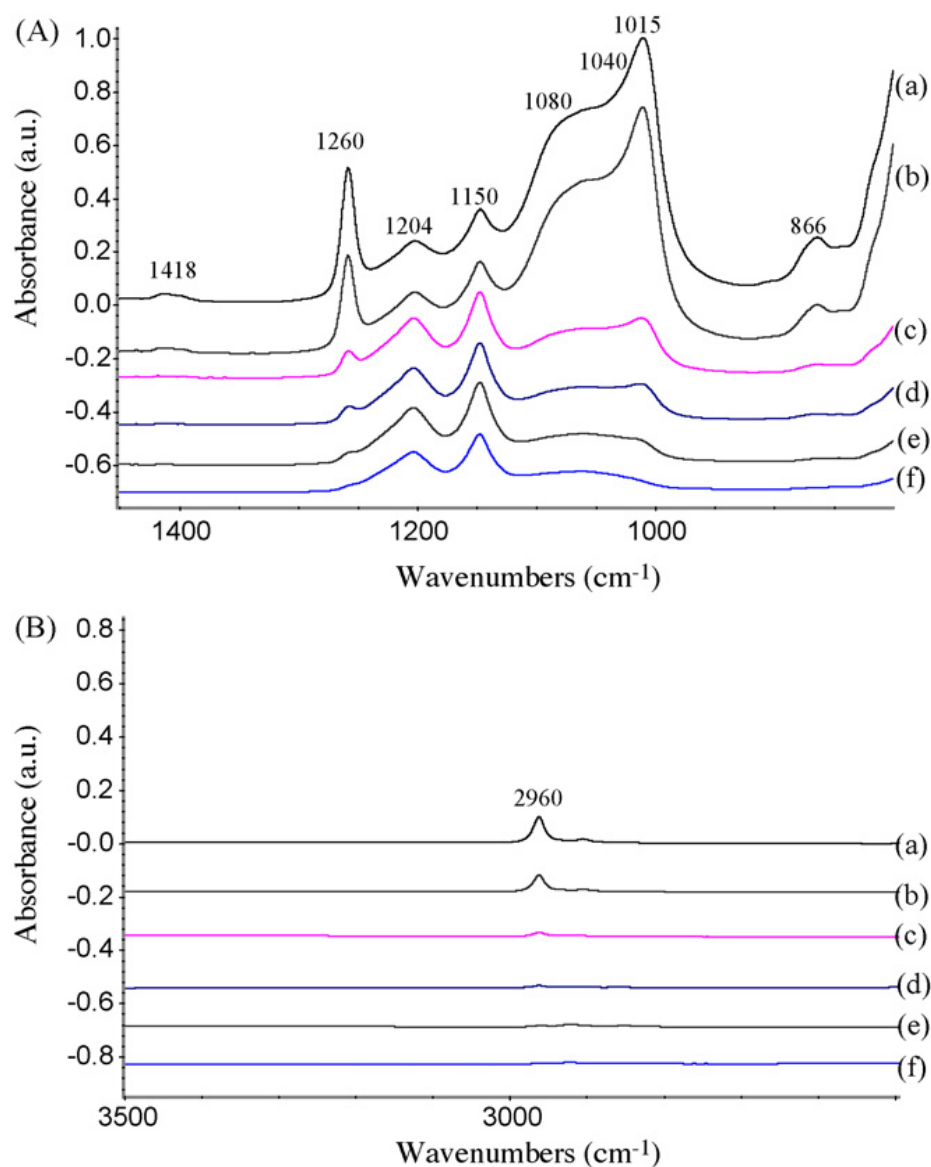


Figure 4.8. ATR-FTIR results for silicone rubber material exposed to aging solution at 80°C and subjected to compressive load : a-without exposure and after b-3 week, c-5 week, d-7 week, e-10 week and f- 12 week exposure. ATR-FTIR spectra from (A) 800 – 1450cm –1 and (B) 2500 – 3500 cm⁻¹ ²⁸

EPDM

The ATR – FTIR technique was also employed to identify the changes in the chemical structure of EPDM gasket material with accelerated aging by Tan et al.²⁸. Figure 4.9 shows that the spectra did not change much with aging time. Only the peaks at 1740 cm^{-1} and 1100 cm^{-1} experienced some changes. The decrease in intensity of the peak at 1100 cm^{-1} was accounted for by the filler (SiO_2) reacting with the acid. The change of the peak at 1740 cm^{-1} could be as a result of carboxylates or vulcanisation products present on the material surface.

The study²⁸ concluded that EPDM material did not undergo significant chemical change after being subjected to the acidic aqueous solution with a pH value of 3.35 at 60°C and 80°C .

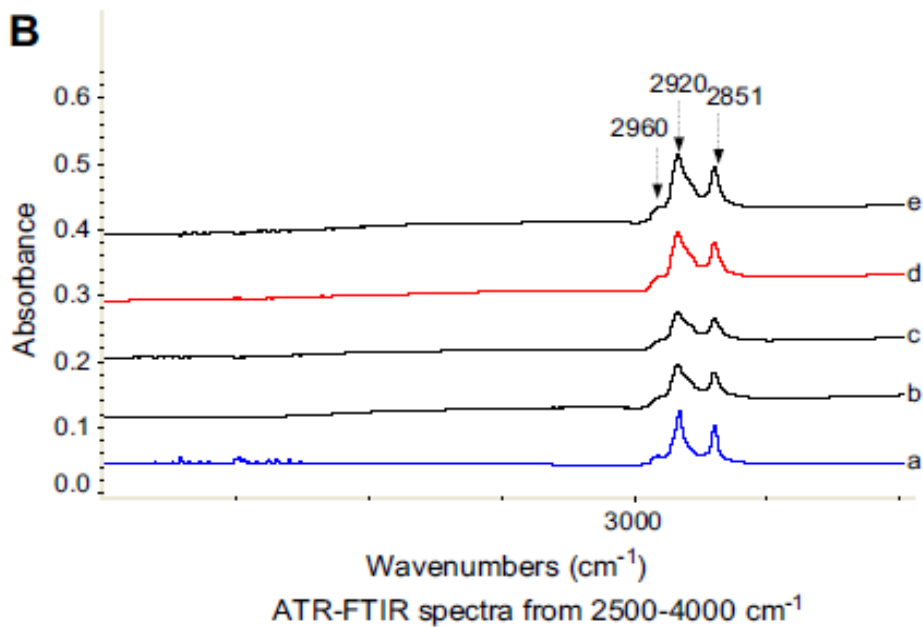
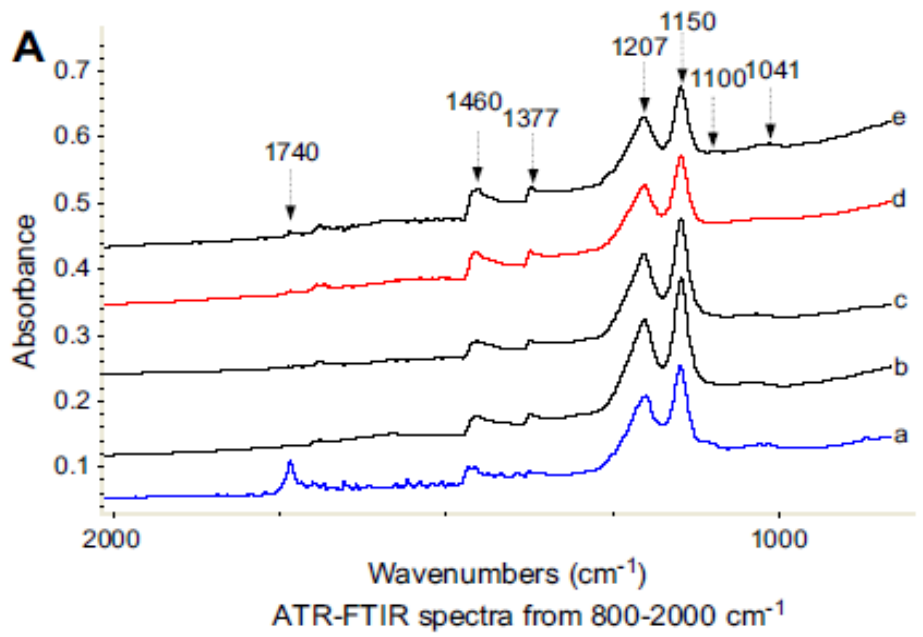


Figure 4.9. ATR-FTIR results for EPDM material in the aging solution at 80°C : a-without exposure and after b-5 week, c-24 week, d-28 week and e-35 week exposure²⁸

Other Seal Materials (FKM, FSR)

Lin et al.²² investigated the changes in the surface chemistry of CR, LSR, FSR, EPDM and FKM gasket materials in both a Regular solution with the pH value of 3.35 and an ADT solution with a stronger acidity (i.e., pH < 1). ATR-FTIR results showed that all the materials were affected more by the ADT solution than the Regular solution in terms of surface degradation. FKM and EPDM were more chemically stable than CR and LSR in the ADT solution. FSR appeared to be the most stable of the five materials as its FTIR spectrum did not change in either Regular or ADT solution over time. This was parallel to the weight change results for FSR which were observed to be constant in both solutions²².

X-ray Photoelectron Spectroscopy (XPS)

XPS is another surface technique, like ATR-FTIR, used to study the surface chemistry of the PEM fuel cell gasket materials exposed to accelerated aging test²⁶.

Silicone Rubber

Tan et al.²³ performed an XPS study on silicone rubber before and after exposure to an ADT solution (pH <1) at 80°C. The XPS spectra are shown in Figure 4.10 and atomic concentrations and ratios are shown in Table 4.1. The C/Si ratio decreased significantly with increasing exposure time. This may indicate that the methyl (CH₃) group on the silicone atom were attacked and oxidized to form Si –O bonds. The O/Si ratio increased slightly with exposure time possibly due to the hydrolytic breakage of the Si –O – Si backbone²³. The oxidation of the methyl groups would also have this effect.

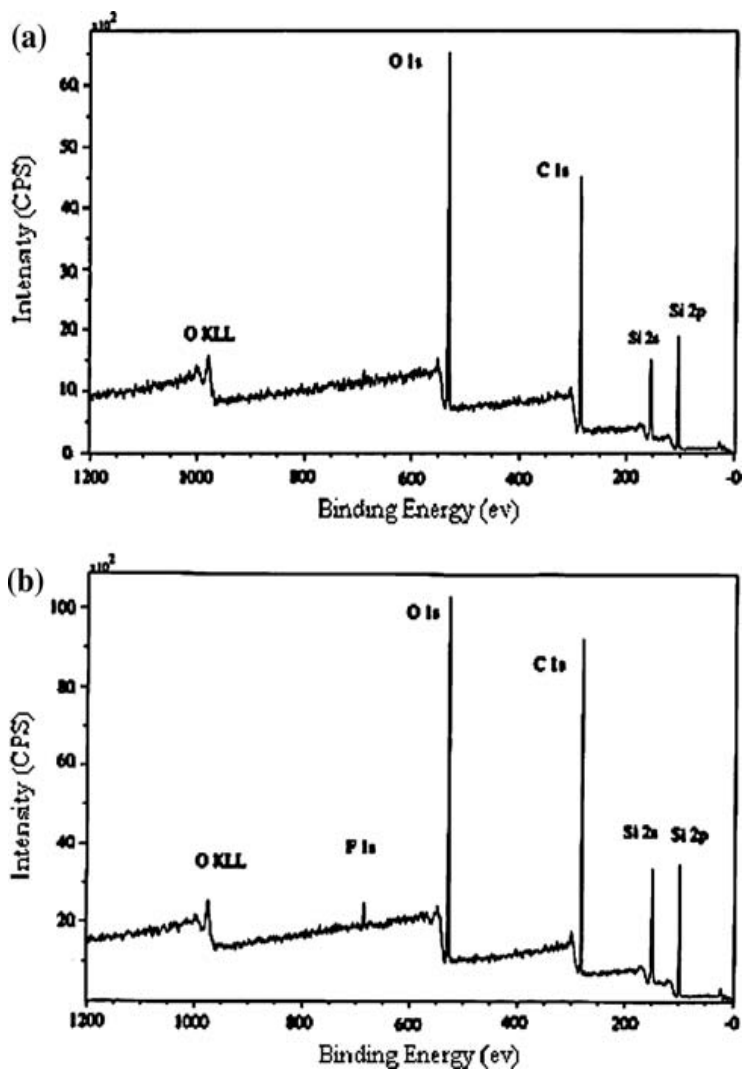


Figure 4.10. XPS spectra for silicone rubber sample (a) before and (b) after 4 week exposure to ADT solution at 80°C²³

Table 4.1. Surface atomic concentration of each element and ratios of atomic concentrations of O and C to Si²³

Sample	Atomic Concentration (at.%)				Ratios to Si	
	C	O	Si	F	C/Si	O/Si
Before exposure	53.29	26.0	20.71	0.0	2.57	1.26
1 week exposure	48.69	29.22	21.51	0.58	2.26	1.36
4 week exposure	48.38	28.87	22.03	0.72	2.19	1.31

The XPS results are consistent with the FTIR observations, indicating degradation progressed via de-cross-linking and chain scission in the backbone^{23,26}.

On top of basic XPS examination, Li et al.^{24,27} carried out a high – resolution XPS analysis. After exposure to accelerated aging solutions with different acidity levels for 1992 h (~ 12 weeks) an additional peak due to SiO₂ appeared indicating further oxidation of the silicone material.

Atomic Adsorption Spectrometry

Atomic adsorption spectrometry has been employed to analyse used accelerated aging solution for the presence of metal ions²³.

Silicone Rubber

Tan et al.^{21,23,25} analysed ADT (pH < 1) solutions which had been used to age silicone rubber at 80°C and 60°C. It was observed that silicon ions had the highest concentration in the solution, followed by calcium and magnesium ions. The authors suggested that these metal ions came from fillers such as silicon dioxide and calcium carbonate present in the silicone rubber which was broken down by the influence of acidic aqueous solution and temperature. The technique is important as leaching chemicals may poison the cell and be harmful to the electro-chemical process of PEM fuel cells²⁵.

EPDM

Atomic adsorption spectrometry analysis was also carried out in the investigation of the chemical degradation of EPDM²⁸. Silicon and calcium ions were detected in the solution due to the presence of silicone dioxide and calcium carbonate fillers in EPDM gasket material.

The Effect of Hardness (Shore A) of the Sealing Materials on Degradation

Silicone Rubber

Very recently Feng et al.³⁰ investigated the influence of the hardness of the silicone rubber sealing material on its durability. Generally, the hardness (Shore A) of sealing materials which is suitable for PEMFC application, lies in the range of 20– 60.

In this paper, silicone rubber gasket materials with different hardness (30, 40 and 50 Shore A) were exposed to various aqueous solutions at 80°C for 30 days.

Apart from the typical ageing solutions which were used in the other degradation studies as previously explained, an acetic acid solution with pH of 5.0 was employed as a weak acid. Figure 4.11(a) displays the percentage of weight loss of silicone rubber with different hardness over exposure time in the simulated solution (12 ppm H₂SO₄, 1.8 ppm HF in DI water, pH ~3.35). It can be clearly seen that the weight loss increases with increase in hardness. It was suggested in the study that, whilst exposed to aqueous solution, polysiloxane backbone of silicone rubbers swells up and causes the fillers (silicon dioxide and calcium carbonate) to leach out, resulting in the weight loss of the tested material.

The hardness is proportional to the amount of filler in the compound. Therefore, as the hardness increases so does the weight loss due to the leaching out of the filler. The presence of F⁻ in both simulated and strong acid solutions could also cause the chemical decomposition of silicone rubbers under acidic environment.

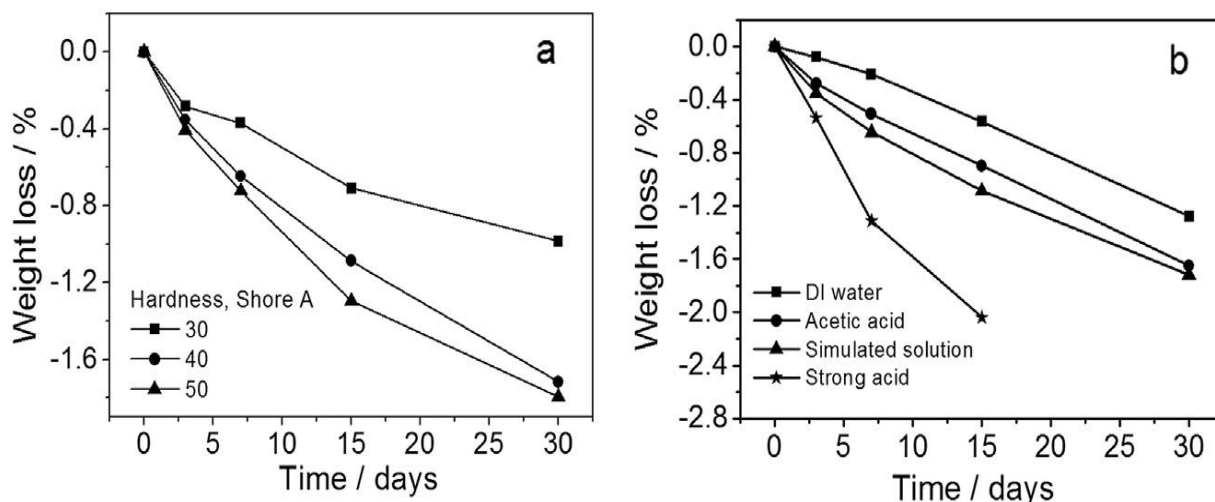


Figure 4.11. Weight loss of silicone rubbers with different hardness after exposure to simulated solution (a) and of silicone rubber with hardness of 40 exposure to different aqueous solutions (b) ³⁰

Change in Physical and Mechanical Properties with Chemical Degradation

Chemical degradation of seals can cause an alteration in the physical and mechanical properties and eventually can lead to a loss in the gasket's sealing function and affect the durability of the fuel cell operation.

There are several standard mechanical test methods to evaluate the mechanical properties of elastomeric gasket materials, including tensile and compressive tests, compression set, compression modulus, Durometer hardness and stress relaxation test. In addition, durometer hardness test gives the shore hardness values as number between 0 and 100, which does reflect a material property (The Modulus). Yet most of these test methods require large size samples³⁰. Thus, microindentation test and dynamic mechanical analysis (DMA) are regularly employed in the degradation studies of fuel cell gasket materials.

Microindentation Test:

Silicone Rubber

Tan et al. and co-workers used the microindentation test in a number of studies^{21, 23,25,31}. The load-indentation depth curves of silicone rubber (S Grade) before and after 35 week exposure to the aging solution (pH 3.35) at temperatures of 60°C and 80°C are shown in Figure 4.12²¹. These tests used displacement control at a peak indentation depth of 0.20mm for the samples. The indentation load at the peak indentation was used as an indication of the surface hardening of the samples with aging. In addition, Figure 4.13 demonstrates the bar charts of indentation load for the same samples represented in Figure 4.12. It can be seen from Figures 4.12 and 4.13 that the samples exposed to the simulated PEM fuel cell (aging) solution (pH ~ 3.35) at 80°C had the largest indentation load, followed by the sample at 60°C and then the unexposed sample. The results imply that the samples exposed to the test environment hardened over time. The extent of surface hardening at 80°C was more than that at 60°C.

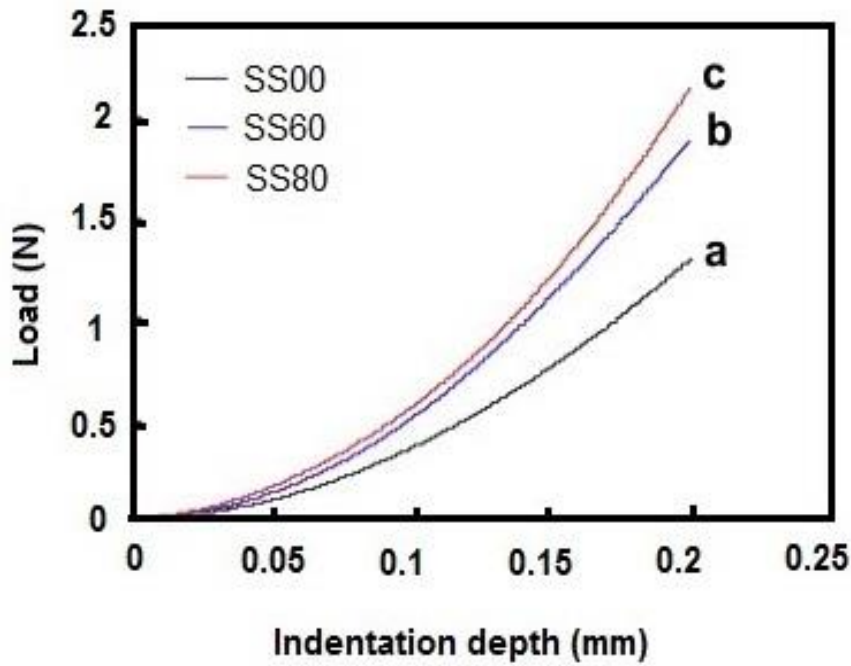


Figure 4.12. Load-indentation depth curves of the silicone samples before exposure (a) and after 35 week exposure to the aging solution (pH ~ 3.35) at 60°C (b) and 80°C (c) at a peak indentation depth of 0.20mm²¹

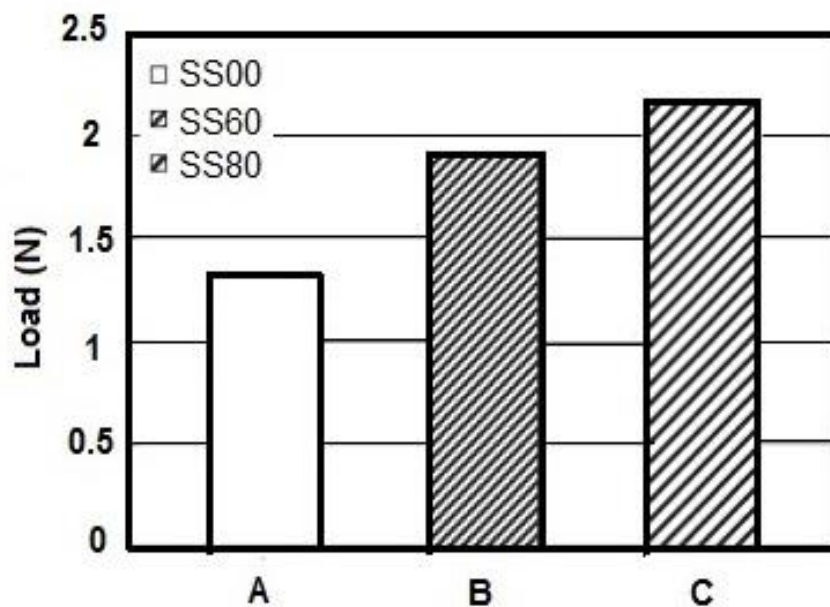


Figure 4.13. Bar charts of indentation load for silicone (SS) samples before exposure (a) and after 35 week exposure to the aging solution (pH ~ 3.35) at 60°C (b) and 80°C (c)²¹

EPDM

The mechanical properties of EPDM²⁸ sealing material was also evaluated, in the study performed by Tan et al., using microindentation test under similar aging conditions as those used for silicone rubber. Figure 4.14 displays the indentation load-depth curves for the unexposed EPDM (EP00) and the samples after 35 week exposure to the simulated fuel cell solution (pH ~ 3.35) at 60°C (EP60) and 80°C (EP80). The bar charts of the indentation load for the same samples were also presented in Figure 4.15.

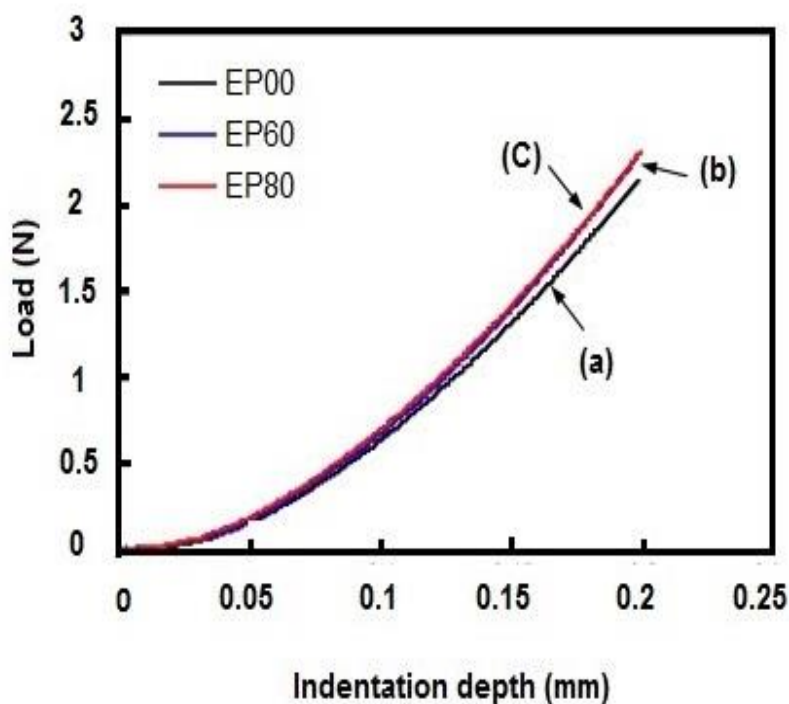


Figure 4.14. Load-indentation depth curves of the EPDM samples before exposure (a) and after 35 week exposure to the solution (pH ~ 3.35) at 60°C (b) and 80°C (c) at a peak indentation depth of 0.20mm²⁸

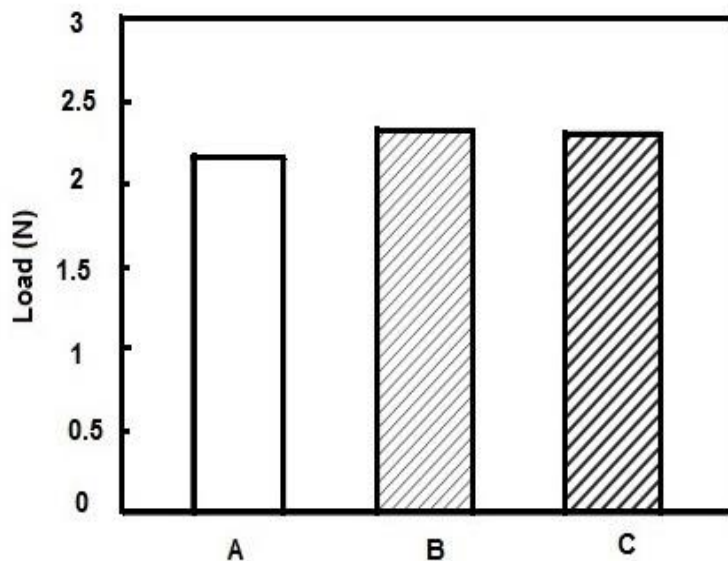


Figure 4.15. Bar charts of indentation load for the EPDM samples before exposure (A) and after 35 week exposure to the aging solution (pH ~ 3.35) at 60°C (B) and 80°C (C) at a peak indentation depth of 0.020 mm²⁸

The data from both Figures 4.14 and 4.15 shows that the samples exposed to the solution at 60°C and 80°C have almost identical indentation load compared to the unexposed sample. It was reported in the study²⁸ that the EPDM samples were not apparently hardened after 35 exposures to the simulated PEM fuel cell environment.

The Other Seal Materials (Fluoroelastomer)

In another experimental work by Tan et al.³² the microindentation test was employed on the Fluoroelastomer (FL) samples along with the ones of EPDM (EP) to compare the mechanical stability of the two gasket materials under compression and upon exposure to an accelerated aging environment. The samples were compressed at three stress level, 0.18, 0.36 and 0.77 MPa and soaked in ADT solution (pH < 1) at 60°C and 80°C for 47 week. Hysteresis loss energy, indentation load, elastic modulus and hardness were acquired from the loading and unloading curves of the indentation test. The results showed that EPDM did not experience any surface hardening after being exposed to accelerated aging.

However, for the Fluoroelastomer samples all these three mechanical properties (e.g., hysteresis loss energy, elastic modulus and hardness) increased.

The study suggested that the exposure medium, temperature and applied compressive load contributed to the degradation of Fluoroelastomer. It was stated that EPDM was more stable than Fluoroelastomer under the accelerated test conditions.

To summarise the above-mentioned findings of the degradation studies for the current and potential gasket materials Chemical degradation of seal materials is observed as weight loss, break – down of the chemical structure as well as leaching of Si, Mg and Ca atoms as a result of fillers in the rubber. Consequently, physical and mechanical properties were affected from the chemical degradation to some extent. However, bulk mechanical properties (i.e., Modulus) of elastomeric gasket materials do not change significantly on aging although surface hardness may increase. Silicone rubber currently used as a PEMFC gasket material is heavily degraded in both simulated (i.e. less acidic pH ~ 3.35) and strong acid (pH <1) solutions. By contrast, EPDM appears to be the most suitable material for PEM fuel cell amongst the other materials, silicone rubber, LSR, FSR and FKM. Especially, resistance of EPDM towards the acidic environment of the PEM fuel cell is an important advantage as chemical degradation seems to be the main issue affecting the seal durability.

4.2.3. Degradation of Silicone Rubber Seals during PEM Fuel Cell Operation Short Term Operation

Husar et al.³³ performed a detailed study on a 7 cell PEM fuel cell stack where the failure of the stack was due to silicone rubber gasket degradation. The fuel cell stack was operated under a variety of pressures (1– 4.5 bar_a), temperatures (25°C –60°C), relative humidity (0 –100 %), and current (0 –5 A). Both air and oxygen were used on the cathode and only pure hydrogen was used on the anode. The cell failed after about 20 h of operation due to a crossover leak (i.e. gas crossed over from one side of the membrane to the other).

Figure 4.16 shows white discoloration at the interface between the GDL and the silicone gasket, indicating chemical degradation had occurred.

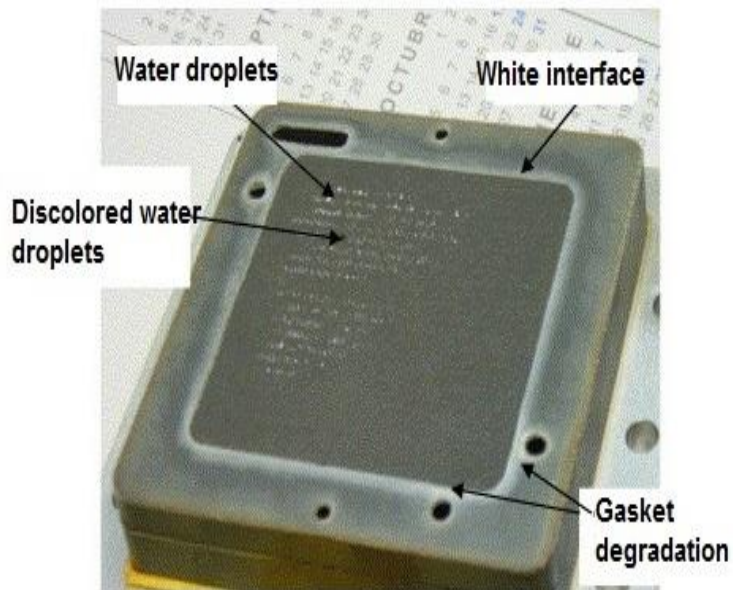


Figure 4.16. Silicone gasket of cell # 2 and cathode GDL attached to the bipolar plate³³

Long Term Operation

Schulze et al.³⁴ studied the degradation of silicone based seals during long term fuel cell operation. They found that silicone seals in direct contact with a perfluorosulphonic acid (Nafion®) membrane degraded chemically at the anode as well as at the cathode resulting in discoloration of the membrane and detectable amounts of silicone on the electrodes. The parts of the membrane surfaces which were in direct contact with the seal became coloured yellow suggesting a chemical decomposition of the sealing material. Silicon from the silicone rubber gasket was detected by XPS in the used electrode, indicating that silicone decomposition products had a high mobility. The combination of this high mobility and the attraction between the decomposition fragments and the platinum catalyst led to poisoning of the catalyst surface. The study concluded that the chemical degradation of the silicone seal was caused by the acidic character of Nafion® membrane along with the thermal stressing of the sealing material but that this occurred without any alteration in its mechanical functionality³⁴.

In another investigation by Ahn et al.³⁵ a very significant decay was observed in the fuel cell performance because of migration of silicone seal degradation products to both anode and cathode catalyst layers.

St-Pierre and Jia³⁶ used a Ballard's PEM fuel cell stack, to carry out an 11000 hours life test for NASA space shuttle applications. Seal samples from both active and humidification areas were analysed by FTIR after completion of the life test. The results revealed that seal was subjected to oxidation and it was more intensive in the humidification section than in the active section.

Cleghorn et al.³⁷ conducted a PEM fuel cell life test of a three years (26.300 h) continuous operation which was the longest life test operation reported. Both the cell temperature and the reactant inlet humidity were regulated at 70°C and 100 % RH, respectively. They measured a reduction in the gasket thickness (approx. 25µm) and observed that the degradation of the silicone was so severe where the gasket was in direct contact with the MEA that only the glass-reinforcement remained.

All the findings suggested that the presence of silicone contamination on both the surface of MEA and GDL, due to the degradation of silicone gasket, may cause decay in the cell performance.

Proposed Degradation Mechanism of Silicone Rubber Gasket Material in PEMFC

In accordance with the ATR-FTIR and XPS results, Tan et al.²⁴ suggested a possible degradation mechanism for the silicone rubber over prolonged exposure to the accelerated test environment (i.e. ADT solution with the pH <1 at 60°C and 80°C) (Figure 4.17). The disappearance of –CH₂– crosslinking in the IR spectra may signify that Si –C bonds (cross-links between polymer chains) were broken through hydrolysis to form Si –OH (silanol groups) as shown in Figure 4.17.

Upon continued exposure to the aging solution, Si –OH groups could be further cross-linked (by the formation of new Si – O – Si bonds as revealed in Figure 4.17).

IR results also indicated that, Si –CH₃ bond may experience similar alteration to that of Si –CH₂ in cross-linking sites to form Si–O. The Si–O could be joined with other Si–O to create new Si – O – Si.

It was concluded that the proposed mechanism for the degradation of silicone rubber was due to de-crosslinking via hydrolysis of crosslink sites and chain scission in the backbone. In addition, the silicone backbone (Si – O – Si) could be attacked by the strong acid (pH < 1), especially hydrofluoric acid (i.e. in ADT solution) to form Si – OH and then Si – OH could be converted into Si –O. This confirms that the acidic aqueous environment is the main reason for the silicone rubber degradation (acid hydrolysis). Siahkali - G. et al.⁹ reported a similar degradation mechanism for cross-linked liquid silicone rubber (LSR) exposed to DI water at 100°C for two years where the chain scission of Si – O – Si backbone occurs via hydrolytic attack upon prolonged exposure (See Figure 4.1).

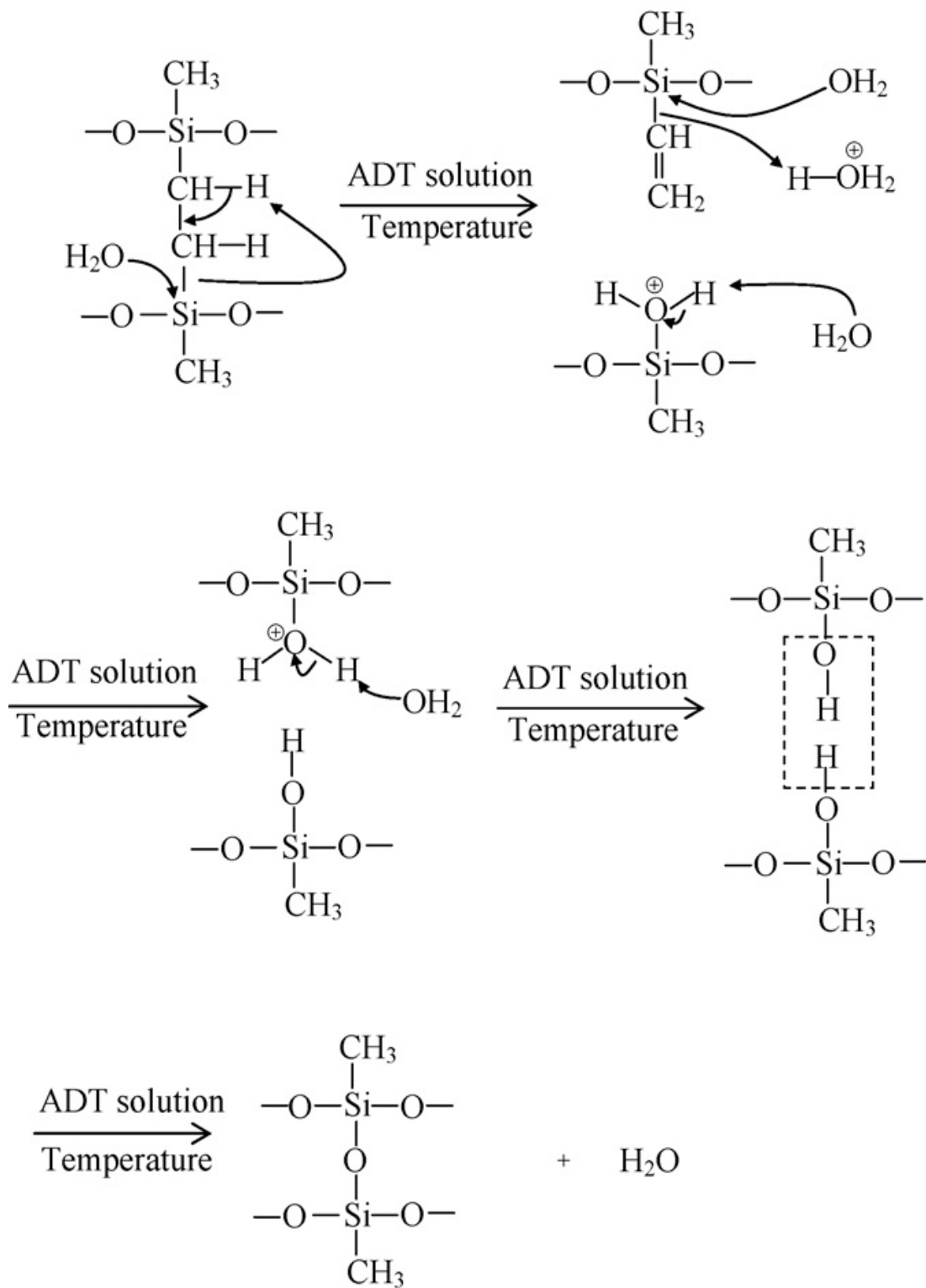


Figure 4.17. The degradation mechanisms of silicone rubber at cross-linked sites of the rubber and combination reaction (in the ageing solution $\text{pH} < 1$)²⁴

4.3. Stress Relaxation in Sealing Materials

The level of compressive stress or pressure at the seal determines its sealing ability. The viscoelastic property of elastomeric seals can result in stress relaxation which can lead to leaking of gas inside PEMFCs during long term operation³⁸. When a constant strain is applied to a rubber sample, the force (stress) required to retain that strain is not constant but declines with time; this behaviour is called *stress relaxation*. Conversely, when a rubber sample is subjected to a constant stress (force), an increase in deformation takes place over time; this behaviour is called *creep*³⁹.

Stress relaxation of an elastomer can be caused by a mixture of factors such as physical relaxation, chemical relaxation and thermal degradation. Physical relaxation occurs when molecular chains rearrange themselves. Physical relaxation usually happens at the beginning of stress relaxation and is largely recoverable upon removal of the strain. Chemical relaxation and thermal degradation is caused by chemical bonds breaking or forming. Either the cross-links or the polymer backbone can be broken, or additional crosslinks can be created. Chemical relaxation typically occurs later in the stress relaxation process and is believed to be irreversible^{38,39-40}. Usually, at normal to low temperatures and for short times, stress relaxation is dominated by the physical processes, whereas, at high temperatures and long time periods, the chemical processes are dominant.

Stress relaxation tests have been commonly applied to seals used in many applications in order to validate seal performance and estimate the lifetime of the seal. Stress relaxation measurements can be carried out in compression, shear or tension, but in practice, usually only tension and compression are used⁴¹. Compression stress relaxation (CSR) tests are more relevant to sealing applications because service lifetime is determined mainly by the deterioration in compressive force between seal and its joining surface. Typically, CSR techniques measure the decrease in stress (force) with time under constant strain conditions⁴².

4.3.1. Modelling of Stress Relaxation Behaviour and Lifetime Predictions of Seals

In general, the reaction rate of a chemical reaction usually increases with increasing temperature. Hence, in the degradation studies of elastomers, lifetime predictions are based on the relationship between the reaction rate of degradation and temperature. The rate of degradation can be determined by exposing the test samples to a series of elevated temperatures and measuring a property change with time. The change in property could be the stress in relaxation tests or relaxation modulus $[E(t)]$ ⁴³.

Viscoelastic Model

A polymer responds differently depending on the speed at which its molecules deform. This is known as *viscoelastic* behaviour⁴³. In the case of elastomeric seals, small or slow deformations can result in *linear viscoelasticity*. The three-parameter Maxwell model is used to describe the linear viscoelastic response of a material to an applied strain. The model consists of a spring (with a spring constant E) and a dashpot (with the coefficient of viscosity η) connected in series^{38,44-45}. The stress at any time is based on the linear Maxwell model and can be written as:

$$\sigma(t) = \sigma_0 \exp\left(-\frac{t}{\tau}\right) \quad (4.1)$$

Where σ_0 is the stress at $t = 0$ and τ is the relaxation time, equal to η / E . According to this model stress decays exponentially with time³⁸.

However, the Maxwell model cannot estimate stress relaxation behaviour accurately, especially over a broad range of temperature and time. For this reason, the generalized Maxwell model, also called "*the Prony series*" has been developed and is considered the most popular linear model for the stress relaxation of polymeric materials^{43,38,46,45,47}. A generalized Maxwell model (Prony series) would result in the following equation:

$$\sigma(t) = \sigma_{\infty} + \sum_{i=1}^n \sigma_i \exp\left(-\frac{t}{\tau_i}\right) \quad (4.2)$$

Where σ_{∞} is the equilibrium stress after a long time, σ_i depends on the applied strain level and material properties and τ_i are material constant³⁸.

Time – Temperature Superposition (TTS) Principle / WLF Equation

Molecular motion in polymers causes the stress relaxation of the bulk material. Molecules normally move faster at high temperatures resulting in shorter relaxation times. The time –temperature superposition (TSS) principle suggests that time and temperature are generally equivalent in affecting the relaxation modulus of polymers as shown by Eq. (4.3)³⁸.

$$G_r(t, T_2) = G_r(a_T(T_1, T_2)t, T_1) \quad (4.3)$$

Where G_r is the relaxation function of time (mechanical response) and temperature, T_1 , and T_2 are two different temperatures, t is the time, and a_T is the shift factor.

Increasing the temperature shortens all relaxation times by the same factor (shift factor). The stress relaxation curve established at a certain temperature can then be horizontally shifted to another temperature when displayed on a logarithmic scale as shown in Figure 4.18. The TTS has been widely used in investigations of creep and stress relaxation of polymeric materials, allowing short term stress relaxation tests at a higher temperature to be used to predict stress relaxation at a lower temperature^{38, 43}. Using the TTS principle, master stress relaxation curves can be created for any temperature and then from these master curves, the service life of the polymeric seals can be predicted³⁸.

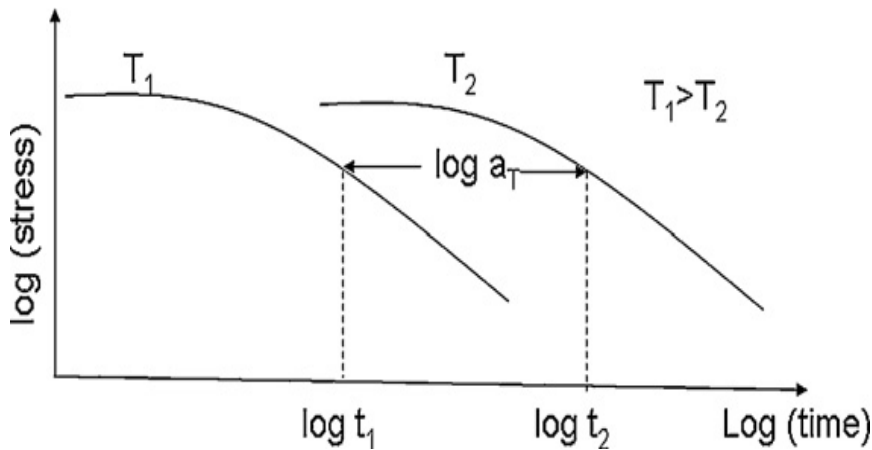


Figure 4.18. Time – temperature superposition³⁸

Williams, Landel and Ferry (WLF) observed that for the transition from the rubbery to the glassy state for many amorphous polymers the dependence of the shift-factor on temperature follows the same general relationship⁴⁸. The WLF empirical formula describes this time - temperature relationship via the shift factor, a_T :

$$\log a_T = - \frac{C_1 (T - T_{ref})}{C_2 + T - T_{ref}} \quad (4.4)$$

Where C_1 and C_2 are material dependent constants which are a function of material type and reference temperature, T_{ref} , and test temperature, T ⁴⁹. The WLF function is based on free volume theory which suggests that the free volume is a linearly increasing function of temperature above the glass transition temperature (T_g)⁵⁰. Above T_g , the polymer is viscoelastic or elastomeric and can withstand large recoverable deformations without fracture. Below T_g , the polymer chains are largely immobilised and there are no big changes in viscoelastic behaviour associated with time and temperature differences. The typical temperature range in which WLF can be used effectively is between T_g and $T_g + 100^\circ\text{C}$. At the temperatures well below T_g the WLF equation is not applicable⁴⁹⁻⁵⁰.

Arrhenius Model

As discussed in the previous section the WLF equation is able to represent the shift factors in the region of glass-transition temperature (T_g) only. An Arrhenius equation might be applied to fit the shift factors in the low as well as in the higher temperature range⁴³.

The Arrhenius model describes how the rate of chemical reaction changes with temperature and is mostly used for life estimation of stress relaxation, creep, time to failure and others, since many failures and degradation of elastomers arise from chemical reactions (e.g., failure of seals in PEMFC due to chemical degradation)^{37, 43, 51-52}. The Arrhenius equation which expresses the rate of chemical reaction as a function of absolute temperature is shown below (Eq. 4.5):

$$k = A e^{-Q/RT} \quad (4.5)$$

Where k is any chemical reaction rate and Q is a constant known as the activation energy of the reaction. Activation energy is the energy which has to be overcome for molecular motion to happen. A is a coefficient, R is the universal gas constant and T is the absolute temperature in Kelvin. The original Arrhenius equation (Eq.4.5) has been adapted to give stress relaxation at a specific time and in logarithmic form can be written as³⁷ :

$$\log t_c = \frac{0.217Q}{T} + \log \theta_c (t, T) \quad (4.6)$$

In accordance with Eq. 4.6, the activation energy Q can be acquired by plotting a straight line with the variables $1/T$ and $\log t_c$ ³⁷. Where t_c is the critical time at which the material is said to fail. The slope of the straight line is then $0.217Q$. Utilising this straight line generated by fitting with limited test data points, the service life t at any other temperature can be predicted by extrapolation.

The shift factor (i.e., the amount of shifting along the horizontal axis) which is required to create the master curve can be calculated using the following equation (Eq.4.7)

$$\log a_T = \frac{-\Delta E}{2.303 R (T - T_{ref})} \left[\frac{1}{T} - \frac{1}{T_{ref}} \right] \quad (4.7)$$

Where, ΔE is the activation energy associated with stress relaxation, R is the gas constant, T is the test temperature, T_{ref} is the reference temperature and a_T is the shift factor.

4.3.2. Stress Relaxation Studies for PEMFC Seals Liquid Silicone Rubber (LSR)

Cui et al.³⁹ investigated stress relaxation behaviour of LSR in DI water and ambient air at different temperatures and strain levels. Figure 4.19 shows the stress relaxation curves for LSR both obtained from the experimental data and also predicted from the Prony series. It can be seen that the model fits the experimental data reasonably well.

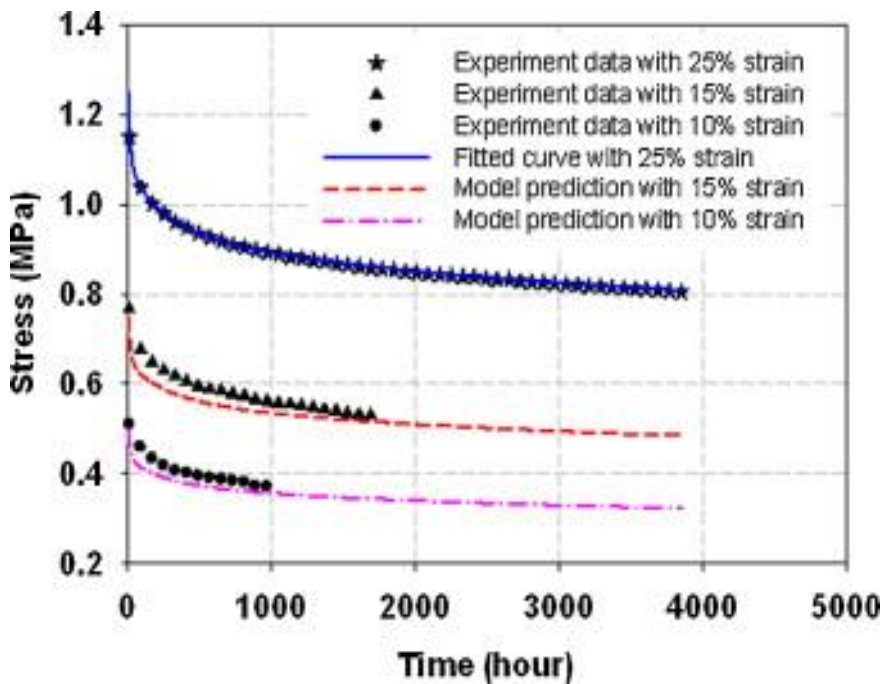


Figure 4.19. Stress relaxation curves of LSR – comparison of test data with the estimation from the Prony series³⁹

The “*Young’s Modulus $E(t)$* ”, which is normally a ratio of stress (σ) to strain (ϵ), is a function of time only, whatever the level of the applied constant strain (ϵ_0) is. Young’s (Relaxation) Modulus E in this study³⁹ was obtained from the modified Prony series in Eq. 4.8.

$$E(t) = \frac{\sigma(t)}{\epsilon_0} = \frac{1}{\epsilon_0} \left[\sigma_\infty + \sum_{i=1}^n \sigma_i \exp\left(-\frac{t}{\tau_i}\right) \right] = E_\infty + \sum_{i=1}^n E_i \exp\left(-\frac{t}{\tau_i}\right) \quad (4.8)$$

In addition, using the TTS principle discussed previously, the sealing life of LSR as a potential PEM fuel cell gasket was predicted in air and DI water.

Figure 4.20 demonstrates the normalised stress relaxation curves of LSR at three temperatures (70°C, 100°C, and 120°C) in DI water all with 25 % applied strain, on a logarithmic scale. These curves are normalised with respect to initial stress³⁹. Generally, the stress relaxation test data is normalised to determine how linear the viscoelastic material behaviour is. If the overlaid normalised curves are situated top of each other, the material is considered to be linearly viscoelastic. If the curves differ, it means that there is some nonlinear viscoelastic behaviour present⁴².

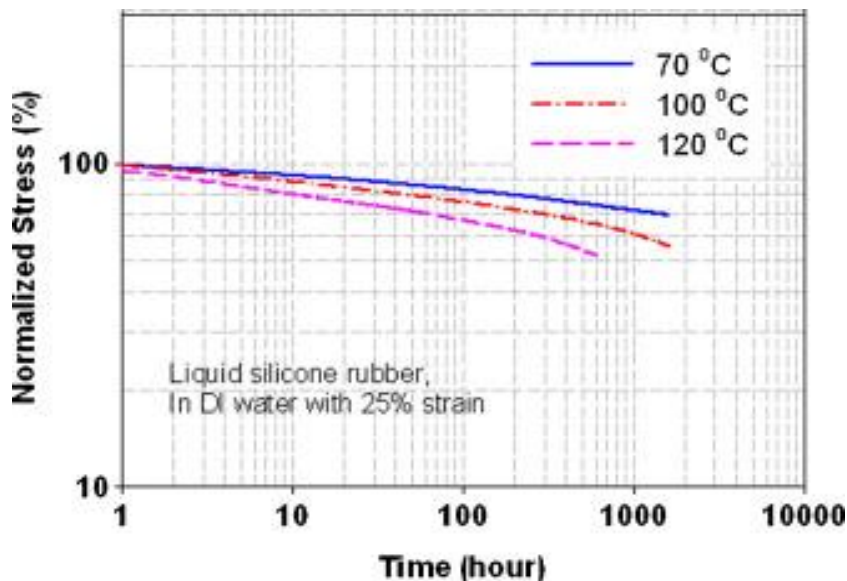


Figure 4.20. Stress relaxation data of LSR in DI water at three temperatures in logarithmic scale³⁹

Figure 4.20 shows that the curve at 70°C is more linear than the ones at 100°C and 120°C. This linear behaviour at 70°C curve implies that physical relaxation is observed during the test period. The linearity for the 100°C ends at about 700 h. After that, the data gradually deviated from the linearity suggesting an additional chemical relaxation. On the other hand, the linear area for the 120°C is limited to about 40 h. These data show that chemical relaxation is likely to arise more rapidly at higher temperature⁴⁶. Applying TTS (Eq.4.3 and Figure 4.18), the curves in Figure 4.20 were shifted to form the master curve at a reference temperature of 70°C.

The overlapping of the three curves at the different temperatures as shown in Figure 4.21, signifying good correlation with the master curve at this reference temperature (70°C).

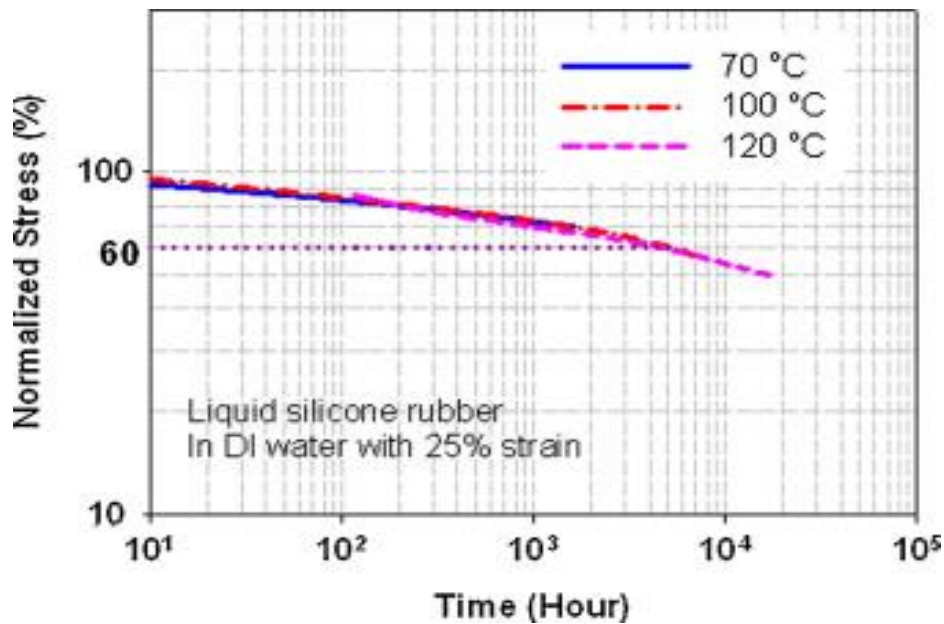


Figure 4.21. Master curve of stress relaxation of LSR at a reference temperature of 70°C³⁹

The data in Figure 4.21 shows that if LSR is used as seal in the PEMFC at the operating temperature of 70°C (in DI water with 25 % strain), service life of the seal would be estimated about 5000 h (6.9 months) provided that 60% of the sealing force has to be retained. This limit (60 %) was chosen in the study in relation to the internal pressure of the FC and other physical factors. In the case of ambient air, the service life of LSR as a seal was predicted from the CSR test results (under identical conditions) to be about 9000 h (12.5 months).

As conclusion, it was reported that temperature was an important factor in the stress relaxation of LSR. Moreover, water in particular, had an adverse effect on stress relaxation at 70°C, presumably by accelerating the chemical degradation of LSR³⁹. To validate this assumption and also the recognised susceptibility of LSR to hydrolysis, Cui et al.³⁷ further investigated the effect of water on the compression stress relaxation. They found that stress relaxed faster in DI water than in air indicating that water might attack the backbone of polymer (e.g, chain scission) and thus accelerated the stress relaxation.

Moreover, high temperature is likely to worsen this process (chain scission) which coincides with the results from hydrothermal degradation of LSR as reported by Siahkali - G. et al.

Their results from the same study³⁷ also showed that the stress relaxation behaviour of LSR was the same in both simulated acidic solution (pH 3.35) and DI water up to 1500 h revealing that the bulk properties of elastomeric gasket materials aged in the test solution did not alter. This outcome was confirmed by the findings of other aging studies of seal materials as previously discussed^{21, 22, 24,25, 27,30}.

In addition to TTS approach³⁹, Cui et al. also utilised the Arrhenius model in another study³⁷ to predict the failure (service life) of the LSR seal material and also to compare the stress relaxation mechanisms of LSR in DI water and ambient air. It can be seen from Figure 4.22 that the Arrhenius plot is almost a straight line for the test data in air, whereas a curve is observed for that in DI water when the temperature is above 100°C. The straight line for the data in air indicates the stress relaxed with a single mechanism in the temperature range 25-120°C. By contrast, this is not the case in water, which suggests that a different stress relaxation mechanism might have happened near 100°C since the slope of the line begins to change as the temperature becomes higher than 100°C. This curved line in the Arrhenius plot is often called non-Arrhenius behaviour and is explained as the occurrence of two competing processes with different activation energies that come from different mechanisms³⁷.

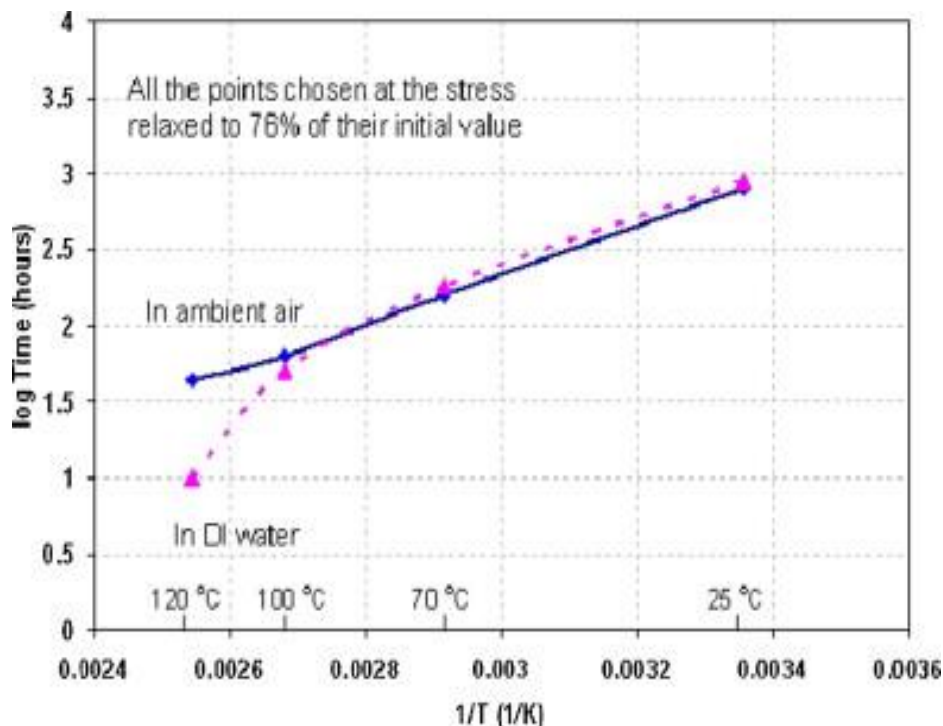


Figure 4.22. Arrhenius plot for stress relaxation tests of LSR in air and DI water³⁷

Most of the studies^{37, 39, 46} on stress relaxation behaviour of elastomeric seals were performed at constant temperature. However, in actual PEMFC applications, the temperature can change from operation to shut-down. For this reason Cui et al.⁵³ investigated the stress relaxation and thermal stress of LSR under temperature cycling (-10°C to 120°C). They found that in addition to stress relaxation, thermal expansion or contraction occurred during temperature change which caused a compressive stress in the seal. In other words, apart from stress relaxation, thermal expansion and contraction during temperature rise and fall was the main reason for the variation of the sealing force of LSR. Their experimental data also showed that the material stiffness changed due to thermal aging (increased stiffness after aging at higher temperature).

EPDM

The stress relaxation behaviour of EPDM seal material was also studied by Cui et al.³⁸ under similar conditions of those for LSR as discussed previously⁴⁶. It was reported that both temperature and water in which EPDM seal is exposed to had an effect on the stress relaxation of the material. From their experimental results, it appeared that higher temperature as well as water environment caused faster stress relaxation.

4.4. Compression Set

When a stress or strain is applied to a rubber sample, it does not fully return immediately to its original dimensions upon the removal of stress but displays a certain level of permanent deformation. When in compression the permanent deformation is known as “*compression set*” and is very important for sealing applications. The extent of the set is governed by the time for which the rubber is deformed, also the time which is allowed for the test sample to recover and the temperature of the test⁴⁰.

Tobolsky⁵⁴ originally proposed that one of the causes of permanent set is that the original network structure is damaged by scission when under strain which leads to a decrease in the force responsible for returning the sample to its initial length. The second reason is the formation of a new network structure by cross-linking, while the sample is under strain.

Similar to stress relaxation, there will be both physical and chemical ageing mechanisms affecting compression set. The compression set test is used more often than stress relaxation because simpler and cheaper equipment is required⁴⁰.

Compression set is an important property to consider in the design of and compound selection for seals in PEM fuel cells. It is typically measured during durability testing in a real or simulated fuel cell condition. If the measured compression set value is large, it means that a higher compression force is required during fuel cell stack operation to retain a low electrical resistance and good sealing.

On the other hand, over compression might be detrimental to other fuel cell components for instance, the gas permeability of the GDL will be altered, affecting the fuel performance ².

As with stress relaxation, the Arrhenius model has also been used to model compression set behaviour in accelerated thermal aging studies of elastomers ^{2, 55–59}. In order to model the changes in the compression set up to high levels, it is necessary to use an exponential or logarithmic function which is self-limiting between 0 and 100 % set ⁴¹.

Patel and Skinner measured the compression set properties of polysiloxane rubber samples exposed to thermal aging⁵. The data obtained from thermo mechanical (TMA) analysis, which was used to monitor compression set with time at various temperatures and under 25% compression, appeared to be adaptable to the time-temperature superposition (TTS) principle (See Figure 4.40). TMA measures a specimen's dimensions (length or volume) as a function of time under a constant mechanical stress. Applying the Arrhenius treatment to shift factors (a_T) originating from the TTS, activation energies were calculated. The results indicated the presence of two different degradation processes, which had an impact on the compression set properties. They concluded that the low activation energy mechanism could come from either hydrolysis of the Si – O backbone or diffusion processes. The degradation mechanism related to the higher activation energy could be due to the beginning of the depolymerisation (head to tail unzipping) reactions along the siloxane chains⁵. In addition, the study predicted that the compression set is expected to reach the failure criterion of 25% over a period of 18.8 (+13.3 /–5.5) years.

In another accelerated thermal ageing study by Patel et al.⁵⁶ the compression set properties of a thermally aged foam polysiloxane elastomer was investigated. Similarly, the TTS principle was applied to evaluate the TMA results and the acceleration factors (a_T) derived from TTS were analysed and fitted to Arrhenius kinetics. The isotherms were superimposed on the lowest test temperature (i.e., 21°C) by horizontally shifting each isotherm along the time axis using a constant shift factor for each temperature.

Quantum- NMR analysis suggested that the compression set was due to viscoelastic relaxation as well as breaking of siloxane linkages and forming new crosslinks leading to a major change in the overall network structure. These results confirmed performance findings of Patel and Skinner⁵ as previously discussed.

Bernstein and Gillen⁵⁸ investigated the connection between compression set and the loss in the sealing force of fluorosilicone o-rings at elevated temperatures. It was found that there was a reasonable linear relationship between the compression set and sealing force reduction with ageing time and temperature. According to previous studies by the same group, silicone o-rings also presented the same linear correlation between compression set and force decay values.

Slater et al.⁵⁷, focused on the impact of moisture as well as temperature on the compression set of the elastomeric TPU materials. Their results showed that in the presence of water, higher compression set values were observed than in the absence of water. It was found that the compression set was influenced by both the temperature and the moisture, but the effect of water occurred only at the higher temperatures (i.e., 70°C and 80°C) which were similar to the operating temperatures of PEMFCs under a humid environment.

The stress relaxation and compression set studies of sealing materials under accelerated aging conditions can be very beneficial in terms of understanding how the stress and the environmental factors cause degradation loss of sealing function.

4.5. REFERENCES

- [1] J. Z. Zhang, Jianlu Huamin Zhang, Jinfeng Wu, "Fuel Cell Degradation and Failure Analysis," in *PEM Fuel Cell Testing and Diagnosis*, Oxford: Elsevier, 2013, pp. 326–27.
- [2] B. L. and J. M. Daijun Yang, Junsheng Zheng, "Degradation of Other Components," in *PEM Fuel Cell Failure Mode Analysis*, H. H. Wang, H. Li 1964-, and X.-Z. Yuan, Eds. Boca Raton, Fla.: CRC Press, 2012.
- [3] D. Graiver, K. W. Farminer, and R. Narayan, "A Review of the Fate and Effects of Silicones in the Environment," *J. Polym. Environ.*, vol. 11, no. 4, pp. 129–136, 2003.
- [4] D. Thomas, "Network scission processes in peroxide cured methylvinyl silicone rubber," *Polymer (Guildf)*., vol. 7, pp. 99–105, 1966.
- [5] M. Patel and a. R. Skinner, "Thermal ageing studies on room-temperature vulcanised polysiloxane rubbers," *Polym. Degrad. Stab.*, vol. 73, no. 3, pp. 399–402, 2001.
- [6] A. N. Chaudhry and N. C. Billingham, "Characterisation and oxidative degradation of a room-temperature vulcanised poly(dimethylsiloxane) rubber," *Polym. Degrad. Stab.*, vol. 73, no. 3, pp. 505–510, 2001.
- [7] I. Umeda, K. Tanaka, T. Kondo, K. Kondo, and Y. Suzuki, "Acid Aging of Silicone Rubber Housing for Polymer Insulators Field Conditions of Aged Insulator," *Int. Symp. Electr. Insul. Mater.*, pp. 2–5, 2008.
- [8] Y. Koshino, I. Umeda, and M. Ishiwan, "Deterioration of Silicone Rubber for Polymer Insulators by Corona Discharge and Effect of Fillers," *Polym. Insulator Div. Power Bus. Group, Japan*.
- [9] A. Ghanbari-Siahkali, S. Mitra, P. Kingshott, K. Almdal, C. Bloch, and H. K. Rehmeier, "Investigation of the hydrothermal stability of cross-linked liquid silicone rubber (LSR)," *Polym. Degrad. Stab.*, vol. 90, no. 3, pp. 471–480, Dec. 2005.
- [10] S. Mitra, A. Ghanbari-Siahkali, P. Kingshott, H. K. Rehmeier, H. Abildgaard, and K. Almdal, "Chemical degradation of crosslinked ethylene-propylene-diene rubber in an acidic environment. Part I. Effect on accelerated sulfur crosslinks," *Polym. Degrad. Stab.*, vol. 91, no. 1, pp. 69–80, 2006.
- [11] S. Mitra, A. Ghanbari-Siahkali, P. Kingshott, H. K. Rehmeier, H. Abildgaard, and K. Almdal, "Chemical degradation of crosslinked ethylene-propylene-diene rubber in an acidic environment. Part II. Effect of peroxide crosslinking in the presence of a coagent," *Polym. Degrad. Stab.*, vol. 91, no. 1, pp. 81–93, 2006.

- [12] S. Mitra, A. Ghanbari-Siahkali, P. Kingshott, S. Hvilsted, and K. Almdal, "An investigation on changes in chemical properties of pure ethylene-propylene-diene rubber in aqueous acidic environments," *Mater. Chem. Phys.*, vol. 98, no. 2–3, pp. 248–255, 2006.
- [13] S. Mitra, A. Ghanbari-Siahkali, P. Kingshott, S. Hvilsted, and K. Almdal, "Surface characterisation of ethylene–propylene–diene rubber upon exposure to aqueous acidic solution," *Appl. Surf. Sci.*, vol. 252, no. 18, pp. 6280–6288, 2006.
- [14] S. Kole, S. K. Srivastava, D. K. Tripathy, and .A. K. Bhowmick, "Accelerated hydrothermal weathering of silicone rubber, EPDM, and their blends," *J. Appl. Polym. Sci.*, vol. 54, no. 9, pp. 1329–1337, 1994.
- [15] S. Mitra, A. Ghanbari-Siahkali, P. Kingshott, K. Almdal, H. Kem Rehmeier, and A. G. Christensen, "Chemical degradation of fluoroelastomer in an alkaline environment," *Polym. Degrad. Stab.*, vol. 83, no. 2, pp. 195–206, Feb. 2004.
- [16] T. Sugama, "Surface Analyses of Fluoroelastomer Bearings Exposed to Geothermal Environments," *Mater. Lett.*, vol. 50, no. 2–3, pp. 66–72, 2001.
- [17] R. H. S. S.H. Kalfayan, "Accelerated Heath Aging of Fluororubber in Various Media pdf.pdf," 1976.
- [18] R. H. S. S.H. Kalfayan, "Accelerated Heat Aging Studies of Fluorosilicone Rubber.pdf," *Jet Propulsion Lab. Calif. Inst. Techonology*, 1975.
- [19] D. K. Thomas, "High temperature stability in fluorosilicone vulcanisates," vol. 13, no. March, pp. 479–484, 1972.
- [20] F. A. De Bruijn, V. a. T. Dam, and G. J. M. Janssen, "Review: Durability and degradation issues of PEM fuel cell components," *Fuel Cells*, vol. 8, no. 1, pp. 3–22, 2008.
- [21] J. Tan, Y. J. Chao, M. Yang, W.-K. Lee, and J. W. Van Zee, "Chemical and mechanical stability of a Silicone gasket material exposed to PEM fuel cell environment," *Int. J. Hydrogen Energy*, vol. 36, no. 2, pp. 1846–1852, Jan. 2011.
- [22] C.-W. Lin, C.-H. Chien, J. Tan, Y. J. Chao, and J. W. Van Zee, "Chemical degradation of five elastomeric seal materials in a simulated and an accelerated PEM fuel cell environment," *J. Power Sources*, vol. 196, no. 4, pp. 1955–1966, Feb. 2011.
- [23] J. Tan, Y. J. Chao, M. Yang, C. T. Williams, and J. W. Van Zee, "Degradation Characteristics of Elastomeric Gasket Materials in a Simulated PEM Fuel Cell Environment," *J. Mater. Eng. Perform.*, vol. 17, no. 6, pp. 785–792, 2008.

- [24] G. Li, J. Tan, and J. Gong, "Degradation of the elastomeric gasket material in a simulated and four accelerated proton exchange membrane fuel cell environments," *J. Power Sources*, vol. 205, no. 0, pp. 244–251, May 2012.
- [25] J. Tan, Y. J. Chao, X. Li, and J. W. Van Zee, "Degradation of silicone rubber under compression in a simulated PEM fuel cell environment," *J. Power Sources*, vol. 172, no. 2, pp. 782–789, Oct. 2007.
- [26] J. Tan, Y. J. Chao, J. W. Van Zee, and W. K. Lee, "Degradation of elastomeric gasket materials in PEM fuel cells," *Mater. Sci. Eng. A*, vol. 445–446, no. 0, pp. 669–675, Feb. 2007.
- [27] G. Li, J. Tan, and J. Gong, "Chemical aging of the silicone rubber in a simulated and three accelerated proton exchange membrane fuel cell environments," *J. Power Sources*, vol. 217, no. 0, pp. 175–183, Nov. 2012.
- [28] J. Tan, Y. J. Chao, H. Wang, J. Gong, and J. W. Van Zee, "Chemical and mechanical stability of EPDM in a PEM fuel cell environment," *Polym. Degrad. Stab.*, vol. 94, no. 11, pp. 2072–2078, Nov. 2009.
- [29] C. W. Lin, C. H. Chien, J. Tan, Y. J. Chao, and J. W. Van Zee, "Dynamic mechanical characteristics of five elastomeric gasket materials aged in a simulated and an accelerated PEM fuel cell environment," *Int. J. Hydrogen Energy*, vol. 36, pp. 6756–6767, 2011.
- [30] J. Feng, Q. Zhang, Z. Tu, W. Tu, Z. Wan, M. Pan, and H. Zhang, "Degradation of silicone rubbers with different hardness in various aqueous solutions," *Polym. Degrad. Stab.*, vol. 109, no. 0, pp. 122–128, Nov. 2014.
- [31] J. Tan, Y. J. Chao, X. Li, and J. W. Van Zee, "Microindentation Test for Assessing the Mechanical Properties of Silicone Rubber Exposed to a Simulated Polymer Electrolyte Membrane Fuel Cell Environment," *J. Fuel Cell Sci. Technol.*, vol. 6, no. 4, p. 41017, Aug. 2009.
- [32] J. Tan, Y. J. Chao, J. W. Van Zee, X. Li, X. Wang, and M. Yang, "Assessment of mechanical properties of fluoroelastomer and EPDM in a simulated PEM fuel cell environment by microindentation test," *Mater. Sci. Eng. A*, vol. 496, no. 1–2, pp. 464–470, Nov. 2008.
- [33] A. Husar, M. Serra, and C. Kunusch, "Description of gasket failure in a 7 cell PEMFC stack," *J. Power Sources*, vol. 169, pp. 85–91, 2007.
- [34] M. Schulze, T. Knöri, A. Schneider, and E. Gülzow, "Degradation of sealings for PEFC test cells during fuel cell operation," in *Journal of Power Sources*, 2004, vol. 127, pp. 222–229.
- [35] S.-Y. Ahn, S.-J. Shin, H. Y. Ha, S.-A. Hong, Y.-C. Lee, T. W. Lim, and I.-H. Oh, "Performance and lifetime analysis of the kW-class PEMFC stack," *J. Power Sources*, vol. 106, no. 1–2, pp. 295–303, Apr. 2002.

- [36] J. St-Pierre and N. Jia, "Successful Demonstration of Ballard PEMFCS for Space Shuttle Applications," *J. New Mater. Electrochem. Syst.*, vol. 5, no. 4, pp. 263–271, 2002.
- [37] S. J. C. Cleghorn, D. K. Mayfield, D. A. Moore, J. C. Moore, G. Rusch, T. W. Sherman, N. T. Sisofo, and U. Beuscher, "A polymer electrolyte fuel cell life test: 3 years of continuous operation," *J. Power Sources*, vol. 158, no. 1, pp. 446–454, Jul. 2006.
- [38] T. Cui, Y. J. Chao, X. M. Chen, and J. W. Van Zee, "Effect of water on life prediction of liquid silicone rubber seals in polymer electrolyte membrane fuel cell," *J. Power Sources*, vol. 196, no. 22, pp. 9536–9543, Nov. 2011.
- [39] T. Cui, Y. J. Chao, and J. W. Van Zee, "Stress relaxation behavior of EPDM seals in polymer electrolyte membrane fuel cell environment," *Int. J. Hydrogen Energy*, vol. 37, no. 18, pp. 13478–13483, Sep. 2012.
- [40] T. Cui, C.-W. Lin, C. H. Chien, Y. J. Chao, and J. W. Van Zee, "Service life estimation of liquid silicone rubber seals in polymer electrolyte membrane fuel cell environment," *J. Power Sources*, vol. 196, no. 3, pp. 1216–1221, Feb. 2011.
- [41] S. Siouris, B. Shaw, and C. Wilson, "Method for the evaluation of elastomeric seals by compression stress relaxation," *Polym. Test.*, vol. 32, no. 8, pp. 1299–1305, Dec. 2013.
- [42] S. Ronan, T. Alshuth, S. Jerrams, and N. Murphy, "Long-term stress relaxation prediction for elastomers using the time–temperature superposition method," *Mater. Des.*, vol. 28, no. 5, pp. 1513–1523, 2007.
- [43] K. T. Gillen, M. R. Keenan, and J. Wise, "New method for predicting lifetime of seals from compression-stress relaxation experiments," *Macromol. Mater. Eng.*, vol. 261–262, no. 1, pp. 83–92, 1998.
- [44] K. Cousins, "Polymers in Building and Construction," 2002.
- [45] T. Osswald, "Understanding Polymer Processing."
- [46] E. Of and L. Support, "Encyclopedia of Life Support Systems," vol. 1, no. 905, 2011.
- [47] T. Cui, Y. J. Chao, and J. W. Van Zee, "Sealing force prediction of elastomeric seal material for PEM fuel cell under temperature cycling," *Int. J. Hydrogen Energy*, vol. 39, no. 3, pp. 1430–1438, Jan. 2014.
- [48] M. Mottahedi, "Numerical analysis of relaxation test based on Prony series material model (4th International Joint Conference on integrated system design and technology)."
- [49] M. Herdy, "ViscoData & ViscoShift," pp. 1–29, 2003.

- [50] D. . Fan, B., Kazmer, "Effect of Low Temperature Shift Factor Modelling on Predicted Part Quality," in *ANTEC 2003, annual technical conference, May 4-8, 2003*, p. 5.
- [51] C. Briody, B. Duignan, S. Jerrams, and S. Ronan, "Prediction of Compressive Creep Behaviour in Flexible Polyurethane Foam Over Long Time Scales and at Elevated Temperatures," 2012.
- [52] T. Cui, Y. Chao, and J. Van Zee, "Understanding the Stress Response of Seals in Fuel Cell Subject to Temperature Cycling," *ECS Trans.*, vol. 41, no. 1, pp. 1927–1934, 2011.
- [53] K. Darlymple, T., Choi, J., Miller, "Elastomer Rate-Dependence : a Testing and Material Modeling Methodology Elastomer Rate-Dependence : a Testing and Material Modeling Methodology," *Rubber Div. Am. Chem. Soc. Inc*, 2007.
- [54] T. Cui, Y. J. Chao, and J. W. Van Zee, "Thermal stress development of liquid silicone rubber seal under temperature cycling," *Polym. Test.*, vol. 32, no. 7, pp. 1202–1208, Oct. 2013.
- [55] A. V Tobolsky, *Properties and structure of polymers*. Wiley, 1960.
- [56] J. E. Coons, M. D. McKay, and M. S. Hamada, "A Bayesian analysis of the compression set and stress–strain behavior in a thermally aged silicone foam," *Polym. Degrad. Stab.*, vol. 91, no. 8, pp. 1824–1836, Aug. 2006.
- [57] M. Patel, S. Chinn, R. S. Maxwell, T. S. Wilson, and S. A. Birdsell, "Compression set in gas-blown condensation-cured polysiloxane elastomers," *Polym. Degrad. Stab.*, vol. 95, no. 12, pp. 2499–2507, Dec. 2010.
- [58] C. Slater, C. Davis, and M. Strangwood, "Compression set of thermoplastic polyurethane under different thermal–mechanical–moisture conditions," *Polym. Degrad. Stab.*, vol. 96, no. 12, pp. 2139–2144, 2011.
- [59] R. Berstein and K. T. Gillen, "Fluorosilicone and Silicone O-ring Aging Study," *Sandia Rep. No. SAND2007-6781*, no. October, pp. 1–42, 2007.
- [60] K. C. Wittich, R. Wensel, R. Larose, S. Kuran, and C. River, "UPGRADING ELASTOMER SEALS FOR NUCLEAR SERVICE Fluid Sealing and Dynamics Branch , Chalk River Laboratories, Atomic Energy of Canada Limited," pp. 113–121.

5. CHAPTER 5: Experimental

An investigation of the durability of the PEM fuel cell seals has been carried out to determine the effects of the accelerated aging on elastomeric gasket materials and the changes in their properties with ageing. In this chapter, information about the gasket materials, experimental test methods and characterization techniques are explained.

5.1. Materials

The sealing materials used in this study were:

- Silicone Rubber compound
- Commercial EPDM compound
- Developed EPDM compounds

The compounds are listed in Table 5.1.

Table 5.1. The rubber compounds used in the project

Material	Supplier Company	Colour	Curing State
Silicone Rubber	Primasil	Grey	Uncured
Commercial EPDM	James Walker	White	Uncured
EPDM Compounds	Mixed in the Lab	Grey	Uncured

Silicone Rubber

A grey-coloured peroxide cured polydimethylsiloxane (VMQ) silicone rubber compound filled with silica was supplied by the sponsor company, Intelligent Energy (IE), as a moulded fuel cell gasket and uncured silicone rubber sheet approximately 1 mm thick. The specifications of the compound are shown in Table 5.2 which was provided by the supplier company called Primasil (via Intelligent Energy).

Table 5.2. Properties of the Silicone Rubber compound

Properties	Typical Values	Units
Density	1.14	g/ cm ³
Hardness	61	Shore A
Tensile Strength	12.5	MPa
Elongation @ Break	520	%
Tear Strength	28	kN/m
Compression Set (25 %) 22 hrs @ 177°C	7	%

Commercial EPDM Compound

White coloured pure grade peroxide cured EPDM compound was provided free of charge by James Walker & Co. Ltd. It was originally used in pharmaceutical sealing applications. This grade was specifically chosen due to the potential low amount of leachants to the environment which was crucial for PEMFCs seal applications.

Developed EPDM Compounds

Two EPDM material candidates were developed over the course of the project.

1. EPDM Compound F
2. EPDM 2 Compound

EPDM Compound F

Initially, we formulated a series of compounds (A – F). A and B are unfilled; C,D,E, F are filled compounds. The purpose of using those different combinations was to observe the influence of the fillers (coated and uncoated silica), coagent (HVA -2) and plasticiser (lithene AH) on the mechanical properties. Table 5.3 and Table 5.4. summarise the formulation of these compounds and the functions of the ingredients in them respectively.

Table 5.3. Formulation of initial EPDM compounds (A–F)

Recipe	Formulation (phr)					
	A	B	C	D	E	F
EPDM	100	100	100	100	100	100
Zinc Oxide	5	5	5	5	5	5
Stearic Acid	0.5	0.5	0.5	0.5	0.5	0.5
Luperox DC40	6.5	6.5	6.5	6.5	6.5	6.5
HVA-2	2.5	-	2.5	-	2.5	-
Lithene AH	-	8	-	8	-	8
Uncoated Silica	-	-	20	20	-	-
Coated Silica	-	-	-	-	20	20

Table 5.4. Functions of the ingredients in EPDM compounds

Ingredient	Function	
Zinc Oxide	Activator	Increase the rate of curing
Stearic Acid	Activator	
Luperox DC 40	Peroxide	Curing System
HVA-2	Coagent	Crosslink Formation
Lithene AH	Plasticiser/Crosslinker	Reduce the hardness & increase the flexibility / Improve the crosslink density
Silica	Filler	Reinforcing agent
Coated silica: with silane coating	Adhesion of silica to EPDM	

Between all the recipes shown in Table 5.3, compound F was chosen, in line with the tensile test results, as a potential gasket material to carry out further testing.

Although the compound was resistant to chemical degradation in the simulated fuel cell environment, it had a high viscosity which could cause a difficulty in the processing and also had a high hardness with the potential for possible sealing problems. Moreover, its oxidation resistance was low. In order to address these issues we improved the formulation of EPDM Compound F and carried out final compounding.

EMDM 2 Compound

Table 5.5 summarises the new EPDM compounds with the lithene concentrations of 0, 8, 16 and silica (coated) concentrations of 5, 12.5, 20.

Table 5.5 Formulation of final EPDM compounds

Recipe	Formulation (phr)								
EPDM	100	100	100	100	100	100	100	100	100
Perkadox (40%)	6.5	6.5	6.5	6.5	6.5	6.5	6.5	6.5	6.5
Zinc Oxide (80%)	6.25	6.25	6.25	6.25	6.25	6.25	6.25	6.25	6.25
TMQ	1	1	1	1	1	1	1	1	1
Stearic Acid	0.5	0.5	0.5	0.5	0.5	0.5	0.5	0.5	0.5
Silica (Coated)	5	5	5	12.5	12.5	12.5	20	20	20
Lithene PH	0	8	16	0	8	16	0	8	16

Table 5.6 and 5.7 show the recipes of (EPDM) compound F and EPDM 2 respectively which were used in the study.

Table 5.6. Recipe for the EPDM Compound F

EPDM Compound F		
Ingredients	Phr	Function
EPDM (Vistalon 7500)	100	Rubber (EPDM)
Zinc Oxide	5	Curing Activator
Stearic Acid	0.5	Curing Activator
Luperox DC 40	6.5	Peroxide Curing Agent
(Lithene AH)	8	Coagent & Plactizier
Silica (Coated with a silane coupling agent)	20	Reinforcing Filler

Table 5.7. Recipe for the EPDM 2 Compound

EPDM 2 Compound		
Ingredients	Phr	Function
EPDM (Vistalon 2504)	100	Rubber (EPDM)
Zinc Oxide (80 %)	6.25	Curing Activator
Stearic Acid	0.5	Curing Activator
Perkadox (40%)	6.5	Peroxide Curing Agent
TMQ	1	Antioxidant
Silica (Coated with a silane coupling agent)	20	Reinforcing Filler

Ingredients

EPDM is a type of rubber which consists of ethylene and propylene co-monomers with ethylidene norborne (ENB) as diene. Two different grades of EPDM were used in this study: Vistalon 7500 and Vistalon 2504 and they were provided from ExxonMobil Chemical. The former contains 56 wt % ethylene content and 5.7 wt % diene (ENB) content; the latter is a low Mooney viscosity polymer with 58 wt % ethylene and 4.7 wt % diene content^{1,2}.

Zinc oxide and stearic acid are the most commonly used activators. They are added to decrease the vulcanisation time by increasing the speed of vulcanisation³. Zinc oxide with the trade name Zinkoxyd Aktiv was supplied by Lanxess.

Dicumyl peroxide with the trade name of Luperox DC 40, which was supplied by Arkema, is a vulcanising or cross-linking agent. Luperox DC 40 is a 40% dicumyl peroxide formulation extended on calcium carbonate and silica. The composition is 38-42 % dicumyl peroxide and 55-57 % calcium carbonate.

HVA-2 curative from Dupont, is a trade name for N,N'-m-phenylene-bis-maleimide and it is a widely used coagent which enhance the cross-linking of the EPDM matrix.

Lithene AH and PH are also coagents which improve the crosslink density of the elastomer compounds. They are liquid butadiene with low molecular weight and are usually used to promote the processing characteristics of EPDM compounds⁴. However, Lithene AH is more viscous (i.e., 400 – 700 dPa.s) than Lithene PH (i.e., 65 – 90 dPa.s). The supplier company was Synthomer.

Uncoated and coated silica fillers were used in the formulation to improve the mechanical properties of the EPDM compounds. Uncoated silica with the trade name of Ultrasil VN 2 was provided from Evonik Degussa GmbH in the form of precipitated silica granules (Synthetic amorphous silicon dioxide). Coated silica, which is coated in silane coupling agent, with the trade name of Ultrasil VN 2 GR, was supplied by Egesil Kimya A.S. Silane coupling agent is used extensively to improve reinforcing efficiency of silica.

TMQ is an oxidant and used with rubber compounds to increase their oxidation resistance.

5.2. Mixing

Small scale mixing of the EPDM compounds (Compound F) was carried out in a lab scale mixer. A Thermo Haake Poly Lab Mixer and Extruder Rheocord 300p was employed with a mixing chamber volume of 78cm³. The mixer was operated at a constant rotor speed of 40 rpm using Banbury-Rotors R600. The temperature of the mixer was set at 24 ± 5°C and the mixing duration for each compound took 10 minutes. The batch size used per compound ranged from 43 to 48 grams which constituted to an approximate fill factor of 0.6 of the chamber volume so as to achieve homogeneous mixing.

After selecting the optimum EPDM compound (Compound F), as a consequence of the results of the tensile and compression set testing, a large batch of this compound (3.5 kg) was mixed in a water cooled K1 intermix MK4 (internal mixer) having a volume of 5.51L. A fill factor of 0.6 was used and mixing was done at a speed of 45 rpm, the rotors and mixing chamber was cooled with circulating water at 40°C. Prior to mixing EPDM rubber was cut into small pieces on a bale cutter.

It was then masticated first with the zinc oxide (activator) in the internal mixer for 2 minutes. Lithene AH (plasticiser) and coated silica mixture was then added and the compound was mixed for a further 3 minutes before the addition of stearic acid (activator) and peroxide curing agent. The mixing was then carried out for a further 1 minute (i.e, total mixing of 4 minutes), before dropping the uncured compound from the mixer on to two roll mill to form into sheet. The order for the mixing is shown in Figure 5.1.

Mixing procedure was exactly the same for EPDM 2 compounding. The only difference was that an antioxidant (TMQ) was added at the stage where the stearic acid and peroxide curing agent were combined into the compound.

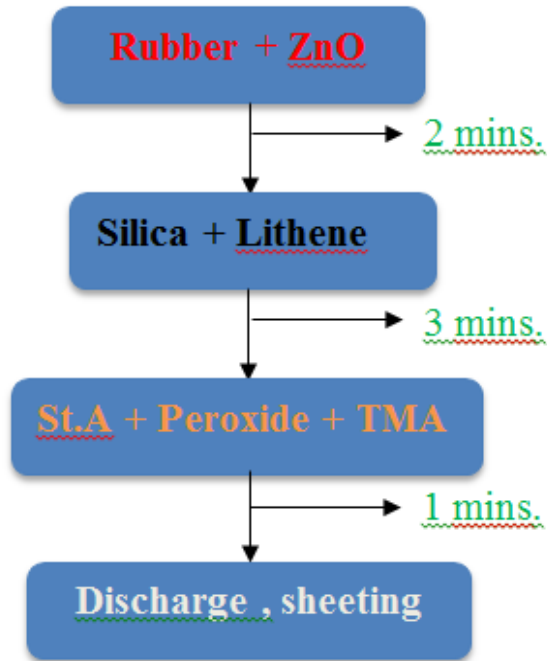


Figure 5.1. The order for compound mixing

5.3. Curing Properties & Conditions

Cure parameters were determined by using a Wallace Test Equipment Precision Cure Analyser. The cure time for each material was obtained from the rheograph at 100% cure. A compression mould using an electrically heated 20 ton lab press was then used to cure either flat sheets (1 mm thick) for tensile testing or the cylindrical (12 mm in diameter) samples for compression set test. Table 5.8 shows the curing time and temperature of the gasket materials.

Table 5.8. Cure Properties of Gasket Materi

Material	Curing temp. (°C)	Curing time (min.) (1mm Flat Sheet)	Curing time (min.) (16 cylinder samples)
Silicone	170	10	15
Com.EPDM	175	20	25
EPDM Compound F	175	11	16
EPDM 2	175	11	16

5.4. Characterization Methods

5.4.1. Scanning Electron Microscopy (SEM)

Scanning electron microscopy (SEM) was performed to measure the thickness of the silicone rubber gaskets before and after service in the real fuel cell. The measurement was used to detect any permanent change in thickness caused by service use. The permanent change in thickness is a similar property to compression set, although the measurement is not carried out under standard conditions, and the level of compression in service is not known. The razor cut surfaces of the unused and used silicone rubber gaskets were examined using a Carl Zeiss (Leo) 1530 VP SEM. A gold coating was applied to the samples prior to the SEM examination by using Polaron Emitech SC7640 Sputter Coater at low voltage (2kV) for 40 seconds in order to avoid electrostatic charging and poor image resolution. The SEM was operated with an accelerated voltage of 5 kV and a working distance of 10mm'

5.4.2. Atomic Force Microscopy (AFM)

Atomic force microscopy (AFM) is a technique to measure modulus mapping on a scale from angstroms to 100 microns. A tip or a probe is used to image a sample. Variations in tip height are recorded while the tip is scanned repeatedly across the sample, producing a topographic image of the surface.

In this project, AFM measurements were carried out on the surface of samples cut from both unused gaskets and the degraded part of the used gaskets using a Veeco Explorer AFM with a pulsed force-imaging mode.

This technique was employed to observe any differences brought about by degradation in the stiffness of the material at a microscopic level.

5.4.3. X-Ray Photoelectron Spectroscopy (XPS)

The atomic composition and surface chemistry of the degraded parts of the silicone rubber gaskets, which had been used in a fuel cell, were identified by applying X-ray photoelectron spectroscopy (XPS). The XPS used in this study was a VG Escalab Mk I with the detection limits of 0.1–1 atom % and an analysis area typically of 3–10 mm².

5.4.4. Attenuated Total Reflection Fourier Transform Infrared Spectroscopy (ATR-FTIR)

Attenuated total reflectance Fourier transform infrared (ATRFTIR) spectroscopy was conducted on the surface of the samples from unused and degraded parts of gaskets used in a fuel cell, along with the silicone rubber material before and after exposure to accelerated aging tests. A Shimadzu FTIR-8400S fitted with Specac Golden Gate ATR Mk II was used in this study. The spectroscopy ran at a resolution of 0.85 cm^{-1} and peak-to-peak S/N ratio of 20.000:1. IR spectrum for the materials were analysed from 4000 to 600cm^{-1} .

5.4.5. Solvent Swelling Method

A solvent swelling method was used to determine the change in the crosslink density of the silicone rubber gaskets on aging.

The degree of swelling is inversely related to crosslink density when the material, solvent, and temperature are kept constant, as in this test. Samples with dimensions of approximately $24 \times 7 \times 0.58\text{ mm}^3$ were cut from unused gaskets and close to the degraded areas of gaskets used in a fuel cell. Each sample was weighed on a digital balance (to four decimal places) then was immersed into a glass tube containing 5 mL solvent (toluene) at room temperature for a total of 6 days.

After 1 day (24 h), the swollen sample was removed from the solvent and dabbed on paper tissue to get rid of any excess solvent, placed in a pre-weighed empty plastic sample bag and weighed immediately. The sample then was put back in to the glass tube containing toluene for the rest of the swelling test.

This procedure was repeated after 24 h (1 day), 96 h (4 days), and 144 h (6 days), and the weights of the samples were recorded. The percentage of swelling was calculated for each sample using the following equation:

$$\text{Swelling (\%)} = \frac{W_2 - W_1}{W_1} \quad 5.1$$

where W_1 is the weight of the test sample before immersion; W_2 is the weight of the swollen sample after immersion.

5.5. Accelerated Acid Ageing Method

An accelerated aging test was developed in order to assess the acid and time/temperature aging resistance of gasket materials, which is relevant to the fuel cell environment.

An accelerated aging temperature of 140°C was selected so that 1 week of accelerated aging would roughly correspond to a real life time of 10000 h at 80°C, on the crude assumption of an expected doubling of degradation rate for every 10°C increase in temperature. Accelerated aging solutions were used to represent the acidity of the fuel cell environment. Because of the elevated temperature and aqueous environment it was necessary to carry out the accelerated aging in pressurised vessels.

Each pressure vessel included a metal base (stainless steel) for holding a polytetrafluoroethylene (PTFE) lining cup and a screw fitting metal cap with a PTFE lid for sealing as shown in Figure 5.2. The PTFE liner in which the samples were aged had internal dimensions of 30 mm diameter and 44mm in height. Accelerated aging solution (7 mL) was placed in the liner and four dumbbells of gasket samples were added. The necks of the dumbbell samples were submerged completely into the solution. Figure 5.3 shows (a) the pressure vessel and (b) the layout of the samples in the liner.

The PTFE liner containing the samples was then put into the metal base and sealed tightly with the lined metal cap before placing in the oven at 140°C for the appropriate period.

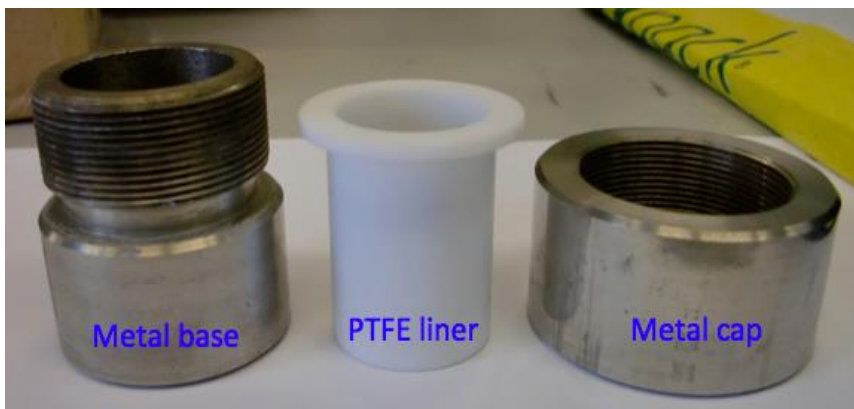


Figure 5.2. The parts of a pressure cooker

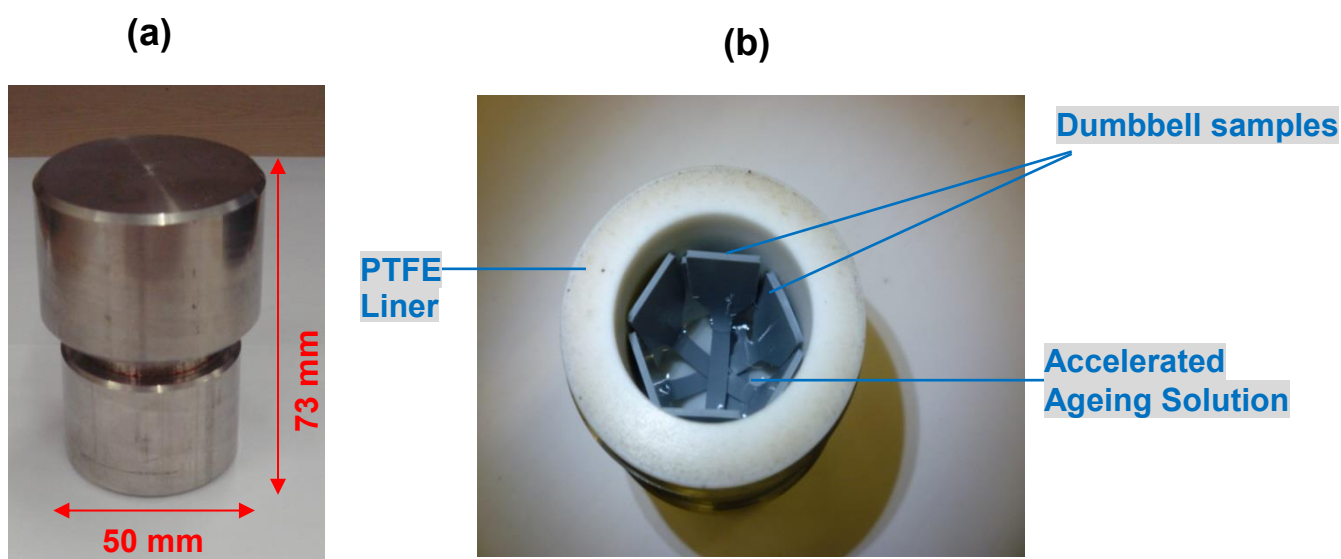


Figure 5.3. (a) Accelerated aging test pressure cooker and (b) arrangement of the samples in the cooker

5.5.1. Accelerated Ageing Solutions

The accelerated aging solutions used in the study were as follows:

1. Sulfuric acid (H_2SO_4) solution with various acidity (i.e. pH 1, 2, 3 and 4) levels
2. Nafion® accelerated ageing solution with the pH values of 3 to 4
3. TFA (Trifluoroacetic acid) solution of pH 3.3

Sulfuric acid (H_2SO_4) solution was prepared by diluting 2M H_2SO_4 with distilled water. The pH values of the aging solutions were chosen to create acidity, which is similar to that in a real PEM fuel cell, i.e., pH ranging from 3 to 4,⁵ but also to include those of greater acidity to accelerate the aging process.

In addition to the sulfuric acid solutions, an acidic environment more closely related to that of the fuel cell, where the acidity is due to the sulfonate groups in the membrane, was created using pieces of Nafion® suspended in distilled water.

Nafion® accelerated aging solution was prepared by using 0.7 wt % of Nafion®, in 7-mL distilled water, heated in the pressure vessel at 140°C for 3 days until pH values of between 3 and 4 were reached. The Nafion® membrane was left in the water when dumbbell samples were added for accelerated aging.

A Trifluoroacetic acid (TFA) solution of pH 3.3, which is close to the pH value of Nafion® solution, was also employed. It was prepared by diluting 0.1% (v/v) trifluoroacetic acid with distilled water. From published literature,^{6,7} trifluoroacetic acid (TFA) has been shown as a major degradation product of Nafion® membrane. Hence it was chosen to establish whether TFA could be the ageing agent in fuel cells.

Upon completion of accelerated aging test, the weight change of the seal materials with exposure time was monitored. The surface condition of the gasket samples, which were exposed to aging solutions, was also visually examined. Additionally, the pH value (i.e., acidity) of the used accelerated aging solutions was measured to reveal any possible reactions between the gasket samples and the acid solutions.

5.5.2. Weight Change

Weight changes of the gasket samples after exposure to ageing solutions were measured. The weight change can reflect the degree of corrosion of the materials caused by acidic solutions. At the end of the ageing periods, the pressure cookers were taken out from the oven and left to cool down to room temperature before opening. After the pressure cookers were opened, the dumbbell samples were taken out and rinsed with deionised water to remove the excess ageing solution from the sample surface. The samples were then left at room temperature to dry before the weight was measured. The percent weight change was calculated by the following equation:

$$\text{Weight Change (\%)} = \frac{W_2 - W_1}{W_1} \times 100 \quad (5.2)$$

where W_1 is the initial weight of the sample in air, and W_2 is the weight of the aged sample in air.

5.6. Tensile Testing

Fuel Cell Hydrogen Energy Association (FCHEA) issued the recommended standard test methods including tensile testing, hardness, compression set and chemical resistance test for PEMFC gaskets in their report⁸ to provide a source for assessing the suitable gasket materials for PEMFCs.

Tensile tests were carried out in our study on the aged gasket samples in order to examine the effect of acid aging on mechanical properties. A Hounsfield universal testing machine fitted with a laser extensometer was used to measure tensile properties in accordance with BS 903: Part A2⁹ at a constant head speed of 500 mm/min and with a 100 N load cell. A Hounsfield laser extensometer was attached to the test machine to measure the extension. The dumbbell test pieces were prepared by punching with a die cutter from 1 mm thick vulcanized test sheets. Figure 5.4 (a) shows the dimensions of the dumbbell sample. The two reflective tapes were then placed 1 cm apart from each other at the centre of the each specimen before testing as shown in Figure 5.4 (b).

Four dumbbell samples were measured for each aging time. Values of tensile strength, elongation at break and 50% and 100 % modulus were recorded. The modulus is a measure of stiffness used for elastomers and is the stress recorded at 50% and 100% elongations.

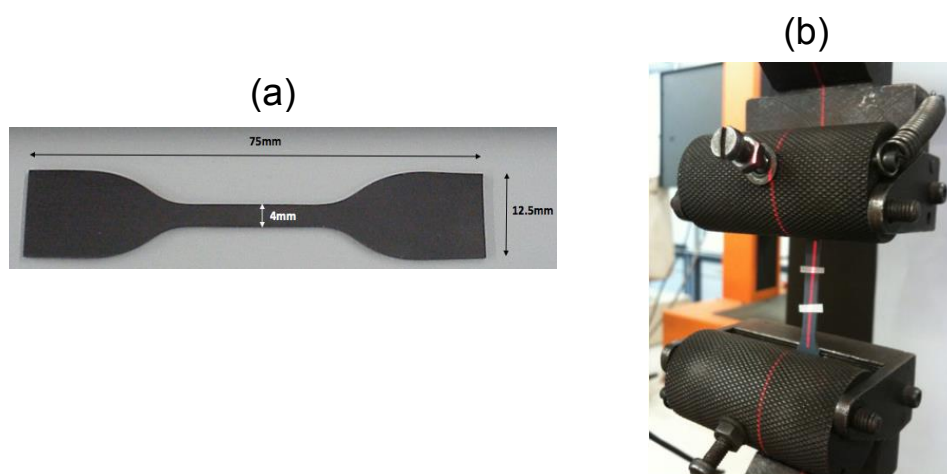


Figure 5.4. (a) Dimensions of a tensile test piece and (b) tensile grip with specimen clamped on

5.7. Compression Set

Compression set measurements were conducted on type B cylindrical test pieces with 13.0 ± 0.5 mm diameter and 6.3 ± 0.3 mm thickness according to BS ISO 815-1:2008¹⁰. The test specimens were compressed to 25 % of their original thickness for 72 hours at elevated temperatures of 70°C and 140°C.

After the test period, the specimens were removed from the oven and were left at the room temperature to recover for 30 minutes before the measurements were carried out. Compression set was calculated using the following equation:

$$\text{Compression set (\%)} = \frac{h_0 - h_1}{h_0 - h_s} \times 100 \quad (5.3)$$

where h_0 is the initial thickness of the test piece

h_1 is the thickness of the test piece after recovery

h_s is the height of the spacer.

5.8. Hardness

Hardness is essentially a measurement of the small strain elastic modulus of the rubber and is determined by measuring its resistance to a rigid indenter under a specified load.

A Wallace Shore A Hardness Tester H17 was used in this experiment with a test specimen of at least 6 mm in thickness. The result is stated as a value between 0 and 100 Shore A.

5.9. REFERENCES

- [1] "Vistalon™ 7500 Ethylene Propylene, Terpolymer, Diene," 2010. [Online]. Available: <http://exxonmobilchemical.ides.com/en-US/ds244666/Vistalon>. [Accessed: 22-Jul-2015].
- [2] E. Propylene and D. Terpolymer, "Vistalon™ 2504," 2014. [Online]. Available: <https://exxonmobilchemical.ides.com/en-US/ds244653/Vistalon™2504.aspx?l=74710&U=0>. [Accessed: 17-Sep-2015].
- [3] J. S. Dick and R. A. Annicelli, *Rubber technology : Compounding and testing for performance*. Munich : Cincinnati, Ohio: Hanser, 2001.
- [4] Synthomer, "Technical Data Sheet Lithene AL," 2014. [Online]. Available: http://www.synthomer.com/pkt/pdf_3.php?ProdId=7226&TdsId=48050&template_id=3&ProdBez=LITHENE ULTRA® AH. [Accessed: 17-Sep-2015].
- [5] J. Tan, Y. J. Chao, H. Wang, J. Gong, and J. W. Van Zee, "Chemical and mechanical stability of EPDM in a PEM fuel cell environment," *Polym. Degrad. Stab.*, vol. 94, no. 11, pp. 2072–2078, Nov. 2009.
- [6] C. Zhou, M. a. Guerra, Z.-M. Qiu, T. a. Zawodzinski, and D. a. Schiraldi, "Chemical Durability Studies of Perfluorinated Sulfonic Acid Polymers and Model Compounds under Mimic Fuel Cell Conditions," *Macromolecules*, vol. 40, no. 24, pp. 8695–8707, Nov. 2007.
- [7] C. Chen and T. F. Fuller, "The effect of humidity on the degradation of Nafion® membrane," 2009.
- [8] "Fuel Cell and Hydrogen Energy Association, Recommended Standard Test Methods for Fuel Cell Gasket Material," 2011.
- [9] British Standard Institution, *BS ISO 37:2011.Rubber, vulcanized or thermoplastic. Determination of tensile stress-strain properties*. London: British Standard Institute, 2011.
- [10] British Standard Institution, *BS ISO 815-1:2008.Rubber, vulcanized or thermoplastic. Determination of compression set. At ambient or elevated temperatures*, no. March. London: British Standard Institute, 2009.

6. CHAPTER 6: Degradation of Silicone Rubber Gasket

Material

In this chapter, the change in properties and structure of a silicone rubber gasket brought about by use in a fuel cell is compared to the changes in the same silicone rubber gasket material brought about by accelerated aging. The mechanisms of degradation in the two environments are discussed and the effects of temperature and acidity on the rate of degradation in the accelerated aging environment are quantified.

6.1. Aging of Silicone Rubber Gasket in an actual PEM Fuel cell Environment

As shown in Figure 6.1, degradation occurs in the gasket close to the cathode (outlet / top part of the gasket) where it is exposed to membrane as well as air and acidic product water (caused by sulfonate groups in the Nafion® membrane). product water. This acid hydrolysis degradation can be seen more clearly on the surface of the silicone rubber gasket in Figure 6.2 (b). However, there is no / very little degradation observed in the gasket close to the anode (inlet / bottom part of the gasket) which is drier in the nature and only hydrogen gas (fuel) is present. At the inlet port gasket is exposed to gas diffusion layer (GDL) or fuel cell cavity.

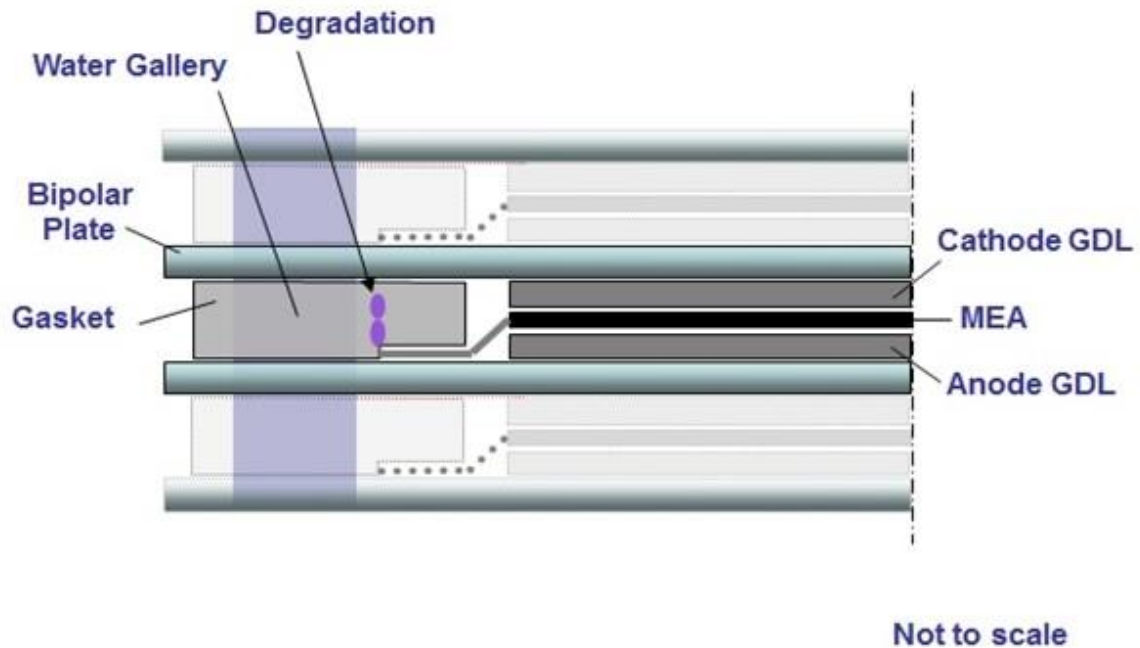


Figure 6.1. Cross section of a PEM fuel cell showing gasket

The silicone rubber gasket used in a real fuel cell environment for a period of up to 8000 hours was examined and the results are discussed in the following sections.

6.1.1. Observed Surface Degradation of the Silicone Rubber Gasket

Figure 6.2 shows the sections from unused and used silicone rubber gasket after 8000 hours operation in the fuel cell at the temperatures of around 80 to 90°C (fuel cell temperature). It can be seen clearly that, severe degradation occurred in the used silicone rubber gasket which has caused the formation of holes and whitened areas, particularly where it was against the edge of the membrane [Figure 6.2(b)]. This degradation resulted in the failure of the gasket during fuel cell operation. In some cases, silicone rubber gaskets failed even after 5000 hours of service in the cell. Therefore, initial work on the project was carried out to identify the mechanisms of silicone rubber gasket degradation and the factors that affect it.

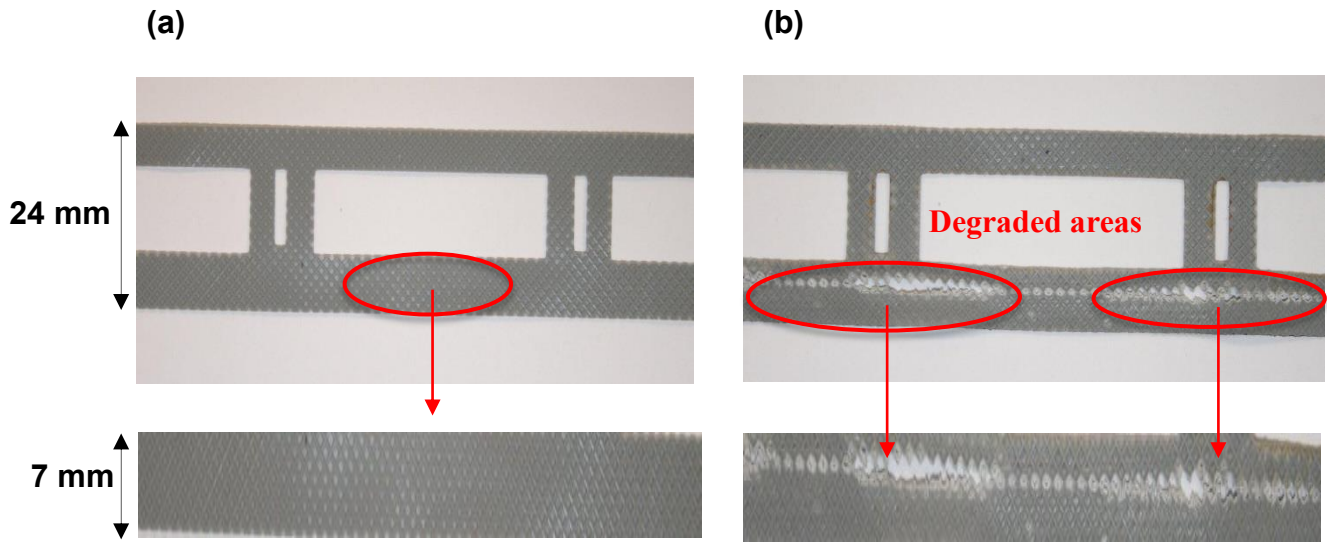


Figure 6.2. Sections of silicone rubber gasket (a) unused (b) after 8000 h use in fuel cell

6.1.2. Scanning Electron Microscopy (SEM) – Change in the Thickness of the Gasket

The cut surfaces of the unused and used silicone rubber gaskets which were used in a fuel cell for 5000 and 8000 hours were studied by employing SEM in order to compare the thicknesses of the gaskets before and after service in the fuel cell. Figure 6.3 shows the SEM images of the gaskets.

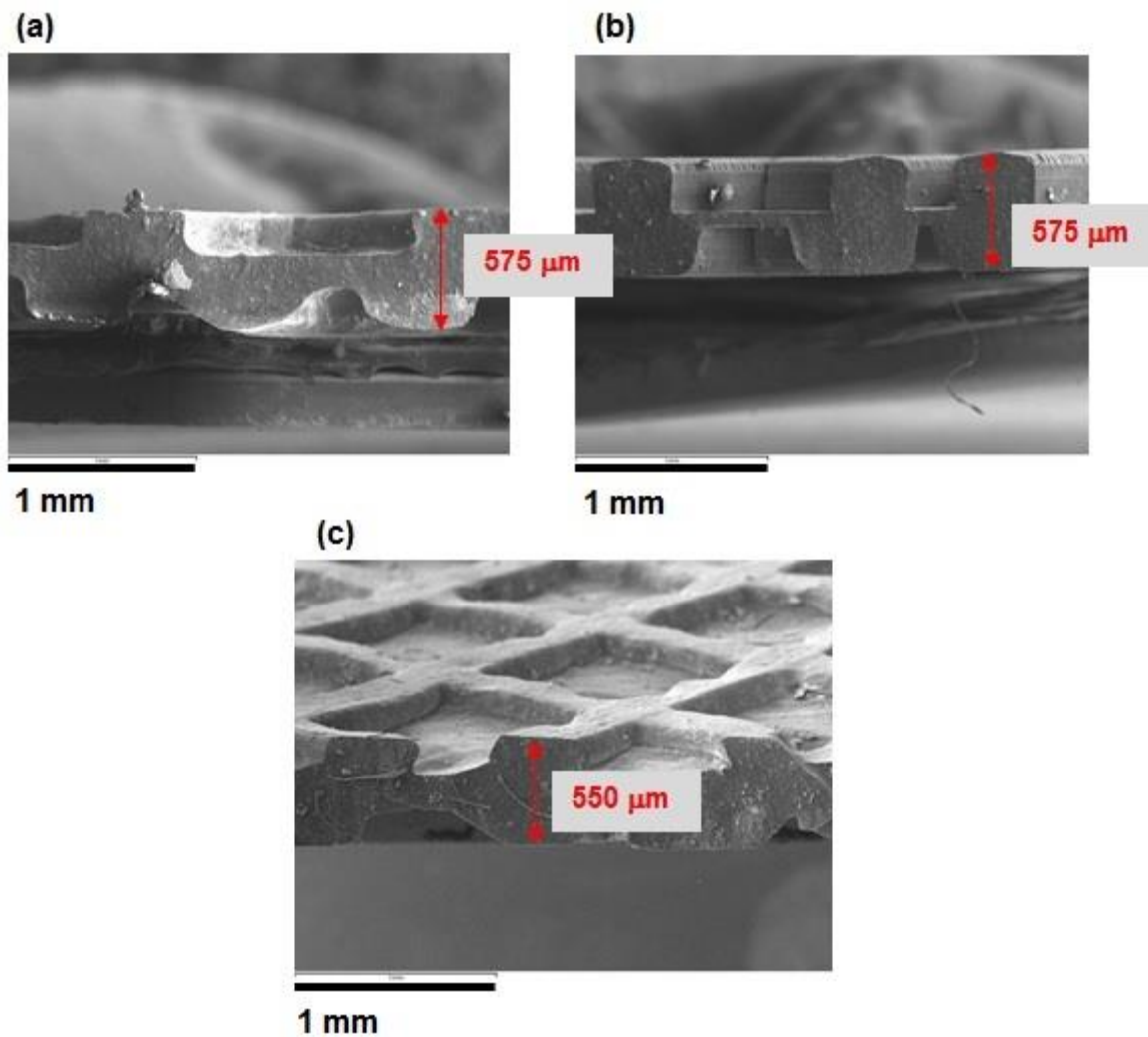


Figure 6.3. SEM images of silicone rubber gasket (a) unused (b) used for 5000 h (c) used for 8000 h

As shown in Figure 6.3 (b), the thickness of the silicone rubber gasket did not change after 5000 hours use in the fuel cell. Even after 8000 h [Figure 6.3 (c)], there was not a considerable reduction in the thickness.

The individual and average thickness of six samples (i.e., top, bottom, left and right sections of the gasket) each of unused and used (5000 and 8000 h) gaskets were measured from SEM images (See Figure 6.4). The mean thicknesses were 580, 622, and 568 μm for the unused, in service for 5000 h and in service for 8000 h samples, respectively.

There was a standard deviation of 60 μm for each batch of samples. The results indicate that there was no significant change in the thickness of the gaskets with service time and suggest that compression set is unlikely to be a cause of failure for these silicone rubber gaskets.

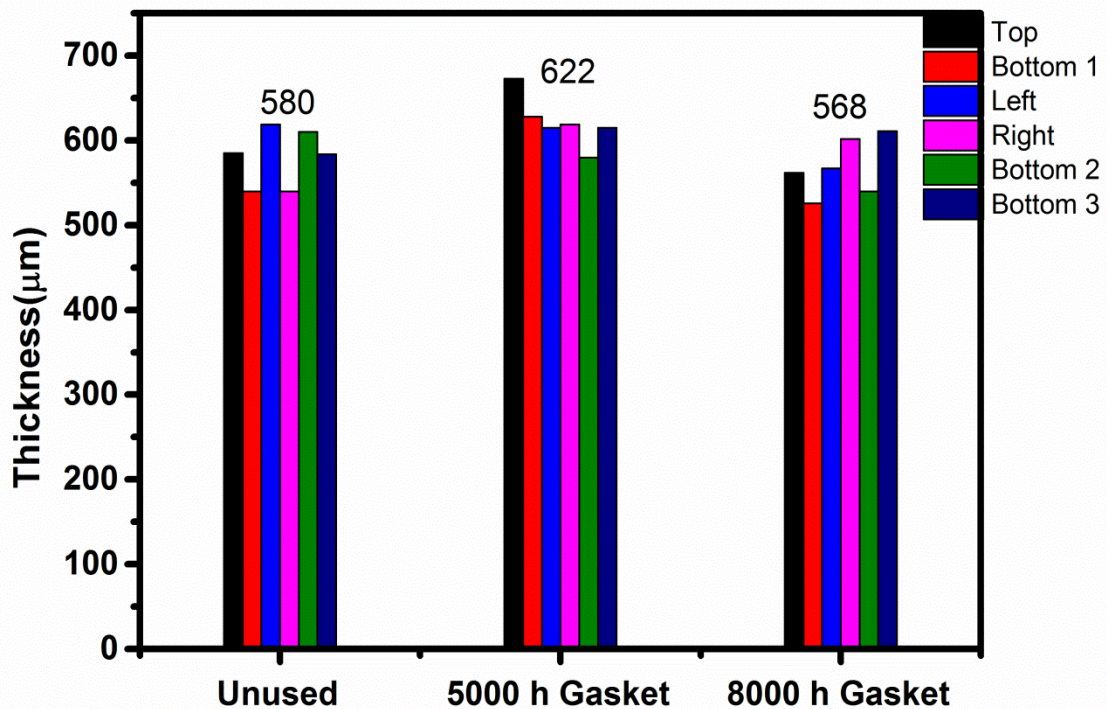


Figure 6.4. Average thicknesses of silicone rubber gaskets measured from SEM images

6.1.3. Atomic Force Microscopy (AFM) – Change in the Stiffness of the Gasket

As stated in section 6.1.1, silicone gaskets that had been used in a fuel cell showed clear areas of degradation particularly where the edge of the membrane rested against the gasket. Degradation appeared as a white powdery substance on the surface and in some cases the surface was degraded away and holes could be observed. For one of these degraded gaskets, AFM measurements were carried out to determine whether changes in stiffness of the material could be detected where degradation had started but had not progressed to a visible degree.

Topographic images obtained from AFM measurement contain qualitative information about the topography and form of the surface.

For instance, the top left image of Figure 6.5 gives information about the height of the surface. The black areas in the picture represent a low point (i.e., a hole) and white parts signify the high points. The top right image is a tip-deflection image with shaded areas in the picture accentuating the edges. The bottom left image is a phase topographic image, which expresses the phase of the reaction related to the force that is applied in the measurement. Darker parts in the image correspond to a lower phase lag and probably indicate the presence of rigid fillers, whereas the light areas could be explained as soft, rubbery parts. Finally, the image on the bottom right illustrates the points at which force/distance curves were acquired (i.e., +1, +2, +3, and +4).

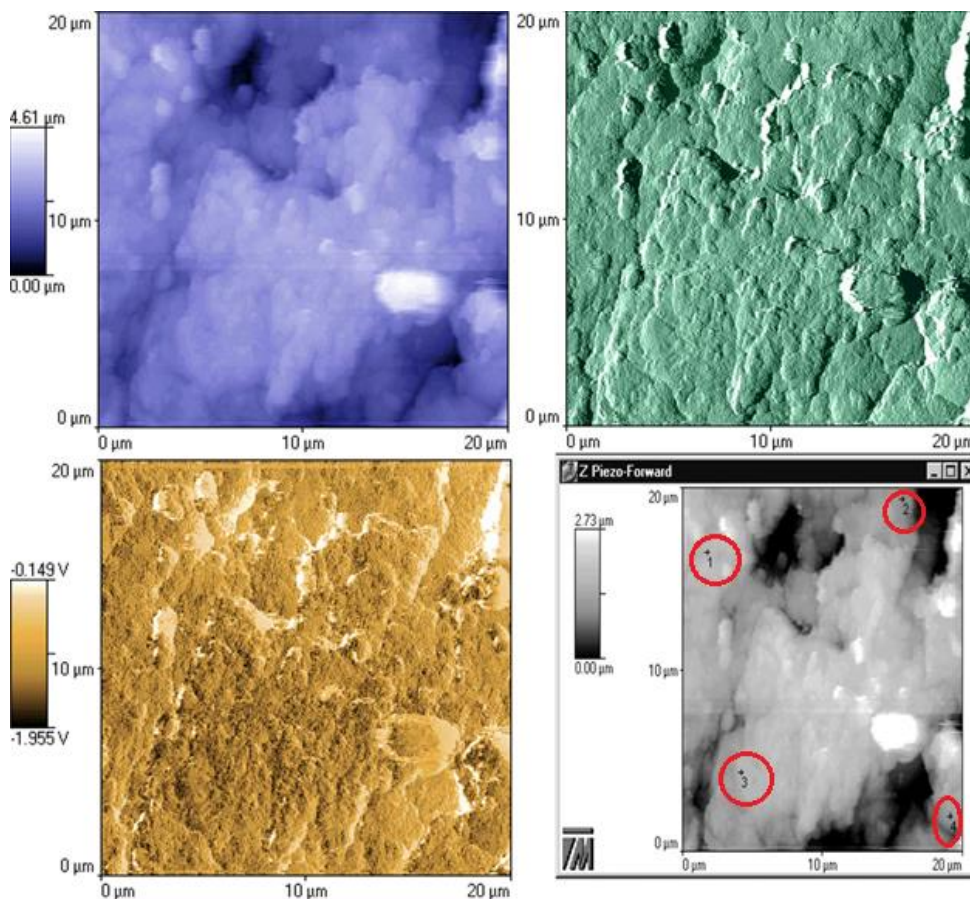


Figure 6.5. Topographic images of used silicone rubber gasket: Location 4. The points (1, 2, 3, and 4) on right bottom image indicate the points at which AFM modulus was calculated for each location

In addition to the qualitative information, force/distance curves were measured at four points for each location. For example Figure 6.6 depicts the force/distance curves, for Location 4. The slope of the force/distance curve is taken as the AFM modulus and has arbitrary units. Figure 6.7 presents the AFM modulus values of unused and used gaskets which were calculated at four points for each location. The AFM modulus for the four points measured at each location are very scattered, showing as great a variation as that observed between the five different locations of supposed differing degradation. The variation in AFM modulus may well be due to local distribution of filler particles rather than differences in level of degradation of the polymer. Hence, these results suggest that AFM is not a useful tool for determining degree of degradation for this particular compound.

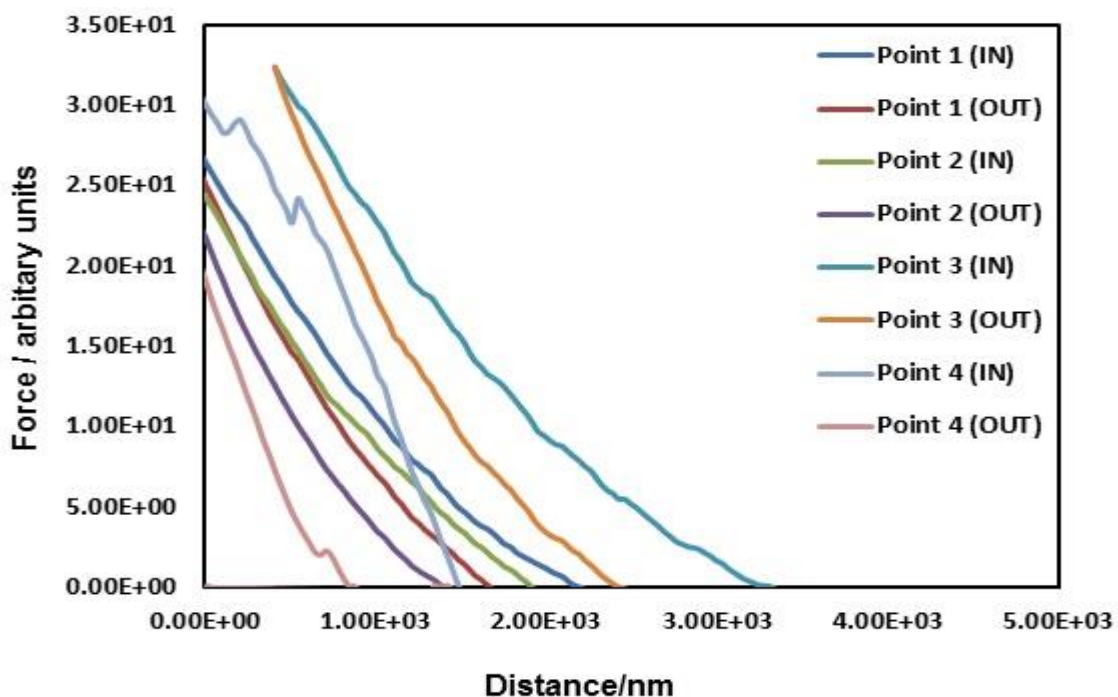


Figure 6.6. Force/distance curves of the used silicone rubber gasket – location 4 (In and out represents the force measurement of the AFM probe with the amount of indentation on the surface)

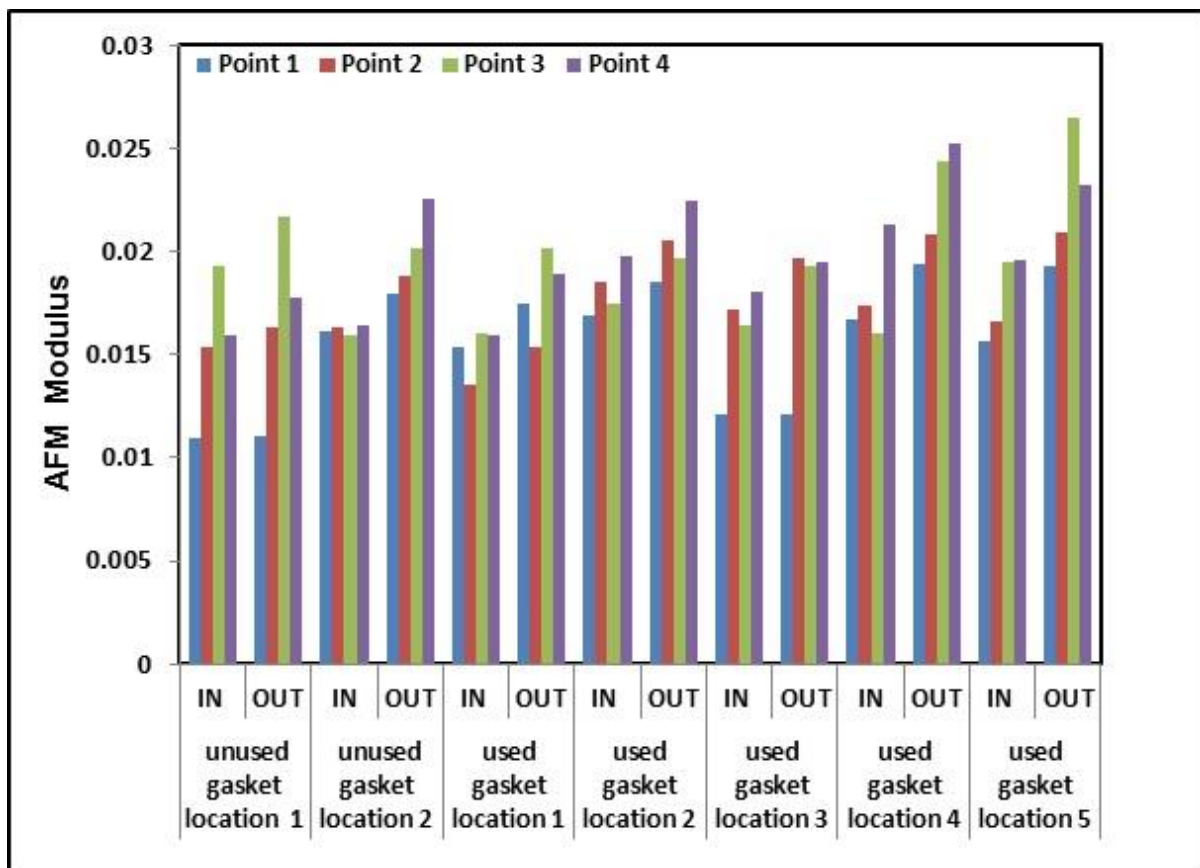


Figure 6.7. AFM Modulus of unused and used (5000 h in the fuel cell) silicone rubber gaskets (from less degraded area, Location 1, to highly degraded area, Location 5, and at each location four different points were measured)

6.1.4. X-Ray Photoelectron Spectroscopy (XPS) – Change in Surface Atomic Composition

The samples for XPS measurements were obtained by cutting pieces from unused silicone rubber gasket and different parts of a gasket used in a fuel cell (i.e., 5000 hours) including, undegraded, stained (brown), and degraded (white) areas as displayed in Figure 6.8. Brown areas may indicate the presence of iron oxide on the surface of the gasket, which might be the result of the corrosion of bipolar plates in the fuel cell. White degraded parts might be caused by hydrolysis due to the aqueous acidic environment in the fuel cell.

The XPS spectra in Figure 6.9 reveal the presence of carbon (C), oxygen (O), silicon (Si), and a small amount of fluorine (F). The atomic concentrations of these elements are also shown in Table 6.1.

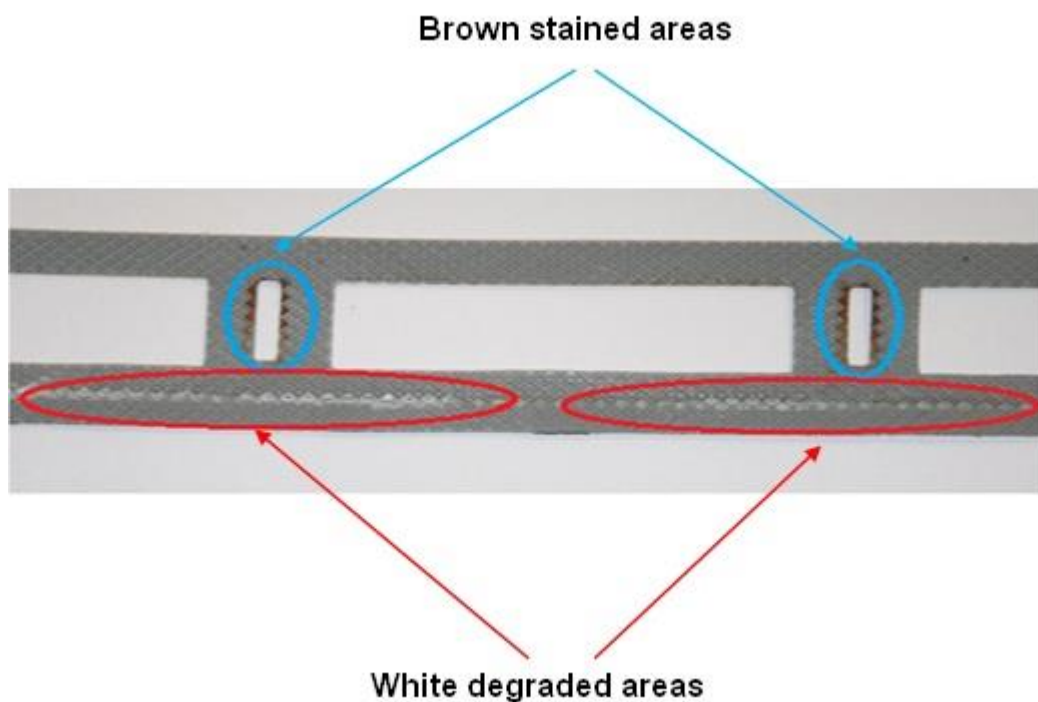


Figure 6.8. Stained and degraded areas of used silicone rubber gasket

Table 6.1. Atomic Composition of Silicone Rubber Gasket from XPS Measurements

Sample	Atomic Concentration (atom %)				Ratios to Si	
	C	O	Si	F	C/Si	O/Si
Unused Gasket	50.9	24.2	24.9	Trace	2.04	0.97
Used Gasket (Undegraded area)	47.2	25.6	25.9	1.3	1.82	0.98
Used Gasket (Close to stained area)	46.4	26.4	25.5	1.7	1.81	1.03
Used Gasket (Degraded area)	34.4	35.0	30.6	–	1.12	1.14

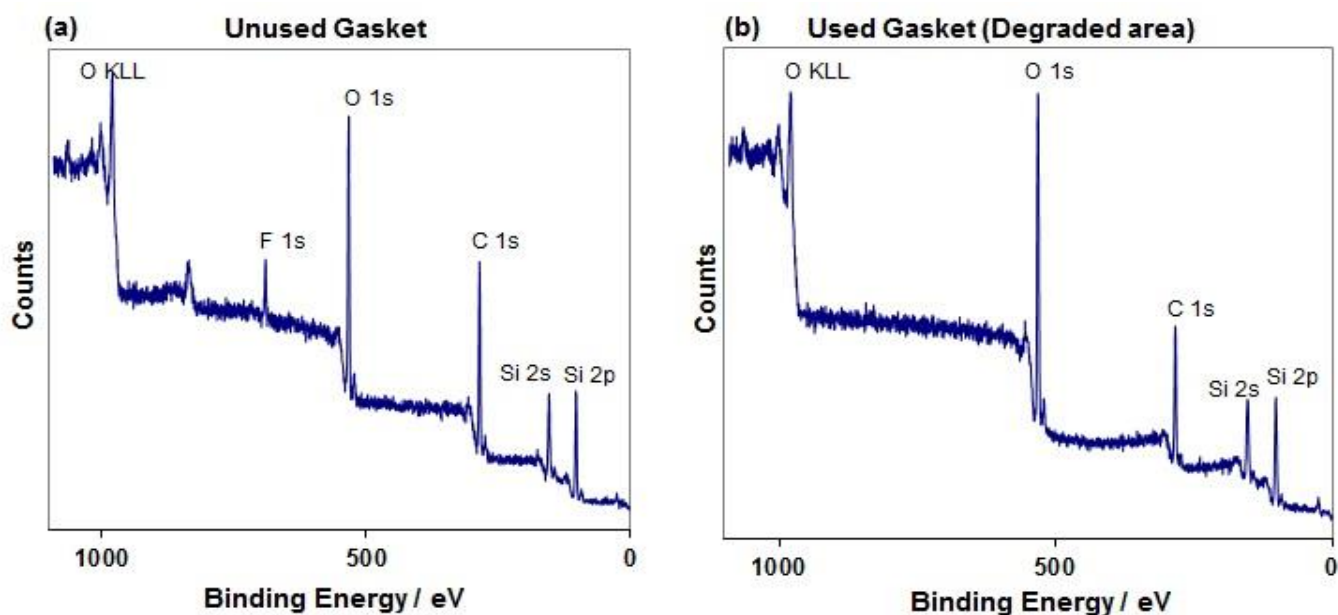


Figure 6.9. XPS spectra for silicone rubber (a) unused gasket (b) degraded area of used (5000 h in the cell) gasket

In XPS, samples are exposed to X-rays. Photons are absorbed by elements in the top few nanometres of the sample surface causing ionization (the gain or loss electrons) and the release of core (inner shell) electrons of the molecules. The kinetic energy distribution of the emitted photoelectrons is measured in the spectrometer and electron binding energies are determined. For each element, there will be a characteristic binding energy associated with each core atomic orbital and therefore any given element produces a characteristic peak in the photoelectron spectrum. Peak intensities can be related to the concentration of the given element allowing XPS to provide a quantitative analysis of surface composition¹.

It can be seen from Figure 6.9 (b) that the carbon peak is lower and the oxygen peak higher in the degraded area of the used gasket compared to the ones in the spectra of the unused gasket [Figure 6.9 (a)]. This can be observed also from the ratios of C/Si and O/Si shown in Table 6.1. XPS did not detect iron atoms on the surface of the gasket sample and so it is assumed the concentration of iron (Fe) atom was less than 1% (the detection level of this equipment). The presence of fluorine (F) may be due to contamination of the surface of the samples from the membrane. As shown in Table 6.1, the C/Si ratio is lower for the used gaskets than the unused gaskets, but is particularly low for the degraded part of the used gasket.

This could be due to the methyl group (CH₃) on the silicone atom being attacked and oxidized to form Si –O bonds. This behaviour would also account for the increase of the O/Si ratio with use and degradation of the gasket (Table 6.1). Additionally, hydrolytic breakage of the Si – O – Si backbone could cause this increase in O/Si ratio.

6.1.5. Attenuated Total Reflection Fourier Transform Infrared Spectroscopy (ATR-FTIR) – Change in Surface Chemistry with Degradation

Initially, unused and degraded parts of the used silicone rubber gasket were analysed. There was no detectable change in the FTIR spectra. For this reason, we scraped the white powdery degraded deposit from the surface of this decomposed part of the used gasket and investigated on ATR-FTIR.

However, there were only relatively small alterations in the FTIR spectra of this degraded part in comparison with the unused silicone rubber part, as reflected in Figure 6.11 (A) and (B). It is assumed that the presence of silica filler in the silicone rubber gasket makes it difficult to detect chemical degradation of the silicone rubber gasket using FTIR. This is because the degradation product of silicone has an almost identical structure to silica (See Figure 6.10).

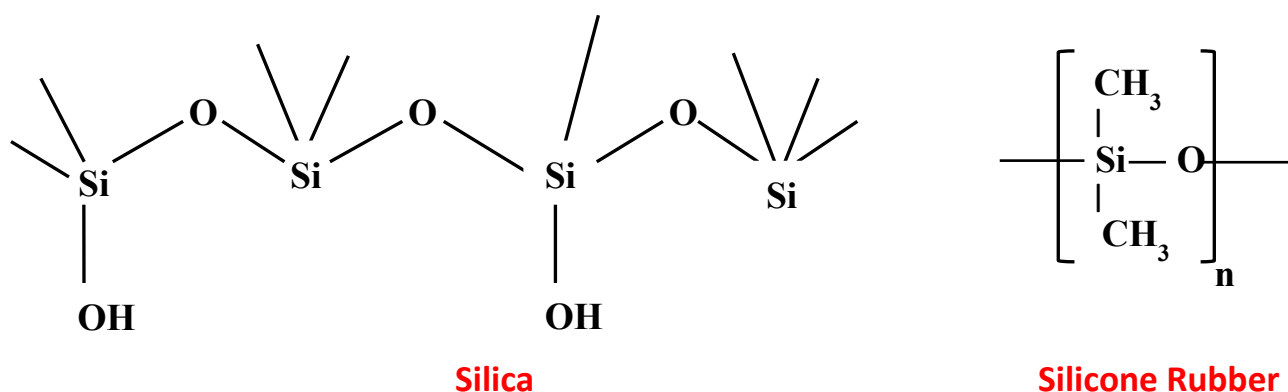


Figure 6.10. Chemical Structure of Silica and Silicone Rubber

Figure 6.11 shows the comparison of the ATR-FTIR results for degraded silicone rubber gasket (operating in the fuel cell for 5000 h) (A) & (B) and silicone rubber material after exposure to the accelerated aging test (pH 1 accelerated aging solution for 2 days) (C) & (D).

The largest peaks for both unused and unexposed silicone rubber are between 1007 and 1050 cm^{-1} [See Figure 6.11 (A) and (C)], which are characteristic of siloxanes and are, associated with asymmetric and symmetric stretching vibrations of Si – O – Si bonds. The peak arising at 694 cm^{-1} is due to the asymmetric deformation of Si – CH_3 bonds. The peak at 790 cm^{-1} corresponds to the bending mode of Si – C and C – H wagging [See Figure 6.11 (A) and (C)]. The peaks at 864 and 1259 cm^{-1} result from the rocking vibration of Si – CH_3 and the bending vibration of Si – CH_3 . The peak near 1411 cm^{-1} is due to the rocking vibration of – CH_2 – as a part of the silicone rubber cross-linked domain. The peak at 2963 cm^{-1} is related to the stretching vibration mode of CH_3 [See Figure 6.11 (B) and (D)]. It can be seen from Figure 6.1 that in general all the peaks did not experience any significant change with degradation.

Of particular significance is the similarity of the spectra for the degraded materials from the fuel cell and accelerated aging environment, which means that the accelerated aging conditions bring about a similar type of degradation to that of the real fuel cell environment. It was concluded at this point of the investigation that ATR-FTIR was not a very sensitive technique to examine the surface degradation of silicone rubber. Thus, the tensile test was applied instead to investigate the degradation.

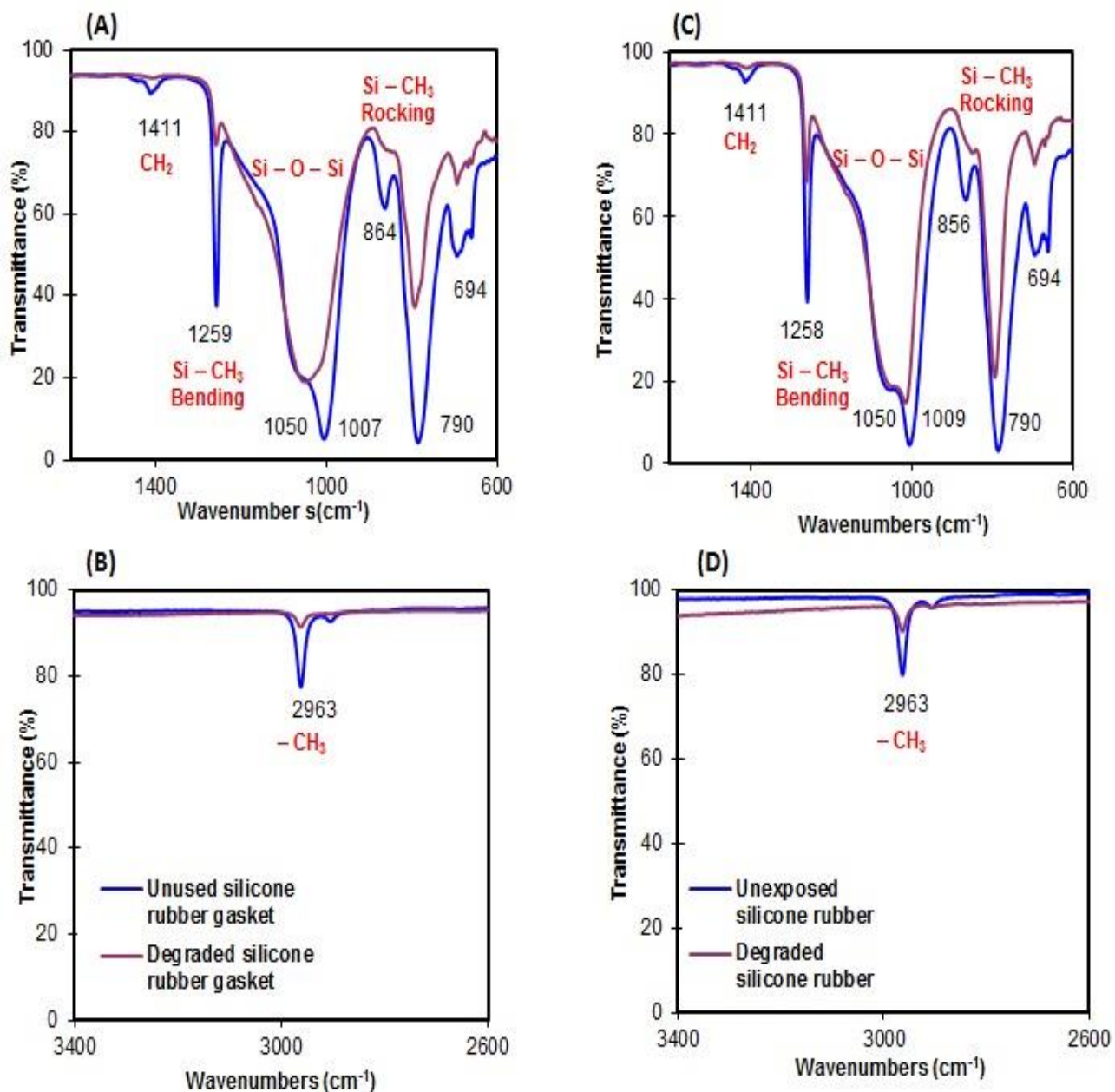


Figure 6.11. ATR-FTIR spectra after exposure to: (A) and (B) actual fuel cell environment, (C) and (D): accelerated aging test

6.1.6. Solvent Swelling Method – Change in the Cross-link Density

Solvent swelling was used to determine whether there were changes in crosslink density brought about by aging of the gaskets. Unused and used silicone rubber gaskets after 5000 and 8000 h service in the fuel cells were analysed by solvent swelling. Figure 6.12 shows the average volume after 6 days (144 h) of swelling in toluene. The percentage changes in volume of the samples were 118, 114, and 109 for the unused, after 5000 and after 8000 h service, respectively. Although the trend suggests a slight decrease in swelling and hence increase in crosslink density, given the very small difference in swelling between the samples in relation to the large amount of swelling of all the samples and a standard deviation of 4 on the swelling measurements, it is considered that the gaskets generally, did not experience significant crosslinking or breakage of crosslinks up to 8000 h in service. The result is a little surprising because both the XPS and the FTIR results indicated that crosslink cleavage and chain scission had occurred in the degraded samples. However, solvent swelling is a bulk measurement, whereas XPS is a surface technique, and the FTIR was carried out on a sampled piece of rubber exhibiting significant degradation. Considering the swelling and spectroscopic sets of results together, it seems likely that there is little degradation in the bulk of the sample, but severe degradation at the surface.

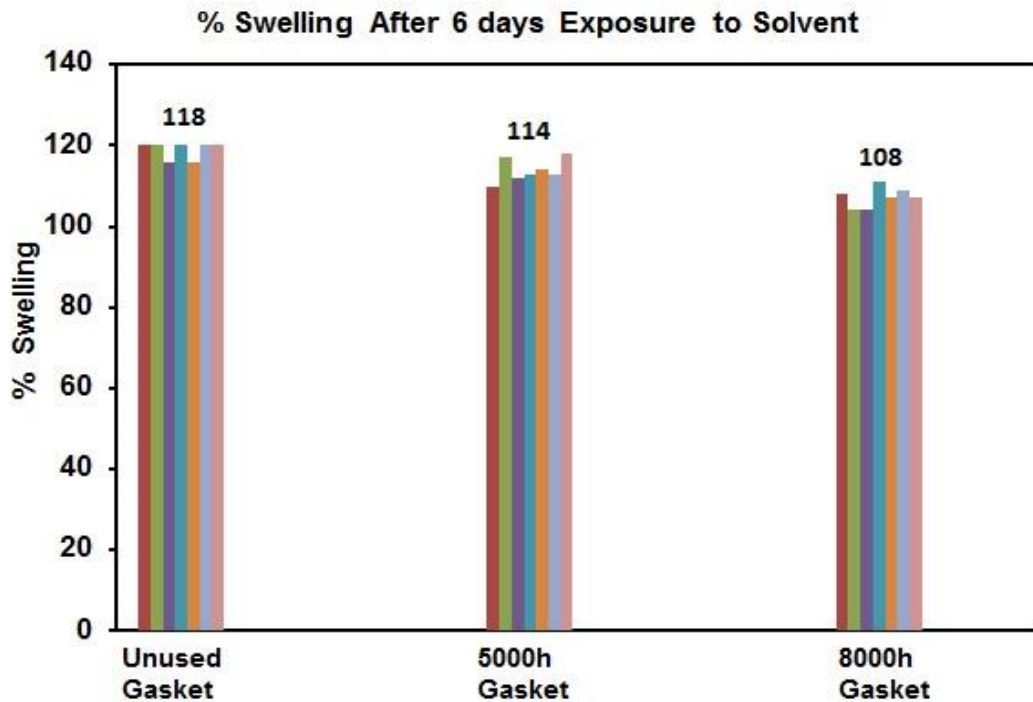


Figure 6.12. Average swelling after 6 days exposure to toluene

6.2. Aging of Silicone Rubber Gasket Material in an Accelerated Aging Environment

6.2.1 In Acidic H₂SO₄ Solutions of pH 1, 2 and 4

Effect of Aging on the Mechanical Properties

Tensile tests were carried out on the silicone rubber samples aged in H₂SO₄ solutions with pH values of 1, 2 and 4 at 140°C. The Figures 6.13, 6.14 and 6.15 reveal the data for tensile strength, elongation at break and 50 % modulus respectively.

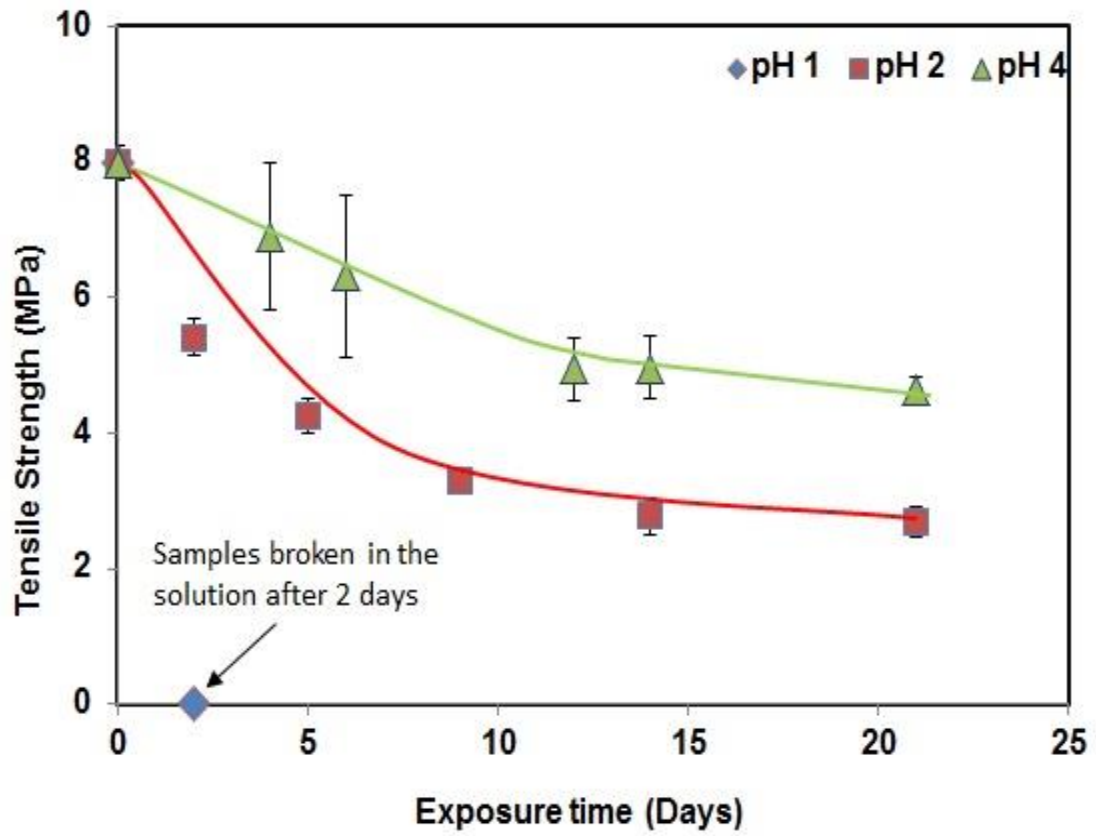


Figure 6.13. Tensile strength of silicone rubber after exposure to H₂SO₄ solutions of pH 1, 2 and 4 at 140°C

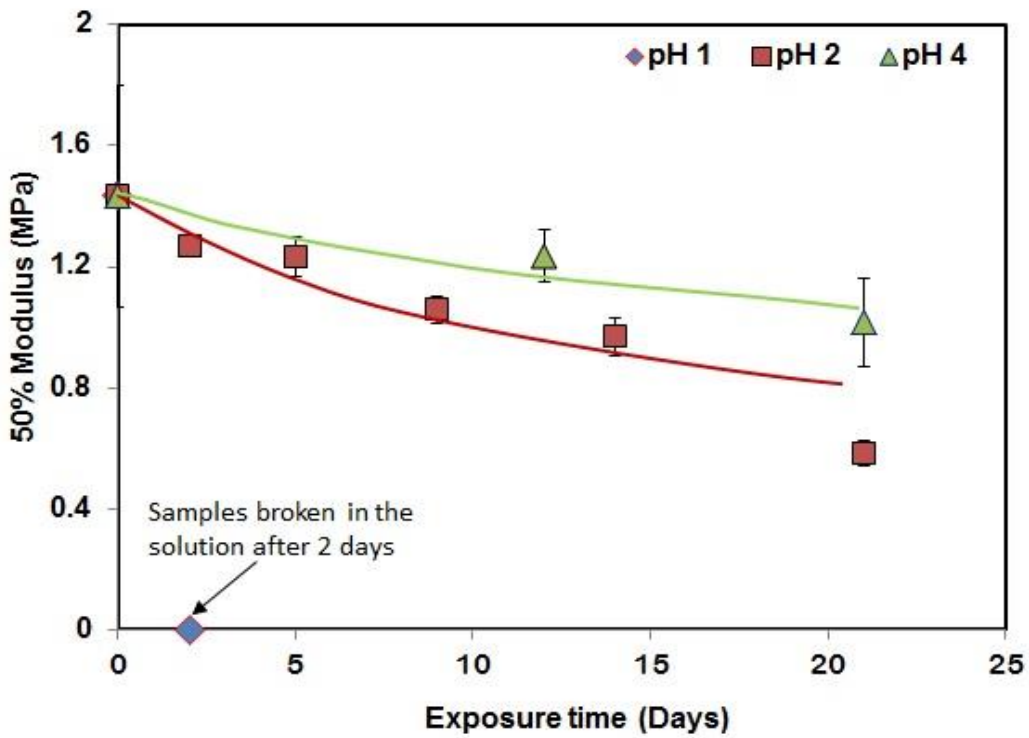


Figure 6.14. Elongation at break of silicone rubber after exposure to H₂SO₄ solutions of pH 1, 2 and 4 at 140°C

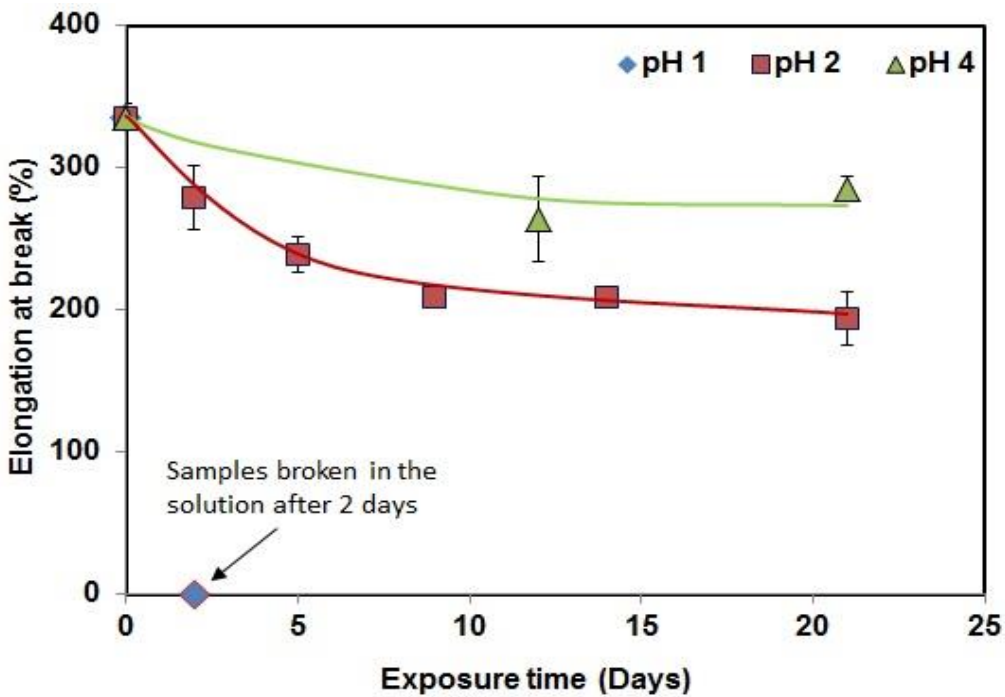


Figure 6.15. 50% Modulus of silicone rubber after exposure to H₂SO₄ solutions of pH 1, 2 and 4 at 140°C

As illustrated in Figures 6.13 – 6.15, tensile strength, elongation at break, and 50% modulus of silicone rubber decreased significantly with time and the rate of decrease was higher in more acidic solutions. However, the decrease in tensile strength is relatively greater than the decrease in modulus. For example, after 15 days at pH 2, the tensile strength has decreased by 70% (See Figure 6.13), whereas the modulus has decreased by 30% (See Figure 6.15). It is likely that the difference is due to the fact that tensile strength is particularly sensitive to surface degradation while modulus is more of a bulk effect. As was suggested by the swelling and spectroscopic results discussed previously, it seems that severe degradation occurs at the surface but very little occurs in the bulk and as aging progresses the degradation front moves inwards. The thickening of the severely degraded layer, which in itself has very little strength, would inevitably result in a decrease in strength and modulus of the sample due to the smaller amount of undegraded rubber remaining that can take the load. In addition, a brittle degraded layer may also be a site for crack initiation, which would also tend to reduce tensile strength. The particular sensitivity of tensile strength to accelerated aging makes it a good means of quantifying aging, being much more sensitive and quantitative than the imaging and spectroscopic methods studied. It would have been beneficial to compare these accelerated aging results with the decrease in tensile strength of the gaskets with service life. However, the geometry of the gaskets was not suitable and sites of degradation so localized that a sensible set of tensile data could not be obtained.

Effect of Aging on the Surface Appearance

The surface degradation of the silicone rubber samples before and after exposure to diluted H₂SO₄ aging solution (pH 1, 2, and 4) at different time intervals is shown in Figure 6.16. It can be seen clearly that the colour of the samples in the neck region which was submerged in pH 2 accelerated aging solution started to change from grey to white after 5 days [Figure 6.16(d)], and the degradation became even more significant (white colour in the neck region) after 9 days. The extent of the degradation was more severe in the more highly acidic solution (pH 1); hence, the silicone rubber samples were ruptured in pH 1 solution after only 2 days exposure [Figure 6.16 (b)].

By contrast, there was no sign of degradation on the surface of the samples after exposure to pH 4 accelerated aging solutions for 21 days [Figure 6.16 (h)].

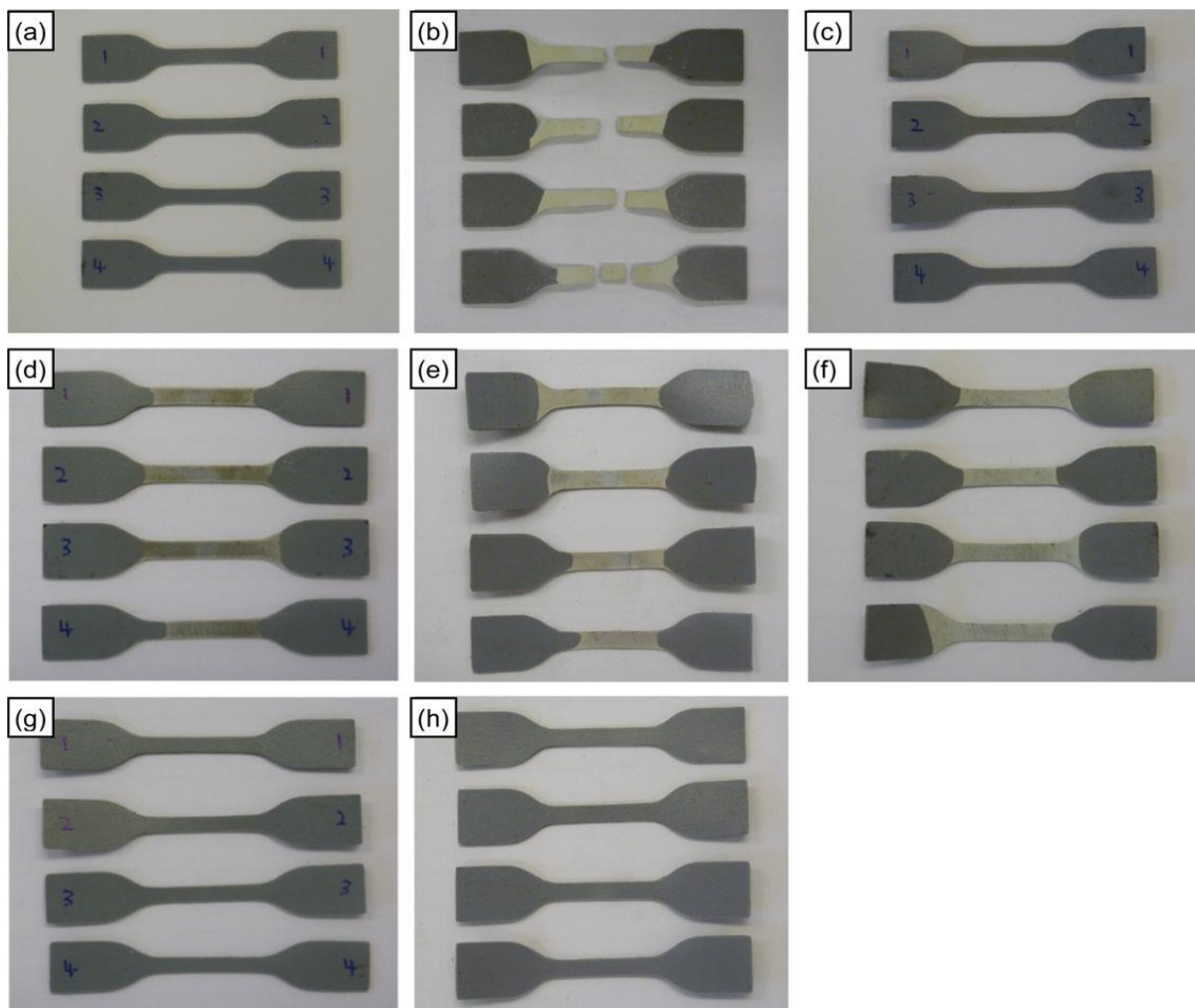


Figure 6.16. (a) Unexposed silicone rubber, (b) after exposure to H_2SO_4 pH 1 solution for 2 days; (c) after exposure to H_2SO_4 pH 2 solution for 2 days, (d) 5 days, (e) 9 days, and (f) 14 days; and (g) after exposure to H_2SO_4 pH 4 solution for 12 days and (h) 21 day at $140\text{ }^\circ\text{C}$

6.2.2. Aging of Silicone Rubber Gasket Material in Nafion® Solution with pH 3 to 4

Acidity (pH) of Nafion® Solution

The acidity of a PEM fuel cell environment is due to the presence of the sulfonated fluorinated hydrocarbon membrane, and for this reason, it was considered worthwhile to carry out accelerated aging experiments using the membrane as the source of the acid. Nafion® samples, which were cut from different parts of a sheet of Nafion® membrane (the edge and central parts), were placed in the pressure vessels containing distilled water and were kept at 140°C for up to 14 days. The weight percentages (wt %) of the Nafion® in water were 0.7 and 1.4. It can be observed from Figure 6.17 that despite the differences in the location on the membrane and in amounts used, the pH was found to be consistent, between 3 and 4 over the 14 day period. Considering that the pH of distilled water was 7 at the beginning, the decrease in pH in other words, the increase in acidity proves the acidic effect of the Nafion® membrane and indicates that the fuel cell environment is likely to be in the range of pH 3 to 4. The water that has been acidified by the presence of Nafion® is referred to as “Nafion® solution” for convenience although the polymer membrane as a whole is clearly not soluble in water.

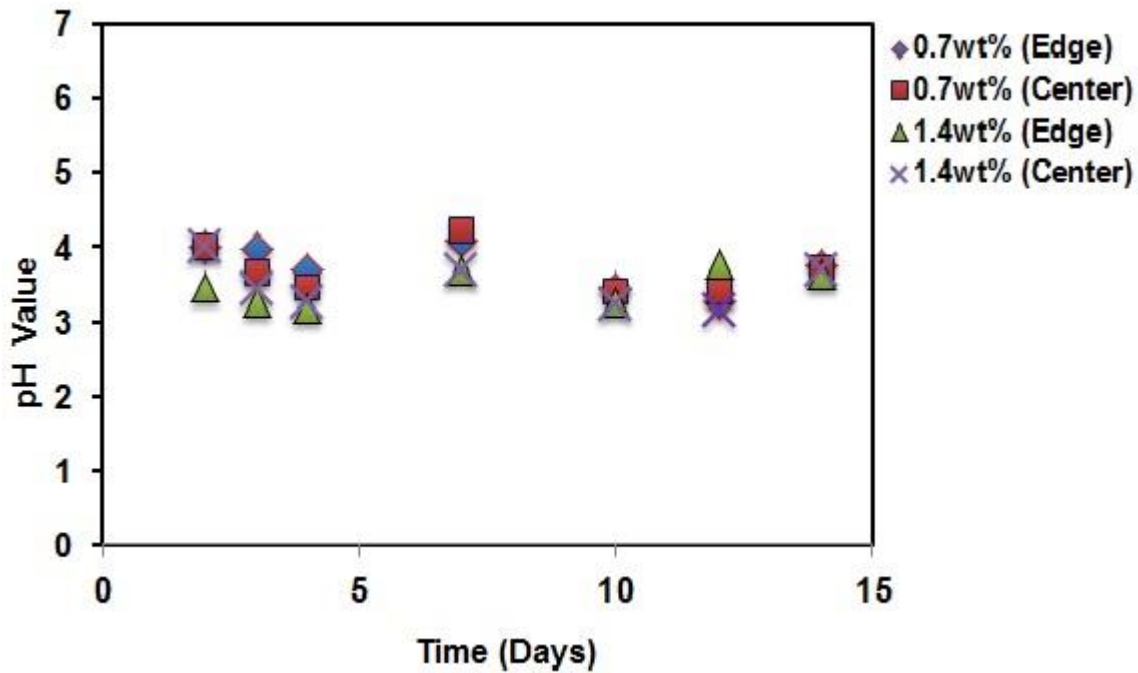


Figure 6.17. Acidity (pH) change with Nafion® samples taken from different locations on the Nafion® membrane and with different concentrations at 140°C for 14 day

Comparison of Degradation in Nafion® (pH 3–4) and H₂SO₄ (pH 2 & pH 4) Solutions

The tensile properties of silicone rubber samples which were exposed to Nafion® aging solution and diluted H₂SO₄ solution with pH of 2 and 4 at 140°C for over 8 days were measured. In Figures 6.18 and 6.19, it is clear that the decrease in both tensile strength and elongation at break of silicone rubber, which was aged in Nafion® solution, was greater than the one that was aged in diluted H₂SO₄ solution with a pH of 2. The result is surprising since the pH of the Nafion® aging solution was higher and so less degradation might have been expected. This suggests that there is something else coming from the membrane that is accelerating the aging process or it could be that the membrane in close proximity to the rubber gives locally a lower pH, which degrades the rubber more significantly.

On the other hand, the 50 % modulus of silicone rubber did not experience any change after exposure to all three solutions which was attributed to the bulk effect of the modulus as discussed beforehand (See Figure 6.20).

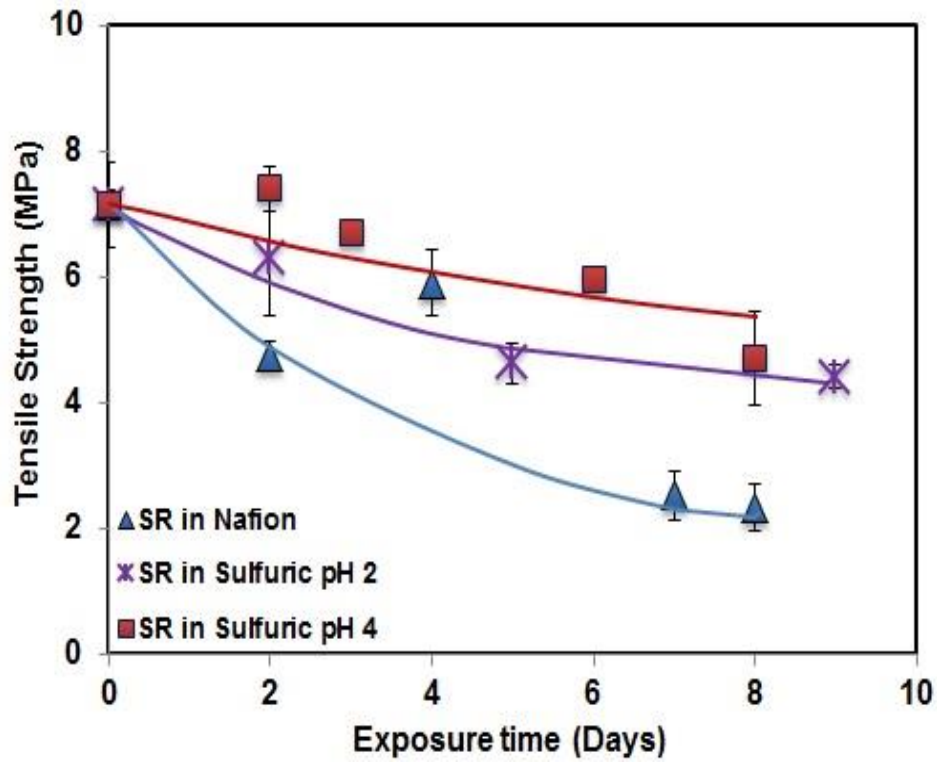


Figure 6.18. Tensile strength of silicone rubber (SR) after exposure to Nafion® (pH 3 – 4), and H₂SO₄ (pH 2 and pH 4) solutions at 140°C

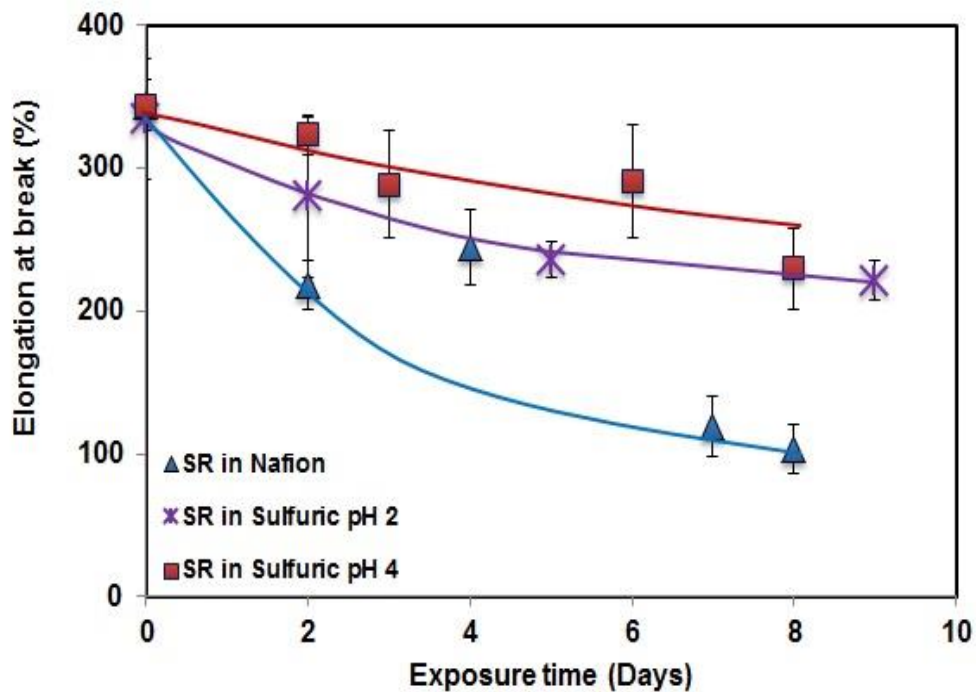


Figure 6.19. Elongation at break of silicone rubber (SR) after exposure to Nafion® (pH 3 – 4) and H₂SO₄ (pH 2 and pH 4) solutions at 140°C

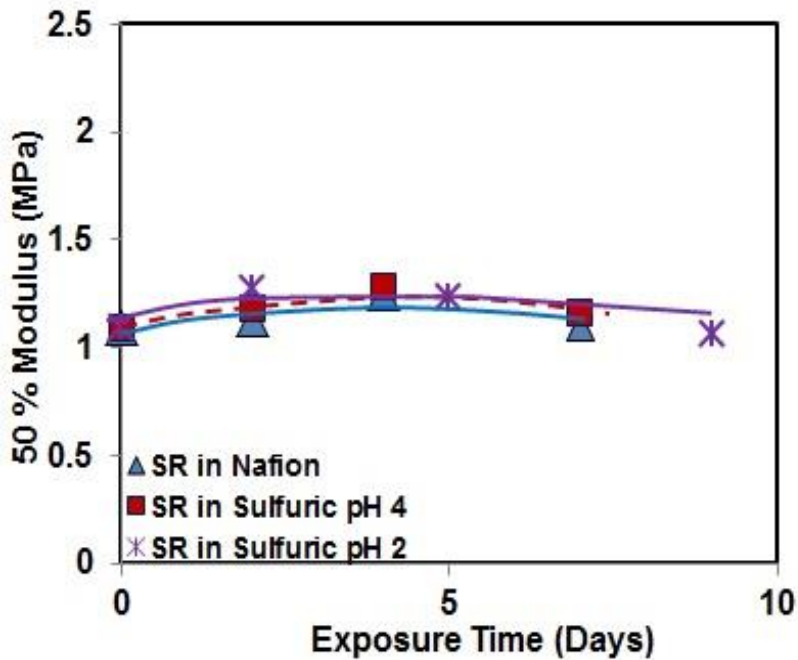


Figure 6.20. 50 % Modulus of silicone rubber (SR) after exposure to Nafion® (pH 3 – 4) and H₂SO₄ (pH 2 and pH 4) solutions at 140°C

6.2.3. Aging of Silicone Rubber in Trifluoroacetic acid (TFA) (pH 3.3), Nafion® (pH ~ 3.2) and H₂SO₄ (pH ~ 3) Solutions

The tensile test results in previous section supported the idea that the degradation of the silicone gasket in the fuel cell is brought about by acid attack coming from the Nafion® membrane. Apparently, it is not the pH value which affects this degradation process but probably the components or degradation products of the Nafion®. In published literature^{2,3}, trifluoroacetic acid (TFA) has been identified as a major degradation product of Nafion® membrane. Therefore, TFA could be the aging agent in PEM fuel cells. In the current study, a TFA solution of pH 3.3 was chosen for aging experiments because it is close to the pH value of the Nafion® solution. The extent of silicone rubber degradation in TFA solution (at constant pH 3.3), Nafion® solution (~ pH 3.2), and H₂SO₄ (~ pH 3) solutions at 140°C was assessed by employing weight change and tensile test measurements. The results are discussed in the following sections.

Acidity (pH) Change of the Aging Solutions

The change of the pH value of the acid solutions after being used to age silicone rubber samples was measured as a way of revealing the reaction between rubber samples and the acid solutions. Figure 6.21 demonstrates the change of the pH values of the acid solutions at 140°C over time.

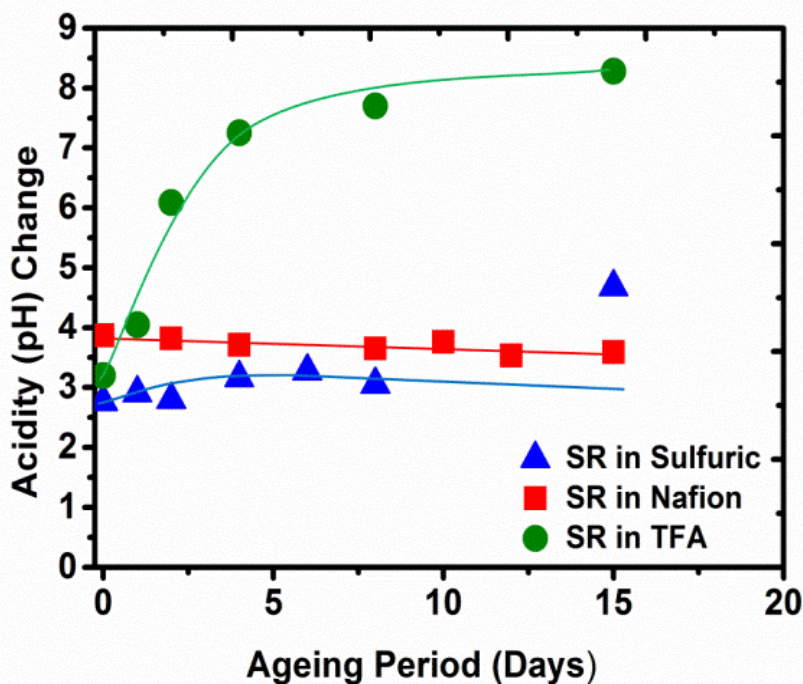


Figure 6.21. Change of the pH values of aging solutions containing silicone rubber (SR) at 140°C

The pH of the TFA solution (containing the silicone rubber) increased sharply with aging time compared to the ones of the Nafion® and sulfuric acid solutions. The TFA acid solution became neutral after 4 days and slightly alkaline after that, so it was clear that there was a chemical reaction between the TFA solution and silicone rubber samples, rather than just acid catalysed hydrolysis. This rapid change in the pH value of the TFA solution indicates that the TFA was used up in reactions relatively soon after the silicone samples were added. Therefore, the aging effect of the solution disappeared after 4 days when the TFA had been consumed. For this reason, an aging experiment was carried out with the TFA solution being refreshed every 2 days so that a fairly constant pH (3.3) was maintained. By contrast, sulfuric acid and Nafion® solutions had no significant change in pH after aging the silicone samples (See Figure 6.21).

This could be explained by the fact that the degradation of silicone rubber in those (i.e., sulfuric acid and Nafion®) solutions is considered to be an acid catalysed hydrolysis, in which acid is just a catalyst and remains the same before and after the reaction.

Weight Change

The weight change of silicone rubber samples which were exposed to sulfuric acid (H_2SO_4 ~ pH 3), Nafion® (pH ~ 3.2) and TFA (at constant pH of 3.3) Aging solutions at 140°C over time was monitored and results are shown in Figure 6.22. In all solutions, silicone rubber (SR) showed increasing weight loss with exposure time which was probably due to loss of the degraded material.

The largest decrease in weight was observed in TFA solution (~ 4 %) compared to the ones in sulfuric acid and Nafion® solutions (~ 1.5 – 2%) of the same pH.

This indicates that TFA solution was more aggressive than sulfuric acid and Nafion® solutions and also confirms the more rapid change in the acidity (pH) of TFA solution with time as explained above.

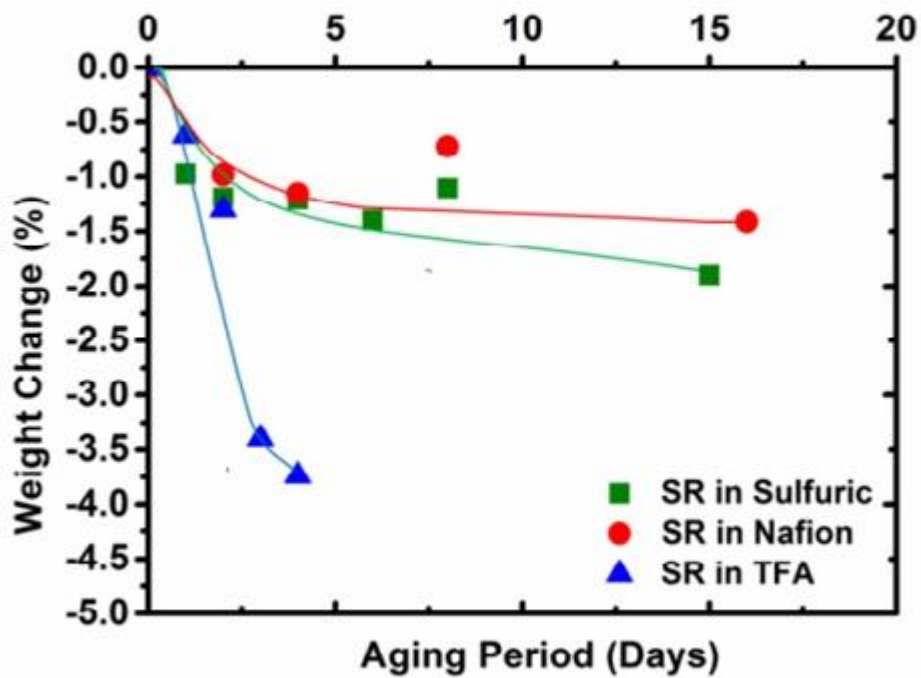


Figure 6.22. Weight Change of silicone rubber aged in Nafion®, TFA and sulfuric acid (~ pH 3) solutions @ 140°C

Effect of Aging on the Mechanical Properties

Figure 6.23 indicates that the tensile strength of silicone rubber in both Nafion® and TFA solutions declined significantly with time whereas it showed only a slight decrease in sulfuric acid solution of similar pH.

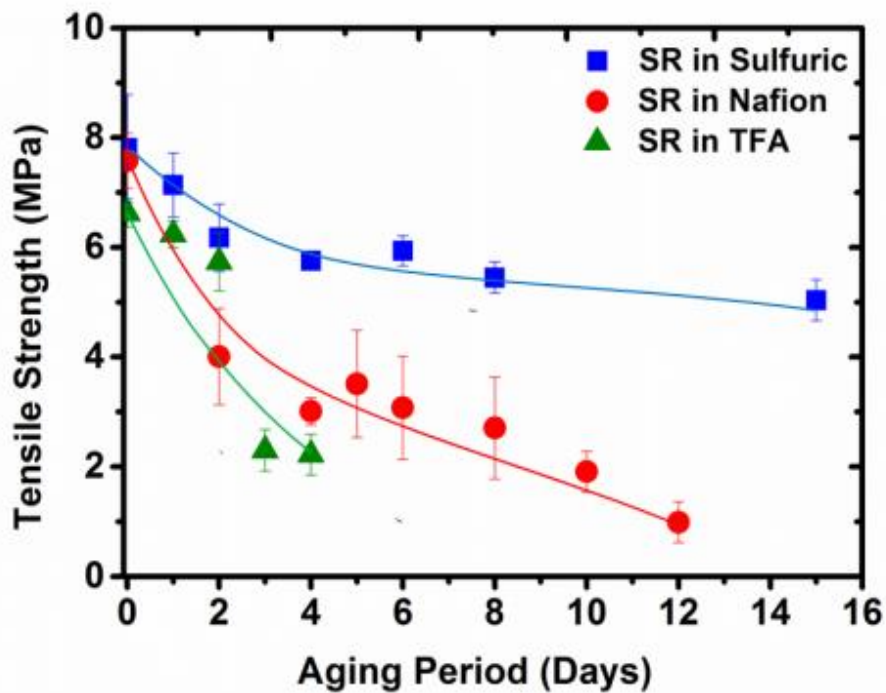


Figure 6.23. Tensile strength of silicone rubber aged in pH 3 (Nafion®, TFA and sulfuric acid) solutions @ 140°C

Effect of Aging on the Surface Appearance

Surface observations of silicone rubber samples exposed to pH 3 accelerated aging solutions of sulfuric acid, Nafion® and TFA solutions at 140°C for four days are presented in Figure 6.24. The silicone sample surfaces showed a similar colour change from grey to white after exposure to Nafion® and TFA solutions (c and d), however, there was no colour change observed after exposure to sulfuric acid solution (b). This confirms the more aggressive attack by TFA indicated in the weight change and tensile test results.

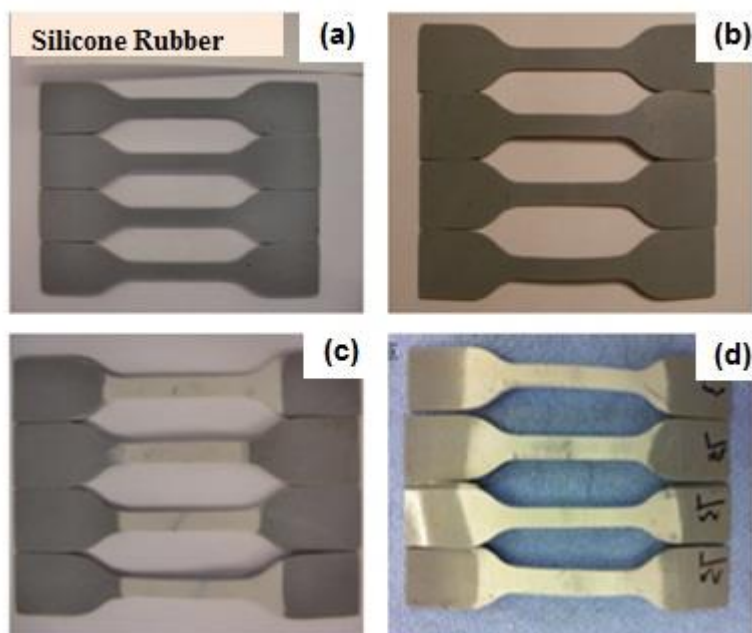


Figure 6.94. (a) Unexposed silicone rubber and after 4 days exposure to pH 3 solutions (b) sulfuric acid, (c) Nafion[®] and (d) TFA at 140°C

6.3. Summary

Examination of the silicone rubber seals used in the fuel cells for up to 8000 hours suggested that failure of the seals would not be due to compression set, but rather due to chemical degradation that made holes in the gasket in places and left a white powdery deposit on the surface in others.

Accelerated aging of the same rubber in sulfuric acid solution at 140°C resulted in visibly similar degradation and FTIR analysis of both samples confirmed the same type of hydrolysis reactions occurred in both the real fuel cell and accelerated aging test. Greater degradation occurred at lower pH levels confirming acid hydrolysis as the main degradation mechanism. AFM proved ineffective as a tool for determining the effect of aging on surface hardness of the rubber, probably because of variations, at a microscopic scale, in hardness caused by the presence of filler particles or agglomerates. Solvent swelling tests carried out on the gaskets used in fuel cell seals for up to 8000 h showed an insignificant change in crosslink density while modulus values of the accelerated aging samples showed a relatively small change in modulus compared to the large change in tensile strength.

Therefore, it is concluded that the fuel cell seals degrade by acid hydrolysis at the surface exposed to the acid but little degradation occurs in the bulk. Thus, degradation progresses as the degradation front moves inwards from the original surface. The similarity in degradation reactions occurring in the real fuel cells and accelerated aging tests at 140°C means that the accelerated aging tests could potentially be used to predict functional life of silicone seals in real fuel cells.

Furthermore, aging carried out using hydrated Nafion® membrane as the source of acid as well as TFA solution revealed that there was greater degradation of silicone rubber in the Nafion® and TFA solutions than was achieved with sulfuric acid solution of the same pH. This implies that the major degradation product of the Nafion® membrane, particularly the TFA, accelerates the acid hydrolysis of silicone rubber.

6.4. REFERENCES

- [1] “The University of Nottingham, Isaac Interface and Surface Analysis Center, X-Ray Photoelectron Spectroscopy(XPS).” [Online]. Available: <https://www.nottingham.ac.uk/isac/facilities/xps.aspx>. [Accessed: 14-Jun-2016].
- [2] J. Tan, Y. J. Chao, H. Wang, J. Gong, and J. W. Van Zee, “Chemical and mechanical stability of EPDM in a PEM fuel cell environment,” *Polym. Degrad. Stab.*, vol. 94, no. 11, pp. 2072–2078, Nov. 2009.
- [3] C. Chen and T. F. Fuller, “The effect of humidity on the degradation of Nafion® membrane,” 2009.

7. CHAPTER 7: Material Development for Improved PEM Fuel Cell Seal

7.1. Commercial EPDM

As the results previously revealed in Chapter 6, silicone rubber gaskets fail in a fuel cell after a relatively short functional life (i.e.5000h), due to acid hydrolysis where it is in contact with the membrane. Therefore, alternative gasket materials were investigated, in particular with regard to their resistance to aging under fuel cell conditions. Initially, a literature review identified EPDM as a potential alternative material. Consequently, a commercial EPDM compound was used in a study for comparison with the existing silicone rubber. This chapter reports the results of acid aging and compression set experiments which were used to guide the development of an EPDM compound optimised for use as a fuel cell gasket.

7.1.1. Accelerated Aging of Commercial EPDM Compound and Silicone Rubber (in pH 2 sulfuric acid solution)

Tensile tests were carried out on the aged commercial EPDM and silicone rubber samples. The tensile strength of the rubber materials exposed to sulfuric acid (H_2SO_4) of pH 2 and Nafion® (pH 3 – 4) solutions are shown in Figures 7.1 and 7.2 respectively. It can be clearly seen that, in both solutions, the strength of silicone rubber decreased significantly with aging whereas commercial EPDM did not show a substantial change in strength with aging.

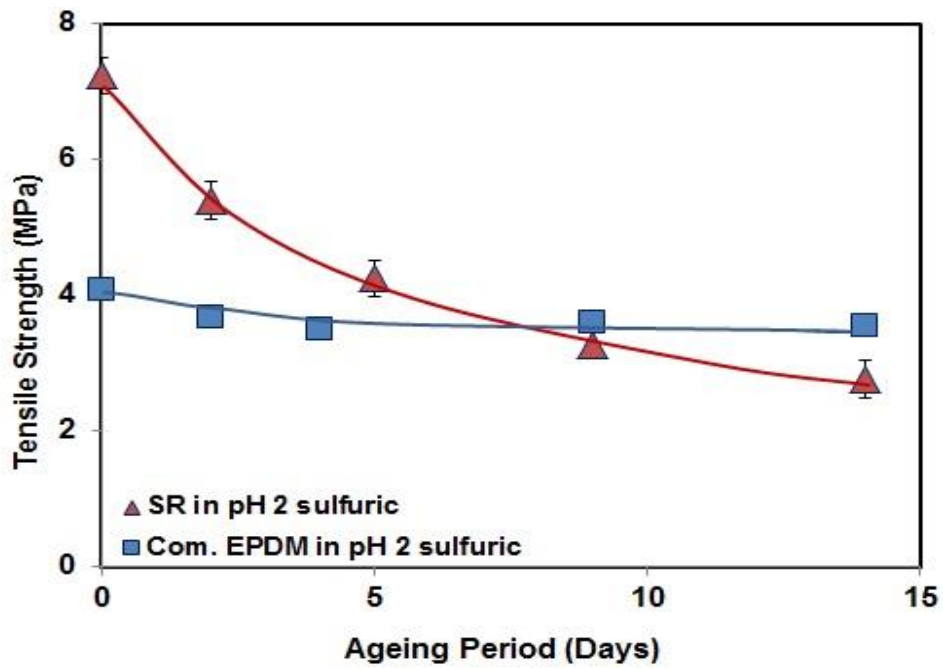


Figure 7.1. Tensile strength of commercial EPDM and silicone rubber compounds in pH 2 sulfuric acid (H₂SO₄) solution at 140°C

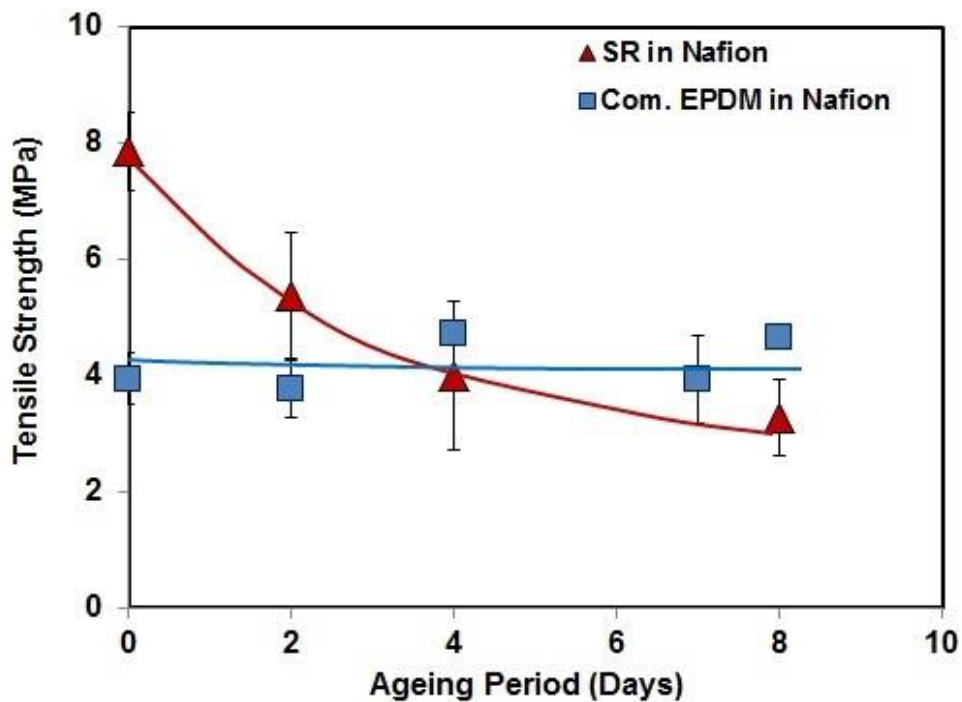


Figure 7.2. Tensile strength of commercial EPDM and silicone rubber compounds in pH 3 – 4 Nafion® solution at 140°C

7.1.2. Compression Set

Figure 7.3. shows the compression set behaviour of commercial EPDM and silicone rubber samples which were compressed to 25 % of their original thickness at 140°C for 72 hours. In Figure 7.3, it is clear that commercial EPDM had a very high compression set compared to silicone rubber.

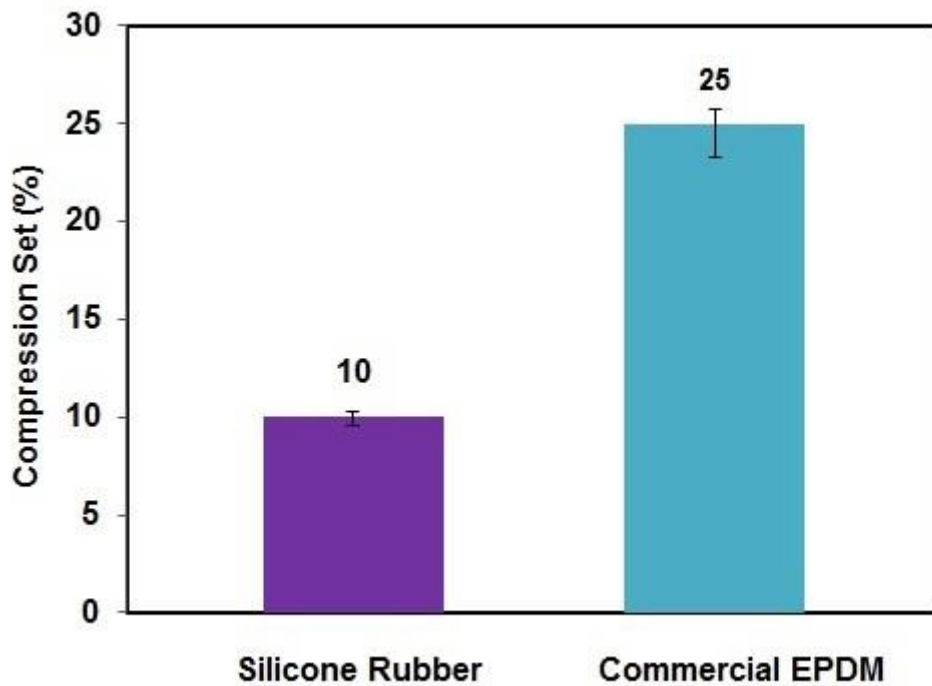


Figure 7.3. Compression set of commercial EPDM and silicone rubber at 140°C and 25% compression for 72 hrs

The experimental results above signify that, commercial EPDM compound exhibited good acid aging resistance but it had a high compression set. Thus, we concluded that EPDM compound is a promising fuel cell gasket material and decided to carry out further investigation such as developing our own EPDM compound with good acid aging resistance and better compression set than the commercial compound.

7.2. The Requirements For an Ideal EPDM Fuel Cell Seal Compound

Based on the our earlier findings, the requirements for an EPDM compound to replace the current silicone compound were determined as follows:

- Similar hardness to the existing silicone rubber (60 Shore A).

- Adequate tensile strength (> 5 MPa, but no advantage in a very high value) and elongation at break (> 200% – useful for easier handling in assembly).
- Similar compression set value to the existing silicone rubber (~10 % at 140°C at 25 % compression) since it seems that compression set is more likely to be a problem for EPDM than silicone rubber.

In addition to the above physical and mechanical property requirements, the EPDM compound for the PEM fuel cell seal must be electrically insulating and any plasticiser must not be extractable. Usually, EPDM compounds are heavily filled with carbon black, which is conductive, and plasticiser which may be extractable and clearly would not be suitable for this application. However, unfilled EPDM can be difficult to process and may not have sufficient strength. Silica as an alternative filler may need silane coating in order to adhere to EPDM. For the curing system, a peroxide cure with coagent would be appropriate for the best heat aging properties. In order to meet these requirements and to acquire a compound with optimal properties, tensile test and compression set tests were performed on the EPDM compounds.

7.3. EPDM Compound Optimisation

7.3.1. Initial Compounding

Firstly, various EPDM compounds (A–F) were made with various combinations of the ingredients in order to assess the effect of the fillers (coated & uncoated silica) as well as the effect of plasticiser (Lithene AH) and coagent (HVA -2) on the mechanical properties. Table 7.1 summarises the compounds with different combinations of those ingredients.

Table 7.1. EPDM Compounds with different combinations

A	B	C	D	E	F
HVA-2	Lithene	HVA + Uncoated Silica	Lithene + Uncoated Silica	HVA + Coated Silica	Lithene + Coated Silica

Tensile Properties of the initial EPDM Compounds

Tensile tests were conducted on the EPDM compounds (A – F) to compare their mechanical properties to identify the optimum compound. Tensile strength, elongation at break and 50 % modulus of EPDM compounds are represented in Figures 7.4, 7.5 and 7.6 respectively.

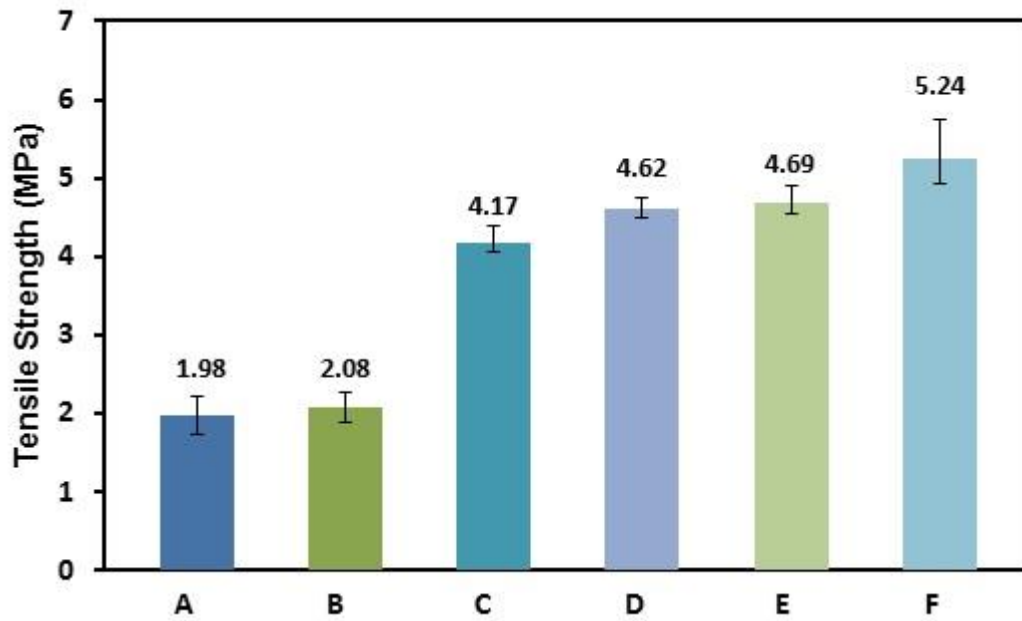


Figure 7.4. Tensile strength of EPDM compounds (A to F)

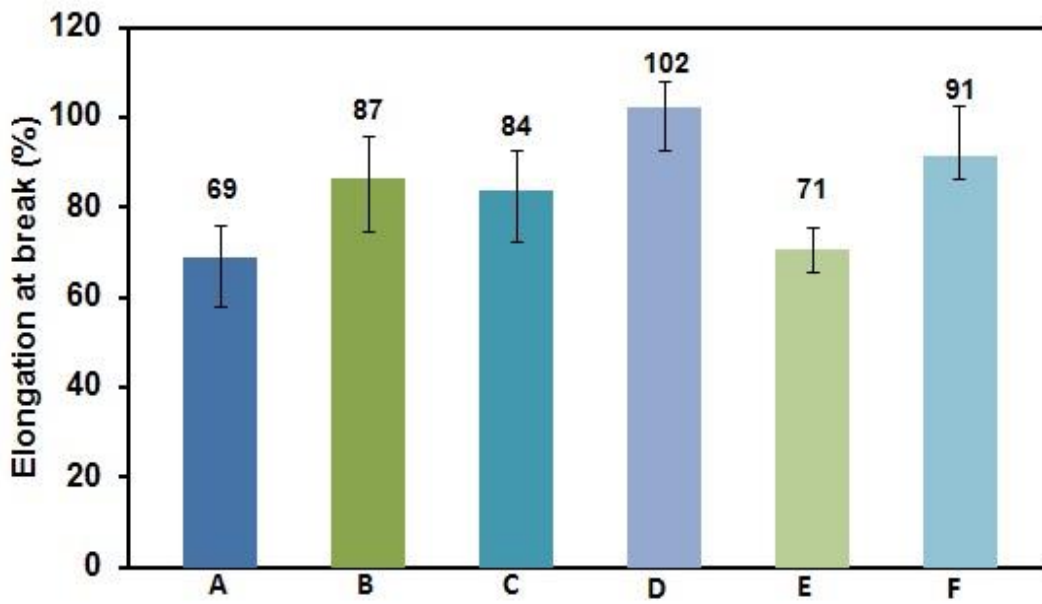


Figure 7.5. Elongation at break of EPDM compounds (A to F)

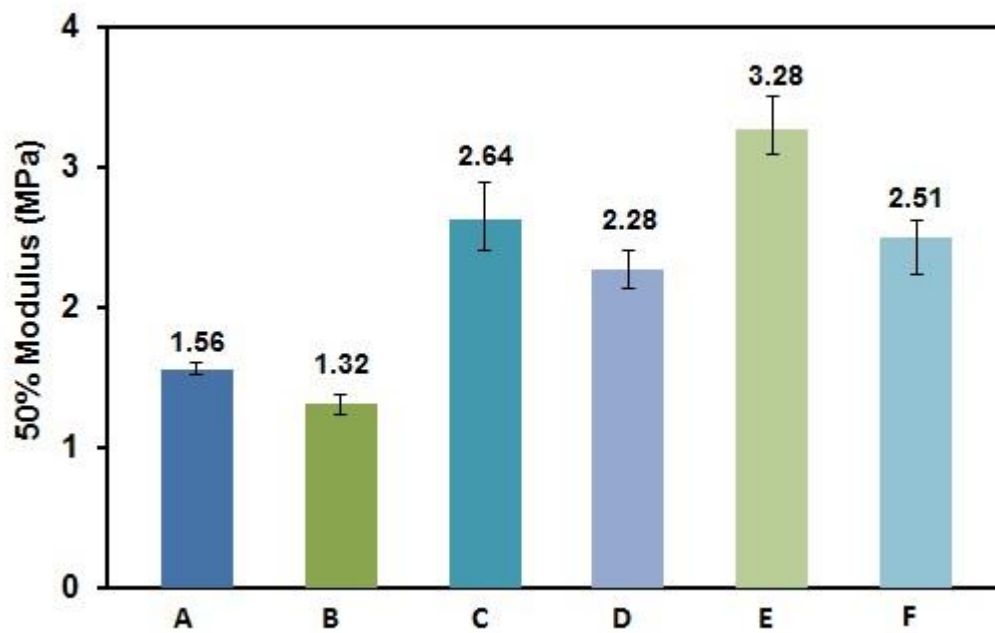


Figure 7.6. 50 % Modulus of EPDM compounds (A to F)

As seen in Figure 7.4, the compounds with reinforcing filler (from C to F) exhibited higher tensile strength compared to the unfilled compounds A and B.

Overall, compound F which contained coated silica with lithene (See Table 7.1) showed the highest tensile strength. In contrast, the addition of fillers in compounds C to F does not have a significant effect on the elongation at break as reflected in Figure 7.5. However, compounds containing lithene (B, D and F) exhibited higher elongation at break than those containing HVA-2 (A, C and E). This is because lithene as a plasticiser reduces the hardness leading to softer end products with higher elongation at break. By contrast, HVA-2 promotes the cross-linking which results in harder products therefore lower elongation at break (See Figure 7.5). Figure 7.6 shows the 50 % modulus of the EPDM compounds. It can be seen clearly that the addition of the fillers to compounds C to F increased the stiffness resulting in higher stress values and 50 % modulus.

Tensile test results showed that compounds containing coated silica (E & F) had better mechanical properties (i.e. tensile strength) than those containing uncoated silica (C & D). This could be attributed to the fact that silica coated in silane was chemically bonded to the elastomer matrix. Silane coupling agent has two functionally active end groups, i.e., the readily hydrolysable alkoxy group and the organo-functional group. The former can react chemically with the silanol groups on silica surface to form stable siloxane linkages whereas the latter, which is relatively non-polar, is more compatible with rubbers and also can participate in the sulfur vulcanization to form chemical linkages with rubbers. As a consequence, silane coupling agent could act as a bridge between silica and rubber to enhance the rubber–filler interaction and, thus, give a significant improvement in properties of silica-filled compounds.

Compression Set of the initial EPDM Compounds

The data in Figure 7.7 shows that compounds A and B had the lowest therefore, the best compression set among the other EPDM compounds due to the fact that there were no fillers in the formulation. This is because, the addition of the fillers to the rubber compounds increases the crosslinking density which inhibits the mobility of the rubber chains causing increased stiffness and lower elasticity resulting in less recovery after compression¹.

All compounds showed higher compression set at 140°C than those of at 70°C (Figure 7.7). However, EPDM compound D showed a large increase in the compression set value from 70°C to 140°C. This is probably due to the combination effect of the temperature and plasticiser on the compression set.

Between the compounds with filler (C, D, E and F) compound E and F had a slightly better (lower) compression set which was probably due to the fact that they had coated silica as a filler in the formulation whereas compound C and D contained uncoated silica instead (See Table 7.1).

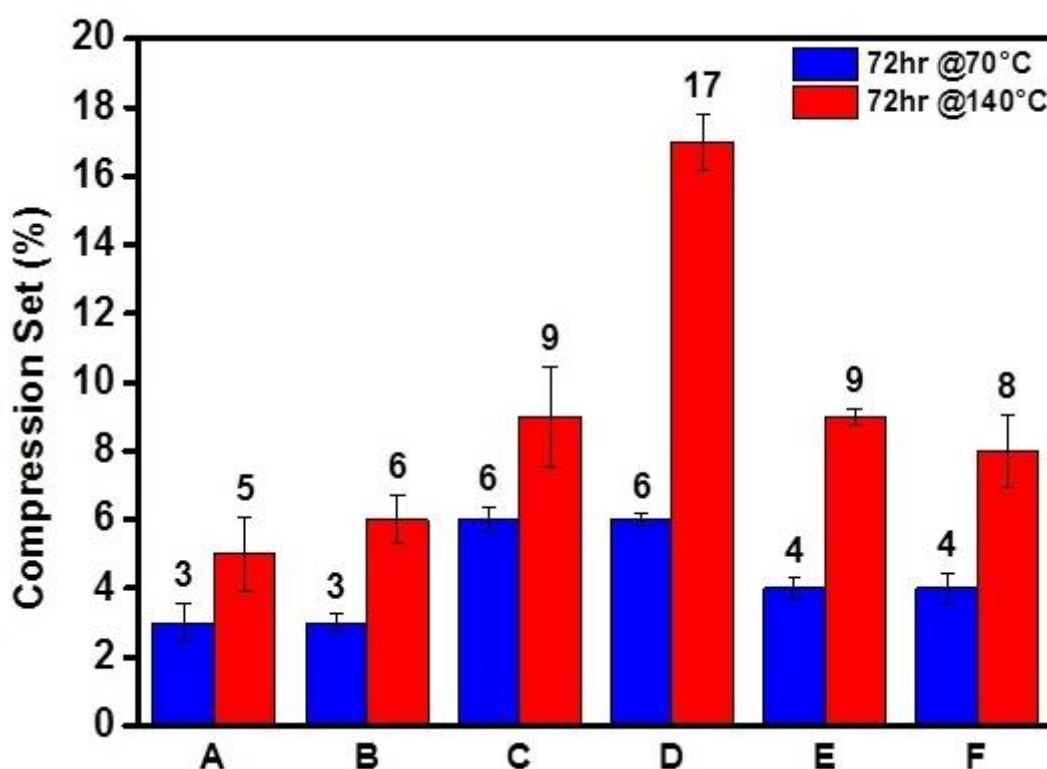


Figure 7.7. Compression set of EPDM compounds (A to F)

Based on the above mechanical properties obtained from tensile test results, EPDM compound F demonstrated the best performance between all the compounds (A to F). However, the compound had a higher viscosity and hardness than those of silicone rubber. The high viscosity could cause potential problems in the processing of the gasket, such as the moulding of the seals. As is shown in Table 7.2, the hardness of EPDM compound F is much higher (~ 70 Shore A) than the one of silicone rubber (~ 60 Shore A).

Table 7.2. Hardness of EPDM compound F and silicone rubber

Material	Hardness (Shore A)
Silicone Rubber	57 – 58
EPDM Compound F	67 – 68

This greater stiffness (hardness) can also create possible sealing problems because the compound could be too hard to compress and hence seal against gases. Additionally, oxidation resistance was also low and tensile strength properties need to be enhanced. To address these problems final EPDM compounding trials were carried out.

7.3.2. Final Compounding

The second and final compounding trial was performed to tackle the above – mentioned issues relating to compound F. A low viscosity EPDM with 25 (MU) in Mooney Unit was used this time compared to the previous EPDM rubber (i.e., from initial compounding) which had a higher viscosity of 82 (MU). Furthermore, a lower viscosity (65 – 90 dPa.s) lithene (i.e., Lithene PH) was added to the formulations as the former lithene (Lithene AH) was highly viscous (i.e., 400 –700 dPa.s).The main purpose of using these low viscosity grand EPDM and lithene was to reduce viscosity and stiffness of the compound F.

The new EPDM compounds with the lithene concentrations of 0, 8, 6 and silica (coated) concentrations of 5, 12.5, 20 were prepared. The range of concentrations was chosen using results from the earlier experiments where compound F was developed. Tensile test, hardness and compression set measurements were carried out to obtain optimum compound.

Tensile Properties of the final EPDM Compounds

The results for tensile strength, elongation at break and 100 % modulus of new EPDM compounds and EPDM compound F are shown in Figures 7.8, 7.9 and 7.10 respectively.

It can be observed from Figure 7.8 that tensile strength increases with silica loading, however it is interesting that there is also an increase in strength with increase in lithene concentration.

Elongation at break is not significantly affected by silica and lithene concentrations but it is much improved in comparison with the previous compound F as reflected in Figure 7.9. This is most likely due to the change in EPDM viscosity (i.e., using low viscosity grade EPDM in the formulation). Figure 7.10 demonstrates that 100 % modulus also increases with silica content however; surprisingly the plasticiser (lithene) has little effect. This may indicate that it is crosslinking, effectively behaving more as a co-agent than a plasticiser.

This is supported by the effect on tensile strength (See Figure 7.8). The modulus of new compound containing the same silica and lithene concentrations (i.e., 20 phr silica and 8 phr lithene), is much lower than compound F, yet again due to the grade of EPDM.

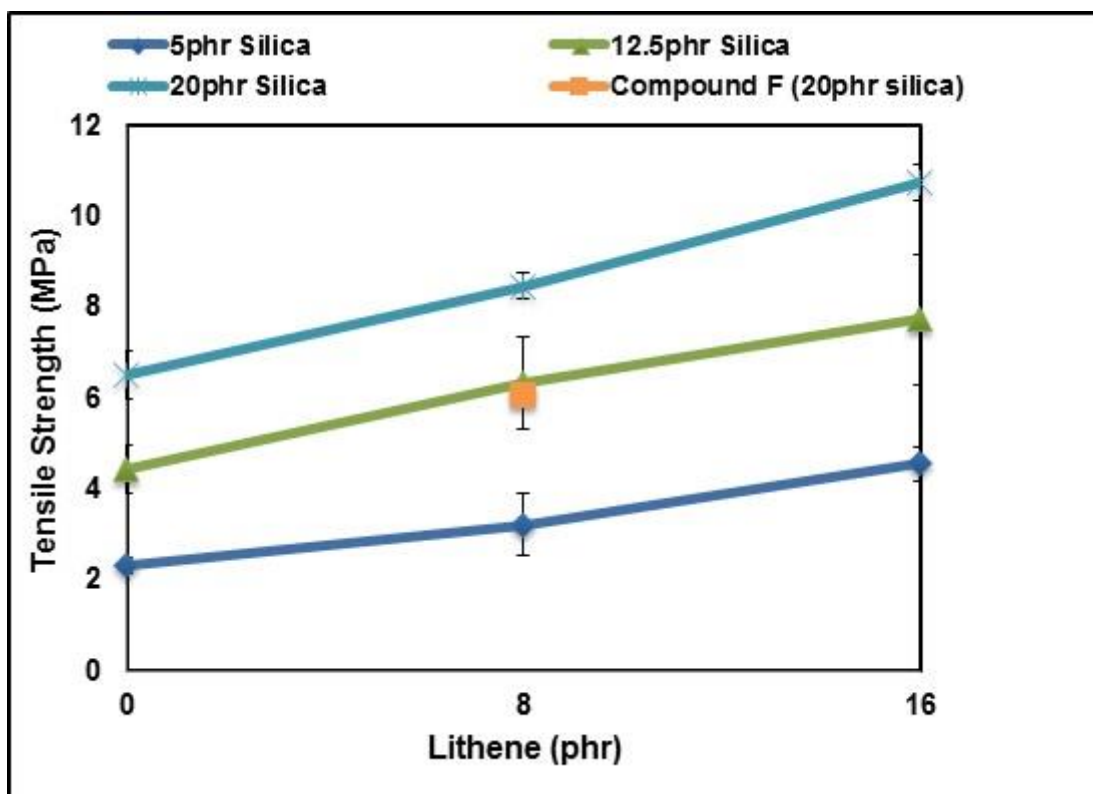


Figure 7.8. Tensile Strength of new EPDM compounds and compound F

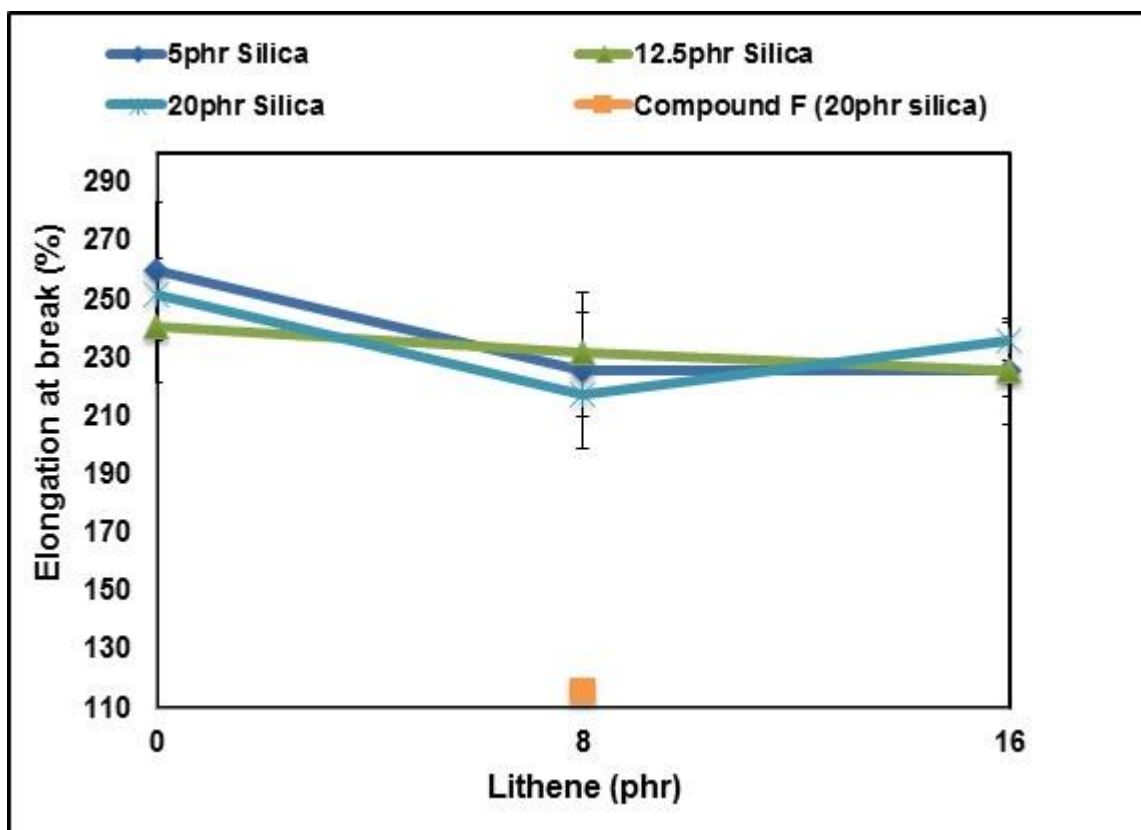


Figure 7.9. Elongation at break of new EPDM compounds and compound F

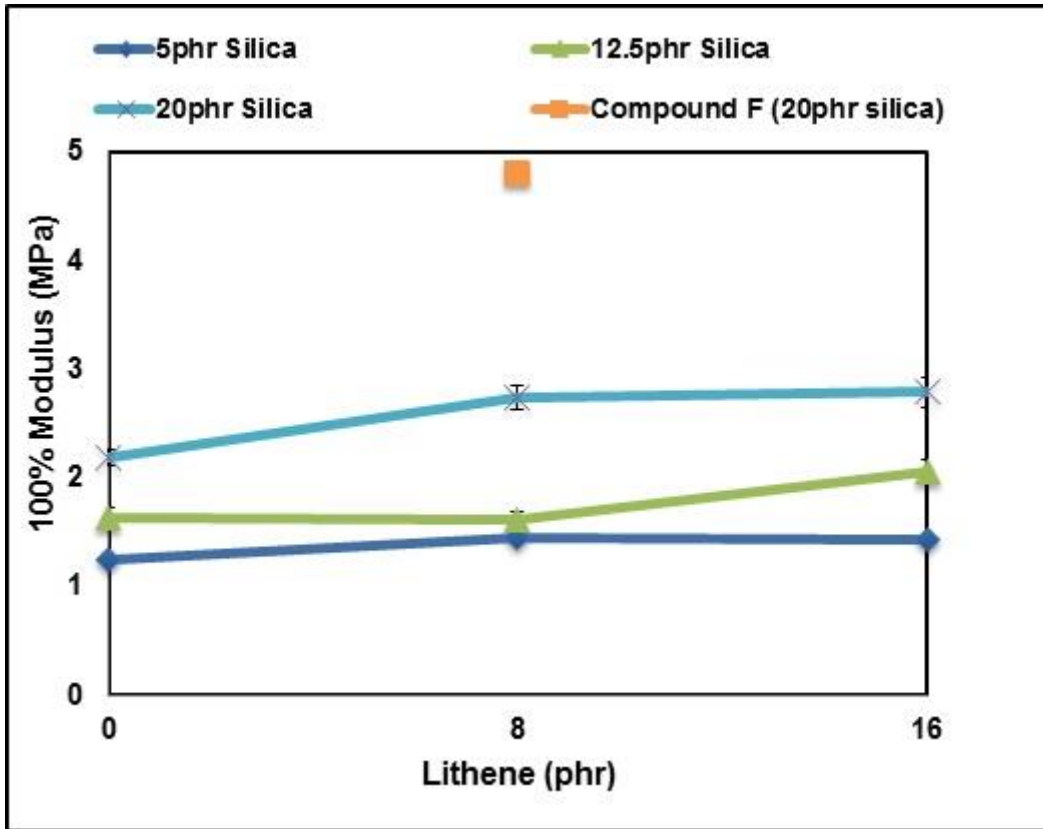


Figure 7.10. 100 % Modulus of new EPDM compounds and compound F

Hardness of the final EPDM Compounds

As with the modulus values (See Figure7.10), the hardness increases with addition of silica, but is not affected significantly by lithene as revealed by the data in Figure7.11. The lower hardness than compound F is likely to be due to the EPDM grade.

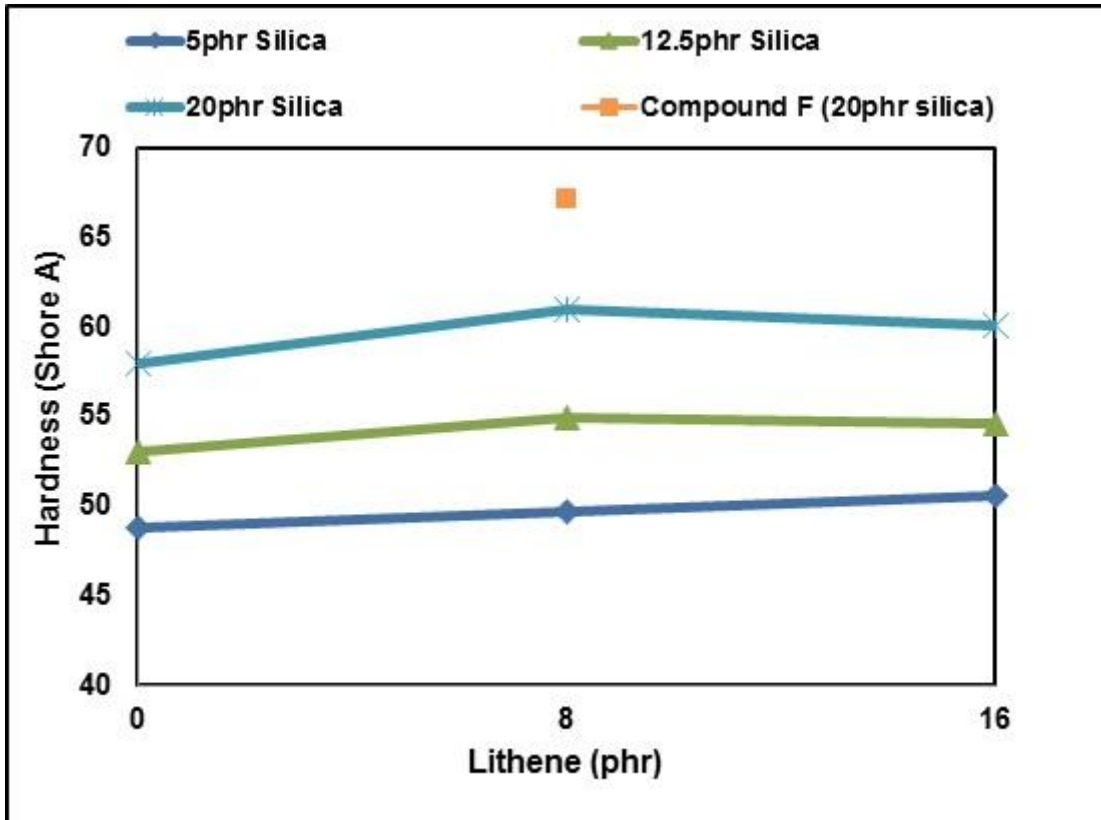


Figure 7.11. Hardness of EPDM new compounds and compound F

Compression Set of the final EPDM Compounds

Figure 7.12 shows the compression set of new EPDM compounds comparison with the compound F. It can be seen that the best (i.e., lowest) compression set value (10.97 %) was achieved with 20 phr silica and no lithene which was also not far from the compression set of compound F (10 %). Both set values are very close to that of silicone rubber (10 %) under identical conditions (i.e., at 140°C for 72 hrs at 25 % compression). In Figure 7.12 it is also clear that compression set increases with an increase in the filler amount indicating the undesirable effect of filler on set.

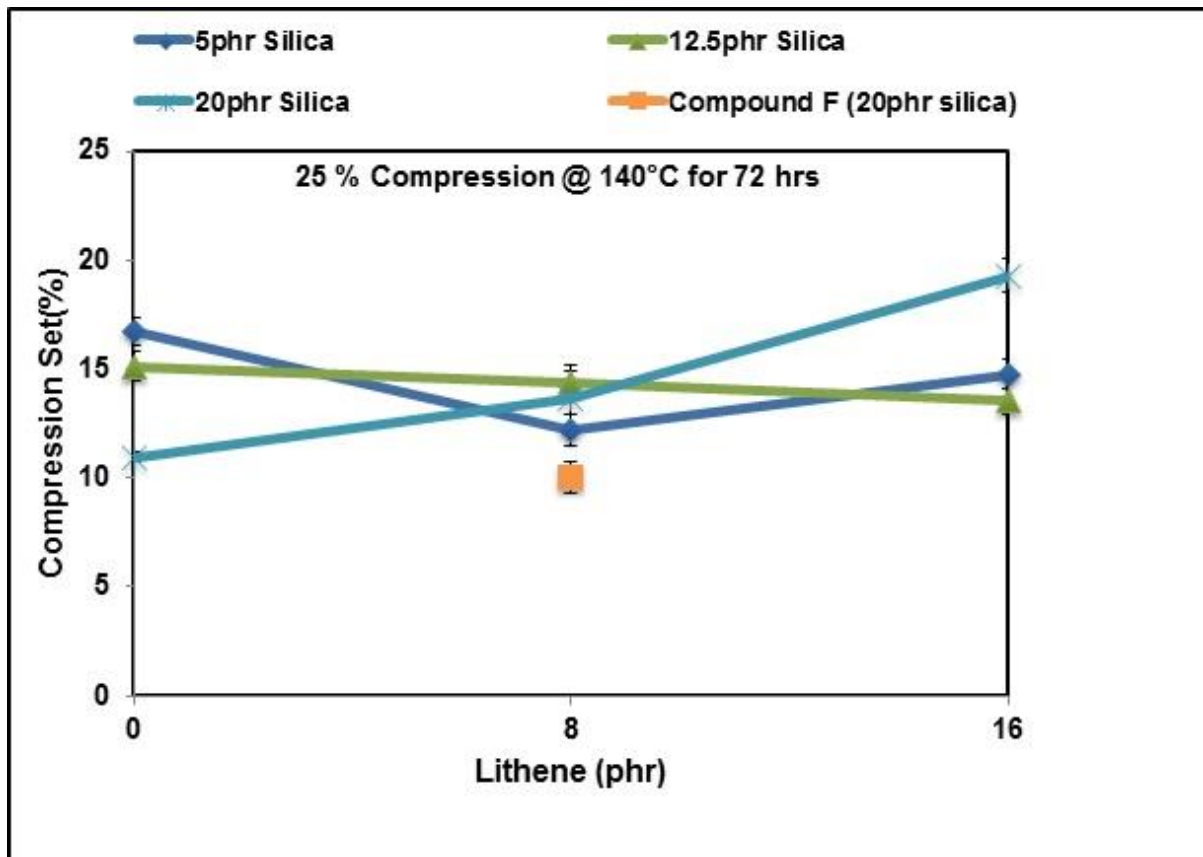


Figure 7.12. Compression set of EPDM new compounds and compound F at 140°C and 25% compression for 72 hrs

So far, compounding of the EPDM to optimise properties for the seal has shown that increasing the silica content increases stiffness and strength. Increasing the lithene content increases strength but does not reduce stiffness, suggesting that it is crosslinking effectively in the system.

Additionally, the following figures (Figures 7.13 – 7.16) show the results in the form of contour plots to indicate the combined effects of silica and lithene concentrations on the physical properties and to allow easier identification of the optimum composition for each property.

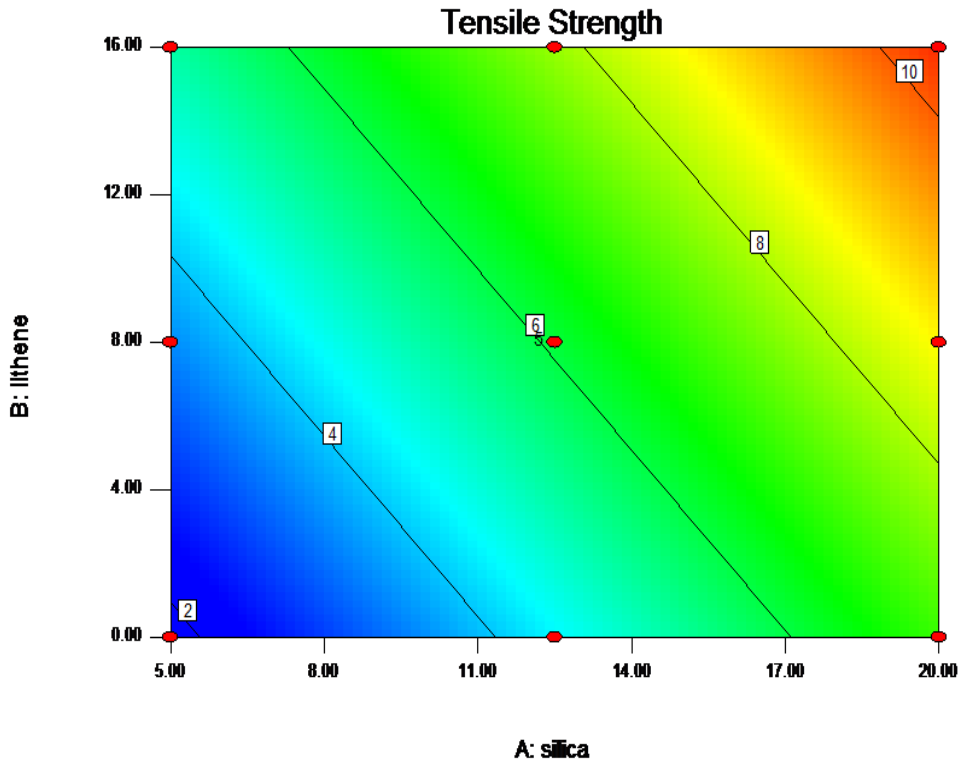


Figure 7.13. Effect of lithene and silica concentrations on the tensile strength of EPDM compounds

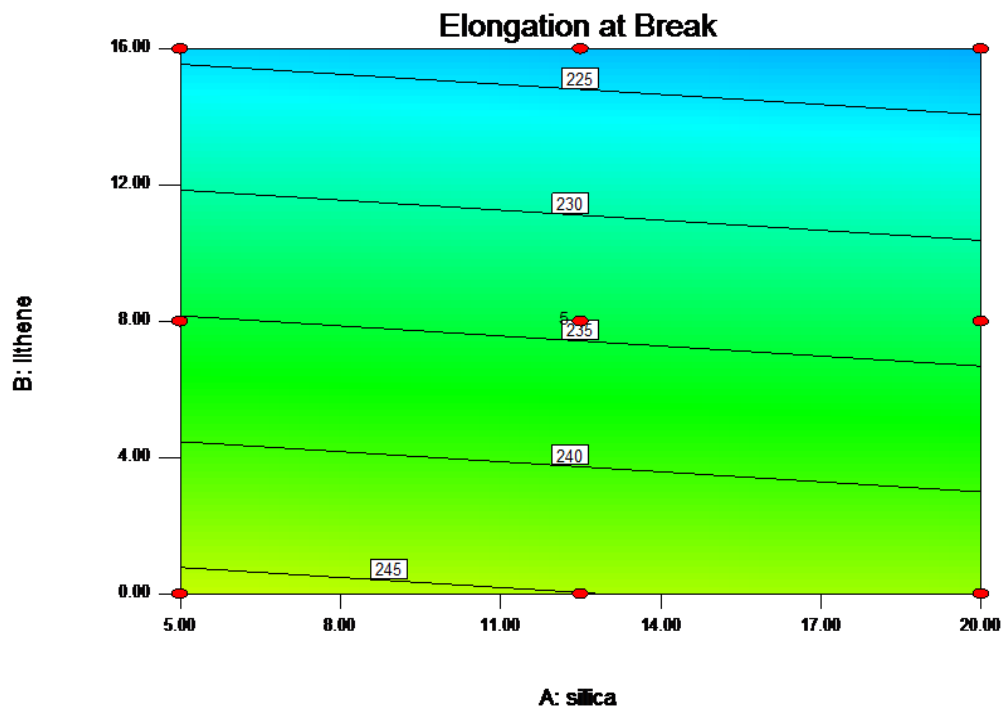


Figure 7.14. Effect of lithene and silica concentrations on the elongation at break of EPDM compounds

As seen in Figure 7.13, the tensile strength increases with both silica and lithene concentration confirming that silica is acting as reinforcing filler while the lithene is acting as a coupling agent rather than a plasticiser in the cured compound. Silica at 20 phr, with or without lithene will give an adequate tensile strength (>7 MPa). Elongation at break is not very sensitive to compound composition, but the lower the lithene content, the greater the elongation at break (See Figure 7.14).

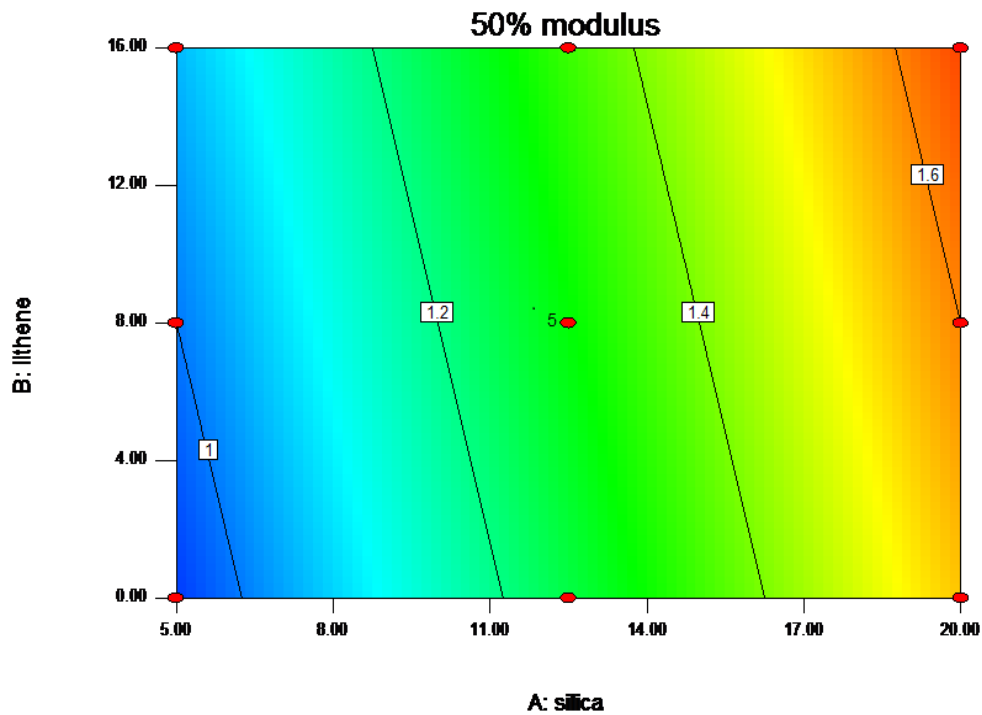


Figure 7.15. Effect of lithene and silica concentrations on the 50 % modulus of EPDM compounds

The 50% modulus (stress at 50% elongation) is another measure of stiffness, at higher strain. The compositions with <15 phr silica give modulus values similar to the silicone compound (~ 1.4 %) as reflected in Figure 7.15. However, it is not likely that the higher modulus values at higher silica concentrations would be a problem.

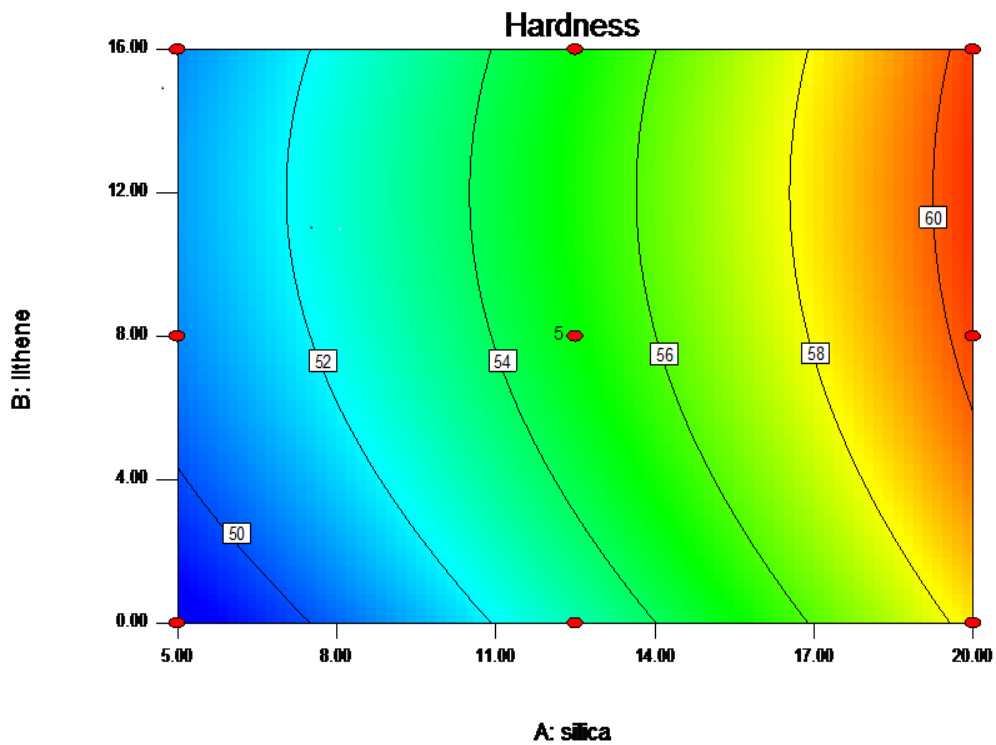


Figure 7.16. Effect of lithene and silica concentrations on the hardness of EPDM compounds

Hardness is a measure of modulus or stiffness at low strain and would reflect the amount of force required to compress the seal. Figure 7.16 shows that the highest silica composition (20 phr) has a hardness of 60, which is similar to the silicone, while all other compositions are softer. This means that from a hardness point of view any of the compositions are suitable.

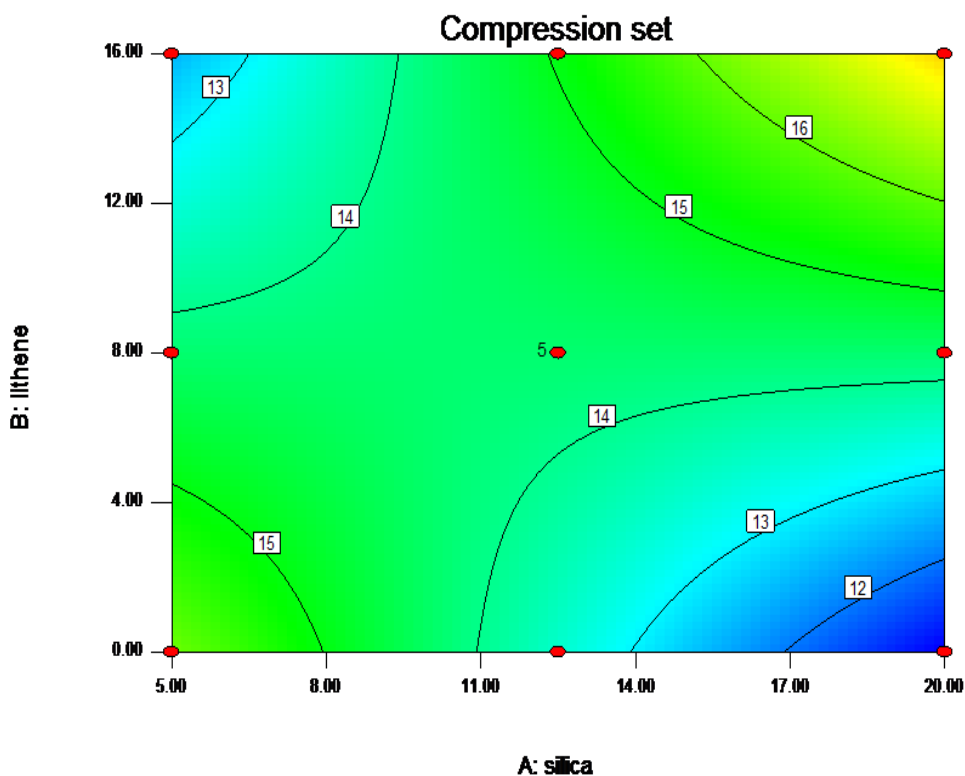


Figure 7.17. Effect of lithene and silica concentrations on the compression set of EPDM compounds

Compression set is a key property to optimise since, although it is not known what a critical value of compression set is for the sealing in the fuel cell, silicone rubber has a generally lower value (~11) than the EPDM compounds tested so far. Compression set is minimised at about 11 to 12% at the highest loading of silica (20 phr) and with no lithene present as shown in Figure 7.17.

Based on the above results, the optimum compound was identified with 20 phr silica and no lithene. This composition (EPDM 2) gave the lowest compression set while the other properties (i.e. hardness, tensile strength, and modulus) satisfied the estimated design constraints for the seal.

After selecting the best EPDM compound (referred to as EPDM 2) a large batch of this compound (3.5 kg) was mixed in the K1 internal mixer and samples were cured and tested to investigate compression set and acid Aging behaviour, compared to earlier results of silicone rubber.

7.4. Comparison of Accelerated Aging Behaviour of EPDM 2 with Silicone Rubber

Aging was carried out in Nafion® (pH 3 – 4) solution at 140°C to determine whether EPDM2 compound is resistant to aging in Nafion® solution. Nafion® solution was particularly chosen because the previous results in Chapter 6 confirm that the Nafion® accelerates aging of the silicone rubber more than sulfuric acid solution. Silicone rubber also was re-tested alongside the EPDM 2 compound for comparison and to check repeatability.

7.4.1. Weight Change

Figure 7.18 below compares the weight change of silicone rubber and EPDM2 exposed to Nafion® solution (pH 3 – 4) at 140°C. The weight of silicone rubber samples decrease with exposure time indicating the loss of degraded material whereas EPDM2 material has a slight weight gain (~ 3 %) during aging probably due to water adsorption. The increase in weight is only slight for EPDM2, and the trend also suggests that it will level off. It is difficult to know if this absorption may be a problem but it does not significantly affect the tensile properties as shown in the following section (See Figures 7.19 and 7.20).

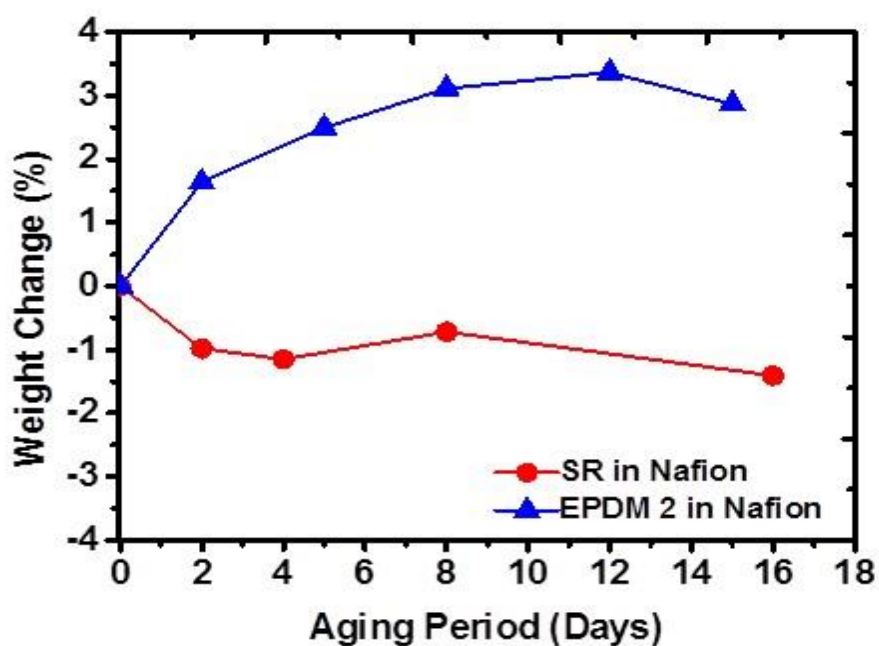


Figure 7.18. Weight change of silicone rubber (SR) and EMPD 2 aged in Nafion® (pH 3-4) solution @ 140°C

7.4.2. Effect of Aging on the Mechanical Properties

Figure 7.19 shows that there is a great reduction in tensile strength of silicone rubber upon exposure to Nafion® solution while EPDM 2 did not experience a significant change in the strength.

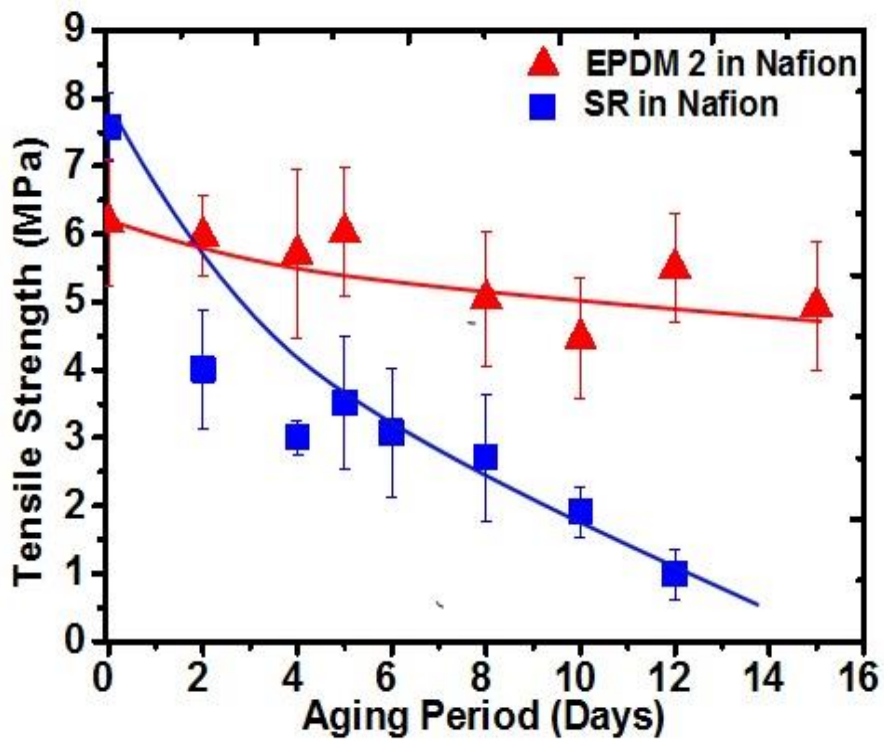


Figure 7.19. Tensile strength of silicone rubber (SR) and EPDM 2 aged in Nafion® (pH 3-4) solution at 140°C

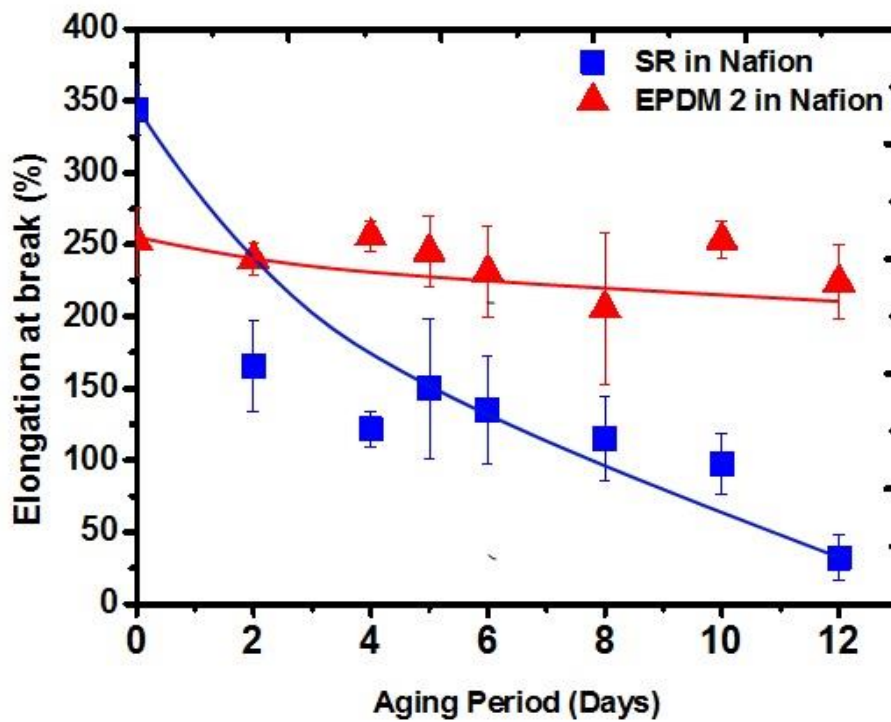


Figure 7.20. Elongation at break of silicone rubber (SR) and EPDM 2 aged in Nafion® (pH 3-4) solution at 140°C

Elongation at break (See Figure 7.20) exhibited a very similar trend to the tensile strength. On the other hand, 100 % modulus for both silicone rubber and EPDM 2 remained almost constant during aging period as seen in Figure 7.21.

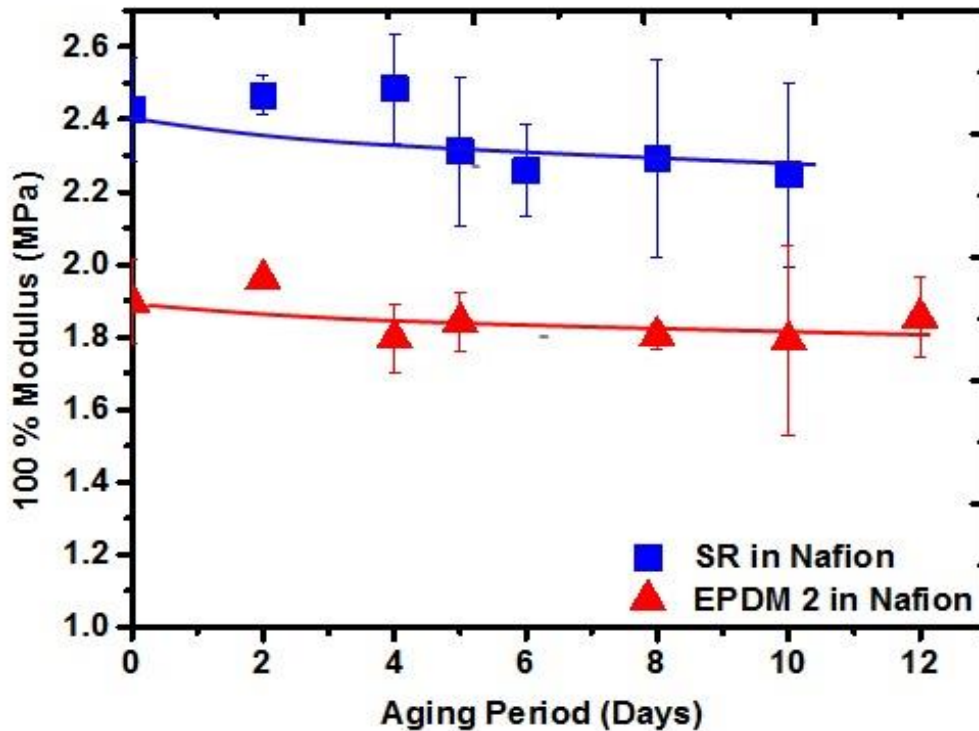


Figure 7.21. 100 % Modulus of silicone rubber (SR) and EPDM 2 aged in Nafion® (pH 3– 4) solution at 140°C

7.4.3. Compression Set

Compression set was measured for EPDM 2 at 140°C for 72 hrs at 25 % compression to establish if the compression set resistance of EPDM 2 is adequate for functioning in the fuel cell as well as to ensure it is as good as the one of silicone rubber. Figure 7.22 shows the compression set behaviour of EPDM 2 and silicone rubber materials. It can be clearly seen that EPDM 2 had a low (good) compression set value which is similar to silicone rubber.

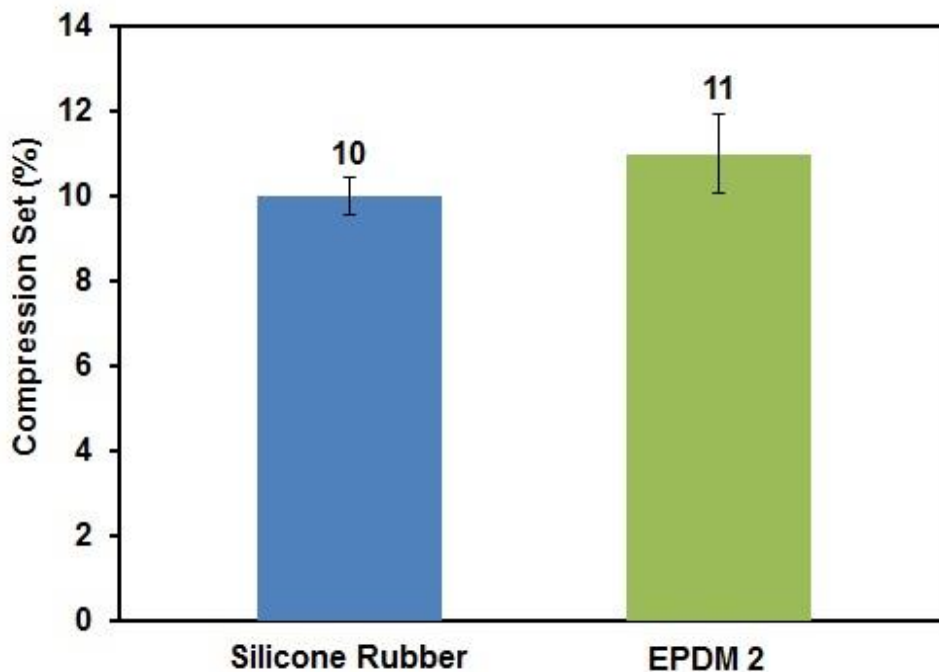


Figure 7.22. Compression set of EPDM 2 and silicone rubber at 140°C and 25% compression for 72 hrs

7.5. Accelerated Aging of Moulded Gaskets in Single Fuel Cells (in stack test)

The fuel cell seals were moulded with EPDM 2 compound and cured (i.e., 175°C for 20 min) using the tool provided by sponsor company (Intelligent Energy) and they were tested along with the silicone rubber seals in their accelerated aging rig for suitability. The accelerated test procedure was as follows:

Gaskets were contained in the 25cm² test rig and were heated to 90°C. 1mmol H₂SO₄ in water (containing MEA) (0.5mLmin⁻¹) and air (331mLmin⁻¹) were pumped through the system. Figure 7.23 shows the basic structure of the accelerated aging rig. A cross over test was carried out daily to check the failure of the gasket. Crossover is when the gas from one side of the membrane crosses over to the other side of the membrane. During the test, the air supply was shut off, while maintaining a steady stream of hydrogen to the anode.

The open circuit voltage was then recorded for approximately 2 minutes². If gas cross over is detected this indicates the end of the test.

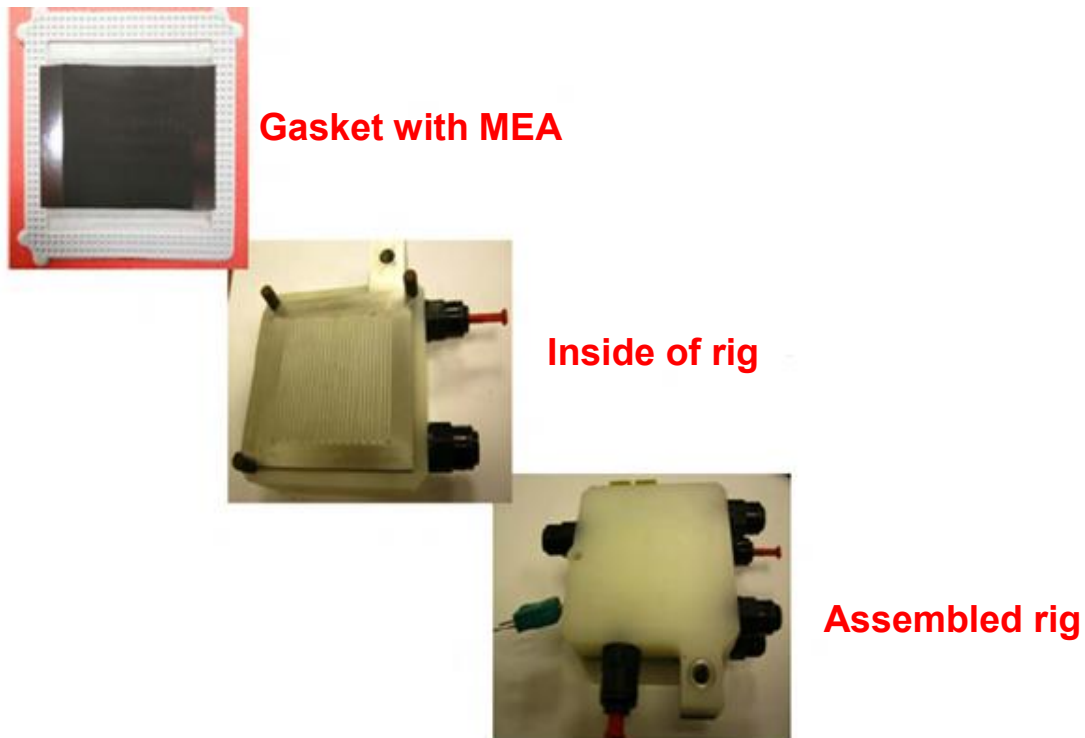


Figure 7.23. Intelligent Energy's accelerated aging test rig

7.5.1. Daily Cross- over Test (Failure Test) of the Gaskets

Generally, there is an expected crossover leak rate of hydrogen and oxygen through the membrane because of the diffusion across the membrane and can be predicted for any given stack depending on the number of the cells in the stack, active area, and type and thickness of the membrane assuming that the seals are perfect. This flow rate due to diffusion is measured in $\text{cm}^3 \text{ }^{-\text{sec}}$ and is also related to the partial pressure and temperature of the gas. However, the loss in voltage due to the hydrogen diffusion could only be seen at open circuit voltage because as the current increases the hydrogen partial pressure decreases on the anode side which reduces the driving force of the diffusion. The oxygen crossover, however, should not be seen in the open circuit voltage³.

Figure 7.24 represents the daily recorded data of flow rate of hydrogen gas in cm^3/sec for EPDM 2 and the standard silicone rubber gaskets which were on the test for a period of time. It is observed in Figure 7.24 that the EPDM 2 gasket did not fail even after 500 hours of the test, compared to the silicone rubber gaskets which all failed after less than 160 hours.

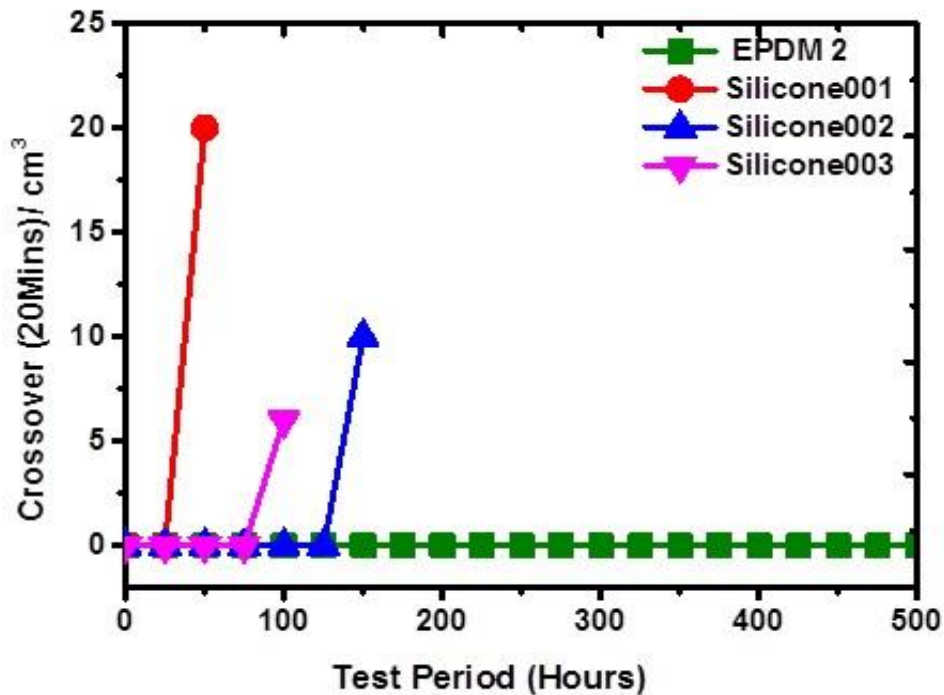


Figure 7.24. Cross over leak rate (flow rate) of hydrogen through the membrane for EPDM 2 and silicone rubber 001,002 and 003 gaskets

7.5.2. Thickness Loss in Gasket Samples

The thickness measurements were carried out by sponsor company (Intelligent Energy) on the silicone rubber, commercial EPDM and EPDM 2 gaskets after 121 to 158 hrs exposure to accelerated aging conditions in the test rig as described in section 7.5. The eight different points on the gasket samples were measured, as reflected in Figure 7.25, by using a constant force micrometer the average thickness loss (i.e., compression) was then calculated for each gasket material and the results are shown in Figure 7.26.

It can be observed clearly that EPDM 2 was comparable to silicone rubber in terms of loss in sample thickness and much better than commercial EPDM.

Considering the thickness of the unused gasket was 0.57 mm (570 μ m), the percentage loss in thickness for silicone rubber, EPDM 2 and commercial EPDM was laid in the range of 5 – 10 %.

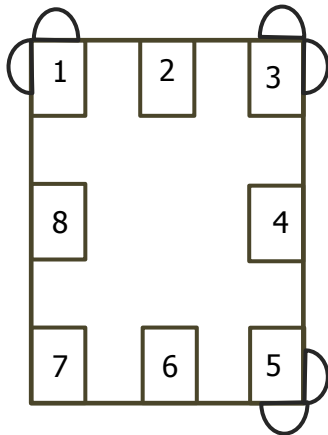


Figure 7.25. Eight points for gasket thickness measurements

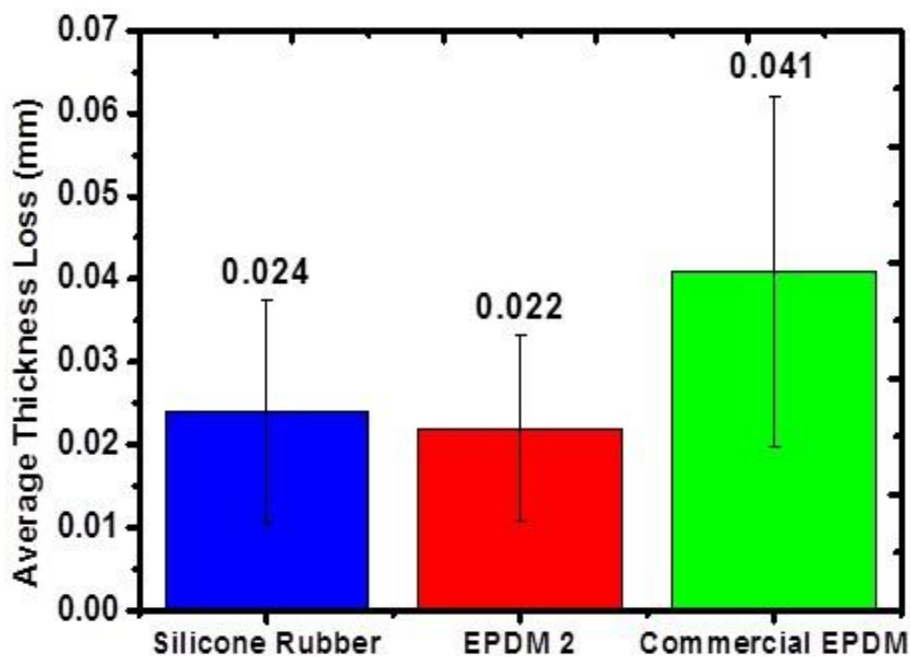


Figure 7.26. Average thickness loss of silicone rubber, EPDM 2 and commercial EPDM gaskets after 121 - 158 hrs exposure to accelerated aging in the fuel cell test rig

7.6. Summary

The study revealed that, the commercial EPDM did not show a significant decrease in tensile strength on Aging but had a high compression set. Our own developed EPDM 2 however, had a good resistance to acid Aging as well as a good (low) compression set. Additionally, it showed a very good performance in the fuel cell test rig and hence it has proved to be an improved material in fuel cell sealing applications.

7.7. REFERENCES

- [1] A. Mostafa, A. Abouel-Kasem, M. R. Bayoumi, and M. G. El-Sebaie, "Effect of carbon black loading on the swelling and compression set behavior of SBR and NBR rubber compounds," *Mater. Des.*, vol. 30, no. 5, pp. 1561–1568, 2009.
- [2] Supramaniam Srinivasan, *Fuel Cells: From Fundamentals to Applications*. Springer, 2006.
3. A. Husar, M. Serra, and C. Kunusch, "Description of gasket failure in a 7 cell PEMFC stack," *J. Power Sources*, vol. 169, pp. 85–91, 2007.

8. CHAPTER 8: Conclusions and Recommendations

8.1. Conclusions

The following sections summarise the outcomes of the study under individual sub-headings.

8.1.1. Effect of Aging on the properties of silicone rubber gasket in a real PEM fuel cell environment

For the silicone rubber gasket used in the actual fuel cell, the following conclusions can be drawn:

- The thickness of the unused and used gaskets, (i.e., after 8000 hours service in the fuel cell) which were measured from SEM images, did not change with service time. This can imply that compression set is unlikely to be the reason for the silicone rubber gasket failure in the fuel cell.
- The degradation of the silicone rubber gasket was due to acid catalysed hydrolysis leading to the failure of the gasket after 8000 hours operation in the cell at the temperatures of 80 to 90°C (i.e., operating temperatures of the PEM fuel cell).
- Acid hydrolytic degradation was detectable on the surface of the silicone rubber gasket to a large extent as the formation of holes and whitened areas, predominantly where it was contacting the edge of the membrane.(i.e., caused by the acidic nature of Nafion® membrane). The degradation appeared to occur only at the surface rather than throughout the bulk of the material and it progressed inwards from the surface.
- The results for AFM modulus showed a large random variation which can be attributed to the local distribution of filler particles instead of variations in degree of degradation of the silicone rubber. Therefore, AFM was proven not to be an effective technique to determine the changes in the surface hardness of the silicone rubber gasket with degradation.

- XPS measurements confirmed that the main degradation mechanism of silicone rubber was hydrolytic cleavage at the cross-link sites and chain scission in the backbone.
- ATR-FTIR was not accurate enough to investigate the surface degradation of silicone rubber gasket. This was most likely due to interference in the spectra from the silica filler used in the rubber which had the same Si – O bonds as those being formed from the chain scissioning in the silicone rubber backbone as a result of acid hydrolysis.
- Solvent swelling measurement revealed that there was no change in the crosslink density of silicone rubber gasket with aging even though XPS and the FTIR results suggested that crosslink cleavage and chain scission had occurred in the degraded sample. This could be rationalized by the fact that solvent swelling is a bulk measurement whereas; XPS and FTIR are the surface techniques. It can be concluded once more that there was little degradation in the bulk of the sample, but severe degradation at the surface.

8.1.2. Effect of Aging on the Properties of Silicone Rubber Gasket Material in an Accelerated Aging Environment

The findings of silicone rubber gasket material exposed to accelerated aging experiments are summarised as follows:

- Accelerated aging test results of silicone rubber gasket material exposed to diluted sulfuric acid solutions with pH levels of 1, 2 and 4 at 140°C demonstrated that tensile strength decreased considerably with Aging time whereas, the decrease in modulus was comparatively smaller. This could be due to the fact that surface degradation causes a reduction in the strength but it does not affect the modulus in the same way because of being a bulk property. In other words, significant amounts of degradation occurred at the surface but not in the bulk of the material. This was parallel to the results from the swelling and spectroscopic analysis of degraded parts of the silicone rubber gasket as highlighted in the previous section.

- It was found out that tensile strength was a good quantitative measure of the extent of degradation due to accelerated aging. In fact, it was much more sensitive than the AFM imaging technique and spectroscopic surface methods (i.e., ATR-FTIR and XPS) applied.
- The same visible damage was observed on the surfaces of the aged silicone rubber samples (i.e., in the sulfuric acid solutions) compared to that of degraded parts of the silicone rubber gasket in the fuel cell. The FTIR analysis of the degraded materials from the real fuel cell and accelerated aging environment confirmed that the same type of hydrolysis reactions occurred in both the fuel cell and accelerated aging test.
- Tensile test results as well as the surface condition of the aged samples showed that the extent of degradation was more severe in the more acidic (i.e., lower pH) solutions indicating acid hydrolysis as the main degradation mechanism.
- The decrease in both tensile strength and elongation at break of silicone rubber in Nafion® solution (pH 3 – 4) was greater than the one that was aged in H₂SO₄ solution with a pH of 2. It seemed that Nafion® solution (i.e., comprising of hydrated Nafion® membrane) accelerated the aging of silicone rubber than did the sulfuric acid solution of a similar pH and may explain the surprisingly high rate of degradation in the vicinity of the Nafion® membrane that was observed in real fuel cells. This can be attributed to the contribution of major degradation products of Nafion® such as TFA, on aging rather than the acidity in the fuel cell.
- The pH of the TFA solution rose substantially after aging the silicone rubber samples while both sulfuric acid and Nafion® solutions did not have any change in the pH. This could be due to the possible chemical reaction occurring between the TFA solution and silicone rubber. On the other hand, the effect of the Nafion® and sulfuric acid solutions on degradation was more likely an acid catalysing reaction in which the acidity (i.e., pH) stayed the same before and after degradation.

- The largest amount of weight lost from silicone rubber with aging time was observed in TFA solution (~ 4 %) compared to the ones in sulfuric acid and Nafion® (~ 1.5 – 2%) of the same pH signifying that TFA caused the greater degradation of silicone rubber.
- Tensile strength of silicone rubber aged in both Nafion® and TFA solutions decreased significantly with time. However, 50 % modulus almost remained the same after exposure to all three solutions which was due to the bulk effect of modulus as discussed previously.
- The Surface condition of the silicone rubber samples exposed to Nafion® and TFA solutions revealed similar change in colour (i.e., from grey to white) with time whereas there was no alteration in the colour after exposure to sulfuric acid solutions (of similar pH). These observations confirmed the out comings of weight change and tensile test measurements which all indicated the more aggressive effect of TFA solution on silicone rubber degradation.

8.1.3. Effect of chemical Aging on the properties of commercial EPDM gasket material with comparison to silicone rubber

- The tensile strength of commercial EPDM aged in both sulfuric acid (pH 2) and Nafion® (pH 3 – 4) solutions at 140°C showed little change compared to silicone rubber aged under identical conditions. However, despite its good acid resistance, the commercial EPDM had a high compression set.

8.1.4. EPDM Compound development

- The best tensile properties and compression set values were obtained with a combination of coated silica (i.e., filler) and lithene (i.e., Lithene AH, plasticiser and coagent) in the initial compounding (i.e., compound F contains 20 phr silica and 8 phr lithene).
- Upon recognising the problems related to the high viscosity and stiffness of the EPDM compound F, a lower viscosity lithene (i.e., Lithene PH) as well as a low viscosity grade EPDM rubber were used in the final compounding trials. The resultant effect of these replacements together with the combined effects of coated silica and lithene on physical properties are summarised below:

- Tensile strength increased with both silica and lithene loading proving that silica worked as reinforcing filler whereas, lithene behaved as coupling agent (i.e., crosslinker) instead of a plasticiser.
- Elongation at break was not influenced by silica and lithene loadings. However, elongation at break was better than for the previous compound F, more likely as a result of using low viscosity grade EPDM in the formulation.
- Both 100 % modulus and hardness increased with silica content but they were not modified by lithene concentration also confirming that lithene acted more as a coagent than a plasticiser. On the other hand, both the modulus and hardness at the same silica and lithene concentrations (i.e., 20 phr silica and 8 phr lithene), were much lower than compound F, yet again due to the grade of EPDM.

From above results, the best properties were obtained for the composition containing 20 phr silica and no lithene (i.e., EPDM 2 compound). Such properties included lowest compression set as well as the desired values for hardness, tensile strength, and modulus which were identified in Chapter 7.2.

8.1.5. Effect of chemical Aging on the properties of EPDM 2 gasket material with comparison to silicone rubber

- The slight increase (~ 3 %) in the weight of EPDM 2 (i.e., exposed to Nafion® solution, pH 3 – 4 at 140°C) with time was attributed to water adsorption during accelerated aging test. Conversely, the weight of the silicone rubber samples declined with exposure time under the same conditions implying the loss of degraded material.
- The tensile strength and elongation at break of EPDM were much more stable than those of silicone rubber when exposed to Nafion® solution, pH 3 – 4 at 140°C.

The steady behaviour displayed by the tensile properties of EPDM 2 towards acid aging indicated that the water adsorption of the material did not affect those properties.

8.1.6. Compression set behaviour of silicone rubber, commercial EPDM and EPDM 2 compound

Silicone rubber had an inherently good (low) compression set value (i.e., 10%). A similar set (i.e., 11 %) was achieved from the EPDM 2 compound under the test conditions of 140°C and 25 % compression for 72 hours. This much improved on the relatively poor compression set of the commercial EPDM compound (i.e., 25%).

8.1.7. Stability of silicone rubber and EPDM 2 gasket materials in the fuel cell accelerated aging test rig

- The daily cross over (failure) test was one of the criteria which indicated the stability of the gasket in the actual fuel cell environment. While silicone rubber gaskets failed after approximately 160 hours, EPDM 2 gaskets were still functioning even after 500 hours of the test.
- The thickness loss of the gaskets after exposure to the fuel cell aging test conditions was another measurement for the stability. EPDM 2 was as good as silicone rubber and much better than commercial EPDM. For example, the average thickness loss was 0.022 mm for EPDM 2 and 0.024 mm for silicone rubber gaskets respectively, while it was 0.041mm for commercial EPDM.

8.2. Recommendations for Future Work

Understanding the degradation mechanisms of silicone rubber as the existing seal material for PEM fuel cells was the starting point of this thesis in order to mitigate them and therefore to prolong the lifetime of the seals. The findings of the research presented here demonstrated a crucial step towards the definition of the relationship between the fuel cell operating parameters and seals as well as the type and extent of degradation of the silicone rubber.

In the search for more durable seal materials for PEMFCs, a new EPDM compound was developed as an alternative gasket material. Although the experimental results confirmed that EPDM was a good sealing material there is still a need to address the issues related to the viscosity of EPDM seals in terms of their successful fabrication. The following recommendations for future work in this area are based mainly on the outcome of investigations of this project:

- Further research could be carried on the development of a lower viscosity EPDM compound suitable for injection moulding. This could increase the processability of EPDM seals for PEMFC applications.
- A lower viscosity liquid EPDM could be investigated which has been recently processed using Liquid Injection Moulding (LIM) for fuel cell seals applications instead of conventional high molecular weight (i.e., higher viscosity) EPDM polymers.

APPENDIX

Publications from this Thesis

1. Comparison of Accelerated Aging of Silicone Rubber Gasket Material with Aging in a Fuel Cell Environment, *Journal of Applied Polymer Science*, 129, 2013, 1446-1454.
2. Improved Elastomeric Materials for Fuel Cell Seals, Conference Paper, Presented at Rubber Conference (Rubbercon) 2014 Advanced Engineering & Materials in Manchester UK.
3. Improved Elastomer Gasket Materials for PEM Fuel Cells, Conference Paper, Presented at the 4th International Symposium on Energy Challenges and Mechanics (ECM4) conference in Aberdeen- Scotland UK.
4. Modelling Degradation of Silicone Rubber in PEM Fuel Cell and other Acidic Environments, Submitted to *Polymer Degradation and Stability*, Manuscript Number: PDST-D-15-00555.

Comparison of Accelerated Aging of Silicone Rubber Gasket Material with Aging in a Fuel Cell Environment

Sebnem Pehlivan-Davis,¹ Jane Clarke,¹ Simon Armour²

¹Department of Materials, Loughborough University, Loughborough, Leicestershire LE11 3TU, United Kingdom

²Intelligent Energy, Charnwood Building, Holywell Park, Ashby Road, Loughborough, Leicestershire LE11 3GB, United Kingdom

Correspondence to: J. Clarke (E-mail: J.Clarke@lboro.ac.uk)

ABSTRACT: A polymer electrolyte membrane (PEM) fuel cell stack requires gaskets in each cell to keep the reactant gases within their respective regions. Both sealing and electrochemical performance of the fuel cell depend on the long-term stability of the gasket materials. In this paper, the change in properties and structure of a silicone rubber gasket brought about by use in a fuel cell was studied and compared to the changes in the same silicone rubber gasket material brought about by accelerated aging. The accelerated aging conditions were chosen to relate to the PEM fuel cell environment, but with more extreme conditions of elevated temperature (140°C) and greater acidity. The dilute sulfuric acid accelerated aging solutions used had pH values of 1, 2, and 4. In an additional test, Nafion[®] membrane suspended in water was used for accelerated aging, to more closely correspond to a PEM fuel cell environment. The analysis showed that acid hydrolysis was the most likely mechanism of degradation and that similar degradation occurred under both real fuel cell and accelerated aging conditions. It was concluded that the accelerated aging test is a good one for rapidly screening materials for resistance to the acidic environment of the fuel cell. © 2012 Wiley Periodicals, Inc. *J. Appl. Polym. Sci.* 000: 000–000, 2012

KEYWORDS: batteries and fuel cells; ageing; elastomers; rubber

Received 13 June 2012; accepted 14 November 2012; published online

DOI: 10.1002/app.38837

INTRODUCTION

Seals (gaskets) are required in polymer electrolyte membrane (PEM) fuel cell stacks to separate the reactant gas compartments (hydrogen and oxygen) from each other.

Long-term durability of the fuel cell stack depends on the performance of these gaskets. If the gaskets fail, the reactant gases (H₂ and O₂) can leak to the environment or mix with each other directly in the fuel cell, causing it to malfunction.

The gaskets used as seals in PEM fuel cell are typically elastomeric materials and exposed to an acidic environment, humid air and hydrogen and subjected to mechanical stress.¹ Thus, elastomeric seals should possess sufficient chemical resistance against the chemically active fuel cell environment. In addition, it should be highly flexible to allow compression of the fuel cell stack when a compressive load is applied.

Silicone rubber is one of the most commercially available elastomeric gasket materials for fuel cell applications due to its low cost and ease of fabrication.

There are many published reports based on the degradation of silicone rubbers in various environments.^{2–12} For instance, Patel et al.² carried out a study on the thermal aging of polysiloxane

rubber¹³ in both sealed conditions and in open air. Schulze et al.¹³ investigated the degradation of seals in a polymer electrolyte membrane fuel cell during fuel cell operation. Tan et al.^{1,14} studied the degradation of silicone rubber in a simulated PEM fuel cell environment. Chemical and mechanical degradation of the elastomeric materials was also reported in other articles.^{15–20}

Although, there is a large amount of literature discussing the degradation of silicone rubbers in various environments, there are only a small number of results reported for the degradation of silicone rubber in a real PEM fuel cell environment or for degradation using Nafion[®] membrane as an accelerated aging agent.

In this article, we report the results from an investigation of silicone rubber gaskets used in an actual fuel cell and from degradation studies of the same silicone rubber gasket material under accelerated aging conditions. The objectives of this study are to (1) determine the effect of exposure to fuel cell conditions on the silicone rubber gasket, (2) identify potential mechanisms of seal failure, (3) determine the effect of acidity on the rate of silicone gasket material degradation, and (4) determine whether the accelerated aging test could potentially be used to predict degradation behavior in a real fuel cell.

© 2012 Wiley Periodicals, Inc.

EXPERIMENTAL

Material

A gray-colored polydimethylsiloxane silicone rubber compound filled with silica was used in this study. Samples of new gaskets and gaskets that had been used in fuel cells for various periods were supplied by Intelligent Energy. The same silicone rubber compound was also provided uncured. Sheets of the silicone gasket material (1 mm thick) were cured to 100% in a heated press at 170°C. Dumbbells (Type 2, BS903:Part A2) were cut from the cured sheet for tensile testing before and after accelerated aging. The fuel cell seal gaskets were cured under similar conditions to the sheets.

Characterization Methods

Scanning electron microscopy (SEM) was used to measure the thickness of the silicone rubber gaskets before and after service in the fuel cell. The measurement was used to detect any permanent change in thickness caused by service use. The permanent change in thickness is a similar property to compression set, although the measurement is not carried out under standard conditions, and the level of compression in service is not known. The razor cut surfaces of the unused and used silicone rubber gaskets which had been used in a fuel cell for 5000 and 8000 h were examined using a Carl Zeiss (Leo) 1530 VP SEM.

Atomic force microscopy (AFM) measurements were carried out on the surface of samples cut from both unused gaskets and the degraded part of the used gaskets using a Veeco Explorer AFM with a pulsed force-imaging mode. This technique was used to observe any differences brought about by degradation in the stiffness of the material at a microscopic level.

The atomic composition and surface chemistry of the degraded parts of the silicone rubber gaskets, which had been used in a fuel cell, were identified by applying X-ray photoelectron spectroscopy (XPS). The XPS used in this study was a VG Escalab Mk I with the detection limits of 0.1–1 atom % and an analysis area typically of 3–10 mm².

Attenuated total reflectance Fourier transform infrared (ATR-FTIR) spectroscopy was performed on the surface of the samples from unused and degraded parts of gaskets used in a fuel cell, along with the silicone rubber material before and after exposure to accelerated aging tests. A Shimadzu FTIR-8400S fitted with Specac Golden Gate ATR Mk II was used in this study. The spectroscopy ran at a resolution of 0.85 cm⁻¹ and peak-to-peak S/N ratio of 20,000 : 1.

A solvent swelling method was used to determine the change in the crosslink density of the silicone rubber gaskets on aging. The degree of swelling is inversely related to crosslink density when the material, solvent, and temperature are kept constant, as in this test. Samples with dimensions of 24 × 7 × 0.58 mm³ were cut from unused gaskets and close to the degraded areas of gaskets used in a fuel cell. Each sample was weighed on a digital balance (to four decimal places) then was immersed into a glass tube containing 5 mL solvent (toluene) at room temperature for a total of 6 days. After 1 day (24 h), the swollen sample was removed from the solvent and dabbed on paper tissue to get rid of any excess solvent, placed in a preweighed empty

plastic sample bag and weighed immediately. The sample then was put back in to the glass tube containing toluene for the rest of the swelling test. This procedure was repeated after 24 h (1 day), 96 h (4 days), and 144 h (6 days), and the weights of the samples were recorded. The percentage of swelling was calculated for each sample using the following equation:

$$\text{Swelling } \delta\% = \frac{W_2 - W_1}{W_1} \times 100 \quad (1)$$

where W_1 is the weight of the test sample before immersion; W_2 is the weight of the swollen sample after immersion.

Tensile properties were measured for the dumbbell samples both before and after accelerated aging. A Hounsfield universal testing machine fitted with a laser extensometer was used to measure tensile properties. Values of tensile strength, elongation at break and 50% modulus were recorded and the mean values determined. The 50% modulus is a measure of stiffness used for elastomers and is the stress recorded at 50% elongation. Four dumbbells were measured for each aging time.

Accelerated aging Method

An accelerated aging test was developed in order to assess the acid and time/temperature aging resistance of the silicone rubber, which is relevant to the fuel cell environment. An accelerated aging temperature of 140°C was selected so that 1 week of accelerated aging would roughly correspond to a real life time of 10000 h at 80°C, on the crude assumption of an expected doubling of degradation rate for every 10°C increase in temperature. Accelerated aging solutions were used to represent the acidity of the fuel cell environment. Because of the elevated temperature and aqueous environment it was necessary to carry out the accelerated aging in pressurized vessels. Each pressure vessel included a metal base (stainless steel) for holding a polytetrafluoroethylene (PTFE) lining cup and a screw fitting metal cap with a PTFE lid for sealing. The PTFE liner in which the samples were aged had internal dimensions of 30 mm diameter and 44 mm in height. Accelerated aging solution (7 mL) was placed in the liner and four dumbbells of cured silicone rubber were added. The necks of the dumbbell samples were submerged completely into the solution. Figure 1 shows (a) the pressure vessel and (b) the layout of the samples in the liner. The PTFE liner containing the samples was then put into the metal base and sealed tightly with the lined metal cap before placing in the oven at 140°C for the appropriate period.

Accelerated aging solutions with acidity levels of pH 1, pH 2, and pH 4 were prepared by diluting 2M sulfuric acid (H₂SO₄) with distilled water. The pH values of the aging solutions were chosen to create acidity, which is similar to that in a real PEM fuel cell, i.e., pH ranging from 3 to 4,¹⁴ but also to include those of greater acidity to accelerate the aging process. In addition to the sulfuric acid solutions, an acidic environment more closely related to that of the fuel cell, where the acidity is due to the sulfonate groups in the membrane, was created using pieces of Nafion[®] suspended in distilled water. Nafion[®] accelerated aging solution was prepared by using 0.7 wt % of Nafion[®], in 7-mL distilled water, heated in the pressure vessel at 140°C

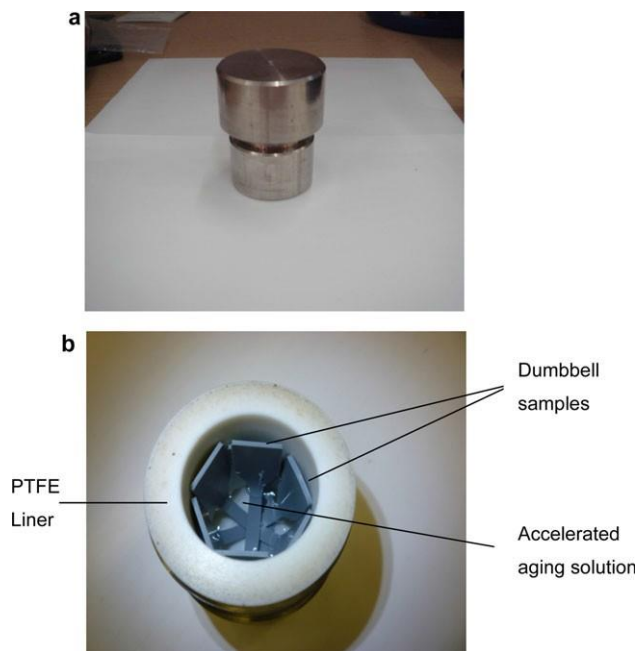


Figure 1. (a) Accelerated aging test pressure cooker and (b) arrangement of the samples in the cooker. [Color figure can be viewed in the online issue, which is available at wileyonlinelibrary.com.]

for 3 days until pH values of between 3 and 4 were reached. The Nafion membrane was left in the water when dumbbell samples were added for accelerated aging.

RESULTS AND DISCUSSION

Scanning Electron Microscopy (SEM)

The individual and average thickness of six samples each of unused and used (5000 and 8000 h) gaskets were measured from SEM images. The mean thicknesses were 580, 622, and 568 μm for the unused, in service for 5000 h and in service for 8000 h samples, respectively. There was a standard deviation of 60 μm for each batch of samples. The results indicate that there was no significant change in the thickness of the gaskets with time and suggest that compression set is unlikely to be a cause of failure for these silicone rubber gaskets.

Atomic Force Microscopy

Silicone gaskets that had been used in a fuel cell showed clear areas of degradation particularly where the edge of the membrane rested against the gasket. Degradation appeared as a white powdery substance on the surface and in some cases the surface was degraded away and holes could be observed. For one of these degraded gaskets, AFM measurements were carried out to determine whether changes in stiffness of the material could be detected where degradation had started but had not progressed

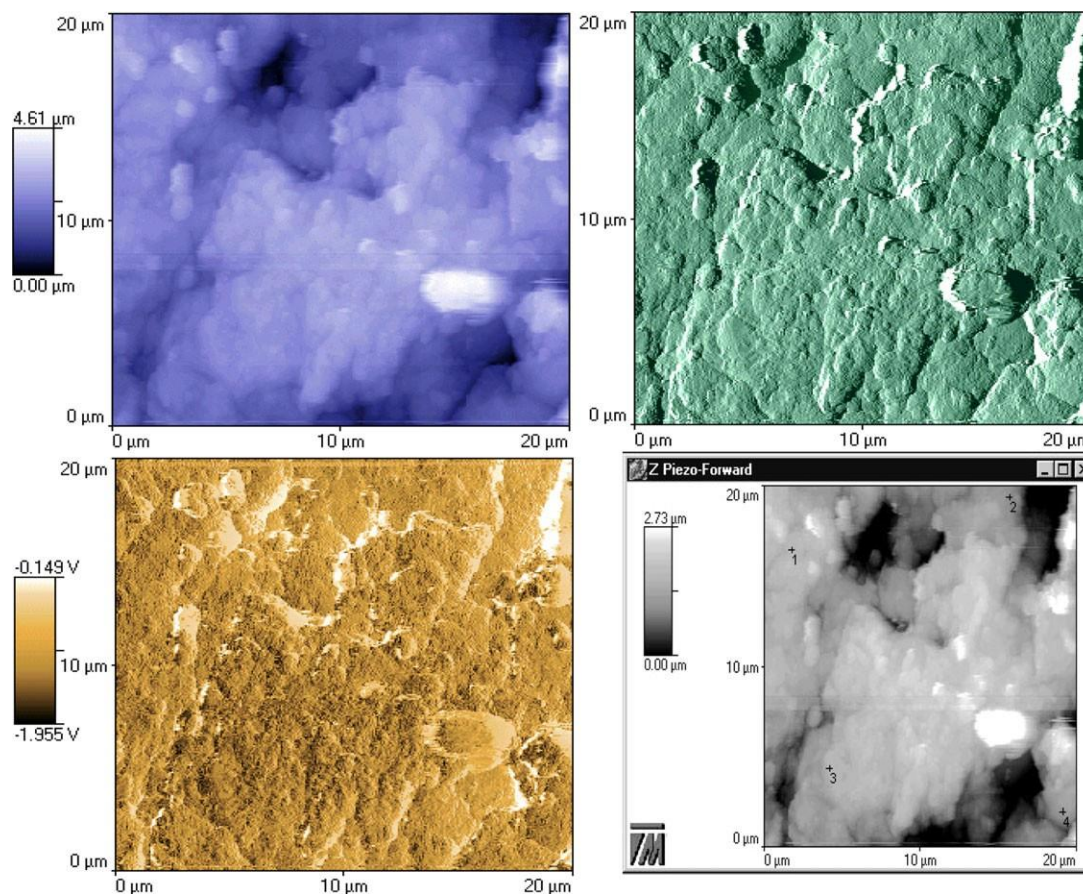


Figure 2. Topographic images of used silicone rubber gasket: Location 4. The points (1, 2, 3, and 4) on right bottom image indicate the points at which AFM modulus was calculated for each location. [Color figure can be viewed in the online issue, which is available at wileyonlinelibrary.com.]

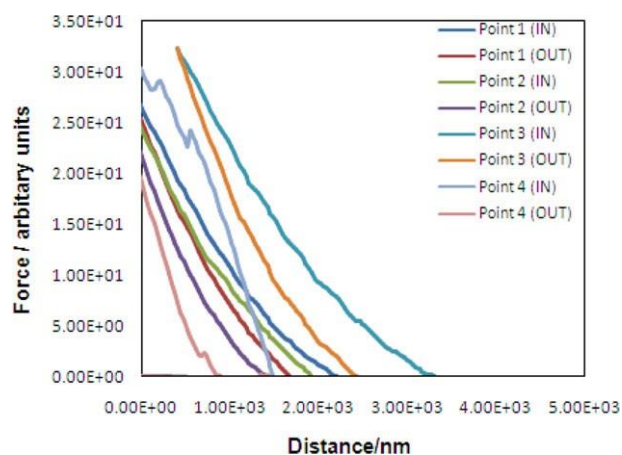


Figure 3. Force/distance curves of the used silicone rubber gasket: Location 4. (In and out represents the force measurement of the AFM probe with the amount of indentation on the surface). [Color figure can be viewed in the online issue, which is available at wileyonlinelibrary.com.]

to a visible degree. The AFM measurement of force/deflection started from a less degraded area of the sample and carried on towards a highly degraded area (i.e., from Location 1, a clean looking edge to Location 5, the area of maximum degradation). At each location, four different points were measured and an AFM “modulus” was then calculated for each location from the slope of the force/distance curves. In addition to these numerical values, images were obtained that also contained qualitative information. An example of these images is given in Figure 2. The top left image of Figure 2 gives information about the height of the surface. The black areas in the picture represent a low point (i.e., a hole) and white parts signify the high points. The top right image is a tip-deflection image with shaded areas in the picture accentuating the edges. The bottom left image is a phase topographic image, which expresses the phase of the reaction related to the force that is applied in the measurement. Darker parts in the image correspond to a lower phase lag and probably indicate the presence of rigid fillers, whereas the light areas could be explained as soft, rubbery parts. Finally, the image on the bottom right illustrates the points at which force/distance curves were acquired (i.e., β_1 , β_2 , β_3 , and β_4). Figure 3 shows the force/distance curves, which were measured at four points at Location 4 of the used silicone rubber gasket. The slope of the force/distance curve is taken as the AFM modulus and has arbitrary units. Figure 4 presents the AFM modulus values of unused and used gaskets which were calculated at four points for each location. The AFM modulus for the four points measured at each location are very scattered, showing as great a variation as that observed between the five different locations of supposed differing degradation. The variation in AFM modulus may well be due to local distribution of filler particles rather than differences in level of degradation of the polymer. Hence, these results suggest that AFM is not a useful tool for determining degree of degradation for this particular compound.

X-Ray Photoelectron Spectroscopy

The samples for XPS measurements were obtained by cutting pieces from unused silicone rubber gasket and different parts of

a gasket used in a fuel cell, including, undegraded, stained (brown), and degraded (white) areas. Brown areas may indicate the presence of iron oxide on the surface of the gasket, which might be the result of the corrosion of bipolar plates in the fuel cell. On the other hand, white degraded parts might be caused by hydrolysis due the aqueous acidic environment in the fuel cell. The XPS spectra in Figure 5 reveal the presence of carbon (C), oxygen (O), silicon (Si), and a small amount of fluorine (F). The atomic concentration of these elements are also shown in Table I.

It can be seen from Figure 5(b) that the carbon peak is lower and the oxygen peak higher in the degraded area of the used gasket compared to the ones in the spectra of the unused gasket [Figure 5(a)]. This can be observed also from the ratios of C/Si and O/Si shown in Table I. XPS did not detect iron atoms on the surface of the gasket sample and so it is assumed the concentration of iron (Fe) atom was less than 1% (the detection level of this equipment). The presence of fluorine (F) may be due to contamination of the surface of the samples from the membrane.¹⁵ As shown in Table I, the C/Si ratio is lower for the used gaskets than the unused gaskets, but is particularly low for the degraded part of the used gasket. This could be due to the methyl group on the silicone atom being attacked and oxidized to form Si–O bonds. This behavior would also account for the increase of the O/Si ratio with use and degradation of the gasket (Table I). Additionally, hydrolytic breakage of the –Si–O–Si backbone could cause this increase in O/Si ratio.¹⁵

Attenuated Total Reflectance Fourier Transform Infrared Spectroscopy

ATR-FTIR analysis was used to study the change in the surface chemistry of silicone rubber with degradation. Figures 6 and 7

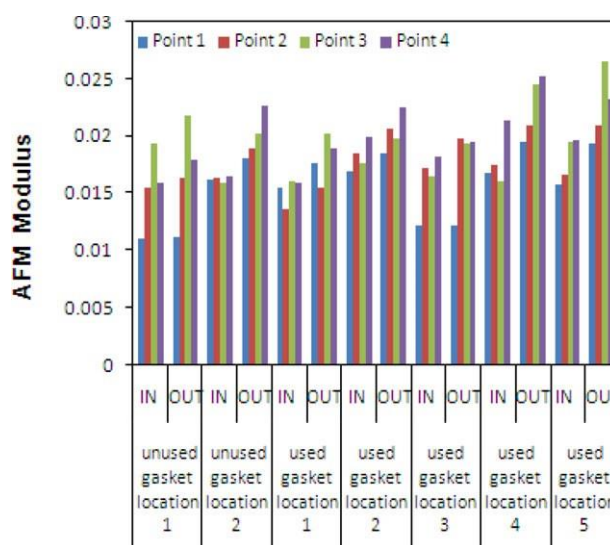


Figure 4. AFM Modulus of unused and used (5000 h in the fuel cell) silicone rubber gaskets (from less degraded area, Location 1, to highly degraded area, Location 5, and at each location four different points were measured). [Color figure can be viewed in the online issue, which is available at wileyonlinelibrary.com.]

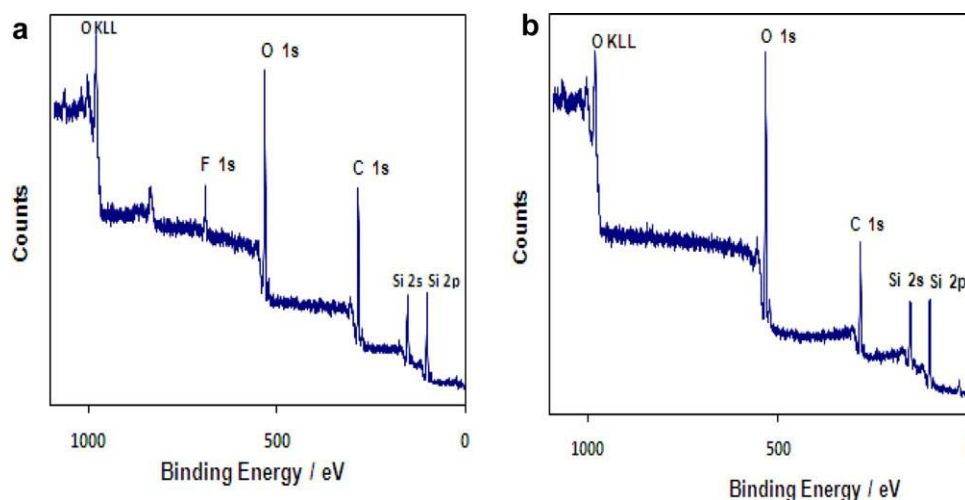


Figure 5. XPS spectra for silicone rubber (a) unused gasket and (b) degraded area of used (5000 h in the cell) gasket. [Color figure can be viewed in the online issue, which is available at wileyonlinelibrary.com.]

show the comparison of the ATR-FTIR results for degraded silicone rubber gasket (operating in the fuel cell for 5000 h) and silicone rubber material after exposure to the accelerated aging test (pH 1 accelerated aging solution for 2 days).

The largest peaks for unused (unexposed) silicone rubber are between 1007 and 1050 cm^{-1} , which are characteristic of siloxanes and associated with asymmetric and symmetric stretching vibrations of Si–O–Si bonds. The peak arising at 694 cm^{-1} is due to the asymmetric deformation of Si–CH₃ bonds.²¹ The peak at 790 cm^{-1} corresponds to the bending mode of Si–C and C–H wagging.²² The peaks at 864 and 1259 cm^{-1} result from the rocking vibration of Si–CH₃ and the bending vibration of Si–CH₃. The peak near 1411 cm^{-1} is due to the rocking vibration of –CH₂– as a part of the silicone rubber crosslinked domain. The peak at 2963 cm^{-1} is related to the stretching vibration mode of CH₃.¹

It can be seen from Figures 6 and 7 that the –CH₂– rocking peak disappeared for the degraded part of the silicone rubber gasket and the silicone rubber material after exposure to accelerated aging. This indicates that crosslinks between the polymer chains were broken during degradation and this might lead to the softening of the silicone rubber. The intensity of the Si–CH₃ bending peak at 1259 cm^{-1} and the peak due to CH at 2963 cm^{-1} decreased significantly in both the degraded silicone rubbers (Figures 6 and 7). This indicates that the methyl (Si–CH₃)

has been hydrolyzed as suggested also by the XPS results. Of particular significance is the similarity of the spectra for the degraded materials from the fuel cell and accelerated aging environment, which means that the accelerated aging conditions bring about a similar type of degradation to that of the real fuel cell environment. A scheme proposing the mechanism of hydrolytic degradation has been included in Tan et al.’s article.

Solvent Swelling

Solvent swelling was used to determine whether there were changes in crosslink density brought about by aging of the gaskets. Unused and used gaskets after 5000 and 8000 h service in the fuel cells were analyzed by solvent swelling. After 144 h of swelling in toluene, the percentage changes in volume of the samples were 118, 114, and 109 for the unused, after 5000 and after 8000 h service, respectively. Although the trend suggests a slight decrease in swelling and hence increase in crosslink density, given the very small difference in swelling between the samples in relation to the large amount of swelling of all the samples and a standard deviation of 4 on the swelling measurements, it is considered that the gaskets generally, did not experience significant crosslinking or breakage of crosslinks up to 8000 h in service. The result is a little surprising because both the XPS and the FTIR results indicated that crosslink cleavage and chain scission had occurred in the degraded samples. However, solvent swelling is a bulk measurement, whereas

Table I. XPS Composition in Atom Percentage

Samples	Atomic concentration (%)				Ratios to Si	
	C	O	Si	F	C/Si	O/Si
Unused gasket	50.9	24.2	24.9	Trace	2.04	0.97
Used gasket (undegraded area)	47.2	25.6	25.9	1.3	1.82	0.98
Used gasket (close to stained area)	46.4	26.4	25.5	1.7	1.81	1.03
Used gasket (degraded area)	34.4	35.0	30.6	-	1.12	1.14

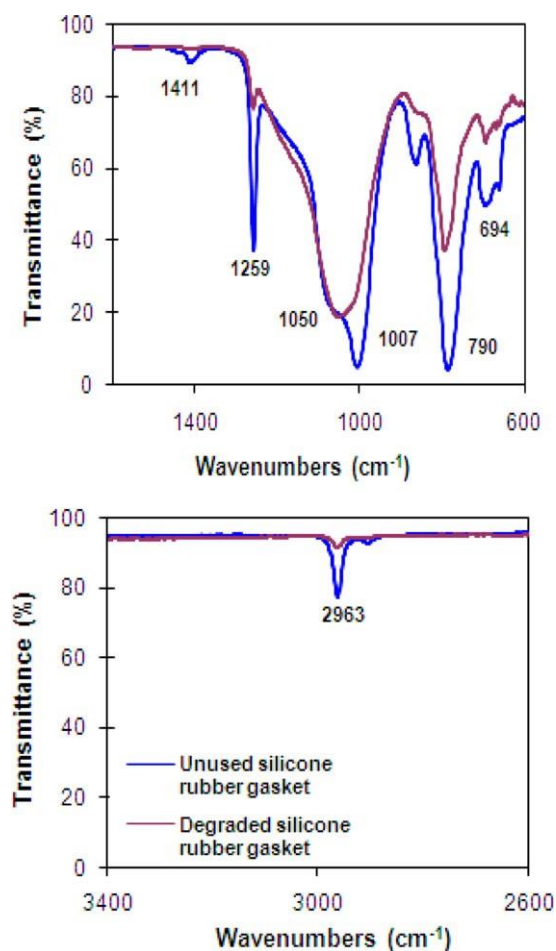


Figure 6. ATR-FTIR spectra after exposure to actual fuel cell environment (comparison of unused silicone rubber gasket with the degraded gasket). [Color figure can be viewed in the online issue, which is available at wileyonlinelibrary.com.]

XPS is a surface technique, and the FTIR was carried out on a sampled piece of rubber exhibiting significant degradation. Considering the swelling and spectroscopic sets of results together, it seems likely that there is little degradation in the bulk of the sample, but severe degradation at the surface.

Accelerated Aging

The surface degradation of the silicone rubber samples before and after exposure to diluted H_2SO_4 aging solution (pH 1, 2, and 4) at different time intervals is shown in Figure 8. It can be seen clearly that the color of the samples in the neck region which was submerged in pH 2 accelerated aging solution started to change from gray to white after 5 days [Figure 11(d)], and the degradation became even more significant (white color in the neck region) after 9 days. The extent of the degradation was more severe in the more highly acidic solution (pH 1); hence, the silicone rubber samples were ruptured in pH 1 solution after only 2 days exposure [Figure 11(b)]. By contrast, there was no sign of the degradation on the surface of the samples after exposure to pH 4 accelerated aging solution for 21 days [Figure 8(h)].

Tensile tests were carried out on these aged silicone rubber samples in order to examine the effect of acid aging on mechanical properties. Figure 9(a–c) shows that tensile strength, elongation at break, and 50% modulus of silicone rubber decreased significantly with time and the rate of decrease was higher in more acidic solutions. The decrease in tensile strength is relatively greater than the decrease in modulus. For example, after 15 days at pH 2, the tensile strength has decreased by 70%, whereas the modulus has decreased by 30%. It is likely that the difference is due to the fact that tensile strength is particularly sensitive to surface degradation while modulus is more of a bulk effect. As was suggested by the swelling and spectroscopic results discussed previously, it seems that severe degradation occurs at the surface but very little occurs in the bulk and as aging progresses the degradation front moves inwards. The thickening of the severely degraded layer, which in itself has very little strength, would inevitably result in a decrease in strength and modulus of the sample due to the smaller amount of undegraded rubber remaining that can take the load. In addition, a brittle degraded layer may also be a site for crack initiation, which would also tend to reduce tensile strength. The particular sensitivity of tensile strength to accelerated aging

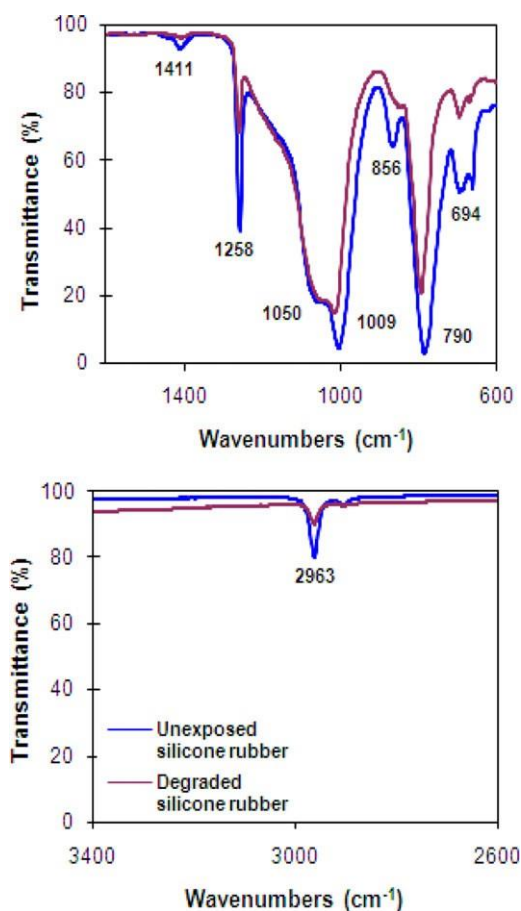


Figure 7. ATR-FTIR spectra after exposure to accelerated aging test (comparison of unexposed silicone rubber with degraded silicone rubber). [Color figure can be viewed in the online issue, which is available at wileyonlinelibrary.com.]

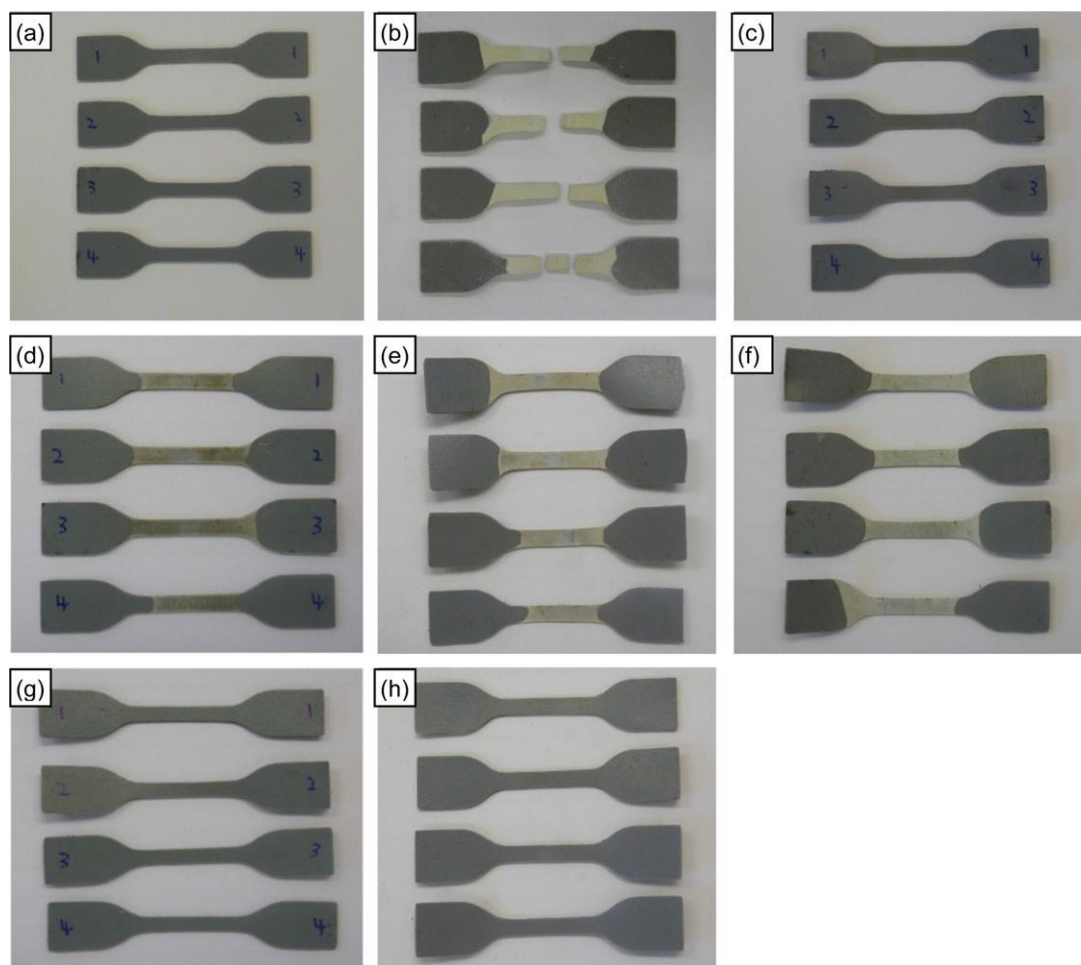


Figure 8. (a) Unexposed silicone rubber, (b) after exposure to pH 1 solution for 2 days; (c) after exposure to pH 2 solution for 2 days, (d) 5 days, (e) 9 days, and (f) 14 days; and (g) after exposure to pH 4 solution for 12 days and (h) 21 days at 140°C. [Color figure can be viewed in the online issue, which is available at wileyonlinelibrary.com.]

makes it a good means of quantifying aging, being much more sensitive and quantitative than the imaging and spectroscopic methods studied. It would have been beneficial to compare these accelerated aging results with the decrease in tensile strength of the gaskets with service life. However, the geometry of the gaskets was not suitable and sites of degradation so localized that a sensible set of tensile data could not be obtained.

3.6.2. Determination of Acidity (pH) Change with Nafion[®]

The acidity of a PEM fuel cell environment is due to the presence of the sulfonated fluorinated hydrocarbon membrane, and for this reason, it was considered worthwhile to carry out accelerated aging experiments using the membrane as the source of the acid. Nafion[®] samples, which were cut from different parts of the Nafion[®] membrane (the edge and central parts), were placed in the pressure vessels containing distilled water and were kept at 140°C for up to 14 days. The weight percentages (wt %) of the Nafion[®] in water were 0.7 and 1.4.

It can be seen from Figure 10 that despite the differences in the location on the membrane and in amounts used, the pH was found to be consistent, between 3 and 4 over the 14 day

period. Figure 11(a,b) shows the comparison of tensile properties of silicone rubber samples which were exposed to Nafion[®] aging solution and to the diluted H₂SO₄ solution with pH of 2 and 4 at 140°C for up to 8 days of aging. The standard deviation is less than 0.8 MPa for tensile strength values and less than 50% for elongation at break. It can be seen clearly that the decrease in both tensile strength and elongation at break of silicone rubber, which was aged in Nafion[®] solution was greater than the one that was aged in diluted H₂SO₄ solution with a pH of 2. The result is surprising since the pH of the Nafion aging solution was higher and so less degradation might have been expected. There is something else coming from the membrane that is accelerating the aging process, or it could be that the membrane in close proximity to the rubber gives locally a lower pH, which degrades the rubber more. Analysis of the Nafion aging solution should be carried out in the future to elucidate possible reasons why the aging is more extreme than in a sulfuric acid solution of similar pH. The assumption that the degree of degradation is solely determined by pH could lead to poor predictions of service life in real fuel cells where Nafion is the source of acidity.

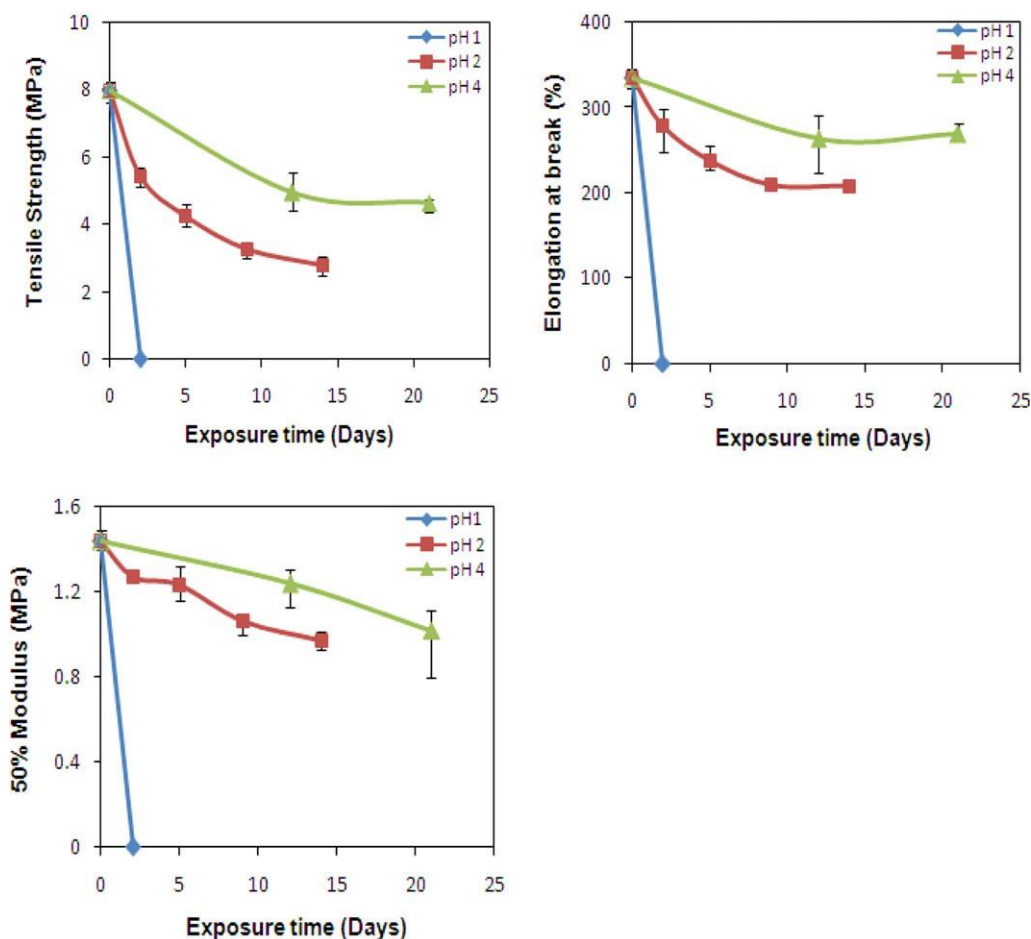


Figure 9. Tensile strength, elongation at break, and 50% modulus of silicone rubber after exposure to acidic solutions of pH 1, pH 2, and pH 4 at 140°C. The error bars indicate plus and minus the standard deviation. [Color figure can be viewed in the online issue, which is available at wileyonlinelibrary.com.]

CONCLUSIONS

Examination of the seals used in the fuel cells for up to 8000 h suggested that failure of the seals would not be due to compression set, but rather due to chemical degradation that made holes in the gasket in places and left a white powdery deposit on the surface in others. Accelerated aging of the same rubber in sulfuric acid solution at 140°C resulted in visibly similar degradation and FTIR analysis of both samples confirming the same type of hydrolysis reactions occurred in both the real fuel cell and accelerated aging test. Greater degradation occurred at lower pH levels confirming acid hydrolysis as the main degradation mechanism. However, aging carried out using hydrated Nafion membrane as the source of acid revealed that there was greater degradation in the presence of Nafion than was achieved with sulfuric acid of the same pH. This suggests that a degradation product from the Nafion membrane accelerates the degradation process in some way. Analysis of the degradation products from the hydrated Nafion should be carried out in future to determine the agent responsible and mechanism by which it achieves degradation of the silicone gasket. AFM proved ineffective as a tool for determining the effect of aging on surface hardness of the rubber, probably because of variations, at a

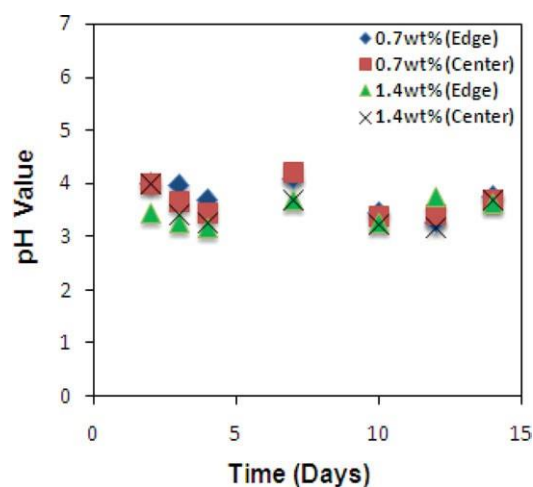


Figure 10. Acidity (pH) change with Nafion[®] samples taken from different locations on the Nafion[®] membrane and with different concentrations at 140°C for 14 days. [Color figure can be viewed in the online issue, which is available at wileyonlinelibrary.com.]

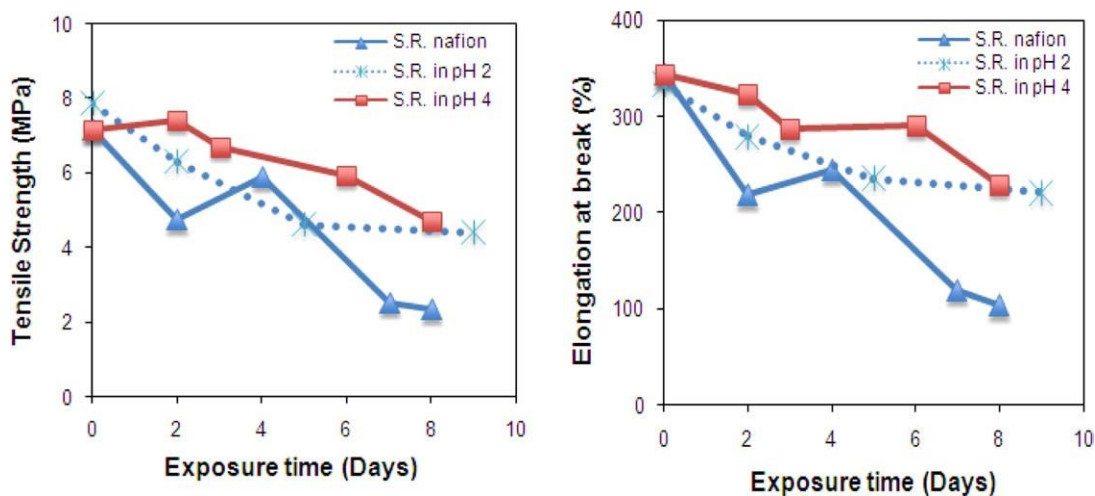


Figure 11. Tensile strength and elongation at break of silicone rubber (SR) after exposure to Nafion[®], pH 2, and pH 4 acidic solutions at 140°C. [Color figure can be viewed in the online issue, which is available at wileyonlinelibrary.com.]

microscopic scale, in hardness caused by the presence of filler particles or agglomerates. Solvent swelling tests carried out on the gaskets used in fuel cell seals for up to 8000 h showed an insignificant change in crosslink density while modulus values of the accelerated aging samples showed a relatively small change in modulus compared to the large change in tensile strength. Therefore, it is concluded that the fuel cell seals degrade by acid hydrolysis at the surface exposed to the acid but little degradation occurs in the bulk. Thus, degradation progresses as the degradation front moves inwards from the original surface. The similarity in degradation reactions occurring in the real fuel cells and accelerated aging tests at 140°C means that the accelerated aging tests could potentially be used to predict functional life of silicone seals in real fuel cells. However, such prediction would require that rates of reaction could be shown to follow Arrhenius behavior over the required temperature range. Furthermore, hydrated Nafion should be used as the acid aging agent.

ACKNOWLEDGMENTS

The work was carried out as part of a research project (BH064B) supported by the UK government agency, the Technology Strategy Board (TSB). Encouragement from the industry partners and financial support from the TSB was greatly appreciated.

REFERENCES

1. Tan, J.; Chao, Y. J.; Li, X.; Van Zee, J. W. *J. Power Sources*, 2007, 172, 782.
2. Patel, M.; Skinner, A. R. *Polym. Degrad. Stab.* 2001, 73, 399.
3. Gravier, D.; Farminer, K. W.; Narayan, R. *J. Polym. Environ.* 2003, 11, 129.
4. Umeda, I.; Tanaka, K.; Kondo, T.; Kondo, K.; Suzuki, Y. Proceedings of 2008 International Symposium on Electrical Insulating Materials, Yokkaichi, Mie, Japan, Sept. 7–11, 2008, 518.
5. Chaudhry, A. N.; Billingham, N. C. *Polym. Degrad. Stab.* 2001, 73, 505.
6. Goudie, J. L.; Owen, M. J.; Orbeck, T. Conference on Electrical Insulation and Dielectric Phenomena, Atlanta, Georgia, USA, Oct. 25–28, 1998, IEEE Annual Report, 1998, 120.
7. Hillborg, H.; Kornmann, X.; Krivda, A.; Meier, P.; Schmidt, L. E. In Conference on Electrical Insulation and Dielectric Phenomena, Vancouver BC, Canada, Oct. 14–17, 2007; IEEE Annual Report, 2007, 360.
8. Youn, B. H.; Huh, C. S. *Trans. Dielect. Elect. Insul.* 2005, 12, 1015.
9. Liu, H.; Cash, G.; Birtwhistle, D.; George, G. *Trans. Dielect. Elect. Insul.* 2005, 12, 478.
10. Gustavsson, T. G.; Gubanski, S. M.; Hillborg, H.; Karlsson, S.; Gedde, U. W. *Dielect. Elect. Insul.* 2001, 8, 1029.
11. Yoshimura, N.; Kumagai, S.; Nishimura, S. *Trans. Dielect. Elect. Insul.* 1999, 6, 632.
12. Oldfield, D.; Symes, T. *Polym. Test.* 1996, 15, 115.
13. Schulze, M.; Kn6ri, T.; Schneider, A.; G6lzew, E. *J. Power Sources* 2004, 127, 222.
14. Tan, J.; Chao, Y. J.; Yang, M.; Lee, W. K.; Van Zee, J. W. *Int. J. Hydrogen Energy* 2010, 36, 1846.
15. Tan, J.; Chao, Y. J.; Van Zee, J. W.; Lee, W. K. *Mater. Sci. Eng. A* 2007 445–446, 669.
16. Tan, J.; Chao, Y. J.; Yang, M.; Williams, C. T.; Van Zee, J. W. *J. Mater. Eng. Perform.* 2008, 17, 785.
17. Tan, J.; Chao, Y. J.; Van Zee, J. W.; Li, X.; Wang, X.; Yang, M. *Mater. Sci. Eng. A* 2008, 496, 464.
18. Tan, J.; Chao, Y. J.; Wang, H.; Gong, J.; Van Zee, J. W. *Polym. Degrad. Stab.* 2009, 94, 2072.
19. Husar, A.; Serra, A. M.; Kunusch, C. *J. Power Sources* 2007, 169, 85.
20. Bruijn, F. A.; Dam, V. A. T.; Janssen, G. J. M. *Fuel Cells* 2008, 8, 3.
21. Paluszkievicz, C.; Gumuła, T.; Podporska, J.; Błażewicz, M. *J. Mol. Struct.* 2006, 792–793, 176.
22. Satoh, K.; Urban, M. W. *Prog. Org. Coat.* 1996, 29, 195.

Title: Improved Elastomeric Materials for Fuel Cell Seals

Authors

Jane Clarke, Sebnem Pehlivan-Davis, Department of Materials, Loughborough University, Loughborough, Leicestershire, LE11 3TU, UK - J.Clarke@lboro.ac.uk, S.Pehlivan-Davis@lboro.ac.uk

Simon Armour, Intelligent Energy, Charnwood Building, Holywell Park, Ashby Road, Loughborough, Leicestershire, LE11 3GB, UK - Simon.Armour@intelligent-energy.com

Abstract

In this paper, the degradation of silicone rubber gaskets used in fuel cells and the same silicone rubber material exposed to accelerated ageing was investigated. The results showed a similar degradation mechanism occurred under both conditions. In addition, alternative gasket materials were investigated, in particular with regard to their resistance to aging under fuel cell conditions. The EPDM compound developed in the study showed the best combination of mechanical properties and resistance to aging both during accelerated aging and in a fuel cell trial.

Introduction

A polymer electrolyte membrane fuel cell (PEMFC) stack requires sealing around the perimeter of the cells to prevent the gases inside the cell from leaking. The overall performance of the fuel cell depends on the long-term stability of the gasket. Silicone rubber is the most commonly used gasket material due to its low cost and ease of processing. In a previous study¹, we investigated the degradation of the existing silicone rubber gasket material. As shown in Fig.1, severe degradation occurred in a silicone rubber gasket (after 8000 h used in the fuel cell), that made holes in the gasket and caused it to fail. Therefore, our intention is to identify more suitable elastomeric compounds for fuel cell applications.



Fig.1. Segments of silicone rubber gaskets (a) unused (b) after 8000 h used in the fuel cell

Experimental

Materials

Five elastomeric materials were used in this study; silicone rubber (SR) as a moulded fuel cell gasket and uncured sheet, fluorosilicone rubber (FSR), commercial ethylene propylene diene monomer rubber (com. EPDM), our EPDM compound (EPDM) and fluoroelastomer copolymer (FKM).

Accelerated Aging

An accelerated aging test was developed in order to assess the acid and time/temperature aging resistance of the sealing materials, which is relevant to the fuel cell environment. The test temperature of 140°C was selected so that 1 week of accelerated aging would roughly correspond to a real life time of 10000 h at 80°C, on the crude assumption of an expected doubling of degradation rate for every 10°C increase in temperature. Because of the elevated temperature and aqueous environment it was necessary to carry out the accelerated aging in pressurized vessels. Fig. 2 shows (a) the pressure vessel and (b) the layout of the samples in the liner. Accelerated aging solutions with acidity levels of pH 1 and 2, were prepared by diluting 2M sulfuric acid (H₂SO₄) with distilled water. The pH values of the aging solutions were chosen to create acidity, which is similar to that in a real PEM fuel cell, i.e., pH ranging from 3 to 4², but also to include those of greater acidity to accelerate the aging process.

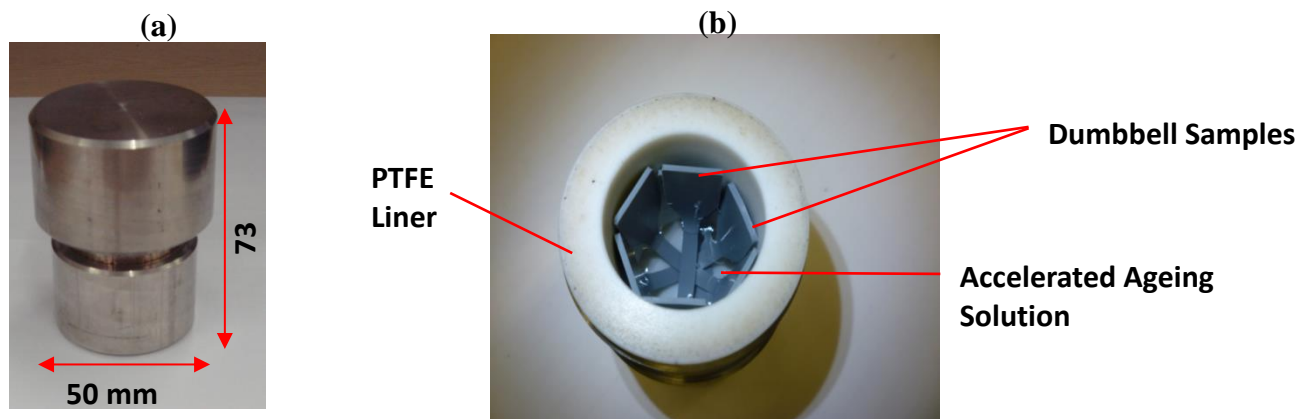


Fig.2 (a) Accelerated aging test pressure vessel and (b) arrangements of the samples in the pressure vessel

Characterisation and testing

ATR-FTIR was used to study the change in the surface chemistry of silicone rubber with degradation. The analysis was carried out on the surface of the samples from unused and degraded parts of gaskets used in a fuel cell, along with the silicone rubber material before and after exposure to accelerated aging tests.

Tensile tests were carried out on the aged rubber samples in order to examine the effect of aging on the mechanical properties.

Compression set tests were carried out in order to predict the suitability of compounds for the sealing application. The test specimens were compressed to 25 % of their original thickness at 140°C for 72 hours.

Results & Discussion

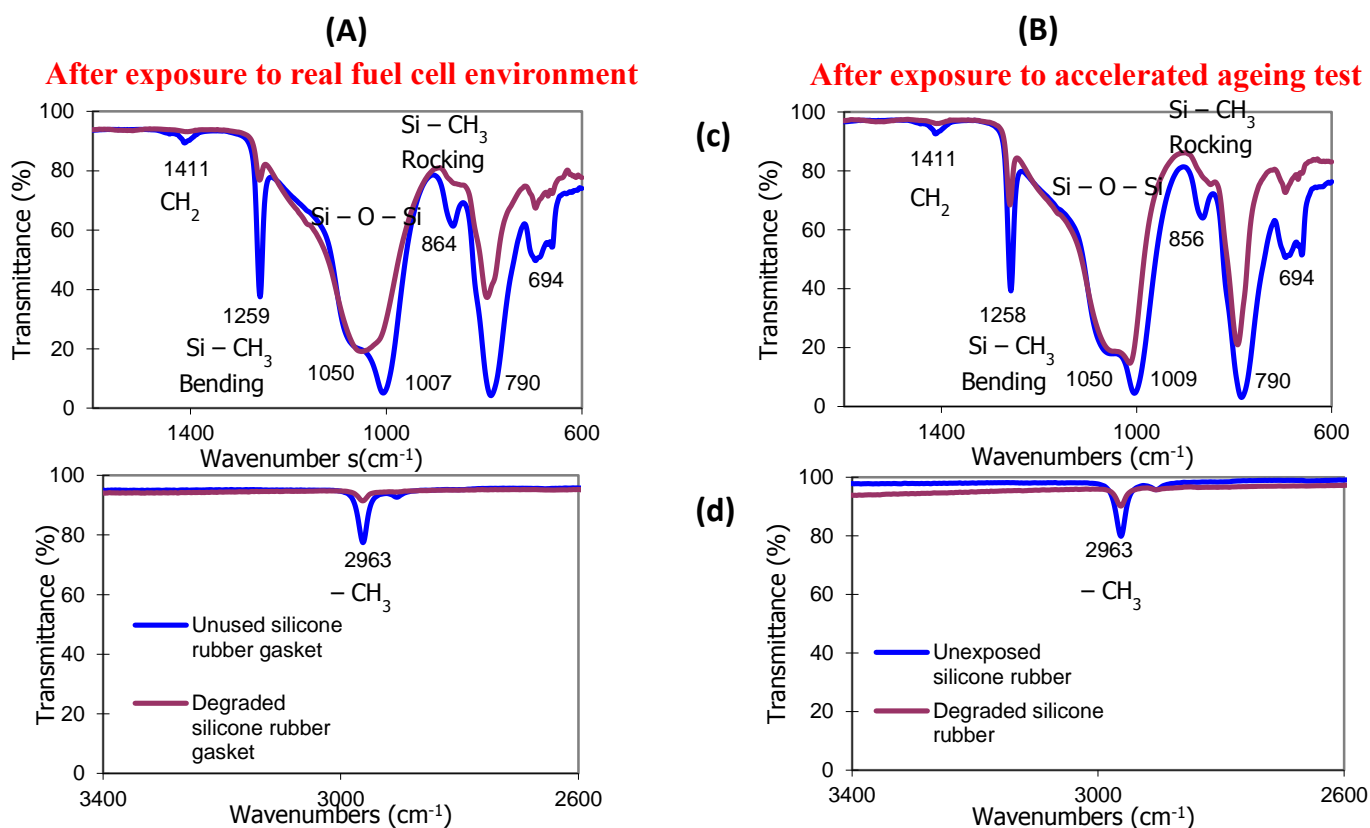


Fig.3. ATR-FTIR spectra of silicone rubber after exposure to (A) actual fuel cell (B) accelerated aging test environment.¹

Fig.3 shows the comparison of the ATR-FTIR results for a degraded silicone rubber gasket (operating in the fuel cell for 5000 h) and silicone rubber material after exposure to the accelerated aging test (pH 1 accelerated aging solution for 2 days). The similarity in the spectra for degraded materials from the fuel cell and accelerated aging environment indicates that accelerated aging conditions bring about a similar type of degradation to that of the real fuel cell environment. A scheme proposing the mechanism of hydrolytic degradation has been included in Tan et al.'s article³.

The decrease in tensile strength of rubber samples aged in pH 2 H₂SO₄ solution @ 140°C for up to 17 days were compared. Fig. 4 shows that SR and FSR had the higher decreases in tensile strength. The strength of FKM remained almost stable with aging. Commercial EPDM showed a relatively small reduction in tensile strength. Although the FKM showed the best resistance to aging, it was excluded from further investigation because it is an expensive material for fuel cell sealing compared to EPDM, which showed reasonably good acid aging resistance.

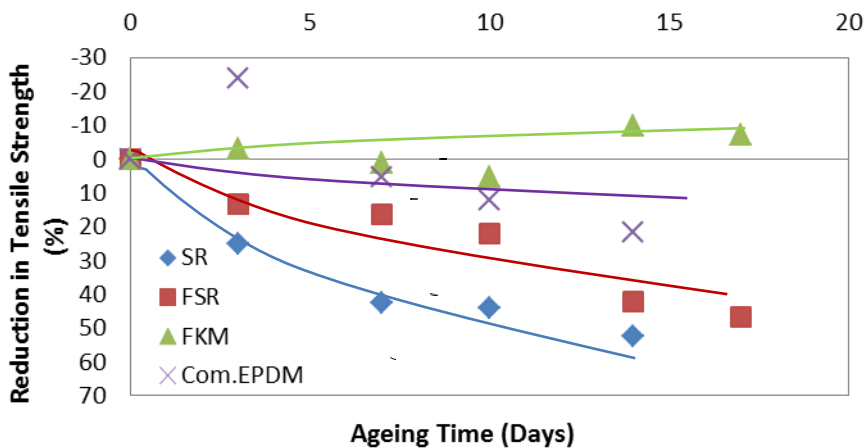


Fig.4. Reduction in tensile strength of SR, FSR, commercial EPDM and FKM samples aged in pH 2 H₂SO₄ solution @ 140°C for up to 17 days

Although the commercial EPDM compound had good acid aging resistance, it had a high compression set, as can be seen in Fig.5. For this reason we developed our own EPDM compound with a desired compression set value, similar to that of silicone rubber.

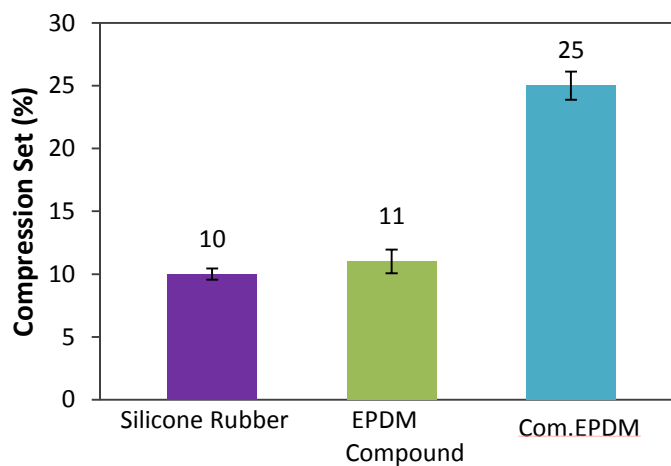


Fig.5. Compression set of the sealing materials @140°C and 25 % Compression for 72 h

Fuel cell seals of our EPDM compound were moulded and cured to test for suitability in a real single fuel cell in Intelligent Energy's test rig (IE) along with silicone rubber seals which were used as existing gaskets by IE. Failure of the gasket was indicated when cross-over of gasses was detected.

Fig.6 shows that the EPDM gasket did not fail even after 500 hours of the test, compared to the silicone rubber gaskets which all failed after less than 160 hours.

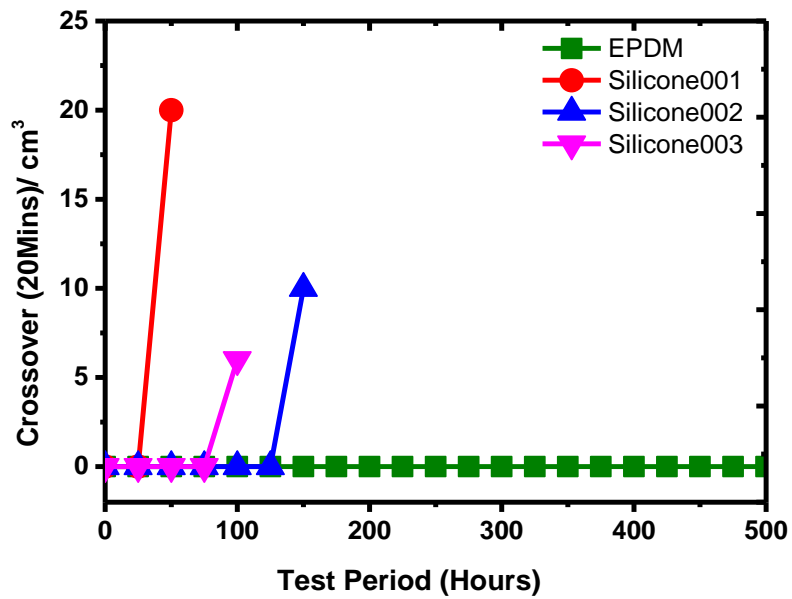


Fig.6.Crossover Test (Failure Test) of Silicone Rubber and EPDM compound Gaskets

Conclusion

The degradation of silicone rubber gasket used in the fuel cell was caused by acid hydrolysis. The EPDM compound developed in the study showed a very good performance in the fuel cell test rig, conforming that it is a potential replacement for silicone rubber in fuel cell applications.

References

1. Pehlivan-Davis, S.; Clarke, J.; Armour, S. J. Appl. Polym. Sci.,2012,129,1446-1454
2. Tan, J.; Chao, Y. J.; Yang, M.; Lee, W. K.; Van Zee, J. W. Int. J. Hydrogen Energy 2010, 36, 1846.
3. Tan, J.; Chao, Y. J.; Li, X.; Van Zee, J. W. J. Power Sources, 2007, 172, 782

Improved Elastomer Gasket Materials for PEM Fuel Cells

Sebnem Pehlivan- Davis^{1*} and Jane Clarke²

^{1,2}Department of Materials, Loughborough University, Loughborough, Leicestershire LE11 3TU, UK
E-mail: S.Pehlivan-Davis@lboro.ac.uk¹, J.Clarke@lboro.ac.uk²

Abstract – The overall aim of this research is to develop improved PEM fuel cell materials. This paper describes a systematic investigation into the degradation of three elastomeric gasket materials (silicone rubber, commercial EPDM and our EPDM compound) using an accelerated ageing experiment. Weight change and the tensile properties of the aged gasket samples were measured. In addition, compression set behaviour of the elastomeric seal materials was investigated in order to evaluate their potential sealing performance in PEM fuel cells. The EPDM compounds showed excellent acid resistance and our EPDM compound also showed good compression set behaviour, indicating great potential for this material in the PEM fuel cell application.

Keywords- PEM Fuel Cell, Elastomeric gaskets, Accelerated Ageing Test, Degradation, Rubber, Acidity

I. INTRODUCTION

PEM fuel cell stacks require gaskets (sealing) for each cell to separate the reactant gas compartments (hydrogen and oxygen) from each other. The seals used in PEM fuel cells are typically made of elastomeric materials and are exposed to acidic liquid solution, humid air and hydrogen and are subjected to mechanical compressive load during fuel cell operation. The combination of these factors can cause the degradation of the seal material. In our previous work, we investigated the degradation of silicone rubber gasket material used in actual fuel cells, as well as under accelerated ageing conditions.^[1] It was found that in both cases, silicone rubber had the same degradation mechanism (acid hydrolysis) which manifested itself as visible surface damage. In the present paper, the ageing processes of two different Ethylene propylene diene monomer (EPDM) compounds, along with the silicone rubber material were studied and the effect of ageing on the material properties was compared. In published literature, there are many reports regarding the chemical degradation of elastomeric gasket materials in simulated and accelerated fuel cell environments and the effect of degradation on their mechanical properties.^[2-12] For instance, Tan et al.^[2-8] investigated the chemical and mechanical

property degradation of silicone rubber, EPDM and fluoroelastomer materials exposed to simulated PEM fuel cell conditions. Schulze et al.^[13] reported that silicone rubber in direct contact with a perfluorosulphonic membrane degraded during fuel cell operation, leading to coloration of the membrane and detectable amounts of silicon on the electrodes. Most of these gasket degradation studies used the same or similar accelerated aging solutions containing hydrogen fluoride (HF) and sulphuric acid (H₂SO₄) and test temperatures of 80°C – 90°C (close to the PEM fuel cell operating temperature). However, in this work, we had a different approach to these accelerated test conditions by applying Nafion® membrane and trifluoroacetic acid (TFA) aging solutions (with sulphuric acid for comparison) to create a more realistic PEMFC environment. The TFA is a degradation product of the Nafion® membrane and since it is a very strong organic acid, it is likely to be a powerful degradation agent in the fuel cell environment. A high ageing temperature (140°C) was used in the current study to accelerate the degradation, since it was previously shown that degradation occurred by the same mechanism at both high and low temperatures.

II. EXPERIMENTAL

Three elastomeric materials, silicone rubber (SR), commercial ethylene propylene diene monomer rubber (EPDM), and our developed EPDM rubber compound (EPDM 2) were used for the experiments. SR was a peroxide cured polydimethylsiloxane (VMQ) silicone rubber compound filled with silica and was supplied by Intelligent Energy as uncured silicone rubber sheet. Commercial (EPDM) was supplied by James Walker & Co. Ltd. and is usually used in pharmaceutical sealing applications. The reason for the choice of this biocompatible and pure grade of EPDM is related to low leachability which is an important issue in PEM fuel cells. EPDM 2 was compounded as per the recipe given in Table1.

Table I. Compound recipe for EPDM 2

Compound Name	Amount (Phr)	Function
EPDM Ethylene and propylene co-monomers with ENB	100.0	Rubber
Perkadox (40 %) (Dicumyl peroxide)	6.5	Curing agent
ZnO (Zinc oxide (80%))	6.25	Curing activator
St.A (Stearic Acid)	0.5	Curing activator
SiO₂ (Silica coated with a silane coupling agent)	20.0	Reinforcing filler
TMQ (2,2,4-Trimethyl-1,2- Dihydroquinoline)	1.0	Antioxidant

Three different accelerated aging solutions were selected to age the gasket samples. The first one was sulphuric acid solution with a pH value of 3 which was prepared by diluting 2M H₂SO₄ with deionised water. Secondly, Nafion® membrane suspended in water was used for accelerated ageing with pH values between 3 and 4. The acidity level of pH 3 was particularly chosen in order to simulate the acidity which the gasket material was exposed to in the real fuel cell, (pH ranging from 3 to 4) [4]. It was assumed that Nafion® solution could create an acidic environment where the acidity was caused by the sulfonate groups in the membrane [1]. As a third solution a Trifluoroacetic acid (TFA) solution of pH 3.3 was employed, which is close to the pH value of the Nafion® solution. This was prepared by diluting 0.1% (v/v) trifluoroacetic acid with deionised water. In published literature TFA was identified as a major degradation product of Nafion® membrane. [14,15] The accelerated aging test was carried out in pressurized vessels at the elevated temperature of 140°C in the same way as in our previous work [1]. The dumbbell test samples were submerged into the ageing solutions which were placed in the vessels.

Weight change of rubber samples after exposure to ageing solutions was measured. The weight change can reflect the degree of corrosion of the materials caused by the acidic solutions. At the end of the ageing periods the dumbbell samples were taken out of the pressure vessels and rinsed with deionised water to remove the extra ageing solution from the sample surface. The samples were then left at room temperature to dry before the weight was measured and the percent weight change was calculated.

Tensile properties were measured for the dumbbell samples both before and after accelerated aging. A Hounsfield universal testing machine fitted with a laser extensometer was used to measure tensile properties in accordance with BS ISO 37:2011. [16] Values of tensile strength, elongation at break and 100 % modulus were recorded and the mean values determined. Four dumbbells were measured for each aging time.

In order to predict the suitability of compounds for the sealing application it was also necessary to assess compression set behaviour. Compression set measurements were conducted on cylindrical test pieces with 13.0 ± 0.5 mm diameter and 6.3 ± 0.3 mm thickness according to BS ISO815-1:2008. [17] The compression set test was carried out for silicone rubber, commercial EPDM and EPDM 2 compound at 140°C for 72 hours (25 % compression) to observe the effect of time on the compression set at this temperature and strain. After the test period, the specimens were removed from the oven and were left at room temperature to recover for 30 min before the measurements were carried out. Compression set was calculated using the following equation.

$$\text{Compression set (\%)} = \frac{h_0 - h_1}{h_0 - h_s} \times 100$$

where h_0 the initial thickness of the test piece, h_1 is the thickness of the test piece after recovery, h_s is the height of the spacer.

III. RESULTS AND DISCUSSION

The change of the pH value of the acid solutions after being used to age silicone rubber samples was measured as a way of revealing the reaction between rubber samples and the acid solutions. Fig. 3.1 demonstrates the change of the pH values of the acid solutions over time.

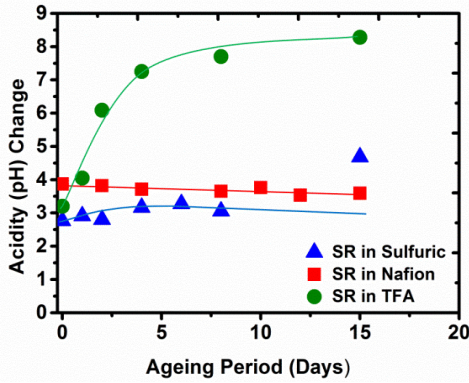


Fig.3.1. Change of the pH values of aging solutions containing silicone rubber

The pH of the TFA solution (containing the silicone rubber) increased sharply with aging time compared to the ones of the Nafion® and sulphuric acid solutions. The TFA acid solution became neutral after 4 days and alkaline after that, so it was clear that there was a chemical reaction between the TFA solution and silicone rubber samples, rather than just acid catalysed hydrolysis. This rapid change in the pH value of the TFA solution indicates that the TFA was used up in reactions relatively soon after the silicone samples were added. Therefore, the aging effect of the solution disappeared

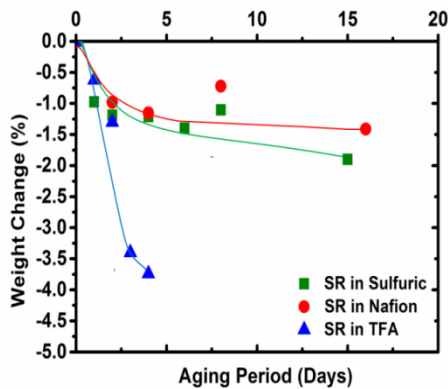


Fig.3.2. Weight change of SR samples aged in Nafion®, TFA and sulphuric acid (~ pH 3) @ 140°C

after 4 days when the TFA had been consumed. For this reason, the aging experiment was repeated, with the TFA solution being refreshed every 2 days so that a fairly constant pH (3.3) was maintained. By contrast, sulphuric acid and

Nafion® solutions had no significant change in pH after aging the silicone samples. (See Fig.3.1)

The weight change of silicone rubber samples which were exposed to sulphuric acid (H_2SO_4 ~ pH 3), Nafion® (pH ~ 3.2) and TFA (at constant pH of 3.3) ageing solutions at 140°C over time was monitored and results are shown in Fig.3.2. In all solutions, SR showed increasing weight loss with exposure time which was probably due to loss of the degraded material.

The largest decrease in weight was observed in TFA solution (~ 4 %) compared to the ones in sulphuric acid and Nafion® solutions of the same pH. This indicates that TFA solution was more aggressive than sulphuric acid and Nafion® solutions and also confirms the more rapid change in the acidity (pH) of TFA solution with time as explained above.

Tensile tests were carried out on the aged silicone rubber dumbbell samples in sulphuric acid, Nafion® and TFA aging solutions with the pH value of around 3 in order to determine the effect of acid aging on mechanical properties.

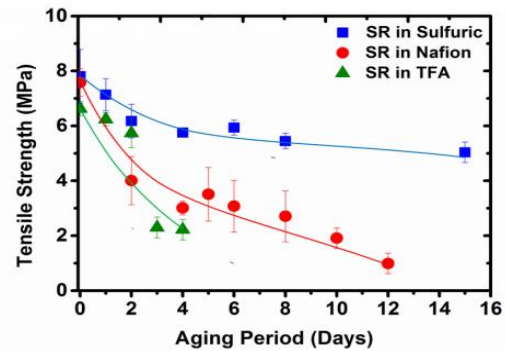


Fig.3.3. Tensile strength of silicone rubber aged in pH 3 (Nafion®, TFA and sulphuric acid) solutions @ 140°C

Fig.3.3 shows that tensile strength of silicone rubber in both Nafion® and TFA solutions declined significantly with time whereas it showed only a slight decrease in sulphuric acid solution of similar pH.

Surface observations of silicone rubber samples exposed to pH 3 accelerated aging solutions of sulphuric acid, Nafion® and TFA solutions at 140°C for four days are presented in Fig.3.4. The major degradation products of Nafion® membrane were reported as HF and TFA[15] and this can explain why the silicone sample surfaces had a similar colour change after exposure to Nafion® and TFA solutions as shown in Fig. 3.4. The colour change from grey to white of the silicone samples in the neck region which was immersed in the Nafion® and TFA accelerated aging solutions indicates a sign of degradation. However, there was no colour change observed on the surface of the samples which were exposed to sulphuric acid solution under identical conditions. This

confirms the more aggressive attack by TFA indicated in the weight change and tensile test results.

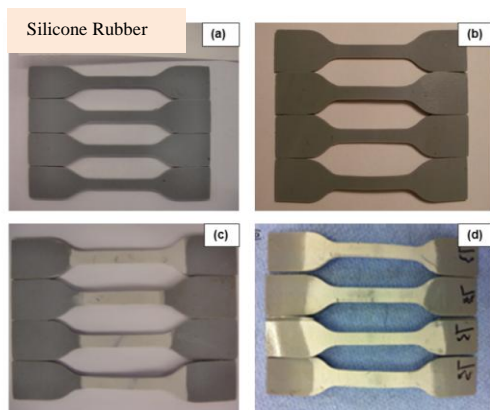


Fig.3.4. (a) Unexposed silicone rubber and after 4 days exposure to pH 3 solutions (b) sulphuric acid, (c) Nafion® and (d) TFA at 140°C.

Fig.3.5. compares the weight change of silicone rubber, commercial EPDM and EPDM 2 exposed to Nafion® solution (pH 3– 4) at 140°C. The weight of silicone rubber samples decreased with exposure time whereas both EPDM materials had weight gain which could be due to the water uptake of these materials.

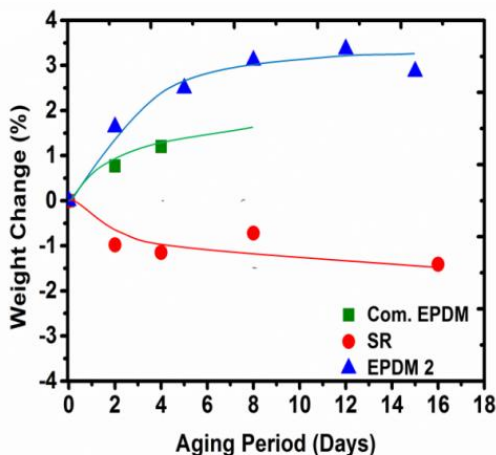


Fig.3.5. Weight change of SR, commercial EPDM and EMPD 2 aged in Nafion® (pH 3-4) @ 140°C

Fig. 3.6 shows the tensile strength of the three gasket materials (SR, com. EPDM and EPDM 2) exposed to Nafion® solution at 140°C. Silicone rubber had the larger decrease in tensile strength with exposure time but both EPDM (com. EPDM and EPDM 2) materials did not experience a significant change.

Fig. 7 shows the compression set behaviour of the rubber materials. It can be clearly seen that EPDM 2 had a low

(good) compression set value which is similar to silicone rubber and much better than the commercial EPDM.

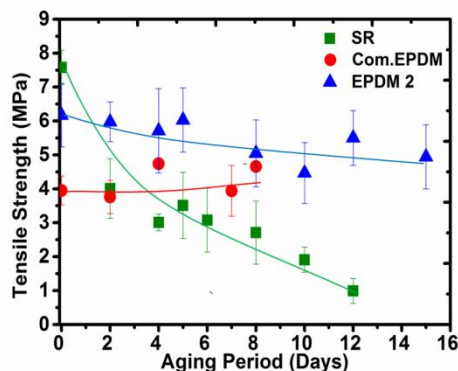


Fig.3.6. Tensile strength of silicone rubber, commercial EPDM and EPDM 2 in Nafion solution at 140°C.

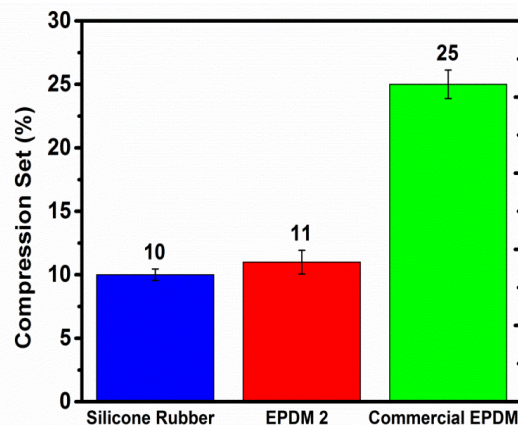


Fig.3.7. Compression set of silicone rubber, commercial EPDM and EPDM 2 at 140°C and 25% com for 72 hrs.

IV. CONCLUSIONS

The degradation of silicone rubber in Nafion® and TFA solutions was greater than that in sulphuric acid of the same pH. This implies that the major degradation products of the Nafion® membrane, particularly the TFA, accelerates the acid hydrolysis of silicone rubber. The commercial EPDM did not show a significant decrease in tensile strength on ageing but had a high compression set. Our own developed EPDM 2 however, had a good resistance to acid ageing as well as a good (low) compression set and hence it has proved to be an improved material in fuel cell sealing applications

ACKNOWLEDGEMENTS

The work was carried out as part of a research project (BH064B) supported by the Technology Strategy Board

(TSB). Encouragement from the industry partners and financial support from the TSB was greatly appreciated. Special thanks to James Walker & Co. for providing the commercial EPDM compound.

REFERENCES

- [1] S. Pehlivan-Davis, J. Clarke, and S. Armour, "Comparison of accelerated aging of silicone rubber gasket material with aging in a fuel cell environment," *J. Appl. Polym. Sci.*, vol. 129, no. 3, pp. 1446–1454, 2013.
- [2] J. Tan, Y. J. Chao, J. W. Van Zee, and W. K. Lee, "Degradation of elastomeric gasket materials in PEM fuel cells," *Mater. Sci. Eng. A*, vol. 445–446, no. 0, pp. 669–675, Feb. 2007.
- [3] J. Tan, Y. J. Chao, J. W. Van Zee, X. Li, X. Wang, and M. Yang, "Assessment of mechanical properties of fluoroelastomer and EPDM in a simulated PEM fuel cell environment by microindentation test," *Mater. Sci. Eng. A*, vol. 496, no. 1–2, pp. 464–470, Nov. 2008.
- [4] J. Tan, Y. J. Chao, M. Yang, W.-K. Lee, and J. W. Van Zee, "Chemical and mechanical stability of a Silicone gasket material exposed to PEM fuel cell environment," *Int. J. Hydrogen Energy*, vol. 36, no. 2, pp. 1846–1852, Jan. 2011.
- [5] J. Tan, Y. J. Chao, X. Li, and J. W. Van Zee, "Degradation of silicone rubber under compression in a simulated PEM fuel cell environment," *J. Power Sources*, vol. 172, no. 2, pp. 782–789, Oct. 2007.
- [6] J. Tan, Y. J. Chao, M. Yang, C. T. Williams, and J. W. Van Zee, "Degradation Characteristics of Elastomeric Gasket Materials in a Simulated PEM Fuel Cell Environment," *J. Mater. Eng. Perform.*, vol. 17, no. 6, pp. 785–792, 2008.
- [7] J. Tan, Y. J. Chao, H. Wang, J. Gong, and J. W. Van Zee, "Chemical and mechanical stability of EPDM in a PEM fuel cell environment," *Polym. Degrad. Stab.*, vol. 94, no. 11, pp. 2072–2078, Nov. 2009.
- [8] J. Tan, Y. J. Chao, X. Li, and J. W. Van Zee, "Microindentation Test for Assessing the Mechanical Properties of Silicone Rubber Exposed to a Simulated Polymer Electrolyte Membrane Fuel Cell Environment," *J. Fuel Cell Sci. Technol.*, vol. 6, no. 4, p. 41017, Aug. 2009.
- [9] C. W. Lin, C. H. Chien, J. Tan, Y. J. Chao, and J. W. Van Zee, "Dynamic mechanical characteristics of five elastomeric gasket materials aged in a simulated and an accelerated PEM fuel cell environment," *Int. J. Hydrogen Energy*, vol. 36, pp. 6756–6767, 2011.
- [10] G. Li, J. Tan, and J. Gong, "Chemical aging of the silicone rubber in a simulated and three accelerated proton exchange membrane fuel cell environments," *J. Power Sources*, vol. 217, no. 0, pp. 175–183, Nov. 2012.
- [11] G. Li, J. Tan, and J. Gong, "Degradation of the elastomeric gasket material in a simulated and four accelerated proton exchange membrane fuel cell environments," *J. Power Sources*, vol. 205, no. 0, pp. 244–251, May 2012.
- [12] C.-W. Lin, C.-H. Chien, J. Tan, Y. J. Chao, and J. W. Van Zee, "Chemical degradation of five elastomeric seal materials in a simulated and an accelerated PEM fuel cell environment," *J. Power Sources*, vol. 196, no. 4, pp. 1955–1966, Feb. 2011.
- [13] M. Schulze, T. Knöri, A. Schneider, and E. Gülzow, "Degradation of sealings for PEFC test cells during fuel cell operation," in *Journal of Power Sources*, 2004, vol. 127, pp. 222–229.
- [14] C. Zhou, M. a. Guerra, Z.-M. Qiu, T. a. Zawodzinski, and D. a. Schiraldi, "Chemical Durability Studies of Perfluorinated Sulfonic Acid Polymers and Model Compounds under Mimic Fuel Cell Conditions," *Macromolecules*, vol. 40, no. 24, pp. 8695–8707, Nov. 2007.
- [15] C. Chen and T. F. Fuller, "The effect of humidity on the degradation of Nafion® membrane," *Polym. Degrad. Stab.*, vol. 94, no. 9, pp. 1436–1447, Sep. 2009.
- [16] British Standard Institution, *BS ISO 37:2011. Rubber, vulcanized or thermoplastic. Determination of tensile stress-strain properties*. London: British Standard Institute, 2011.
- [17] British Standard Institution, *BS ISO 815-1:2008. Rubber, vulcanized or thermoplastic. Determination of compression set. At ambient or elevated temperatures*, no. March. London: British Standard Institute, 2009.

Manuscript Number: PDST-D-15-00555

Title: Modelling degradation of silicone rubber in PEM fuel cell and other acidic environments

Article Type: Research Paper

Keywords: silicone rubber, acid hydrolysis, modelling, fuel cell

Corresponding Author: Dr. Jane Clarke,

Corresponding Author's Institution: Loughborough University

First Author: Jane Clarke

Order of Authors: Jane Clarke; Sebnem Pehlivan-Davis; Minsi Yan

Abstract: The objective of this research was to model the degradation of a silicone rubber sealing material in an acidic environment, such as a fuel cell, under different pH and temperature conditions. Accelerated aging experiments were carried out under controlled conditions of temperature (100, 120 and 140°C) and pH (1, 1.5, 1.7, 2 and 4), with tensile strength being used as a quantitative measure of the extent of degradation.

The decrease in tensile strength due to accelerated aging was found to follow first order kinetics and so degradation rate constants were determined for all the different conditions of temperature and acidity. These rate constants varied with pH, but in a non-linear fashion. It was found that the pH dependency of the degradation rate constant could be modelled by assuming that the overall degradation rate has a component due to an underlying rate of degradation that is not pH dependant and a component due to acid catalysed degradation that is pH dependant. Both the overall rate constants and the individual components were found to obey Arrhenius behaviour, with all having the same activation energy of 81.4 kJ.mol⁻¹. A model was developed that included both the acid and temperature dependency of the rate constants. The model was used to determine rate constants for all the experimental conditions studied and using these, model tensile strength against aging time curves were generated and compared to the experimental values. The model was able to reproduce experimental data reasonably accurately for the different sets of conditions studied and hence, a predictive model for the degradation behaviour of the silicone rubber material was achieved. The model will allow the degradation behaviour of the silicone rubber seal to be predicted in real fuel cells, provided that information about temperatures, times and pHs of operation can be supplied as input for the model. The model may also be more broadly applied to acid aging of silicone rubbers in acidic environments, although as extrapolations become greater, the predictions can be made less confidently.

Suggested Reviewers:

Modelling degradation of silicone rubber in PEM fuel cell and other acidic environments

Jane Clarke^{a*}, Sebnem Pehlivan-Davis^a, and Minsi Yan^a

^a Loughborough University, Loughborough LE11 3TU, Leicestershire, UK,

J.Clarke@lboro.ac.uk, S.Pehlivan-davis@lboro.ac.uk

*Corresponding author. Tel.:+44 1509 223154; fax: +44 1509223949

Abstract

The objective of this research was to model the degradation of a silicone rubber sealing material in an acidic environment, such as a fuel cell, under different pH and temperature conditions. Accelerated aging experiments were carried out under controlled conditions of temperature (100, 120 and 140°C) and pH (1, 1.5, 1.7, 2 and 4), with tensile strength being used as a quantitative measure of the extent of degradation.

The decrease in tensile strength due to accelerated aging was found to follow first order kinetics and so degradation rate constants were determined for all the different conditions of temperature and acidity. These rate constants varied with pH, but in a non-linear fashion. It was found that the pH dependency of the degradation rate constant could be modelled by assuming that the overall degradation rate has a component due to an underlying rate of degradation that is not pH dependant and a component due to acid catalysed degradation that is pH dependant. Both the overall rate constants and the individual components were found to obey Arrhenius behaviour, with all having the same activation energy of 81.4 kJ.mol⁻¹. A model was developed that included both the acid and temperature dependency of the rate constants. The model was used to determine rate constants for all the experimental conditions studied and using these, model tensile strength against aging time curves were generated and compared to the experimental values. The model was able to reproduce experimental data reasonably accurately for the different sets of conditions studied and hence, a predictive model for the degradation behaviour of the silicone rubber material was achieved. The model will allow the degradation behaviour of the silicone rubber seal to be predicted in real fuel cells, provided that information about temperatures, times and pHs of operation can be supplied as input for the model. The model may also be more broadly applied to acid aging of silicone rubbers in acidic environments, although as extrapolations become greater, the predictions can be made less confidently.

Keywords: silicone rubber, acid hydrolysis, modelling, fuel cell

1. Introduction

Silicone rubber has often been used as a Polymer Electrolyte Membrane (PEM) fuel cell sealing material; however, it has been observed that it is prone to degradation, which can limit the performance and durability of the fuel cell. In the PEM fuel cell the sealing material

is exposed at temperatures of about 80°C, to water and acid. The acid comes from the sulphonated tetrafluoroethylene based polymer electrolyte membrane.

There have been many published studies into the weathering or aging of silicone rubber in moist and acidic environments that indicate the probable mechanisms of degradation in the fuel cell and the key factors affecting the process. For instance, Gravier et al. (1) reviewed the possible degradation mechanisms of polydimethylsiloxane (PDMS) in an outdoor environment. It was suggested that, in soil, PDMS hydrolyses into dimethylsilandiol (DMSD) which evaporates and that the Si – C bonds are cleaved by hydroxyl radicals, leading to the degradation products of silica, water and carbonyl compounds. The rate of hydrolysis was found to depend on the type of soil, pH, temperature, organic material, and particularly the moisture content. In studies by Thomas (2) and Patel et al. (3) it was reported that network scission in peroxide cured PDMS rubbers at high temperatures in a closed system was due to hydrolysis reactions, which did not happen in an open system, probably because of evaporation of any water. Chaudhry and Billingham (4) showed that silica filled PDMS rubber was highly resistant towards oxidative degradation at high temperatures (180 – 200°C) in the absence of moisture. From these studies it is apparent that water is the main trigger for the breakage of siloxane bonds, which leads to network scission in PDMS.

It has been found that an acidic environment can accelerate the degradation of silicone rubber to a great extent. Umeda et al. (5) and Koshino et al. (6) investigated aging of a silicone rubber housing for a polymer insulator used at a testing station near the sea coast. The FTIR analysis confirmed that the ageing mode was similar to damage caused by nitric acid. The strong acid environment (pH = 0 – 2.0) was shown to be due to corona discharge under humid conditions.

In our previous work (7), ATR-FTIR analysis suggested a similar type of degradation for silicone rubber materials degraded in an actual PEM fuel cell and an accelerated ageing environment. A number of other studies into aging of silicone rubber in fuel cell environments have been carried out by Tan et al. (8,9,10,11) and Li et al. (12,13) agreed with our findings under similar test conditions. All the ATR-FTIR results from these studies suggest that the silicone rubber backbone and the crosslink sites in the rubber were chemically changed over time as a result of acid hydrolysis.

The objective of the current study is to establish whether it is possible develop a predictive model of the degradation of silicone rubber in acidic environments by determining the quantitative relationships between degree of degradation and degradation time, temperature and pH.

2. Experimental

Sheets approximately 1 mm thick of silicone rubber compound were cured for 10 min. at 170°C in an electrically heated hydraulic press. Type 2 dumbbells (BS 903: Part 2) were cut from the sheets and were used in the accelerated aging tests.

Accelerated aging was carried out in steel pressure vessels fitted with PTFE liners (7). Accelerated aging solutions with acidity levels of pH 1, 1.5, 1.7, 2 and 4 were prepared by diluting 2 M sulphuric acid with deionised water. Four dumbbell samples were placed into a PTFE liner containing the accelerated aging solution filled up to one-third of its depth in order to make sure that the neck of the dumbbell test samples were submerged completely in the solution. The PTFE liner was then put into the metal base and sealed tightly with the metal cap before placing in an oven at 100, 120 or 140°C. The aged samples were taken out of the pressure vessel at selected times from one day to three weeks for tensile testing. They were washed with distilled water and allowed to dry in air at room temperature before testing. Table 1 summarises the experiments carried out.

Table 1: Summary of accelerated aging conditions

pH	Temperature, °C		
	100	120	140
1	√	√	√
1.5	√	√	√
1.7	√	√	√
2	-	-	√
4	-	-	√

Tensile tests were carried out in accordance with BS 903:A Part 2, using a Hounsfield tensile testing machine at constant cross-head speed of 500 mm/min and with a load cell of 1000N. The tensile strength was determined and used as a quantitative measure of degree of degradation in the development of the aging model.

3. Results and Discussion

3.1 Effect of pH, temperature and aging time on tensile strength

The tensile strength was plotted against aging time for all the different experimental conditions. Figure 1 shows an example of the results for a pH of 1.7.

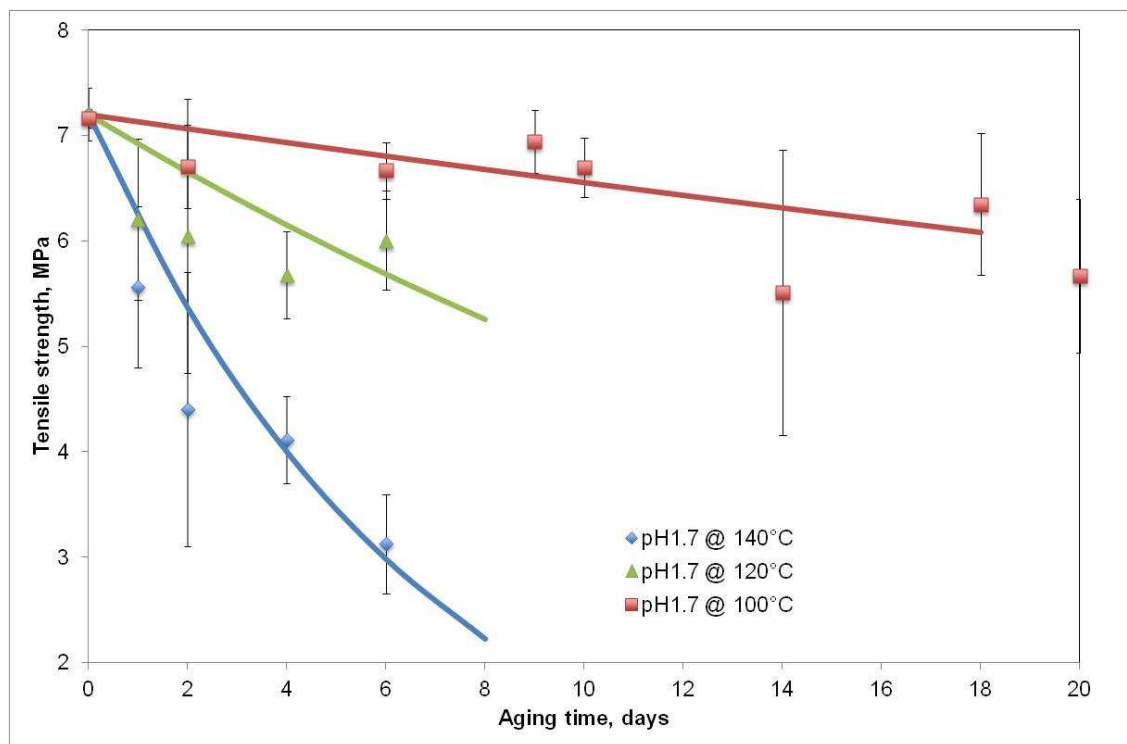


Figure 1. Effect of aging time and temperature on tensile strength of silicone rubber aged at a pH of 1.7 (error bars indicate plus and minus the standard deviation)

The rate of decrease in tensile strength with aging time increased with increase in temperature and decrease in pH. The results are not surprising because the degradation process is a chemical reaction which would be expected to increase in rate with increase in temperature and because it is believed to be an acid catalysed reaction, it would also be expected to increase in rate as the concentration of protons increases.

3.2 Modelling the relationship between tensile strength and aging time

In developing a predictive aging model the rate of degradation must be expressed mathematically. Therefore it is necessary to hypothesise a relationship between aging time and tensile strength. It was noticed that the rate of decrease in tensile strength with aging time was steep at short degradation times but decreased as the aging time increased. This sort of behaviour is typical of first order reactions where the rate of reaction is dependent on the concentration of one of the reactants, which decreases as the chemical reaction progresses. However, in this case, both the acid which is catalysing the reaction and the silicone rubber which is the main reactant are present in excess. In fact the pH at the end of the aging is the same as it was at the beginning. Therefore, there must be another explanation for this behaviour. It is possible that the rate limiting step of the reaction is the time taken for the acid and water to diffuse through the degraded layer to the un-degraded rubber where it reacts to cause further degradation. If this is the case then the rate of diffusion is proportional to the thickness of the degraded layer (Fick's Law) which, in turn, is inversely proportional to the tensile strength. Figure 2 shows the qualitative relationship between the rate of degradation, tensile strength, thickness of the degraded layer and rate of diffusion.

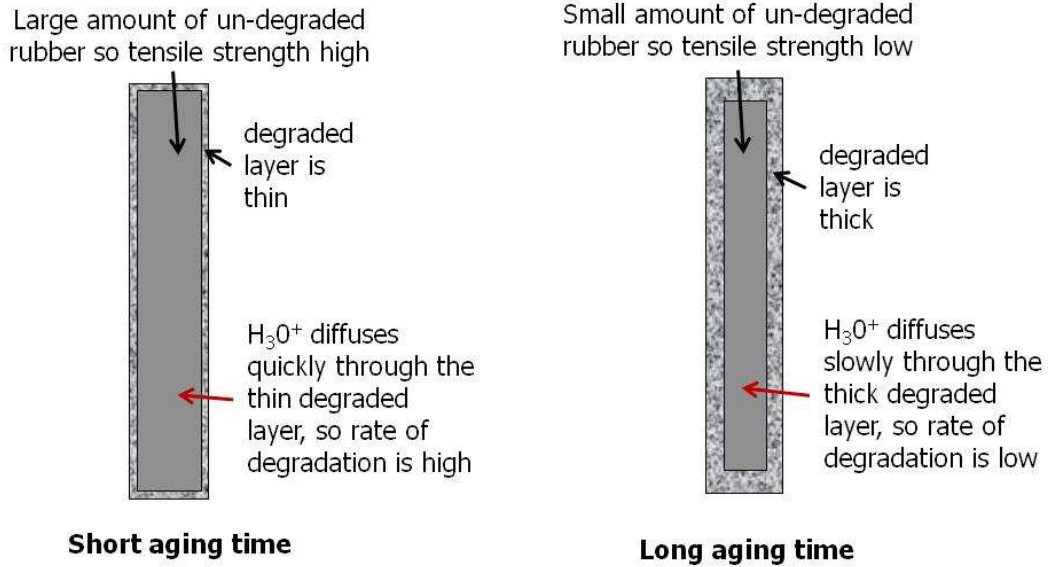


Figure 2: Diagram to show how diffusion of acid through the degraded layer at different aging times may affect degradation rate

If this hypothesis is correct then the situation is analogous to first order kinetics of chemical reactions where the following equation relates the rate of reaction to the concentration of one of the reactants.

$$\text{reaction rate} = k[A]$$

where $[A]$ is the concentration of reactant A

In the current case, rather than the concentration of a reactant, the degradation rate is proportional to tensile strength, because the tensile strength is inversely proportional to the thickness of the degraded layer and the thickness of the degraded layer is inversely proportional to the rate of degradation. The degradation rate can thus be expressed as follows.

$$\text{degradation rate} = -\frac{dT_S}{dt} = kT_S$$

Where T_S is tensile strength at aging time, t and k is the rate constant.

This equation relates the rate of degradation to tensile strength, but it is more useful to relate tensile strength to the aging time, so integration is necessary, giving the equation below.

$$TS = TS_0 e^{-kt}$$

Where TS_0 is the tensile strength of the un-degraded rubber (i.e. at $t=0$)

Hence we can use the characteristic kinetic plot for first order reactions to determine the rate constant, k . In this case, the natural log of tensile strength ($\ln TS$) plotted against aging time (t) will give us a slope of $-k$.

Figure 3 shows an example of a first order plot for degradation carried out at a pH of 1.7. The rate constants are given as the negative gradients of the best fit lines.

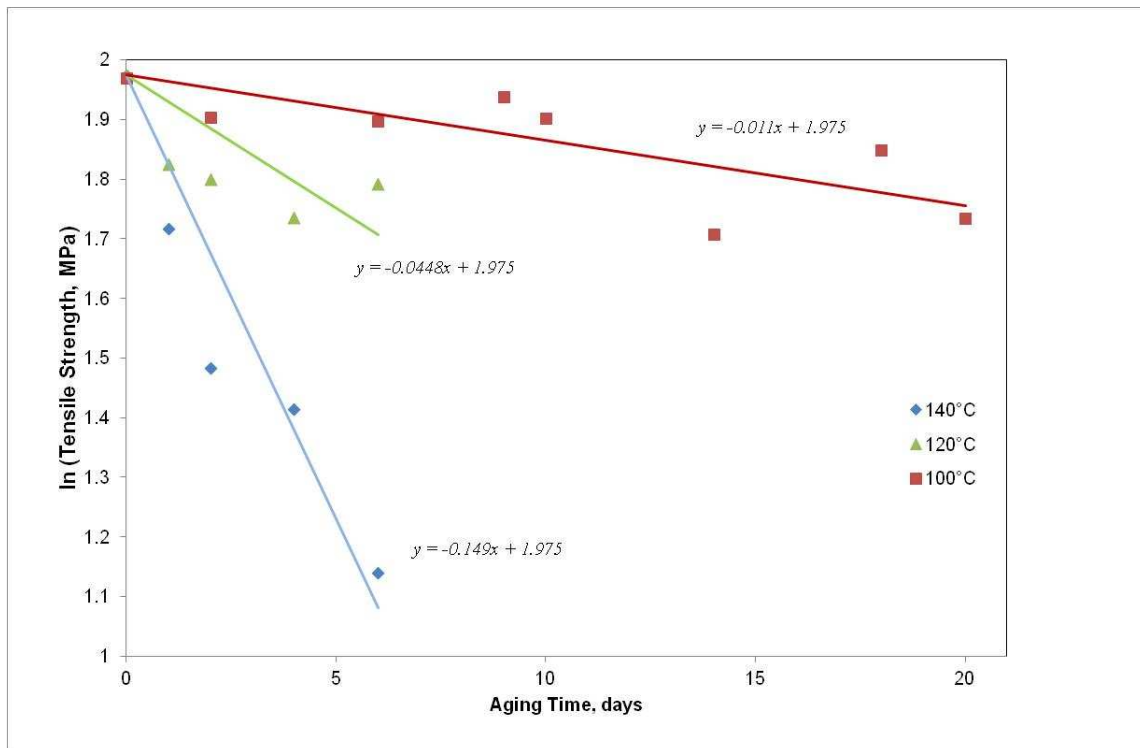


Figure 3: First order rate plots for degradation of silicone rubber aged at a pH of 1.7

First order plots were produced for all the aging experiments and the rate constants determined are shown in Table 2.

Table 2: Rate constants for all the accelerated aging conditions investigated

		Rate constant		
		100	120	140
Temperature, °C				
pH	1	0.1638	0.6753	2.0392
	1.5	0.032	0.1221	0.3889
	1.7	0.011	0.0448	0.149
	2	-	-	0.0727
	4	-	-	0.0285

3.3 Modelling the relationship between degradation rate constant and pH

Since it is known that the degradation mechanism for the silicone rubber is acid catalysed hydrolysis, it is reasonable to assume that the rate of degradation is related to the concentration of H^+ ions by the equation below, where n is the order of reaction.

$$degradation\ rate = [H^+]^n$$

We can assume that the degradation rate can be represented by the rate constant, k and therefore a plot of $\log k$ against $\log[H^+]$ should give a straight line with slope equal to the order of the reaction. Since $pH = -\log[H^+]$, $\log k$ can be plotted instead against pH, in which case the negative of the slope will give the order of the reaction. Figure 4 shows the plot for the experiments carried out at 140°C. From pH1 to pH2 the data does fall on a straight line, however, the pH4 result falls well away from the straight line, indicating a much greater rate of reaction than would be expected from an extrapolation of the straight line through the lower pH results. To account for this behaviour it can be assumed that a level of hydrolysis occurs even in the absence of acid, a reasonable assumption since the acid is acting as a catalyst. Hence, the overall rate of reaction k can be assumed to comprise contributions from

an underlying or non-catalysed rate, k_u , which is the same at all pH values and a catalysed rate, k_c which varies with pH, as shown in the following equation.

$$k = k_c - k_u$$

The catalysed reaction is assumed to give a straight line when $\log k_c$ is plotted against pH, with the negative of the slope giving the order of reaction, n . The intercept on the y axis gives the log of the theoretical value of the catalysed degradation rate at a pH of 0, (k_{cA}).

$$\log k_c = \log k_{cA} - n(pH)$$

By trying different values for the underlying rate and for the order of the acid catalysed reaction, a good fit to the experimental data was found. A value of 0.0284 for the underlying rate and 1.7 for the order of reaction (n) gave the solid line shown in Figure 4. The value of n of 1.7 is surprising since it would be expected that acid catalysed hydrolysis would be first order with respect to hydrogen ions (i.e. $n = 1$).

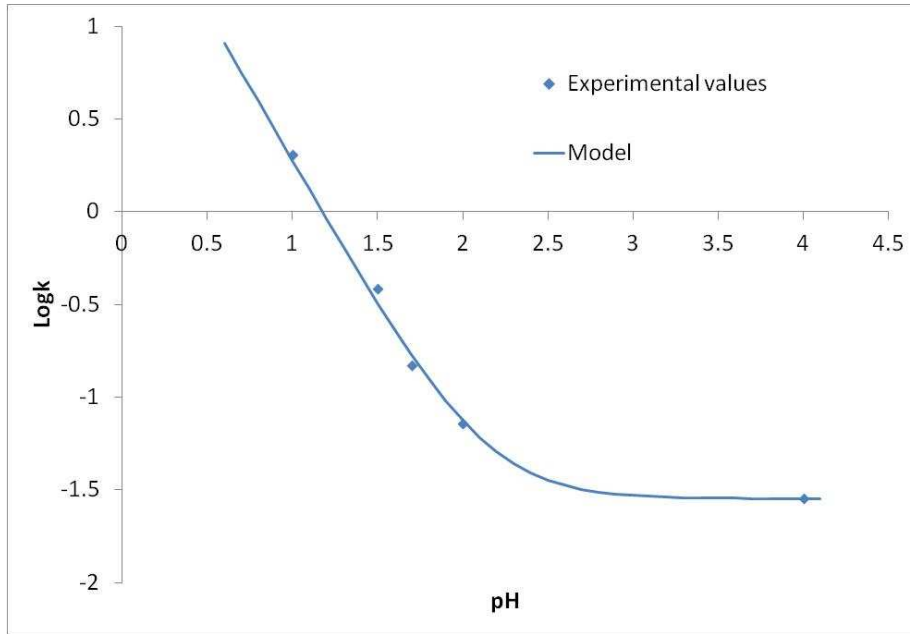


Figure 4: Relationship between pH and degradation rate constant, k (at 140°C)

3.4 Modelling the relationship between degradation rate constant and temperature

The degradation process is a chemical reaction and so would be expected to obey Arrhenius behaviour. Figure 5 shows an Arrhenius plot for the experiments carried out at temperatures of 100, 120 and 140°C.

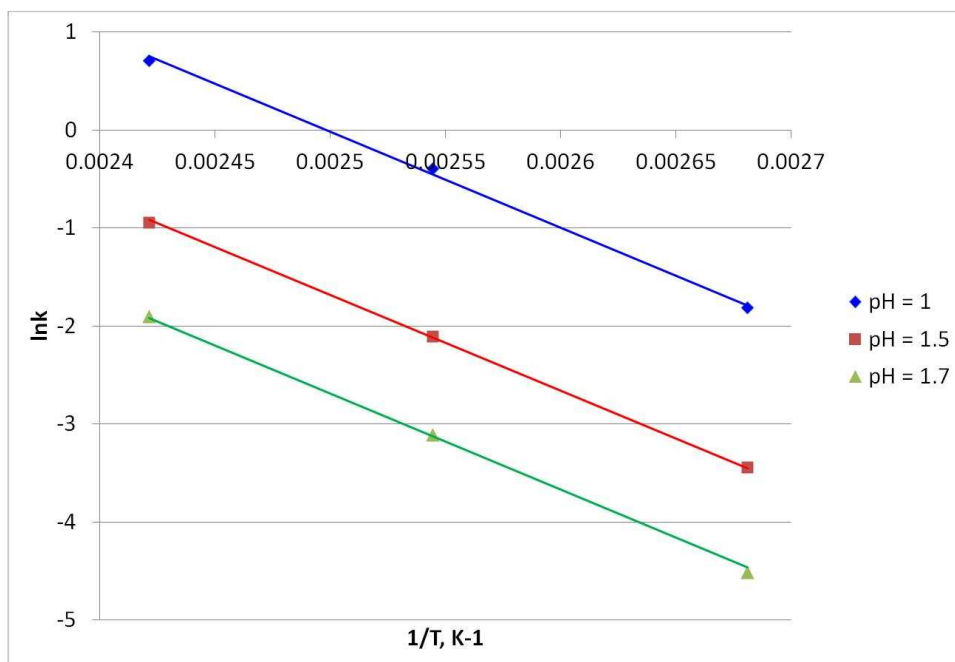


Figure 5: Arrhenius plot for rate constants

The similarity of slopes for the data from different pH values indicates that activation energy is not affected by pH. The difference in rates of degradation brought about by differences in pH is apparently only reflected in the pre-exponential factor (the y intercept of the plots). The average slope of the best fit lines for the different pH values gives an activation energy of $81.4 \text{ kJ}\cdot\text{mol}^{-1}$. Assuming that the underlying rate of hydrolysis, (k_u) also has the same activation energy, values of k_u for 100 and 120°C were calculated from the activation energy and the k_u value measured at 140°C. Values of k_u calculated for 100 and 120°C were 0.002232 and 0.008494 respectively. The intercept on the y axis of the Arrhenius plot for the underlying rate data gives a pre-exponential factor of 5.671×10^8 . Using the calculated values of k_u , model curves of $\log k$ against pH were then plotted for 100 and 120°C, selecting values of k_{cA} that gave the best fit to the experimental data (Figure 6).

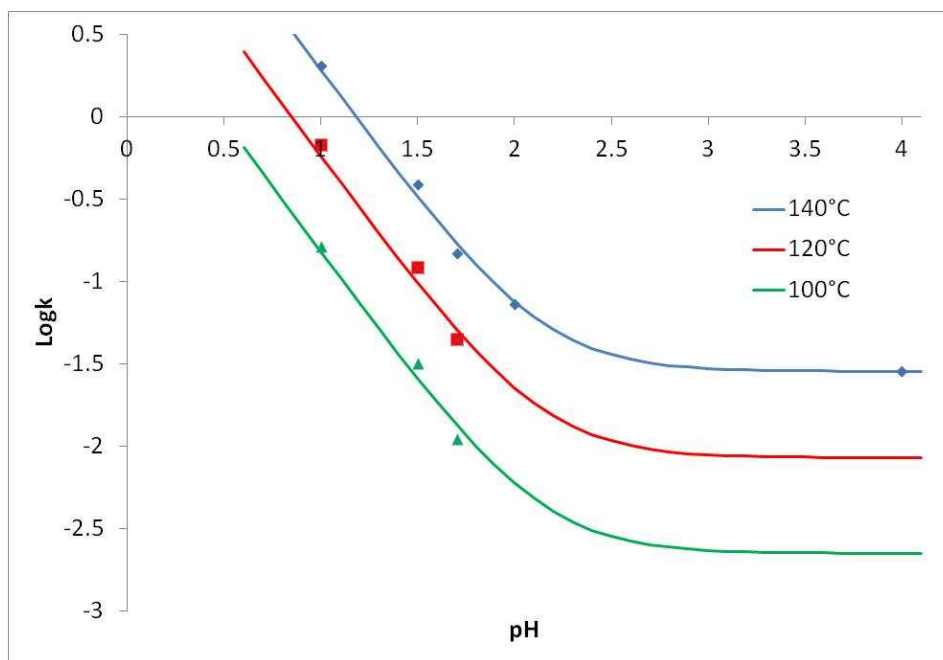


Figure 6: Curve fitting for the dependence of rate constant on pH. Solid lines show calculated values, symbols show experimental data.

The values of k_{cA} reflect a temperature “shift factor” for the curves and so would be expected to follow Arrhenius behaviour. A plot of $\log k_{cA}$ against $1/T$ gave the same activation energy as that obtained for the values of k and a pre exponential factor, A of 1.445×10^{12} .

3.5 Calculation of rate constants for different temperatures and pH values

The model has 4 material dependant constants shown in Table 3 from which values of k can be determined for any temperature and pH value. The Gas constant is also used in the determination of the activation energy.

Table 3: Constants used in the modelling of rate constants

Activation energy	E	
Pre-exponential factor for k_u	k_{uA}	5.671×10^8
Pre-exponential factor for k_{cA}	A	1.445×10^{12}
Order of reaction	n	1.7
Gas constant	R	$8.3145 \text{ J.mol}^{-1}\text{K}^{-1}$

The overall rate constant k is the sum of the underlying rate k_u and the acid catalysed rate k_c .

The value of k_u only depends on temperature and is given by:-

$$k_u = k_{uA} e^{-E/RT}$$

The value of k_c depends on both temperature and pH. Temperature dependence of k_{cA} is given by:-

$$k_{cA} = A e^{-E/RT}$$

The pH dependence of k_c is given by:-

$$k_c = k_{cA} e^{-n(pH)}$$

Using these equations, model values of rate constants were determined for the corresponding experimental conditions and are shown in Table 4.

Table 4: Model rate constants for all the accelerated aging conditions investigated

		Rate constant		
Temperature, °C		100	120	140
pH	1	0.1508	0.5728	1.9118
	1.5	0.0258	0.0979	0.3269
	1.7	0.0135	0.0513	0.1713
	2	x	x	0.0757
	4	x	x	0.0284

3.6 Comparison of the model and experimental values

The model rate constants shown in Table 4 were used to reconstruct tensile strength against aging time curves and are plotted in Figures 7, 8 and 9. Given the scatter of experimental data and the fact that both pH and temperature dependence are included in the model, a good level of agreement is achieved. Hence, it is reasonable to use the model to predict aging behaviour of this silicone rubber at pH values between 1 and 4 and at temperatures of operation of PEM fuel cells (e.g. 80°C). A high level of confidence in extrapolating down to 80°C is justified by the good linear Arrhenius relationships observed and the fact that it is only a short extrapolation from the minimum temperature at which experiments were carried out (100°C).

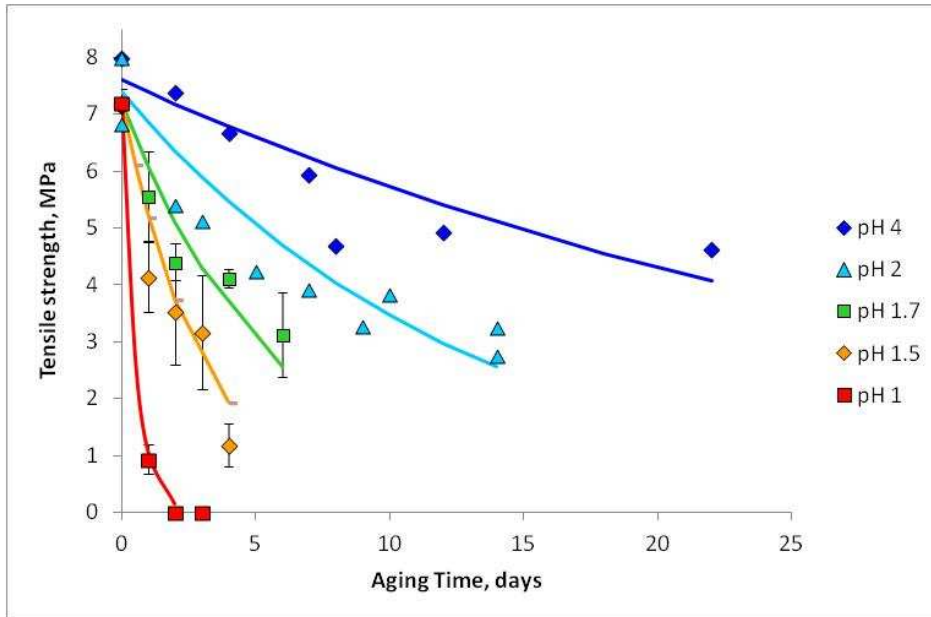


Figure 7: Comparison of model and experimental aging data at 140°C. Solid lines give the model values and symbols give the experimental data.

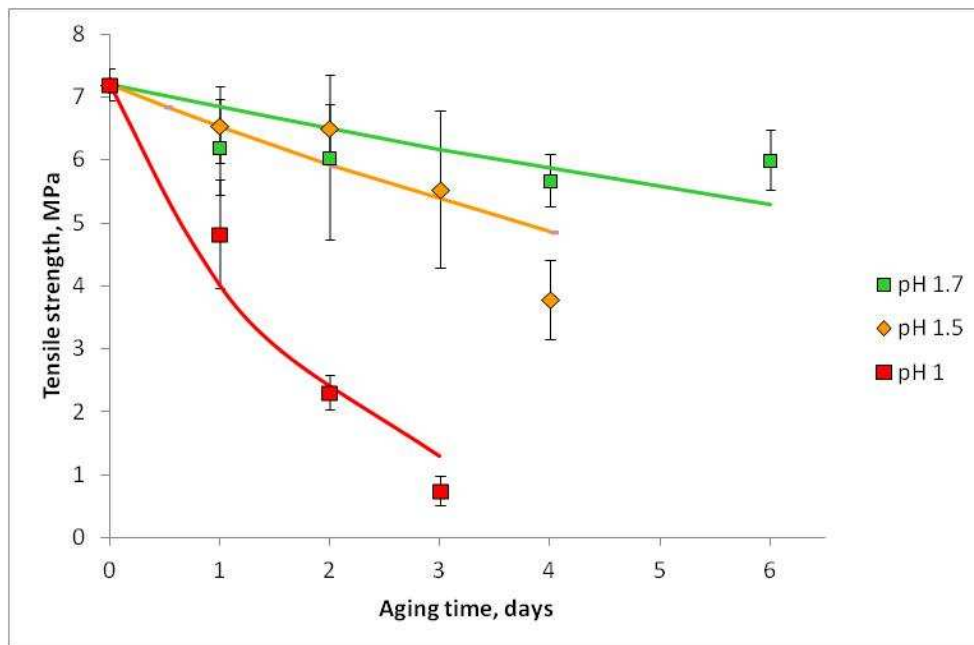


Figure 8: Comparison of model and experimental aging data at 120°C. Solid lines give the model values and symbols give the experimental data.

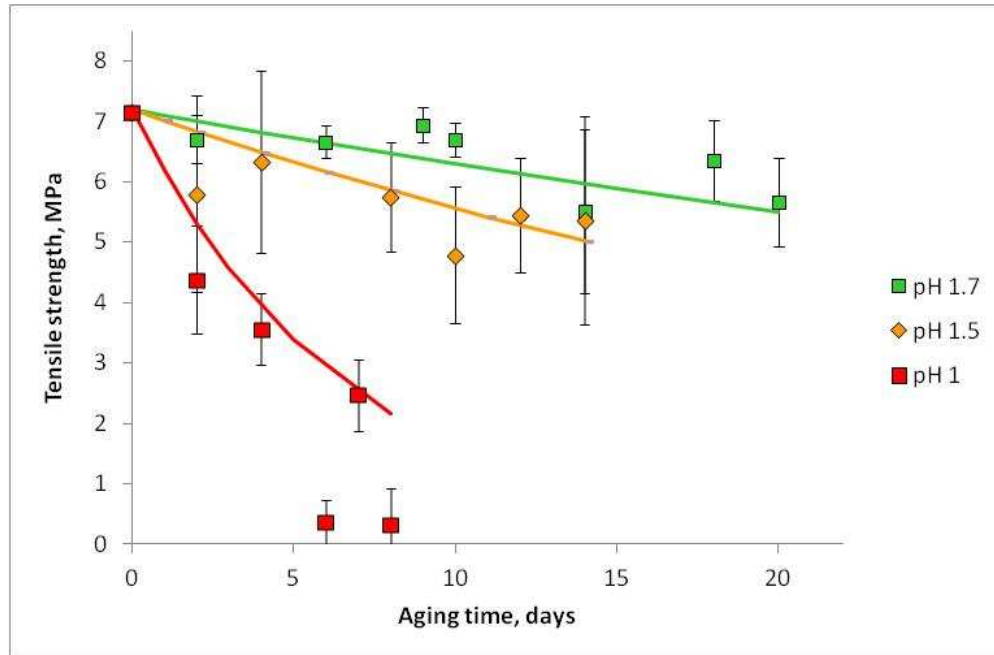


Figure 9: Comparison of model and experimental aging data at 100°C. Solid lines give the model values and symbols give the experimental data.

4. Conclusions

For the silicone rubber used in this project, the following conclusions can be drawn about the degradation brought about by aging in an acidic environment.

1. Tensile strength is a good quantitative measure of the extent of degradation due to accelerated aging.
2. The decrease in tensile strength due to accelerated aging follows first order kinetics, with rate constants characterising the degradation rate for different conditions of temperature and acidity.
3. The pH dependency of the degradation rate constant could be modelled by assuming that the overall degradation rate has a component due to an underlying rate of degradation that is not pH dependant and a component due to acid catalysed degradation that is pH dependant.

4. Rate constants for both the underlying and acid catalysed degradation processes obeyed Arrhenius behaviour, and both had the same activation energy of 81.4 kJ.mol⁻¹.
5. The model was able to reproduce reasonably accurately the tensile strength against aging time curves for the different sets of conditions studied.

Acknowledgements

The work was carried out as part of a research project (BH064B) supported by the UK government agency, the Technology Strategy Board (TSB). Encouragement from the industry partners and financial support from the TSB was greatly appreciated.

References

1. Graiver, D., Farminer, K. W., & Narayan, R. (2003). A review of the fate and effects of silicones in the environment. *Journal of Polymers and the Environment*, 11(4), 129-136.
2. Thomas, D. K. (1966). Network scission processes in peroxide cured methylvinyl silicone rubber. *Polymer*, 7(2), 99-105.
3. Patel, M., & Skinner, A. R. (2001). Thermal ageing studies on room-temperature vulcanised polysiloxane rubbers. *Polymer Degradation and Stability*, 73(3), 399-402.
4. Chaudhry, A. N., & Billingham, N. C. (2001). Characterisation and oxidative degradation of a room-temperature vulcanised poly (dimethylsiloxane) rubber. *Polymer degradation and Stability*, 73(3), 505-510.
5. Umeda, I., Tanaka, K., Kondo, T., Kondo, K., & Suzuki, Y. (2008, September). Acid aging of silicone rubber housing for polymer insulators. In *Electrical Insulating Materials, 2008.(ISEIM 2008). International Symposium on* (pp. 518-521). IEEE.
6. Koshino, Y., Umeda, I., & Ishiwari, M. (1998, October). Deterioration of silicone rubber for polymer insulators by corona discharge and effect of fillers. In *Electrical Insulation and Dielectric Phenomena, 1998. Annual Report. Conference on* (Vol. 1, pp. 72-79). IEEE.
7. Pehlivan-Davis, S., Clarke, J., & Armour, S. (2013). Comparison of accelerated aging of silicone rubber gasket material with aging in a fuel cell environment. *Journal of Applied Polymer Science*, 129(3), 1446-1454.

8. Tan, J., Chao, Y. J., Yang, M., Lee, W. K., & Van Zee, J. W. (2011). Chemical and mechanical stability of a Silicone gasket material exposed to PEM fuel cell environment. *international journal of hydrogen energy*, 36(2), 1846-1852.
9. Tan, J., Chao, Y. J., Yang, M., Williams, C. T., & Van Zee, J. W. (2008). Degradation characteristics of elastomeric gasket materials in a simulated PEM fuel cell environment. *Journal of materials engineering and performance*, 17(6), 785-792.
10. Tan, J., Chao, Y. J., Van Zee, J. W., & Lee, W. K. (2007). Degradation of elastomeric gasket materials in PEM fuel cells. *Materials Science and Engineering: A*, 445, 669-675.
11. Tan, J., Chao, Y. J., Li, X., & Van Zee, J. W. (2007). Degradation of silicone rubber under compression in a simulated PEM fuel cell environment. *Journal of Power Sources*, 172(2), 782-789.
12. Li, G., Tan, J., & Gong, J. (2012). Degradation of the elastomeric gasket material in a simulated and four accelerated proton exchange membrane fuel cell environments. *Journal of Power Sources*, 205, 244-251.
13. Li, G., Tan, J., & Gong, J. (2012). Chemical aging of the silicone rubber in a simulated and three accelerated proton exchange membrane fuel cell environments. *Journal of Power Sources*, 217, 175-183.